

Identification and Analysis of microRNAs Encoded by γ -Herpesviruses

Dissertation

zur Erlangung des Doktorgrades der Naturwissenschaften (Dr. rer. nat.) am
Department Chemie der Fakultät für Mathematik, Informatik und Naturwissenschaften der
Universität Hamburg

vorgelegt von
Dipl. Biochem. Nicole Walz

Hamburg, November 2010

Die vorliegende Arbeit wurde in der Zeit vom September 2006 bis November 2010 im Heinrich-Pette-Institut – Leibniz-Institut für Experimentelle Virologie unter Anleitung von Dr. Adam Grundhoff in der Nachwuchsgruppe Zelluläre Virusabwehr angefertigt und von Prof. Wolfgang Deppert betreut.

1. Gutachter: Prof. Dr. Wolfgang Deppert
2. Gutachter: Prof. Dr. Ulrich Hahn

Tag der Disputation: 28.01.2011

Dedicated to my parents

Zusammenfassung

Mehr als 90% der Weltbevölkerung sind mit dem Epstein-Barr Virus (EBV) infiziert. Das Virus ist mit diversen Tumorerkrankungen wie z.B. dem Burkitt's Lymphom oder dem Nasopharynxkarzinom assoziiert. Die Rolle, die das Virus in der Tumorentstehung spielt, ist dabei nur unzureichend verstanden. Das EBV Genom wird als episomale DNA in der Wirtszelle latent repliziert. In dieser Phase werden nur wenige Proteine, aber alle viralen microRNAs (miRNAs) exprimiert. MiRNAs sind kleine, nicht kodierende RNAs, die post-transkriptionell Genexpression regulieren. MiRNAs werden aus Vorläufermolekülen, den pre-miRNAs, die eine charakteristische Haarnadelschleifenstruktur aufweisen, in ~21 nt lange reife miRNAs prozessiert. Reife miRNAs werden in den „RNA induced silencing complex“ (RISC) inkorporiert und binden meistens nicht vollständig komplementär an die 3'UTR von Ziel-mRNAs, was zur Inhibition der mRNA-Translation führt. MiRNAs sind nicht immunogen und benötigen wenig kodierende Kapazität. Daher stellen sie ideale Werkzeuge für Herpesviren dar, um die Expression des Wirtsgenoms zu modulieren.

Zu Beginn dieser Arbeit waren in der miRNA Datenbank (miRBase) 146 virale miRNA registriert, von denen die große Mehrheit (139) von Herpesviren kodiert wird. Es wird allgemein angenommen, dass virale miRNAs eine wichtige Rolle im herpesviralen Lebenszyklus und der Tumorentstehung spielen. Diese Annahme ließ vermuten, dass virale miRNAs zwischen verschiedenen Viren konserviert sind, um dieselben Funktionen auszuüben. Unter den bislang bekannten miRNAs wurden aber wenige konservierte Vertreter gefunden, mit der Ausnahme von 7 miRNAs von EBV und dem nahe verwandten Rhesus Lymphocryptovirus (rLCV). Daher wurde in dieser Arbeit erstmals eine globale miRNA-Analyse aller komplett sequenzierten γ -Herpesviren durchgeführt. Ein kürzlich etabliertes Programm (VMir) wurde für die *ab initio* Vorhersage von pre-miRNAs in viralen Genomen verwendet. Unter Verwendung des BLAST-Algorithmus wurden nachfolgend konservierte pre-miRNAs identifiziert. Es konnte gezeigt werden, dass viele γ -Herpesviren miRNA-Cluster an denselben genomischen Positionen kodieren. Weiterhin zeigte sich, dass die Sequenzen der miRNAs, im Gegensatz zu der genomischen Position, in der Regel nicht konserviert waren. Eine von zwei Ausnahmen stellten EBV und rLCV dar, für welche wesentlich mehr konservierte pre-miRNAs als bisher bekannt vorhergesagt wurden. Die zweite Ausnahme bildeten die zu den Rhadinoviren gehörenden Rhesus Rhadinovirus (RRV) und Japanese Monkey Herpesvirus (JMHV). In Northern Blot-Analysen wurden 2 neue EBV-, sowie 17 neue rLCV- und 14 neue JMHV-miRNAs identifiziert. Es konnte gezeigt werden, dass die Anzahl partiell konservierter miRNAs zwischen EBV und rLCV signifikant größer ist als bisher angenommen und dass zwischen den näher verwandten Viren RRV und JMHV nahezu alle pre-miRNAs konserviert sind.

Ein weiterer Schwerpunkt dieser Arbeit war die Ziel-mRNA Identifizierung von EBV-kodierten miRNAs. Die computerbasierte Vorhersage von Ziel-mRNAs ist aufgrund der nicht vollständig komplementären Bindung der miRNA äußerst schwierig. Um die Funktion von EBV kodierten miRNAs in biologischen Systemen zu untersuchen, wurden Expressionsplasmide und adenovirale

Vektoren generiert, welche für alle EBV-miRNAs kodieren. Da miRNAs neben der translationalen Inhibierung auch eine Destabilisierung der Ziel-mRNA bewirken, wurden die Transkriptomte von miRNAs stabil exprimierenden Zelllinien und infizierten primären Zellen mittels Expressions-Mikroarrays analysiert. So ermittelte potentielle Ziel-mRNAs wurden dann mit Hilfe computerbasierter Programme hinsichtlich möglicher miRNA-Bindungsstellen weiter eingegrenzt. Der Nachweis einer direkten Bindung der miRNA an ihre Ziel-mRNAs erfolgte mittels Luziferase-Assay. Es konnten so einige potentielle Ziel-mRNAs identifiziert werden, unter anderem die des Interferon-induzierten Proteins myxovirus resistance 1 (MX1). In diesem Zusammenhang weisen preliminäre Analysen auf eine verringerte IFN-Antwort in miRNA exprimierenden Zellen hin, so dass EBV kodierte miRNAs möglicherweise direkt in die Interferon-Antwort eingreifen. Weiterhin wurde Tankyrase 2 (TNKS2) im Luziferase-Assay verifiziert. Überexpression von TNKS2 führt zur Inhibition der latenten Replikation des EBV-Episoms. Eine verringerte Expression von TNKS2 könnte somit für eine effizientere Replikation des Episoms verantwortlich sein.

Diese Daten weisen darauf hin, dass EBV kodierte miRNAs durch Eingreifen in unterschiedliche zelluläre Netzwerke eine für die Replikation des Virus und den Erhalt des Episoms optimale Umgebung schaffen könnten.

Abstract

More than 90% of adults are estimated to be infected with the Epstein-Barr virus (EBV). EBV is not only the aetiologic agent of infectious mononucleosis (IM), but is also associated with different kinds of tumors like Burkitt's lymphoma or nasopharyngeal carcinoma. However, the precise contribution of EBV to tumorigenesis is only partially understood. The virus persists as a benign latent infection throughout the host's lifetime. Gene expression during latency is strictly limited to very few genes. However, all viral miRNAs are expressed in latency. Mature miRNAs are small, non-coding RNAs (~ 21 nt) derived from a pre-miRNA hairpin. Mature miRNAs are incorporated into the RNA-induced silencing complex (RISC) and bind imperfectly to the 3'UTR of target mRNAs to silence post transcriptionally gene expression. Since miRNAs require minimal coding capacity and are non-immunogenic, they are a useful tool for herpesviruses to modulate host cell gene expression. Thus, an important function in the herpesviral life cycle has been proposed.

When this work was started, the miRNA registry listed 146 viral miRNAs, the vast majority (139) of which are encoded by herpesviruses. There is little evidence of evolutionary conservation, except for seven miRNA hairpins shared between EBV and the closely related rhesus lymphocryptovirus (rLCV). Assuming that viral miRNAs have important functions, it was hypothesized that more conserved miRNAs may exist. Therefore, the conservation state of all known and predicted γ -herpesvirus encoded miRNAs was investigated. Pre-miRNA hairpins were predicted with a recently established program VMir. VMir allows the *ab initio* prediction of pre-miRNA hairpins in viral genomes. A subsequent BLAST alignment of viral sequences allowed the identification of conserved miRNAs. In this work, it was shown that γ -herpesvirus miRNAs are encoded in clusters at the same genomic positions. In contrast to the conserved genomic position, the sequences were mostly not conserved. One of two exceptions is presented by EBV and rLCV, which were predicted to encode a significantly higher number of conserved miRNAs. The second exception was found in the rhadinoviruses, rhesus rhadinovirus (RRV) und Japanese monkey herpesvirus (JMHV). Northern blotting confirmed 2, 17 and 14 novel EBV-, rLCV- and JMHV-miRNAs, respectively. The number of partial conserved miRNAs of EBV and rLCV was significantly higher than previously thought. Nearly all of the pre-miRNAs encoded by the closely related RRV and JMHV are conserved.

At the beginning of this work, nearly nothing was known about EBV-encoded miRNA targets and functions. The computational target prediction is very difficult due to the fact that miRNAs bind imperfectly to their target mRNAs. To elucidate functions of EBV-encoded miRNAs, DNA and adenoviral expression vectors that allow simultaneous expression of all EBV-encoded miRNAs were generated. Since miRNAs not only inhibit translation but also destabilize their target mRNAs, gene expression microarrays were used to identify EBV-miRNA targets. Differentially regulated genes were filtered for miRNA binding sites and verified in luciferase reporter assays. A set of putative target mRNAs was identified, including myxovirus resistance 1 (MX1). In line with this, preliminary data point toward a reduced IFN signaling in response to miRNA expression in primary cells. Thus it

can be proposed that EBV-encoded miRNAs might directly influence the IFN pathway. Tankyrase 2 (TNKS2) was also verified in luciferase assays. Overexpression of TNKS2 has been shown to inhibit EBV episome replication. A miRNA dependent reduction of TNKS2 might be responsible for a facilitated replication of the episome. These data indicate that EBV-encoded miRNAs might create an advantageous environment, allowing replication and maintenance of the EBV genome by interfering with different cellular networks.

1. INTRODUCTION.....	1
1.1. Herpesviruses	1
1.1.1. Genome Structure of Herpesviruses	2
1.2. Epstein-Barr Virus.....	4
1.2.1. Epidemiology and Associated Malignancies	4
1.2.1.1. Tropism.....	5
1.2.2. EBV Life Cycle.....	6
1.2.2.1. Lytic Replication.....	7
1.2.2.2. Latency.....	8
1.2.2.3. Burkitt's Lymphoma	11
1.2.2.4. Nasopharyngeal Carcinoma	11
1.2.3. Animal Models to Study γ -Herpesvirus Pathogenesis	12
1.3. miRNAs.....	14
1.3.1. History	14
1.3.2. miRNA Biogenesis	14
1.3.3. miRNA Function.....	16
1.3.4. Viral miRNAs	18
1.3.4.1. Overview.....	18
1.3.5. Lymphocryptovirus miRNAs.....	19
1.3.6. Evolutionary Conservation of miRNAs	21
1.3.7. Functions of miRNAs	22
1.3.7.1. Target Prediction.....	22
1.3.7.2. Functions of Cellular miRNAs.....	23
1.3.7.3. Viral miRNA Targets.....	24
1.3.7.4. EBV miRNA Targets	25
1.4. Objective	26
2. MATERIALS	27
2.1. Chemicals and Expendable Materials.....	27
2.1.1. Chemicals.....	27
2.1.2. Expendables	27
2.2. Bacteria and Cell Lines	27
2.2.1. Bacteria	27
2.3. Enzymes	27
2.4. Oligonucleotides	27
2.4.1. Primers	28
2.4.2. Probes.....	31
2.5. Commercial Systems.....	33
2.6. Instruments and Equipment	34
2.7. Plasmids	34
2.7.1. Generation of Plasmids Encoding all EBV miRNAs and JMHV miRNAs	35
2.7.1.1. EBV miRNA Expression Vectors	35
2.7.1.2. JMHV miRNAs Expression Vector	36
2.8. Antibodies	36

3. METHODS	37
3.1. DNA Techniques	37
3.1.1. Bacteria	37
3.1.1.1. Culture and Storage.....	37
3.1.1.2. Generation of Chemically Competent <i>E. coli</i>	37
3.1.1.3. Transformation of <i>E. coli</i>	38
3.1.1.4. Blue-White Screening of <i>E. coli</i> Colonies	38
3.1.2. Preparation of Plasmid DNA from <i>E. coli</i>	38
3.1.3. Determination of DNA Concentration and Purity	39
3.1.4. Restriction of DNA	39
3.1.5. Purification of DNA.....	40
3.1.6. Ligation.....	40
3.1.6.1. Ligation into a TA-vector.....	40
3.1.7. Agarose Gel Electrophoresis.....	41
3.1.8. Sequencing of Plasmids	42
3.1.9. Isolation of Genomic DNA	42
3.1.10. Polymerase Chain Reaction	43
3.1.10.1. Colony PCR	44
3.1.10.2. Site-directed Mutagenesis	44
3.1.11. Real-time qPCR	45
3.1.11.1. Real-time qPCR with SYBR Green	45
3.1.11.2. Real-time qPCR with TaqMan probes	46
3.1.11.3. Reverse-Transcriptase PCR (RT-PCR).....	47
3.1.11.4. Real-time Stem-loop PCR.....	48
3.2. RNA-Techniques	49
3.2.1. Isolation, Purification and Quantification of RNA	49
3.2.2. Northern Blot	49
3.2.2.1. Small RNA Northern Blot.....	50
3.2.3. Cloning of Small RNAs	52
3.3. Protein Techniques	53
3.3.1. Isolation of Protein from Cultured Cells.....	53
3.3.2. Determination of Protein Yield.....	53
3.3.3. SDS-Polyacrylamide Gel Electrophoresis (SDS-PAGE).....	54
3.3.4. Western Blot	55
3.3.5. Immunoprecipitation RIP-ChIP	56
3.4. Cell Biological Methods	57
3.4.1. Culture of Adherent Mammalian Cell Lines.....	57
3.4.2. Culture of Suspension Mammalian Cell Lines	58
3.4.3. Cryo-freezing of Cell Lines	58
3.4.4. Transfection	58
3.4.4.1. Transfection with Polyethyleneimine (PEI).....	59
3.4.4.2. Transfection with FuGene [®] 6.....	59
3.4.4.3. Transfection with Lipofectamine [™] 2000.....	59
3.4.4.4. Electroporation.....	60
3.4.5. Generation of Stable Cell Lines	60
3.4.6. Fluorescence Activated Cell Sorting (FACS).....	60
3.4.7. Induction of Interferon Signaling.....	61
3.4.8. Adenovirus	61
3.4.8.1. Generation of Virus from DNA	62
3.4.8.2. Propagation and Storage of Adenovirus Stocks	62
3.4.8.3. Titration of Virus Stocks	62
3.4.8.4. Infection with Adenovirus.....	63
3.4.9. Luciferase Assay	63
3.4.9.1. Cloning of Controls for the Luciferase Reporter Assays	64
3.5. DNA Microarrays	65
3.5.1. cDNA Synthesis with Spike-in Controls	66
3.5.2. cRNA Synthesis with Fluorescence Dye Incorporation.....	66
3.5.3. Hybridization of DNA Microarrays	67

3.5.4. Washing of DNA Microarrays.....	67
3.5.5. Scanning and Evaluation of DNA Microarrays	67
3.5.5.1. Scanning.....	67
3.5.5.2. Evaluation	68
3.6. Computational Methods.....	69
3.6.1. Prediction of Pre-miRNA Hairpins with VMir.....	69
3.6.2. Prediction of Target mRNAs	69
3.6.2.1. Genome Browser.....	69
<u>4. RESULTS.....</u>	<u>71</u>
4.1. Identification of Novel miRNAs Within the γ-Herpesvirus Family.....	71
4.1.1. Sequence Conservation Among γ -Herpesviruses	71
4.1.2. VMir Prediction of Pre-miRNA Hairpins.....	74
4.1.2.1. Proof of Principle: VMir Prediction of Novel and Known Pre-miRNA Hairpins.....	75
4.1.3. Confirmation of Novel miRNAs of EBV, rLCV and JMHV by Northern Blot	76
4.1.4. Cloning of novel miRNAs from rLCV and JMHV.....	83
4.1.4.1. Conservation Analysis of Known and Novel Pre-miRNAs from EBV and rLCV.....	87
4.1.4.2. Conservation Analysis of Known and Novel miRNAs from RRV and JMHV.....	90
4.2. Target Identification of EBV miRNAs.....	91
4.2.1. EBV miRNA Delivery Systems.....	91
4.2.1.1. Design of Vectors Encoding EBV miRNAs	91
4.2.1.2. EBV-miRNA Encoding Adenoviruses.....	92
4.2.2. Target Identification on mRNA Level - DNA Microarrays.....	95
4.2.3. Computational Target Prediction	97
4.2.3.1. Genome Browser.....	97
4.2.4. Confirmation of miRNA Targets	98
4.2.4.1. Luciferase Reporter Assay	98
4.2.4.2. Design of Controls for Luciferase Reporter Assays.....	98
4.2.4.3. PUMA from Rhesus Macaques is Not Regulated by the Conserved miRNA rL1-8.....	101
4.2.4.4. MX-1 and PDCD2 Might be Regulated by miR-BART11 and -19, Respectively.....	102
4.2.4.5. CASP3 Was Not Confirmed to be a Direct Target of EBV-encoded miRNAs.....	103
4.2.4.6. Evaluation of Putative Targets identified in Adenovirus-infected Primary Cells	104
4.2.4.7. Gene Ontology of Gene Lists Derived From DNA Microarrays	106
<u>5. DISCUSSION.....</u>	<u>109</u>
5.1. Identification and Conservation of γ-herpesvirus miRNAs	109
5.1.1. VMir Analysis to Identify Conserved Pre-miRNA Hairpins.....	109
5.1.2. Identification of Novel Pre-miRNA Hairpins in γ -Herpesvirus Genomes	110
5.1.3. Conservation State of Predicted Pre-miRNA Hairpins	112
5.2. Target Identification	116
5.2.1. Conserved Targets	117
5.2.2. Expression Systems for miRNAs and Phenotypic Analysis	119
5.2.2.1. High Throughput Methods for the Identification of miRNA Targets	122
5.2.2.2. DNA Microarrays	122
5.2.3. Gene Ontology of DNA Microarrays.....	125
5.2.4. Target Confirmation.....	126
5.3. Outlook	129
<u>6. INDICES.....</u>	<u>131</u>
6.1. Abbreviations	131
6.2. Figure Index	133
6.3. Table Index	134

7. LITERATURE	136
8. APPENDIX	I
8.1. Safety-related Data	I
8.2. Supplementary Figure 1	III
8.3. Supplementary Figure 2	VI
8.4. Supplementary Table 1.....	VIII
8.5. Supplementary Table 2.....	IX
9. ACKNOWLEDGMENT	XI
CURRICULUM VITAE	XII
PUBLICATIONS, PRESENTATIONS AND AWARDS	XIII
EIDESSTATTLICHE ERKLÄRUNG	XIV

1. Introduction

1.1. Herpesviruses

Herpesviruses are large double-stranded DNA (dsDNA) viruses and are prevalent in most species throughout the animal kingdom. Mammalian herpesviruses are estimated to have a common evolutionary origin, from which they have diverged, 180-220 million years ago, into three subfamilies, α -, β -, and γ -herpesvirinae (McGeoch et al., 1995). This was before the major mammal radiation and as such herpesviruses are relatively diverse (Alba et al., 2001). Furthermore, within a subset of the herpesviruses the phylogenetic tree's branching patterns are similar to those of mammalian hosts. This counts for co-evolution of host and virus lineages and allows estimation of timescales. (McGeoch and Cook, 1994; McGeoch et al., 1995; McGeoch and Gatherer, 2005; McGeoch et al., 2005).

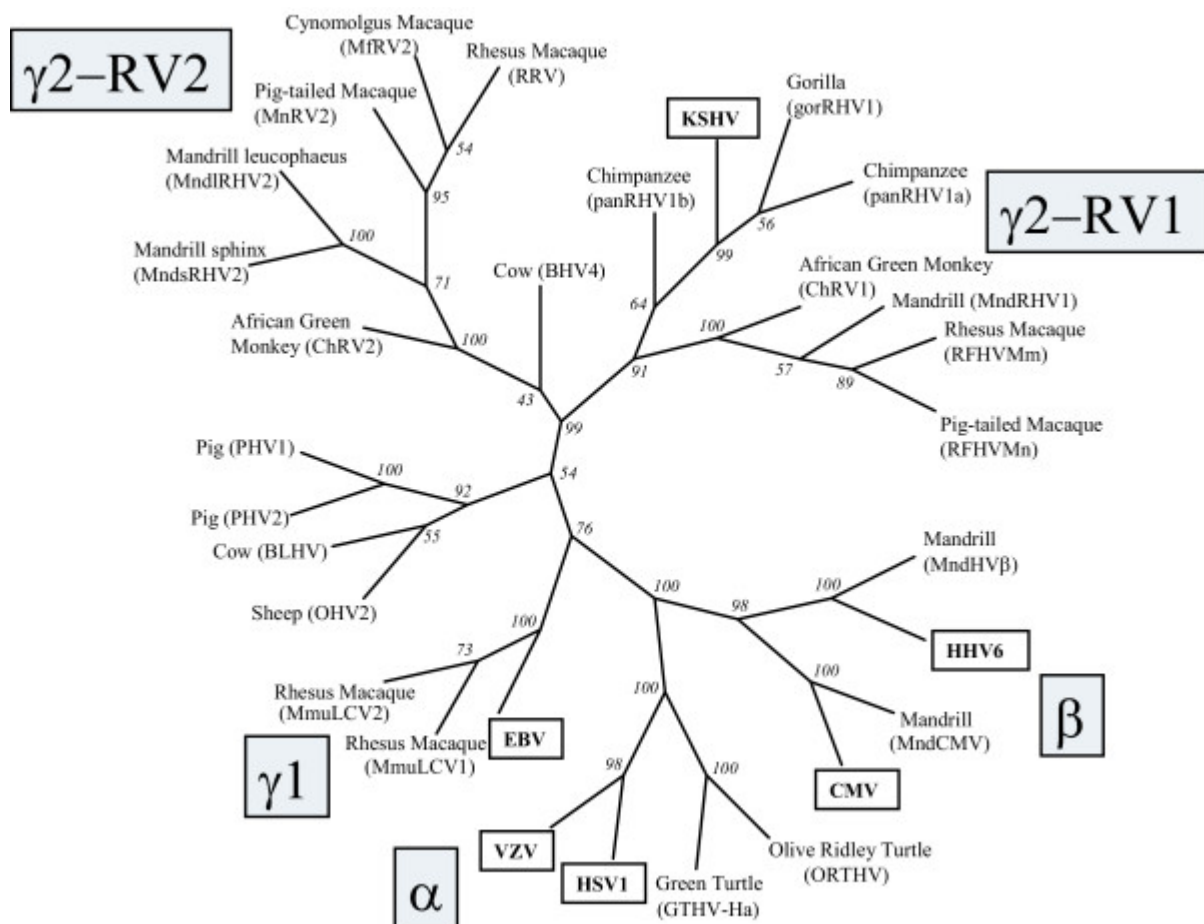


Figure 1-1 Phylogenetic Tree of Herpesviruses

Herpesviruses can be divided into α -, β - and γ -herpesviruses. The phylogenetic tree is based on the analysis of DNA polymerase sequences. Human pathogenic viruses are highlighted with a box (Rose, 2005). (figure: © 2005 Rose; licensee BioMed Central Ltd.)

Herpesviruses are well adapted to their hosts and fatal infections are rare in immunocompetent individuals. If a heterologous host is infected, fatal outcomes may occur as for example in humans infected with simian B virus. Additionally, deregulation of distinct cellular or viral genes can facilitate

tumor development. Consequently the virus has to maintain a good balance between virus growth and regulation of host responses, which are not fully understood. In particular, investigation of the establishment and maintenance of latency as well as the associated mechanisms in host cell gene regulation are important to gain a better insight into herpesvirus pathogenesis (Roizman in Fields Virology, (Fields et al., 2007)).

To date more than 130 herpesviruses have been identified, eight of them infecting humans. Herpes simplex virus 1 and 2 (HSV-1, -2; HHV-1, -2) belong to the α -herpesviruses, whereas varicella-zoster virus (VZV; HHV-3), human cytomegalovirus (HCMV; HHV-5) and human herpesvirus 6 and 7 (HHV-6, HHV-7) belong to the β -herpesviruses. Epstein-Barr virus (EBV; HHV-4) and Kaposi's sarcoma-associated virus (KSHV; HHV-8) are grouped into the family of γ -herpesviruses (Damania and Pipas, 2009)

The γ -herpesviruses are further subdivided in lymphocryptoviruses and rhadinoviruses. The only lymphocryptovirus (LCV) and rhadinovirus (RDV) infecting humans are EBV and KSHV, respectively. EBV and KSHV are lymphotropic viruses which are capable of undergoing lytic replication in epithelial and fibroblast cells, respectively. But a hallmark of herpesviral infection is their ability to establish a life long latent infection. In addition they have been identified as co-carcinogens in different types of malignancies and are related to lymphoproliferative or neoplastic disorders. Other LCVs like rhesus lymphocryptovirus (rLCV) are found in new world primates but not in subprimate mammalian species as it is the case for the RDVs. The DNA of RDVs is more diverse than the DNA of LCVs and so it is suggested, that the RDVs have evolved earlier. Considering that the genomes of RDVs and LCVs are similar and LCVs are restricted to primates it is likely that the LCVs have evolved from an early primate RDV (Damania, 2004).

1.1.1. Genome Structure of Herpesviruses

Herpesviruses contain a toroid shaped protein core wrapped with DNA, a nucleocapsid, a protein tegument between the nucleocapsid and the envelope and an outer envelope with external glycoprotein spikes. Most herpesvirus genomes consist of 70-120 ORFs, with the exception of HCMV, that might encode over 220 genes (Cha et al., 1996). They are transcribed by polymerase II (Alwine et al., 1974) and, in most cases, have their own promoters (Bodescot et al., 1987). Consecutive and similar oriented genes share often a polyadenylation site. While introns are generally found in the minority of herpesvirus genes, it has been shown that β - and γ -herpesviruses have more intron containing genes than alphaherpesviruses.

Although the sequence conservation is low, herpesviruses encode functional homologous proteins. Herpesvirus genomes encode several core genes that are contained in seven conserved gene blocks and are largely located in the central region of the genomes (McGeoch et al., 2006). Apart from that, each virus has a subset of genes characteristic of the subfamily, in which the rate of gene turnover appears higher, and a variable, high number of ORFs specific for the virus (Alba et al., 2001) located mostly

near the termini of the genomes (McGeoch et al., 2006). The less-well conserved functional groups comprise transcription, glycoproteins and genes of unknown functions. It seems likely that these were captured from the specific host in recent time.

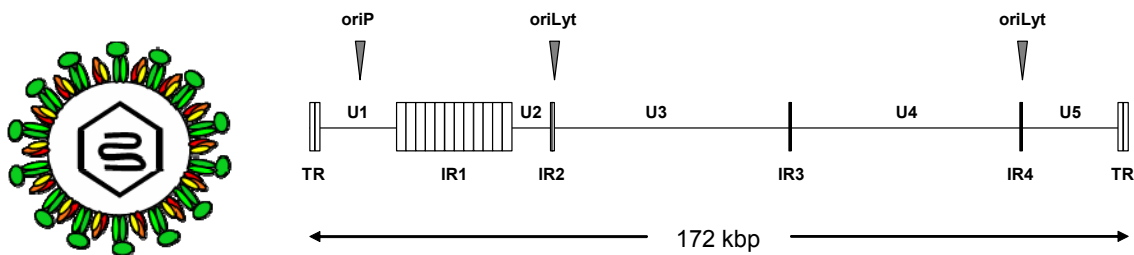


Figure 1-2 EBV Structure

Virus particle, left. Virus envelope with external glycoprotein spikes, toroid shaped capsid and linear DNA genome are schematically shown. Genome structure, right. EBV consists of 172 kbp, containing unique regions (U1-U5), terminal repeats (TR) and internal repeats (IR1-4). Location of the origins of latent (oriP) or lytic (oriLyt) replication are depicted.

However, the known herpesviruses seem to share four biological properties. They specify a large set of enzymes involved in nucleic acid metabolism. Viral DNA synthesis and capsid assembly occurs in the nucleus. Lytic cycle replication and production of viral particles lead to the destruction of infected cells and, next to the lytic cycle, herpesviruses remain latent in their host as episomal circularized genomes, expressing only few genes (Roizman in Fields Virology, (Fields et al., 2007)). Main differences of herpesviruses are their host range (which might be wide as for HSV-1 or very restricted as for EBV) and the set of cells that are latently infected.

In addition to protein coding regions, there are several regions within herpesvirus genomes encoding for RNAs, such as large-non coding RNAs of the latency associated transcripts in HSV-1 (Stevens, 1987) or the EBER RNAs transcribed by polymerase III of EBV (Rosa et al., 1981). Furthermore microRNAs have been identified in members of all herpesviral subtypes (Cai et al., 2005; Grey et al., 2005; Grundhoff et al., 2006; Pfeffer et al., 2005b).

All herpesviruses have evolved strategies to alter the cellular environment to their advantage. A common mechanism is the host shutoff (Child et al., 2004; Covarrubias et al., 2009; Strelow and Leib, 1995), leading to a widespread inhibition of host gene expression. Furthermore they block induction of programmed cell death and inhibit the activation of interferon pathways (e.g. by activation of PKR) (Roizmann in Fields Virology, (Fields et al., 2007)).

EBV contains a 172-kbp linear dsDNA genome encoding for approximately 94 genes (Farrell, 2005). The nomenclature of the open reading frames was initially based on the size of the *Bam*HI fragments generated after digestion of the entire genome (A–X: largest to smallest). Genes in these fragments were further designated based on the sides of their initiation left end genes LFs and right end genes RFs. (Farrell, 2005). For example BZLF1 is the open reading frame (ORF) for the fragment BZ left end gene 1.

1.2. Epstein-Barr Virus

The British missionary surgeon, Denis Burkitt, described extranodal lymphomas in children, which were found frequently in regions of equatorial Africa together with holoendemic malaria but rarely elsewhere (Burkitt and Wright, 1966). In 1964, Epstein-Barr virus (EBV) was discovered in electron micrographs of cultured tumor cells from extranodal lymphomas (Epstein et al., 1964). It was the first candidate for being a human tumor virus.

There are two different types of EBV. Type I and II are represented by the isolate B95.8 and Jijoye, respectively. The major differences are found in the EBV nuclear antigen (EBNA-2 and -3) genes (Dambaugh et al., 1984; Sample et al., 1990). Type I is more common in Europe and the United States, whereas both types are frequent in populations in equatorial Africa and New Guinea and also among people infected with HIV (Yao et al., 1998; Young et al., 1987; Zimber et al., 1986). Furthermore, type I isolates are more efficient in B-cell immortalization *in vitro* (Cohen et al., 1989; Rickinson et al., 1987).

1.2.1. Epidemiology and Associated Malignancies

EBV is ubiquitously found in the world's population and more than 90% of adults are estimated to be infected (Black, 1970; Lang et al., 1977). EBV is strictly a human pathogen and in most cases is transmitted via saliva. Oral transmission is the primary route of infection in young adults explaining the original name of infectious mononucleosis (IM), the "kissing disease". Indirect infection with saliva through contact with contaminated eating utensils for instance is another common route mainly for infants. Since infectious virus is also found in cervical secretions, sexual transmission and perinatal transmission from mother to child during birth are also possible routes. Infection through organ transplantation via infected B lymphocytes in the transplanted organ is a risk factor for the development of post transplant lymphoproliferative disease (PTLD) in EBV-seronegative recipients (Cen et al., 1991; Haque et al., 1996).

The majority of primary infections occur in infants and have an asymptomatic course. The virus remains as a benign latent infection throughout the host's lifetime. In contrast to that, primary infection in young adults can lead to IM, a benign self-limiting disease. EBV is clearly the aetiologic agent of IM, as well as for hairy leukoplakia of the tongue (HLP). Other EBV associated diseases like post-transplantation lymphomas, solitary CNS (central nerve system) lymphomas or leiomyosarcoma exclusively occur in immunodeficient hosts. Another EBV related disease with fatal outcome is the X-linked lymphoproliferative syndrome. It is caused by a heritable genetic disorder, whereas EBV-associated hemophagocytic syndrome and chronic active EBV infection might have genetic components as well. Furthermore, EBV has been linked to B-cell lymphomas like Burkitt's lymphoma (BL) and Hodgkin's disease (HD), as well as epithelial cell derived carcinomas like nasopharyngeal carcinoma (NPC), PTLN and gastric carcinomas. EBV is associated with about 50% of HD cases. In

these cases the EBV genome is monoclonal, displaying that the infection took place before tumor development. In nasopharyngeal carcinoma (NPC) the association of EBV is 100% in contrast to gastric carcinoma with only a subset of 15%.

The association with other types of cancer (e.g. breast cancer) or auto-immune diseases (e.g. multiple sclerosis (MS)) and the interplay between EBV and other infectious diseases e.g. Malaria, which is a clear co-factor for endemic BL, are under investigation (Morrow, 1985).

Since most humans are infected with EBV and the virus has been linked to several diseases it is very important to understand how the virus modulates its host cells and furthermore by which mechanisms it is involved in disease onset and / or progression.

1.2.1.1. Tropism

Efficient EBV infection *in vitro* occurs in primary human B lymphocytes only. In accordance to this EBV infects efficiently B lymphocytes derived from peripheral blood, tonsils or fetal cord blood, whereas B lymphocytes at earlier stages of development e.g. from adult or fetal bone marrow, fetal liver or leukemic and non-EBV infected Burkitt's lymphoma (BL) cell lines are only infectable with low efficiency. EBV infected cells are nonpermissive for virus replication and establish a latent infection with continuous proliferation resulting in long-term lymphoblastoid cell lines underlining the oncogenic potential of EBV. Latency can also be established with very low incidence in T- and NK-cells as well as in epithelial cells. About 10% of *in vitro* infected primary B-cells become latently infected, immortalized and transformed lymphoproliferative cell lines (LCLs). Lytic replication is virtually not detectable in these cells and the whole set of latency genes is expressed (latency III) (Fields et al., 2007).

Infection of epithelial cells with cell free virus *in vitro* has a low efficiency whereas the infection with cell-associated virus is more efficient (Chang et al., 1999; Imai et al., 1998; Tugizov et al., 2003). In contrast to B lymphocytes, epithelial cells are permissive for complete lytic replication of the virus (Ackermann, 2006). Identification of lytic cells is complicated in healthy EBV positive humans, since most EBV infected cells reside in a quiescent state expressing only latent genes. Nevertheless, the abundance of lytically infected cells is necessary for virus spread and the virtual absence of these cells emphasizes the efficient cytotoxic T cell response to lytic gene products (Steven et al., 1997). Lytically infected cells have been identified in oropharyngeal epithelial cells (Pegtel et al., 2004; Steven et al., 1997) and in tonsillar plasma cells (Laichalk and Thorley-Lawson, 2005). In addition, EBV infection occurs in the more differentiated epithelial layers of lytic oral hairy leukoplakia (OHL) lesions (Niedobitek et al., 1991).

1.2.2. EBV Life Cycle

A hallmark of herpesviruses is the dual character of their life cycle. They either replicate lytically or latently. The lytic cycle enables universal gene expression and genome amplification, which leads to viral progeny, whereas most genes are silenced during latent infection and only a small subset of latent genes are expressed. Latent infection allows the virus to establish a life long persistence in the host. However, it is still unknown whether B-lymphocytes or epithelial cells *in vivo* are the first site of infection within the oral cavity. So far, the infection of B-cells has been extensively studied and is characterized in more detail.

The initial step in EBV infection of B-cells *in vitro* is the binding of the major viral glycoprotein gp350/220 to CD21 on the cell surface, which is also the receptor for the complement component C3d (Fingeroth et al., 1984). This binding induces receptor-mediated endocytosis (Nemerow and Cooper, 1984; Tanner et al., 1987). The heterotrimeric complex of the viral glycoproteins gp25 (gL), gp85 (gH) and gp42 mediates the co-receptor interaction by binding of gp42 to the major histocompatibility complex (MHC) Class II (Knox and Young, 1995). This interaction allows fusion of the viral membrane with the endosomal membrane (Miller and Hutt-Fletcher, 1988). The viral nucleocapsid and tegument are then released into the cytoplasm of the cell (Carel et al., 1990; Nemerow and Cooper, 1984; Tanner et al., 1987).

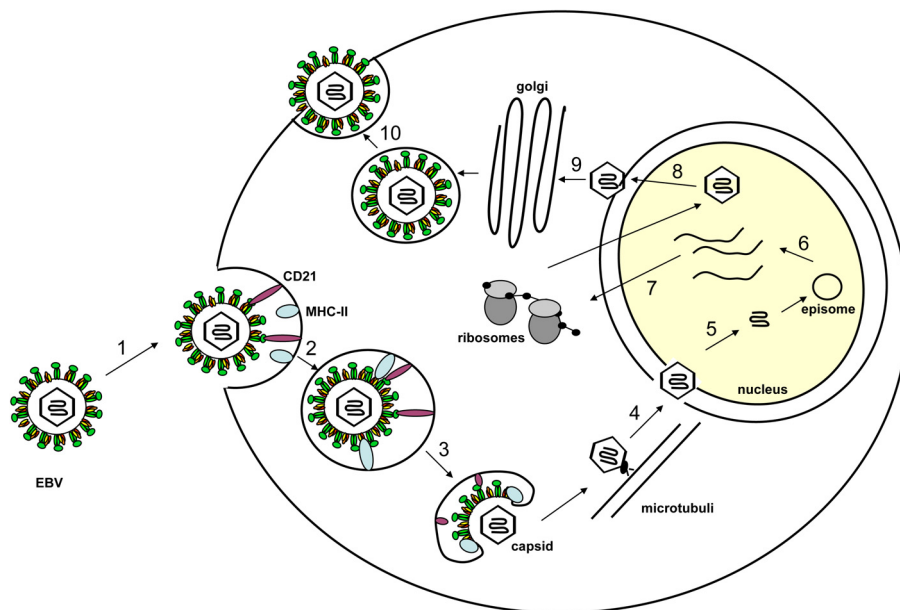


Figure 1-3 EBV Life Cycle

Binding of the viral glycoprotein gp350/220 to CD21 on the cell surface leads to endocytosis (1,2). Binding to the co-receptor MHC-II via the viral gp42 mediates fusion of the virus membrane with the endosomal membrane and results in the release of the tegument and capsid into the cytoplasm (3). The capsid is transported via microtubules to the nucleus (4). In the nucleus the DNA circularizes (5) and the DNA is transcribed into RNA by a cellular polymerase (6). DNA is transcribed in a temporally regulated manner: immediate early, early and late genes are expressed (7). The capsid is assembled in the nucleus and buds through the first nuclear membrane, is exocytosed through the second nuclear membrane and released into the cytoplasm (8). By traversing through the golgi network the virus obtains its envelope (9) and is released out of the cell via exocytosis (10).

In analogy to other DNA viruses, it is likely that the transport of the nucleocapsid to the nucleus is mediated by the cytoskeleton. The EBV genome circularizes in the nucleus and is either lytically or latently replicated. In the reproductive life cycle the herpesvirus DNA is transcribed to RNA by a cellular enzyme (DNA-dependent RNA polymerase I) and is dependent on both nuclear factors of the cell and proteins encoded by the virus. DNA synthesis is enabled by the viral encoded DNA-dependent DNA polymerase (BALF5). The transcription takes place in a temporally regulated manner in which immediate early (IE), early (EA) and late (L) genes are expressed successively. The IE genes are the first class to be expressed. They include proteins involved in transcriptional regulation and the control of expression of the second class of proteins. The EA proteins resemble the second class and encode proteins necessary for DNA replication like DNA polymerases and transcription factors. The L genes are the last to be expressed and encode structural components which allow the virus to be encapsidated and produce infectious virion particles (Fields et al., 2007).

The exact mechanisms of how viral particles are assembled and released are not fully understood. It is suggested, that nucleocapsids are assembled in the nucleus and bud through the inner nuclear membrane, where they receive an initial envelope. Afterwards they are de-enveloped by fusion with the outer nuclear membrane in the cytoplasm, where they acquire tegument proteins and are finally enveloped as they traverse the trans-Golgi or plasma membrane prior to virion release (Gong and Kieff, 1990; Granzow et al., 2001).

In contrast to B-cells, the receptor used for infection of epithelial cells is still unknown. The receptor for gp350/220 binding is missing on the surface of epithelial cells and furthermore the glycoprotein gp42 has been shown to be of no importance for infection of epithelial cells (Li et al., 1995). The heterodimeric complex of gH/gL is able to bind efficiently to epithelial cells but not B-cells and seems to play an important role (Molesworth et al., 2000; Oda et al., 2000). Besides the direct infection of epithelial cells by EBV, they can also be infected by fusion with virus producing B-cells (Bayliss and Wolf, 1980). Most of the viruses docked to B-cells do not enter the cell and remain at the surface. Thereby the virus can be transferred to the epithelial cells (Shannon-Lowe et al., 2006).

1.2.2.1. Lytic Replication

Lytic replication starts at the two lytic replication origins (oriLyt). It is believed that the lytic replication occurs through a rolling circle mechanism, resulting in concatemers of the viral genome, which are cleaved during packaging within the TR domains (Hammerschmidt and Sugden, 1988; Zimmermann and Hammerschmidt, 1995).

The immediate early protein BZLF1 has been shown to play a key role in the switch from latent to lytic replication (Adamson et al., 2005; LaJeunesse et al., 2005; Wen et al., 2007). After induction of the lytic cycle, viral DNA is amplified in a manner dependent on oriLyt yielding monomeric progeny DNA (Tsurumi et al., 2005). During this process BZLF1 binds to oriLyt and the viral DNA is nicked by Dnase I. The amplification of the viral genome is then achieved through the concerted action of diverse viral proteins.

1.2.2.2. Latency

During latent infection, replication of the EBV genome occurs simultaneously to DNA replication of the host cell DNA during S phase. Latency-associated EBV DNA replication starts at the replication origin oriP and requires only one viral protein, EBNA-1, which binds to two distinct elements of oriP. Binding to the family of repeats (FR) allows tethering of the EBV episome to host metaphase chromosomes either via interaction with a cellular chromosome-associated protein (Kapoor et al., 2005; Rawlins et al., 1985; Shire et al., 1999) or interaction with host DNA through an DNA binding motif (so called AT hook) mechanism (Sears et al., 2004). Binding to a region of dyad symmetry (DS), which are inverted repeats, orchestrates the assembly of the host cell replication machinery and initiation of DNA synthesis (Chaudhuri et al., 2001; Deng et al., 2002; Dhar et al., 2001; Schepers et al., 2001). Different studies showed that Qp is constitutively active, when introduced into cells allowing EBNA-1 expression, after infection (Nonkwelo et al., 1996; Sung et al., 1991; Tao et al., 1998) Cellular proteins are additionally necessary for EBNA-1 dependent replication like the origin-recognition complex 2 (ORC2). Since EBV does not express proteins necessary for DNA replication like DNA polymerase, single-stranded DNA binding proteins and other accessory genes during latency, other cellular proteins must be recruited in addition to ORC2 (Dhar et al., 2001; Leight and Sugden, 2001; Lindner and Sugden, 2007; Norseen et al., 2008). Recently, the cellular proteins Tankyrase 1 and 2 have been shown not only to bind directly to EBNA-1 but also that this interaction further leads to down-regulation of oriP replication and episome maintenance. Furthermore this function is poly-ADP ribose polymerase (PARP)-dependent (Deng et al., 2005; Tempera et al., 2010). EBV can establish different latency forms (Thorley-Lawson, 2001) depending on the differentiation state and location of the corresponding B-cell.

The whole set of latent genes encompass 6 EBV nuclear antigens (EBNA-1, -2, -3a, -3b, -3c, -LP), 2 latent membrane proteins (LMP-1, -2), two small non-polyadenylated, non-coding EBV-encoded RNAs (EBER-1, -2) and the *Bam*HI-A rightward transcripts (BARTs). Figure 1-4 lists the genes that are expressed in the different latency programs.

Latency type I is found in Burkitt's lymphoma (BL)-derived cell lines where in addition to the EBNA-1 also the EBER and BART transcripts are expressed. Latency I allows EBV to reside in the resting memory B-cell compartment in a quiescent state. In Latency II, the LMP-1 is expressed in addition to EBNA-1 and the BART transcripts (BARTs). Latency II is common in the epithelial cell derived NPC or Hodgkin's Disease (HD) a B-cell derived lymphoma. The whole repertoire of latent genes is expressed in lymphoblastoid cell lines (LCLs) and in BL-derived cell lines. All six EBNAs, LMP-1 and -2, EBER and the BART transcripts are expressed in this form of latency, referred to as latency III. Latency III is also designated as growth programme.

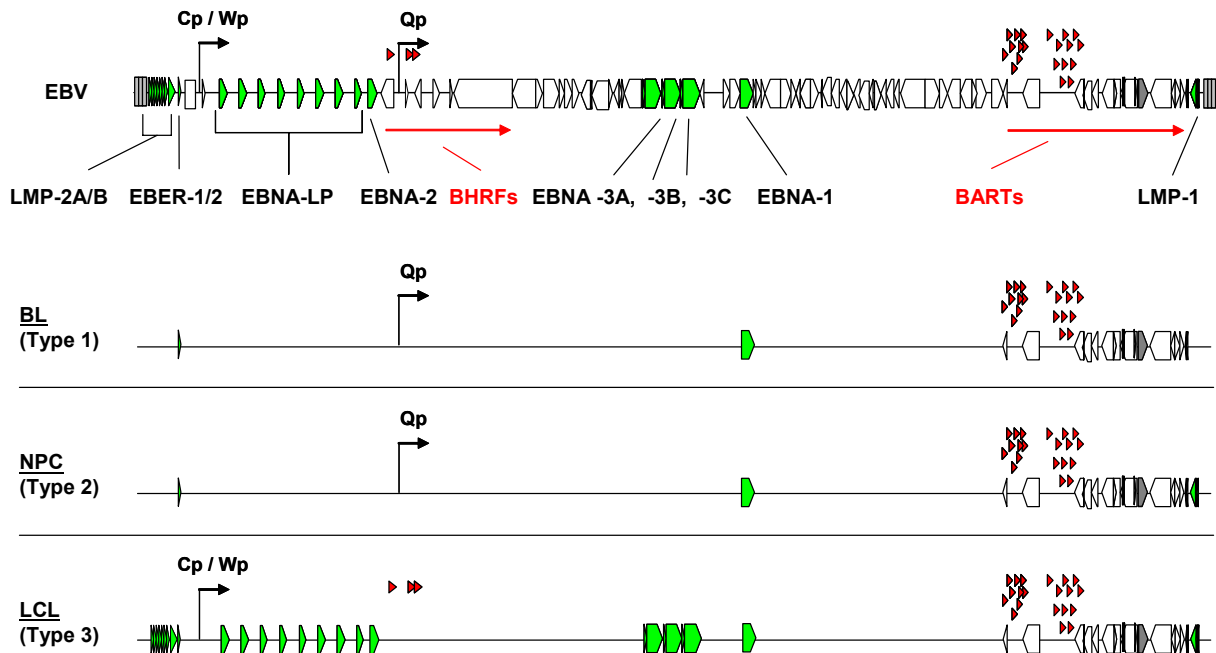


Figure 1-4 Latency Genes and Programs

The EBV genome is shown at the top of the figure. Latency genes are marked as green boxes. Red triangles display viral miRNAs. Burkitt's lymphomas (BL) often show a latency type 1 pattern, in which only EBNA-1 and the BARTs are expressed. The nasopharyngeal carcinoma cells (NPC) display a latency type II pattern, in which EBNA-1, the BARTs and LMP-1 are expressed. All latency proteins are expressed in latency type III, which is found in lymphoblastoid cell lines (LCL) that are established through transformation of B-cells after *in vitro* infection with EBV. Importantly, in all types of latency, the viral miRNAs are expressed. Whereas the BHRF miRNAs are only expressed in Latency I or III, the BART miRNAs are expressed in all types. (figure: Dr. Adam Grundhoff, modified)

EBV nuclear antigen 1 (EBNA1) is expressed in all EBV infected cells regardless of the state of EBV infection. It enables the association of the cis-acting element oriP to genomic DNA and is thereby essential for episome maintenance. EBNA2 can bind to Jk-recombination-binding protein (RBPJk/CBP), a sequence-specific DNA binding protein that mimicks the intracellular domain of Notch (Grossman et al., 1994; Hsieh and Hayward, 1995; Sakai et al., 1998) and abrogates the transcriptional repression mediated by a multiprotein complex containing RBP-Jk. Thereby it activates cellular genes like CD23 and c-myc as well as the viral proteins LMP1 and LMP2A, blocks B-cell differentiation and facilitates growth (Harada et al., 2001). EBNA-LP interacts with EBNA2 and is necessary for the efficient outgrowth of virus-transformed B-cells *in vitro* (Sinclair et al., 1994). EBNA3C is able to facilitate the G1/S transition of activated B-cells by inactivating the function of retinoblastoma tumour suppressor (Rb) (Parker et al., 1996).

LMP-1 and -2 are two integral membrane proteins, that lack significant extracellular domains but are able to act as ligand independent constitutive active receptors. LMP-1 can mimick the activated CD40 receptor preventing B-cells from apoptosis and driving their proliferation (Kilger et al., 1998). CD40 is a key receptor on the surface of memory B-cells and provides a survival signal when it becomes activated by T helper (T_H) cells (Banchereau et al., 1994). Furthermore, LMP-1 has been shown to have transforming effects in continuous rodent fibroblast cell lines and is able of promoting loss of contact inhibition. In contrast however, a very high expression of LMP-1 is toxic. One important effect of

LMP-1 expression is the activation of nuclear factor of 'kappa light chain enhancer' of activated B-cells (NF-kB) by the C-terminal NF-kB activation regions 1 and 2 (CTAR-1, -2) which are transmembrane domains. The CTAR domains interact with tumor necrosis factor (TNF)-associated cytoplasmic factors (TRAFs). Furthermore, the LMP-1 CTAR1 is structurally and functionally homologous to the TNF-receptor CD40 and induces similar effects in B lymphocytes.

The B-cell receptor (BCR) affords a tonic signal in the absence of antigen necessary for B-cell survival. LMP-2A is able to mimic this signal (Caldwell et al., 1998). The amino-terminal domain of LMP-2A contains immunoreceptor tyrosine-based activation motifs (ITAMs) (Beaufils et al., 1993), similar to those of the BCR. The Src family tyrosine kinase Lyn can phosphorylate the tyrosines within the ITAMs providing further survival signals but not growth signals (Caldwell et al., 1998; Miller et al., 1995).

The EBER RNAs are expressed highly in all types of latency. Functionally, they are inhibiting interferon (IFN)-induced protein kinase R (PKR) activation and can block phosphorylation of eukaryotic translation initiation factor 2A (eIF2a). The EBER RNAs are therefore capable of overcoming the IFN dependent block on protein synthesis (Nanbo et al., 2005; Sharp et al., 1993).

The BARTs have been shown to be highly expressed in NPC to a very low level in lymphoid tissue (Gilligan et al., 1991). The many transcripts arising from this locus are derived through differentially splicing. The functions of the putative proteins from these transcripts, which are as of yet not described, are mostly unknown (Thornburg et al., 2004). Interestingly the BARTs encode for 23 viral pre-miRNA hairpins, which are expressed in all types of latency. It is suggested, that these miRNAs might fulfill functions to maintain latency or modulate viral or cellular mRNAs to generate a favourable environment. In addition, a putative role in tumorigenesis is conceivable.

EBV latently infected cells can be activated from this state to lytically replicate. This can be achieved *in vivo* as well as *in vitro* through different mechanisms. During latent infection *in vivo*, the promoters of the IE genes BZLF1 and BRLF1 (Zp and Rp, respectively), are repressed through the binding of a cellular transcription factor zinc finger E-box binding homeobox 1 (ZEB1) to the ZV elements within these regions (Yu et al., 2007). Additionally, the inhibition of BZLF1 expression *in vivo* can be due to epigenetic modifications of viral DNA, like DNA methylation or histone deacetylation (Bhende et al., 2004; Jenkins et al., 2000; Nonkwelo et al., 1996; Nonkwelo and Long, 1993; Paulson et al., 2002; Szyf et al., 1985).

In vitro, cell lines latently infected with EBV can be reactivated by overexpression of BZLF1 (Countryman et al., 1987; Countryman and Miller, 1985; Takada et al., 1986) or crosslinking of the B-cell receptor with anti-immunoglobulin (IgG) (Takada and Ono, 1989). Additionally, the expression of BZLF1 can also be achieved by treatment with chemicals such as phorbol ester, 12-O-tetradecanoyl phorbol-13-acetate (TPA), sodium butyrate (an histone deacetylase (HDAC) inhibitor) and calcium ionophores (Faggioni et al., 1986; zur Hausen et al., 1978). Most of the knowledge about the lytic cycle of EBV derives from *in vitro* studies with EBV positive cell lines.

1.2.2.3. Burkitt's Lymphoma

Depending on the geographic distribution and the association with EBV infection there are three classes of Burkitt's lymphoma: endemic, sporadic and HIV-associated. The endemic form of BL remains the most common childhood cancer in sub-saharan Africa. Interestingly, cells of nearly all (98%) endemic BL tumors in Africa and New Guinea and about 85% in areas of intermediate incidence like Brazil and North Africa harbor the EBV genome. In the sporadic form, which predominantly occurs with low incidence in Western Europe and America, only 20% of tumors are EBV positive. BL is also a frequent tumor in immunocompromised AIDS patients and arises often as the first AIDS defining illness with approximately 30-40% association with EBV (Brady et al., 2007; Fields et al., 2007). The occurrence of the tumor is also different in the three forms. While the most frequent affected tissue in endemic BL is the jaw, the abdomen and lymph nodes are the preferential sites of tumor development in the sporadic and HIV-associated BL, respectively (Brady et al., 2007). All forms of BL have one of three reciprocal chromosomal translocations, that place the c-myc proto-oncogene under the control of the immunoglobulin (Ig)-heavy chain or one of the Ig-light chain loci (8;14 / 8;22 / 8;2). (Dalla-Favera et al., 1982). This translocation is a key factor in the pathogenesis of Burkitt's lymphoma (Kovalchuk et al., 2000; Li et al., 2003; Polack et al., 1996). EBV is a probable co-factor, which might establish growth transforming B-cell infection and thereby generate a pool of target cells that are at risk of a following c-myc translocation (Polack et al., 1996). Both malaria and HIV have been shown to activate B-cells. This subsequently leads to a greater number of B-cells entering the GC reaction and a higher chance to accumulate oncogenic mutations (Donati et al., 2006; Lane et al., 1983). The suppression of T-cell response is another mechanism induced by malaria, which can have an effect during the BL development (Moormann et al., 2007).

The vast majority of EBV positive tumors have a strict latency type I pattern meaning that the only protein expressed is EBNA 1. It is unclear whether EBNA-1 plays a role in BL pathogenesis due to mouse transgene assays, where its oncogenicity is controversial (Wilson et al., 1996) and because its function in vitro seems to be restricted to episome maintenance (Kang et al., 2001). However, the blocking of EBNA 1 in EBV positive BL cell lines does affect cell survival (Kennedy et al., 2003). In addition to EBNA 1 the non-coding EBER RNAs as well as all viral miRNAs are also expressed in latency type I. While the EBER RNAs are able to support in a mechanism including upregulation of IL-10 (Takada, 2001; Takada and Nanbo, 2001), the functions of viral miRNAs are mostly unknown.

1.2.2.4. Nasopharyngeal Carcinoma

The Nasopharyngeal Carcinoma (NPC) is an epithelial derived carcinoma. The EBV-associated undifferentiated form of NPC (World Health Organisation WHO type III) has the highest incidence of EBV associated malignancies. WHO classified NPC into three subtypes: Type I is a rare keratinizing carcinoma, Type II is a nonkeratinizing carcinoma and Type III is an undifferentiated form. It is a common tumor in China and South-East Asia.(Yu and Yuan, 2002), where individuals of Chinese

descent and Cantonese males are genetically pre-disposed. Furthermore, environmental cofactors like dietary components seem to play a role in the aetiology of NPC (Yu et al., 1985).

Undifferentiated carcinoma cells and lymphocytic infiltrates are characteristics of NPC tumors. It shows a latency type II pattern of EBV infection with the expression of the latent membrane proteins LMP-2A and LMP-2B, the oncogenic LMP-1 (in 20% of cases) and the *BamHI-A* transcripts in addition to EBNA-1 (Raab-Traub, 2002). The fact that the tumors show monoclonality of the EBV genome, demonstrates that the EBV infection must have taken place prior to clonal expansion of the population of malignant cells (Raab-Traub and Flynn, 1986).

1.2.3. Animal Models to Study γ -Herpesvirus Pathogenesis

To date, different primate LCVs and RDVs serve as model systems for the study of γ -herpesvirus pathogenesis in animals. For example, rhesus lymphocryptovirus (rLCV) is the next-related LCV to EBV, separated by >13 million years of evolution (Gerner et al., 2004) and infects naturally rhesus macaques (*Macaca mulatta*). It shows a high sequence conservation (65%) and expresses homologous genes during lytic and latent infection (Rivailler et al., 2002). It mirrors in many aspects the infection of humans with EBV, in particular regarding the high rate of adult infection or the latent persistence within peripheral blood and oropharynx. The rLCV induced malignancies are being intensively investigated, since they are similar to diseases found in EBV infected humans, like lymphomas or disorders associated with immunosuppression (Moghaddam et al., 1997; Rangan et al., 1986; Rivailler et al., 2004).

Rhesus rhadinovirus (RRV) infects rhesus macaques as well and has been shown to be closely related to Kaposi's sarcoma-associated herpesvirus (KSHV). KSHV is not only the aetiologic agent of Kaposi's sarcoma but also associated with different neoplastic diseases like Multicentric Castleman disease (MCD) or primary effusion lymphoma (PEL) (Wen and Damania, 2010). As rLCV compared to EBV, RRV possess high genetic similarity to KSHV and shows a similar pathogenicity (Desrosiers et al., 1997; Searles et al., 1999). RRV induced malignancies in SIV-induced immunodeficient macaques serve as a model for KSHV associated disease in HIV-induced immunodeficient patients (Orzechowska et al., 2008; Wong et al., 1999).

Nearly all adult humans are infected with EBV. Although, EBV persists in most cases episomally quiescently within the host without any effects, it is linked to diverse malignancies and involved in tumorigenesis. To date, the knowledge about mechanisms used by EBV to facilitate tumor development is limited. Most of the known malignancies are associated with the latent state of EBV infection and a very strict expression of very few genes. In different tumors like BL only EBNA-1 is expressed, which is necessary for episome maintenance but has not been shown to have a tumorigenic potential. In some cases of NPC a second protein is expressed: LMP-1 which has oncogenic potential, since it mimicks a constitutively active CD40 receptor. But this is not sufficient

to explain how EBV is involved in tumorigenesis, since NPC tumors can also arise without expression of LMP-1. A novel class of small RNAs miRNAs have been identified in EBV and interestingly these miRNAs are all expressed in all types of latency. These miRNAs are very small and need little coding capacity, they are non-immunogenic and have the propensity to regulate a lot of different mRNAs. Thus, they might be a very suitable tool for the virus to modulate different mechanisms and to establish an advantageous environment.

1.3. miRNAs

1.3.1. History

MiRNAs are small (21-24 nt in length) non-coding RNAs, which are able to regulate gene expression at the post transcriptional level. Different researchers overexpressed a pigment synthesis enzyme supposed to produce deep purple flowers but resulted in generating white ones (Napoli et al., 1990; van der Krol et al., 1990). Later it was shown, that both strands of the dsRNA are able to repress gene expression in *C. elegans* (Guo and Kemphues, 1995) after being processed into small siRNAs (21-25 nt in length). These small molecules ultimately triggered gene repression by the targeted degradation of complementary mRNA sequences (Fire et al., 1998; Hamilton and Baulcombe, 1999; Hammond et al., 2000; Zamore et al., 2000). This pivotal finding resulted in the discovery of RNA interference (RNAi).

The first miRNA was later discovered in 1993 by Ambros and colleagues. It was the miRNA *lin-4* (derived from the *lin-4* locus) of *C. elegans* (Lee et al., 1993). They identified not only the precursor of the 22 nt long miRNA, which was 61 nt in length and predicted to form a hairpin like structure, but also proposed that the miRNA could bind imperfectly to the *lin-14* mRNA at multiple sites probably leading to its regulation. In 2001, it was shown, that the RNase III like enzyme Dicer, which converts long dsRNA into small siRNAs (Bernstein et al., 2001; Knight and Bass, 2001) was also capable processing pre-miRNA hairpins into mature miRNAs (Grishok et al., 2001; Hutvagner et al., 2001; Ketting et al., 2001).

To date, a growing number of human (940) and viral (229) miRNAs is listed in the miRNA registry (Griffiths-Jones, 2004; Griffiths-Jones et al., 2006; Griffiths-Jones et al., 2008). Now, that they are extensively studied, their roles in diverse key regulatory pathways, such as apoptosis, differentiation, developmental timing and cell proliferation are elucidated.

1.3.2. miRNA Biogenesis

MiRNA genes are mainly found in intergenic regions (Lagos-Quintana et al., 2001; Lau et al., 2001). They are transcribed by Pol II or Pol III from their own promoters and transcribed mRNAs harbor cap structures and poly A tails. Furthermore, they are located in both exonic or intronic sequences (Cai et al., 2004; Kim, 2005; Lagos-Quintana et al., 2001; Lau et al., 2001; Lee et al., 2004). Interestingly, a lot of miRNAs are found in close proximity to other miRNA loci (Mourelatos et al., 2002) and are generated from polycistronic primary transcripts (Lee et al., 2002). Furthermore, some miRNAs are expressed in a tissue-specific and developmental stage-specific manner (Pillai, 2005).

The transcription of miRNA genes from Pol II bears large pri-miRNAs, that are several kilobases in length. Pri-miRNA hairpins are recognized in the nucleus by a RNase III like enzyme (Drosha) and processed to the pre-miRNA with a length of about 70 nt. Drosha is a large 160 kDa protein that

contains two tandem RNase III domains (RIIDs) and a dsRNA binding domain (dsRBD), which are crucial for catalysis (Han et al., 2004). It is highly conserved in animals (Filipowicz, 2000; Fortin et al., 2002; Wu et al., 2000) and forms a so called large microprocessor complex (650 kDa in humans) by interacting with its cofactor DiGeorge syndrome critical region 8 (DGCR8), which is ubiquitously found in animals such as Pasha in *C.elegans* and *Drosophila melanogaster*. DGCR8 is a 120 kDa protein with two dsRBDs and is believed to assist Drosha in substrate recognition (Denli et al., 2004; Gregory et al., 2004; Han et al., 2004; Landthaler et al., 2004).

Based on the secondary structure of the pri-miRNA hairpin consisting of a stem and a terminal loop of appropriate size, Drosha recognizes and processes the RNA (Lee et al., 2003; Zeng and Cullen, 2003; Zeng and Cullen, 2005; Zeng et al., 2005). Moreover the cleavage site of the Drosha complex is located approximately two helical turns away from the terminal loop, leading to a fragment of about 22 nt in length (Zeng et al., 2005).

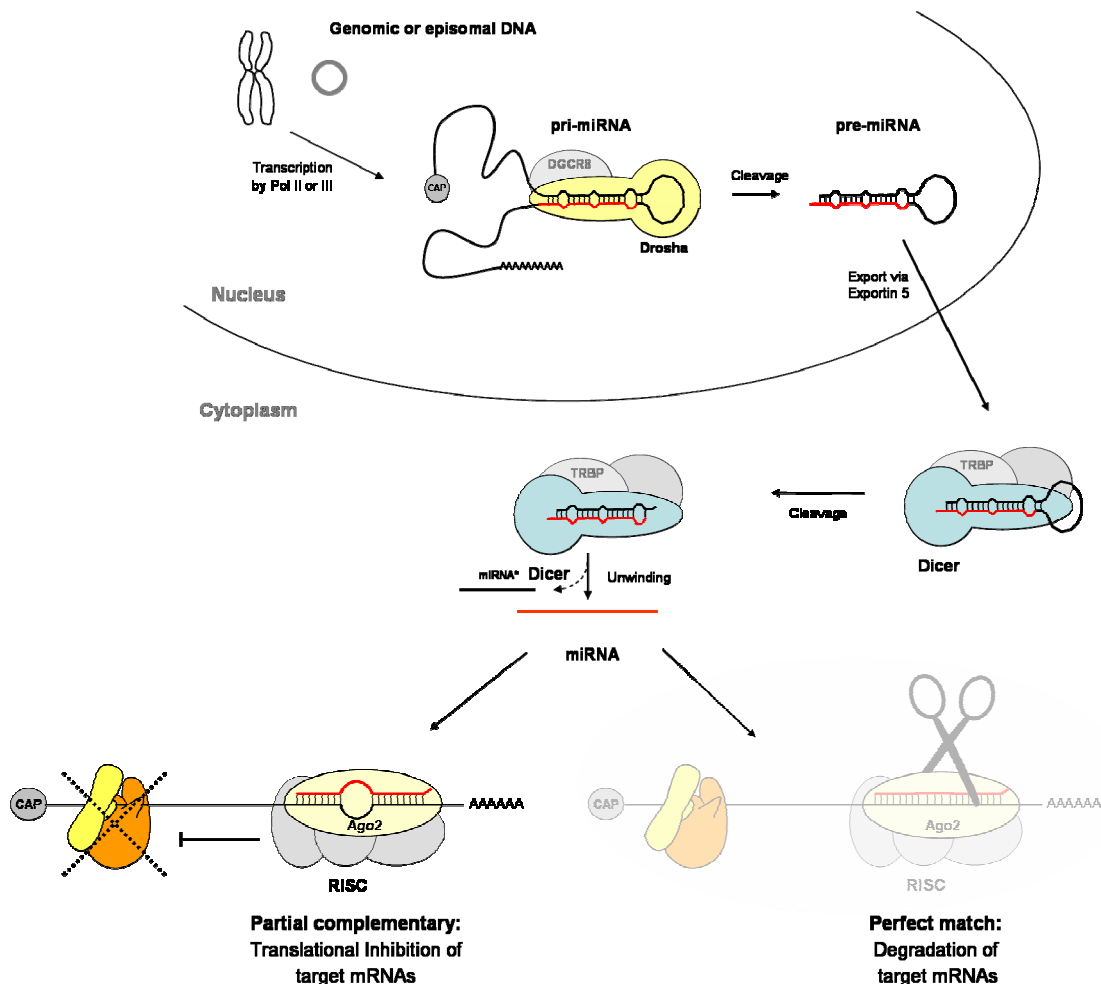


Figure 1-5 miRNA Biogenesis

Pol II or III transcribe the pri-miRNA in the nucleus, which is then recognized through its characteristic secondary structure, the stem-loop, by an RNase III like enzyme Drosha, which processes the pri into the pre-miRNA hairpin. The pre-miRNA is exported out of the nucleus via exportin 5 in a Ran-GTP dependent manner and recognized in the cytoplasm by another RNase III like enzyme Dicer, which processes the hairpin into the mature miRNA duplex. One strand is preferentially incorporated into RISC and mediates translational inhibition of target mRNAs by binding imperfectly to the 3'UTRs. (figure: Dr. Adam Grundhoff, modified)

To further process the pre-miRNA hairpin, it needs to be exported from the nucleus into the cytoplasm. This is accomplished through exportin 5 (Yi et al., 2003), initially known to be a minor transporter of tRNAs (Calado et al., 2002). Considering the high affinity to miRNAs and their abundance in the cell (Lim et al., 2003), one can assume, that miRNAs are the main cargo for exportin 5. The interaction of miRNAs the hairpin with exportin 5 is independent of RNA sequence, but has been shown to require dsRNA region of at least 16 bp and a 3' nt overhang (Bohnsack et al., 2004; Zeng and Cullen, 2004). The transfer to the cytoplasm is enabled in a Ran-GTP dependent manner. Once located in the cytoplasm the pre-miRNA hairpin is recognized by another RNase III enzyme called Dicer. Dicer has been shown previously to process dsRNAs into siRNAs and is also highly conserved among most eucaryotic organisms (Bernstein et al., 2001). It is a multidomain protein with two RIIIDs and a dsRBD (see also Drosha). At its N-terminus, Dicer has a dead-Box RNA helicase domain, a domain of unknown function 283 (DUF283 domain) and a PAZ (Piwi/Argonaute/ Zwillie) domain, which binds to the 3' end of the miRNA-hairpin. The three dimensional structure of Dicer enables the precise cleavage of pre-miRNA hairpins into mature miRNAs with an approximate size of 22 nt. In humans, Dicer interacts with TRBP (the human immunodeficiency virus transactivating response RNA-binding protein), which contains three dsRBD and stabilizes Dicer. Furthermore, TRBP is required for the recruitment of Ago2 (Argonaute 2) to the small interfering RNA (siRNA) bound by Dicer (Chendrimada et al., 2005). Argonaute proteins are important not only for miRNA stability but also for cleavage of mRNA targets.

Mature miRNAs are then incorporated into effector complexes called miRNA containing ribonucleoprotein complexes (miRNPs) or RNA-induced silencing complex (RISC). A lot of different proteins have been identified within the RISC complex (i.e. Gemin 3, -4, Fragile X mental retardation protein (FMRP) and Tudor-SN). However, the functions of most of these proteins are unknown (Sontheimer and Carthew, 2005). The minimal functional RISC consists of a small RNA and Ago protein. In most cases only one strand of a miRNA duplex is incorporated into the RISC whereas the other strand is degraded. Studies by Schwarz and Khvorova (Boese et al., 2005; Schwarz et al., 2003) showed that the thermodynamic stability of the two ends of siRNA duplexes determines which one is selected. The strand with the higher stability relative to the other at the 5' end is preferentially degraded. This seems also to be true for miRNAs (Tomari and Zamore, 2005).

1.3.3. miRNA Function

Within the RISC the miRNAs guide the complex to their mRNA target. If a miRNA is like a siRNA perfectly complementary to the mRNA, a single phosphodiester bond in the mRNA is cleaved between nt 10 and 11 away from the miRNA 5' end (Elbashir et al., 2001). This mode of action occurs predominantly in plants. The so called "slicer" activity is enabled by the Argonaute proteins, which are highly conserved and possess PAZ and P-element induced wimpy testis (PIWI) domains (Carmell et al., 2002). With an oligonucleotide-binding fold of the PAZ domain, Ago can bind the 3' end of

small RNAs (Lingel and Sattler, 2005). The PIWI domain is a structural homolog of the DNA-guided RNA endonuclease RNaseH (Song et al., 2004) and contains a conserved binding pocket for the 5' phosphate of small RNAs (Ma et al., 2005; Parker et al., 2005). From these findings a model arises, in which the small RNA is embedded between the PAZ and PIWI domain whereby the mRNA is positioned in close proximity to the catalytic center (Pillai, 2005). Several publications have shown that even though all Ago proteins are able to bind small RNAs, only Ago 2 can accomplish mRNA cleavage (Liu et al., 2004; Meister et al., 2004). Despite the fact that mammalian miRNAs are believed to inhibit translation by binding imperfectly to their target mRNAs, one example, the human miR196, which is nearly perfectly complementary to its target mRNA Hoxb8, represents the possibility of direct mRNA cleavage and degradation (Yekta et al., 2004).

It has been shown that the Ago proteins co-localize to discrete foci called cytoplasmic processing bodies (PBs). Interestingly, these PBs accumulate proteins necessary for bulk mRNA degradation like the decapping enzymes (e.g. Dcp1/2) and exoribonucleases (e.g. Xrn1) (Bashkirov et al., 1997; Parker and Song, 2004). Furthermore the PBs lack any ribosomes and translation initiation factors (Teixeira et al., 2005). Since Ago bound miRNAs and siRNAs are targeted to the PBs it seems likely, that PBs play a crucial role in mRNA repression (Liu et al., 2005; Sen and Blau, 2005). This is underlined by the fact, that knockdown of GW182 (binds Ago and is the major component of PBs) leads to a reduction in PB formation and inhibition of miRNA initiated translation repression (Jakymiw et al., 2005; Liu et al., 2005). Another important issue is how miRNAs might repress translation initiation.

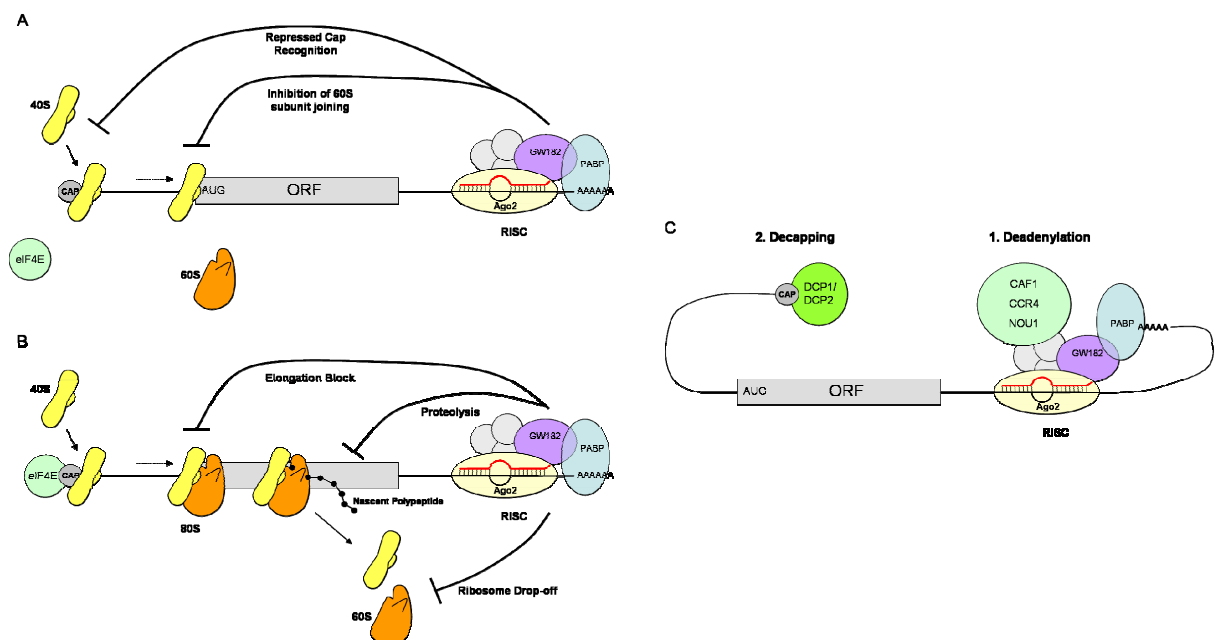


Figure 1-6 Mechanisms of miRNA Target Regulation

Translational repression of miRNA binding may occur by interfering with eIF4F cap recognition, by preventing 80S ribosomal complex formation termed as initiation block (A) or by inhibiting ribosome elongation, ribosome-drop off or by enhanced proteolysis of nascent polypeptides termed post-initiation block (B). Interaction of miRISC with a deadenylase complex enables deadenylation and decapping of mRNA targets (C). (figure: after (Fabian et al., 2010), modified)

The different possible mechanisms of miRNA mRNA repression are under investigation. One possibility is an initiation block, where miRISC (RISC with incorporated miRNA) is interfering with eukaryotic translation initiation factor 4F (eIF4F)-cap recognition and 40S small ribosomal subunit recruitment. In addition, the complex might antagonize 60S subunit joining and thereby inhibiting 80S ribosomal complex formation. GW182 has also been reported to interact with the poly(A)-binding protein (PABP) and might interfere with the loop-formation mediated by eIF4F and PABP and thereby inhibit translation initiation. A block at the post initiation step is also a possible mechanism, by inhibition of ribosome elongation, ribosome drop-off or by facilitating proteolysis of nascent polypeptides. miRNA mediated decay of target mRNAs is facilitated by the binding of miRISC to the deadenylase complex triggering deadenylation of the poly(A) tail. After deadenylation the 5'cap is removed via the DCP1-DCP2 complex. (see (Fabian et al., 2010) and references therein).

The inhibition of protein synthesis and accumulation through miRNAs has been shown in various organisms ranging from *C.elegans* to flies and humans (Brennecke and Cohen, 2003; Reinhart et al., 2000; Wightman et al., 1993; Zeng et al., 2003).

Other than in plants, where the miRNA mostly binds to a single perfect complementary site in the 3'UTR of the corresponding mRNA, the binding of animal miRNAs to their mRNA target is mostly imperfect and may occur at multiple sites in the 3'UTR (Kloosterman et al., 2004). The most important part of a miRNA is the 5'end containing the seed region, which ranges from nucleotide no. 2-8, and is the minimal requirement of mRNA target binding (Tomari and Zamore, 2005).

1.3.4. Viral miRNAs

1.3.4.1. Overview

The first viral miRNAs were identified in 2005 by Pfeffer and colleagues (Pfeffer et al., 2005b). Using a cloning approach they could identify five miRNAs encoded by EBV. The same year, further viral miRNAs were identified for KSHV and EBV.

At present, different methods are used to identify miRNAs. First, different algorithms can predict secondary structures of RNA (e.g. RNA Fold) and thereby hairpin structures, characteristics of pre-miRNAs. Second, small RNA cloning and microarray analysis of the predicted hairpins can give insights into mature miRNA sequences. Finally, small northern blot analysis can confirm the expression of mature miRNAs.

To date, 140 viral miRNAs are known, most of them encoded by members of the herpesviral family. Polyomaviruses and Adenoviruses also encode for a small set of miRNAs. miRNA cloning from cells infected with other viruses like human immunodeficiency virus type 1 (HIV-1), human T cell leukemia virus type 1 (HTLV-1) or hepatitis C virus (HCV) did not result in the identification of new miRNAs (Cai et al., 2006; Lin and Cullen, 2007; Randall et al., 2007). The ability to express miRNAs seems to be mainly restricted to dsDNA viruses. This can be explained by the fact that miRNAs

derived from single stranded RNA viruses would lead to the destruction of the viral genomic RNA (Gottwein and Cullen, 2008).

Similar to cellular miRNAs, viral miRNAs are derived from noncoding RNAs, intronic or noncoding regions or open reading frames of protein coding mRNAs. They are usually transcribed by Pol II, with the exception of murine γ -herpesvirus MHV68, which uses Pol III (Pfeffer et al., 2005b). The adenoviral miRNAs are processed from the viral associated (VA1) noncoding RNA (Aparicio et al., 2006), an inhibitor of cellular protein kinase R (PKR), a sensor of dsRNA. They are transcribed by polymerase III (Pol III) and are expressed highly after infection (Mathews and Shenk, 1991; Thimmappaya et al., 1982).

γ -herpesviral miRNAs are expressed during latency, with the exception of miRNAs of Rhesus Rhadinovirus (Cai et al., 2005; Grundhoff et al., 2006; Landgraf et al., 2007; Pfeffer et al., 2004; Samols et al., 2005; Schafer et al., 2007). In contrast, the miRNAs of α - and β -herpesviruses (human cytomegalovirus hCMV, murine cytomegalovirus mCMV, herpes simplex virus type 1 HSV-1) are associated with the productive lytic life cycle (Buck et al., 2007; Cui et al., 2006; Dolken et al., 2007; Grey et al., 2005).

1.3.5. Lymphocryptovirus miRNAs

EBV was the first virus shown to encode viral miRNAs. Pfeffer and colleagues cloned 5 viral miRNAs out of a Burkitt's lymphoma cell line latently infected with the EBV strain B95.8 (Pfeffer et al., 2004). In 2006 Grundhoff and colleagues identified 22 novel mature miRNAs from another EBV positive Burkitt's lymphoma cell line (Jijoye) by using computational prediction of pre-miRNA hairpins in combination with oligonucleotide arrays and northern blotting for confirmation (Grundhoff et al., 2006). At the same time these novel miRNAs were cloned by another group from BC-1 cells (Cai et al., 2006).

These miRNAs are grouped into two clusters. The BHRF cluster, located next to the *Bam*HI fragment H rightward open reading frame 1 (BHRF1) encodes for 3 pre-miRNA hairpins, and the BART locus, where the miRNAs are located in intronic regions within the *Bam*HI-A region rightward transcript (BART) encodes for 23 pre-miRNA hairpins.

The miRNAs are differentially expressed depending on the type of latency. Several cell lines with different latency states and different EBV strains have been analyzed by several groups. In the nasopharyngeal cell line C666-1 a very high expression of the BART miRNAs was found, but no expression of BHRF miRNAs. In LCL cell lines or BL cell lines, the expression of BHRF miRNAs was detectable, whereas the BART miRNAs were only expressed at very low levels or even not expressed, although the BART locus has been shown to be intact in all cell lines (Cai et al., 2006). EBV utilizes different promoters for the expression of latency genes. In latency III, transcription of EBNA genes is driven by Cp and Wp promoters, whereas in latency I and II the transcription of EBNA1 is performed from the Qp promoter. This promoter is located between the BHRF1 and the EBNA1 ORF

and therefore cannot give rise to the BHRF miRNAs. This correlation has been nicely shown for several cell lines (Cai et al., 2006). Lytic induction of cell lines with TPA and sodium-butyrate results in the higher expression of BART miRNAs and miR-BHRF1-2. The expression level of miR-BHRF1-1 however is not elevated after lytic activation, likely due to the fact that this miRNA lies 5' to the transcription start site of the lytic BHRF1 mRNA (Cai et al., 2006). Cai and colleagues suggested that during latent infection BHRF miRNAs are processed out of the *Bam*HI H intron of the EBNA pre-mRNA rather than from BHRF1 mRNA, since BHRF1 is produced early in lytic infection. Hence, the BHRF1 mRNA can serve as pri-miRNA precursor in early lytic infection. The BART miRNAs have been shown to be produced from a large intron prior to splicing (Edwards et al., 2008).

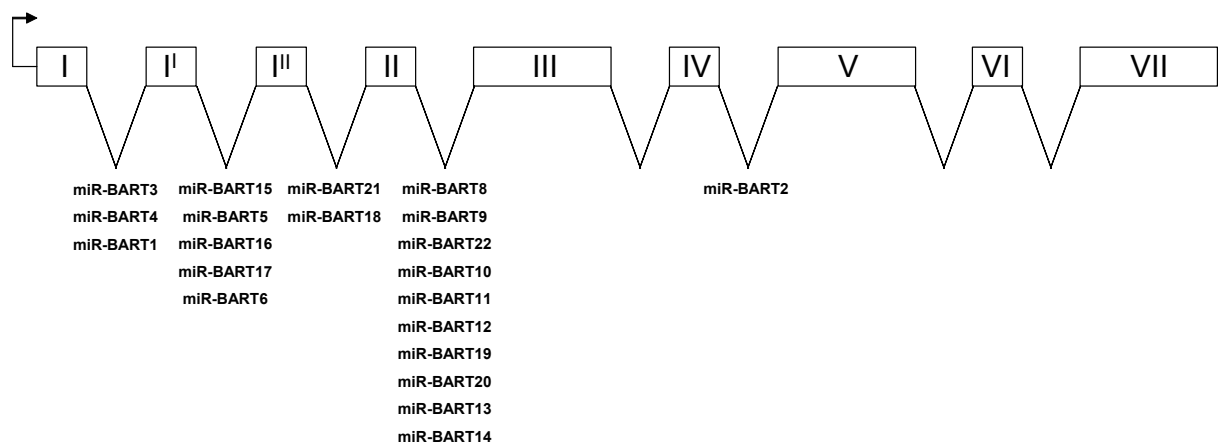


Figure 1-7 *Bam*HI-A rightward Transcripts

Exons are shown as boxes. Viral miRNAs are located within the introns and are listed under the genome.

The expression of BART RNAs has been linked to the abundance of BART miRNAs. Due to the diverse splicing possibilities, there are multiple differently sized BART RNAs detectable. The most prominent is a 4.8 kb RNA, which probably consists of exons 1,3,4,5,6 and 7 starting from the P1 promoter (Edwards et al., 2008; Smith, 2001). In addition, several other transcripts and multiple start sites have been identified (Chen et al., 2005b; de Jesus et al., 2003). Edwards and colleagues identified sequences of exon 1 in RNAs that produce the miRNAs and suggested that these are produced from the intron prior to splicing (Edwards et al., 2008). Their data can be explained by one of two possibilities. One possibility is that the intron lariat has been cleaved at the 3' end but not at the 5' end. The other option assumes, that there might be another 5' splice site, that produces the exon 1 containing intron. However, different splicing patterns might also result from different expression levels of miRNAs. In Jijoye for instance, the BART miRNA expression is relatively high in comparison to other type I or II latency expression patterns, but relatively low in contrast to type III latency in NPC. This can be explained by the fact that the transcript without exon 1a, 1b and 2 is just expressed at low levels.

In conclusion, the BART miRNAs are expressed in all types of latency (I – III) but found to be higher expressed in Nasopharyngeal Carcinoma (Latency II) as in Burkitt's lymphoma (latency I, III). In contrast the BHRF miRNAs are expressed in type I and III latency.

The next related virus to EBV is the Rhesus Lymphocryptovirus and indeed there are miRNAs found at the same loci in the genome with some of them sharing sequence homology. Three pre-miRNAs were identified at the BHRF locus of rLCV and 16 pre-miRNAs at the BART locus of rLCV. The miRNAs were cloned from rLCV positive cell lines. A closer analysis of the sequences illustrates that seven of the pre-miRNAs have a high sequence conservation including the seed region of the miRNAs (Cai et al., 2006). This raises the possibility that these miRNAs are conserved and therefore have important functions and consequences.

1.3.6. Evolutionary Conservation of miRNAs

Cellular miRNAs have been found to be located in highly conserved regions throughout the genome and harbor accordingly conserved sequences (Lewis et al., 2005).

In contrast, virally encoded miRNAs have been shown to be poorly conserved (Cai et al., 2005; Cai et al., 2006; Schafer et al., 2007). Interestingly, miRNAs encoded by relatively close related viruses (e.g. EBV and rLCV, KSHV and RRV, MDV-1 and -2) are located in the same genomic regions (Burnside et al., 2006; Cai et al., 2006; Schafer et al., 2007; Yao et al., 2007; Yao et al., 2008). Cai and colleagues could show in 2006 that 7 out of 23 and 16 miRNAs of EBV and rLCV, respectively, share also sequence homology within the mature miRNA sequences. For KSHV and RRV as well as for MDV-1 and MDV-2 only the genomic positions of miRNAs are conserved (Burnside et al., 2006; Cai et al., 2006; Schafer et al., 2007; Yao et al., 2007; Yao et al., 2008).

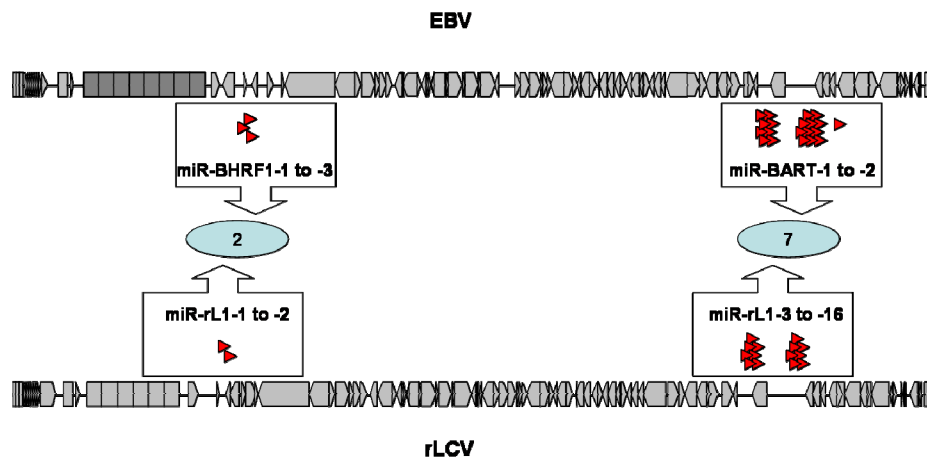


Figure 1-8 miRNA Location within EBV and rLCV Genomes

ORF of EBV and rLCV genomes are shown. The location of viral miRNAs is indicated by red triangles below or above the EBV and rLCV genomes, respectively. Between both viruses two BHRF miRNAs and 7 BART miRNAs have been shown to be conserved (figure: Dr. Adam Grundhoff, modified).

In contrast to the γ -herpesviruses, which encode for clustered miRNAs, the miRNAs encoded by β -herpesviruses are scattered throughout the genome. The identified miRNAs of hCMV and mCMV do not share location or sequence homology (Buck et al., 2007; Dolken et al., 2007; Dunn et al., 2005; Grey et al., 2005; Pfeffer et al., 2005b). The chimpanzee CMV (cCMV) might however share

conserved miRNAs with the hCMV, since several pre-miRNA hairpins are at least predicted to have sequence homology. The homology of cCMV to hCMV miRNAs is awaiting experimental validation (Grey et al., 2005; Pfeffer et al., 2005b). The question now arises if the viral miRNAs have important functions due to the lack of conservation. The relatively poor conservation can be explained by the fact, that herpesviruses in general are highly adapted to their specific host and one would expect a low evolutionary pressure to target regions of highly conserved cellular targets (Gottwein and Cullen, 2008). Contrary, viral miRNAs that target viral mRNAs may have been evolutionarily changed with the alteration in viral target mRNA sequences. Nevertheless, an important and conserved function of viral miRNAs targeting cellular mRNAs is not excluded, since miRNAs can bind at very different loci in a given 3'UTR. In this way different viral miRNAs may cooperate or might target different mRNAs, which lie in the same pathway to achieve a similar regulation.

1.3.7. Functions of miRNAs

1.3.7.1. Target Prediction

Alongside the different experimental methods to identify and confirm miRNA target mRNAs there are also a lot of computational programs to predict putative targets. In plants the complexity of prediction is relatively low in comparison to animal miRNAs, since plant miRNAs are almost perfectly complementary to their targets. To date, different algorithms are available for automated plant miRNA target prediction (Rhoades et al., 2002; Zhang, 2005). Contrarily, the target prediction for animal miRNAs is more challenging. They are for the most part partially complementary to their targets and thereby require different algorithms with more complex prediction criteria. Important features include the perfect or nearly perfect complementarity of the miRNA seed region to the 3'UTR of the mRNA target, putative binding site conservation between closely related species, multiple binding sites in one mRNA target and preferentially low propensity of the mRNA to form secondary structures (Brennecke et al., 2005; Enright et al., 2003; Kiriakidou et al., 2004; Krek et al., 2005; Lewis et al., 2005; Lewis et al., 2003; Rajewsky and Socci, 2004; Stark et al., 2003; Zhao et al., 2005). The mode of action of animal miRNAs has been proposed to fine tune gene expression for a great number of mRNAs rather than the strong regulation of only few mRNAs (Bartel, 2004). Furthermore animal miRNAs are able to act combinatorially to bind a single target and thereby reducing the mRNA translation by more than the sum of their individual effects (Doench et al., 2003). It is also possible to identify miRNA targets the other way around by analyzing one mRNA of interest and searching for a miRNA able to bind to it. Investigations have shown that diverse motifs like the GY-box, Brd-box or K-box within the 3'UTR of Notch mRNAs are mediating post-transcriptional repression and lead to the identification of different miRNAs directly regulating Notch (Lai, 2002; Lai et al., 1998; Lai and Posakony, 1997; Lai et al., 2005; Stark et al., 2003).

1.3.7.2. Functions of Cellular miRNAs

The functions of miRNAs comprise nearly all conceivable cellular mechanisms ranging from normal development and cellular homeostasis to dysregulation in proliferation, differentiation and tumorigenesis.

Various studies have investigated the miRNA expression patterns in normal and tumor tissues using multiple techniques (references). Oligonucleotide miRNA microarrays are a high throughput method to analyze all miRNAs simultaneously in multiple samples. Other approaches utilize the bead-based flow cytometric technique (Lu et al., 2005) or quantitative real time PCR for precursor or mature miRNAs (Schmittgen et al., 2004). The outcome of these experiments was, that more than half of the known human miRNAs are encoded at regions in the human genome, which are frequently affected in cancer by amplification, deletion or rearrangement. This led to the notion that miRNAs play a key role in cancer development or progression (Calin et al., 2004a; Calin et al., 2004b). Furthermore, miRNA profiles can deliver lots of information concerning healthy or altered tissue as well as differentiation states of tumors. This again underlines the importance and usefulness of miRNA expression patterns in diagnostic and prognostic applications (Hwang and Mendell, 2006). To date, many miRNAs that function as tumor suppressors or oncogenes (oncomirs) have been identified.

The first miRNAs that were identified as tumor suppressors were miR-15a and -16-1 which are located within a region that is frequently deleted in B-cell chronic lymphocytic leukemia (Calin et al., 2002). It has been shown, that the miR-16 targets BCL2, an inhibitor of cell death (Cimmino et al., 2005; Xia et al., 2008a) thereby promoting the intrinsic apoptotic pathway to take place and leading to cell death.

Table 1-1 Functions of Cellular miRNAs

Role in:	miRNA	Target	Function	Reference
Cancer	miR-21	PDCD4	enhanced invasion and metastasis	(Asangani et al., 2008)
	miR-16	BCL-2	facilitating cell death	(Cimmino et al., 2005; Xia et al., 2008a)
Autoimmunity	miR-146a	TRAF6	innate immun response	(Taganov et al., 2006)
	miR-155	MMP3	inflammatory response (Rheumatoid Arthritis)	(Pauley et al., 2008; Stanczyk et al., 2008)
Neurodegeneration	miR-107	BACE	disease acceleration (Alzheimer's Disease)	(Wang et al., 2008a)
Development	miR-203	p63	epidermal differentiation	(Hildebrand et al., 2010; Yi et al., 2008)
Cell cycle	miR-34	Cyclin E2	inhibition of inappropriate cell proliferation	(He et al., 2007)

In contrast to the tumor suppressor function of these miRNAs the miR-17 cluster of six miRNAs has oncogenic potential. This cluster is overexpressed in a variety of lymphomas and solid tumours (Ota et al., 2004). In a mouse model for Burkitt's lymphoma, where the proto oncogene c-myc is under the control of the Ig-heavy chain enhancer (see also chapter 1.2.2.3.), overexpression of five miRNAs from the miR-17 cluster resulted in disease acceleration and a high mitosis rate without extensive apoptosis (He et al., 2005).

The finding that cellular miRNAs (oncomirs) playing a role in tumorigenesis exist, raises the possibility, that viral miRNAs, encoded by tumor viruses, could also display oncogenic potential (Gottwein et al., 2007; Skalsky et al., 2007). Table 1-1 shows a list of other miRNA functions and reflects the multifaceted mode of action of human miRNAs.

1.3.7.3. Viral miRNA Targets

In 2005 Sullivan and colleagues identified one pre-miRNA hairpin in simian virus 40 (SV40) that is processed to two mature miRNAs late in infection. Because they are perfectly complementary to the early transcripts of large and small T antigen, they can facilitate their degradation of them and thereby preventing virus infected cells from destruction through cytotoxic T lymphocytes (Sullivan et al., 2005). Since then many polyomaviruses have been shown to encode one miRNA like polyomavirus simian agent 12 (SA12) (Cantalupo et al., 2005), BK and JC virus as well as murine polyomavirus. For all of them the same function could be determined and so the miRNA seems to be of great benefit for the virus and is therefore maintained.

Some putative cellular targets of viral miRNAs have been identified by microarray analyses. Thrombospondin 1 (THBS1), an antiangiogenic and antitumorigenic protein able to activate transforming growth factor (TGF- β) was identified to be target of KSHV miRNAs (Bornstein, 2001). Confirmational luciferase reporter assays showed, that 9 out of 10 miRNAs from one cluster were able to regulate THBS1. These miRNAs may be important for KSHV pathogenesis, since Kaposi's Sarcoma (KS) lesions harbor dysregulated angiogenesis (Ganem, 2006) and since KSHV infected primary effusion lymphoma (PEL) cells are less sensitive to TGF- β induced cell cycle arrest (Di Bartolo et al., 2008).

Another important issue is the cellular miRNA miR-155, which is a product of the BIC gene (Eis et al., 2005) and is transiently expressed in macrophages, T- and B-lymphocytes after inflammatory stimuli or after T- or B-cell receptor ligation. The constitutive expression of miR-155 leads to the development of B-cell lymphomas in humans and is therefore classified as an oncomir. Interestingly, different miRNAs mimick miR-155. KSHV miR-K12-11 and MDV-1 miR-M4 share the same seed region with the cellular miR-155. This is intriguing considering that KSHV is a tumor virus and that MDV-1 is the only α -herpesvirus inducing tumors. The miR-155 target BACH-1 was shown to be a target of KSHV miR-K12-11 (Skalsky et al., 2007) and other targets could at least be identified as being down-regulated in microarrays using BJAB-cells expressing miR-K12-11 (Gottwein et al., 2007). In contrast, there is no miR-155 orthologue in EBV miRNAs, but EBV infection was shown to up-regulate miR-155. EBV miR-BART5 and rLCV miR-rL1-8 do share a common seed region with cellular miR-18a and -18b. These miRNAs are encoded by the miR17-92 cluster and have been shown to have oncomir functions (He et al., 2005). An overlap of mRNA targets between these miRNAs has to be confirmed.

1.3.7.4. EBV miRNA Targets

Very few targets of EBV miRNAs are known so far, but different studies investigated viral as well as cellular mRNA targets. One viral target of BART miRNAs is the Latent Membrane Protein 1 (LMP-1). It is strongly expressed in EBV-positive HD and appears to be important for NPC development although it is not found in all NPC tumors. One major property of LMP-1 is to constitutively mimick the activated tumor necrosis factor (TNF) receptor (Fields et al., 2007)(Kieff and Rickinson 2007). Three EBV miRNAs are capable of down-modulating LMP-1 as well as the LMP-1 induced NF-kB signaling in NPC cell lines, whereby the sensitivity to cisplatin decreases (Lo et al., 2007).

EBV miRNAs also target cellular transcripts, that are important for survival, apoptosis and immune surveillance. Choy and colleagues found that the p53 up-regulated modulator of apoptosis (PUMA) is regulated through miR BART5. The expression of PUMA was found to be significantly decreased in about 60% of NPC tissues, whereas at the same time BART5 is highly expressed in NPC. Depletion of miR-BART5 or induced expression of PUMA leads to a higher susceptibility of NPC cells to apoptotic stimuli. The direct regulation of the PUMA 3'UTR through miR-BART-5 was verified using reporter luciferase assays. Thus, it has been suggested that miR-BART-5 facilitates the establishment of latent infection by promoting host cell survival (Choy et al., 2008). All identified targets of EBV are listed in table 1-2.

Table 1-2 Targets of EBV-encoded miRNAs

Target	miRNA	Function	Reference
BALF5	miR-BART2	switch from lytic to latent	(Barth et al., 2008; Furnari et al., 1992)
CXCL-11	miR-BHRF1-3	possible role in tumorigenesis	(Hensbergen et al., 2005; Xia et al., 2008b)
MICB	miR-BART2	prevents activation of NK cells upon infection	(Nachmani et al., 2009; Raulet, 2003)
TOMM22	miR-BART16	prevention of Bax induced apoptosis	(Dolken et al., 2010; Saeki et al., 2000; Yano et al., 2000)
IPO7	miR-BART3	role in innate immunity	(Dolken et al., 2010; Gorlich et al., 1997; Yang et al., 2009)
LMP-2A	miR-BART22	Undergoing immune surveillance	(Lung et al., 2009)
Dicer	miR-BART6		(lizasa et al., 2010)

Considering the fact, that EBV encodes for a lot more miRNAs compared to the amount of EBV miRNAs already investigated to have functions, a lot of other functions have to be investigated. Additionally the targets investigated so far are all dependent on one single miRNA. Due to the fact, that all EBV miRNAs are expressed simultaneously, it seems likely that several viral miRNAs are capable targeting concordantly the same genes to be more efficient. Furthermore, different genes of one pathway might be regulated by different viral miRNAs to increase regulation.

1.4. Objective

More than 90% of adults are estimated to be infected with EBV. EBV is not only the aetiologic agent of Infectious mononucleosis, but is also associated with different kinds of tumors like Burkitt's lymphoma or Nasopharyngeal carcinoma. The precise contribution of EBV to tumorigenesis is however, only partially understood. The virus persists as a benign latent infection throughout the host's lifetime. The gene expression in latency is strictly limited to very few genes. Apart from that, all viral miRNAs are expressed in all types of latency. Since miRNAs require minimal coding capacity and are non-immunogenic, they are a useful tool for herpesviruses to modulate host cell gene expression. Thus, an important function in herpesviral life cycle was proposed. When this work was started the miRNA registry lists 146 viral miRNAs, the vast majority of which are encoded by herpesviruses. There was little evidence of evolutionary conservation, except for seven miRNA hairpins shared between Epstein-Barr virus and the closely related rhesus lymphocryptovirus (rLCV). Assuming that viral miRNAs have important functions, it was hypothesized that more conserved miRNAs may exist. Therefore, the conservation state of all known and predicted γ -herpesvirus encoded miRNAs was to be investigated.

In the beginning of this work nearly nothing was known about EBV-encoded miRNA targets and functions. Due to the fact that all EBV miRNAs are expressed simultaneously, it seems likely that viral miRNAs cooperate to achieve their function. To elucidate EBV miRNA functions, the task was to generate different vector systems that allow simultaneous expression of all EBV-encoded miRNAs and to establish different biological systems and techniques for the identification of miRNA targets.

Both analyses, the global identification of viral miRNAs and the target identification should lead to a better understanding of viral miRNA function and EBV pathogenesis. Furthermore the identification of direct miRNA targets or miRNA dependent phenotypic effects might shed light on EBV associated tumorigenesis.

2. Materials

2.1. Chemicals and Expendable Materials

2.1.1. Chemicals

All chemicals were purchased from Sigma and Roth. The safety related data are listed in the appendix.

2.1.2. Expendables

Expendables were all purchased from 5 Prime, BD Biosciences, Becton-Dickson, Braun, Costar, Falcon, Greiner, Kimberly Clark, Millipore, Nunc, Sarstedt and Swann-Morton.

2.2. Bacteria and Cell Lines

2.2.1. Bacteria

Table 2-1 Bacterial Strain

Bacterial Strain	Genotype	Reference
E. coli DH5 α	F ⁻ , dcoR, recA1, endA1, hsdR17 (rk ⁻ , mk ⁺), supE44 1-, thi-1, gyr A96, relA1	Invitrogen

Table 2-2 Cell Lines

Cell line	Cell type	Reference
211-98	rLCV positive cell line from Rhesus macaques, suspension	Rivaillier 2004
260-98	rLCV positive cell line from Rhesus macaques, suspension	Rivaillier 2004
Beas-2b	Epithelial cell line, adherent	ATCC-CRL-9609
BJAB	EBV negative Burkitt's lymphoma cell line, suspension	Menezes 1975
C666-1	EBV positive Burkitt's lymphoma cell line, suspension	Cheung 1999
HEK-293	Epithelial cell line, adherent	Louis et al. 1997
HEK 293T	Epithelial cell line, adherent	ATCC-CRL-11268
HNEpC	Human nasal epithelial primary cells, adherent	PromoCell C-12620
HUVEC	Human Umbilical Vein Endothelial Cells, adherent	PromoCell C-22010
Jijoye	EBV positive Burkitt's lymphoma cell line, suspension	Adlinder 1985
Raji	EBV positive Burkitt's lymphoma cell line, suspension	Pulvertaft 1965
SLK	endothelial KS tumor cell line, adherent	Herndier, 1994

2.3. Enzymes

Restriction enzymes were purchased from NEB and Fermentas. All other enzymes were purchased from Invitrogen, NEB or Fermentas.

2.4. Oligonucleotides

All primers and probes were purchased from Invitrogen or Eurogentec.

2.4.1. Primers

Table 2-3 General Cloning Primers

Name	Sequence
5_EBV_C12_BA04	TACGCGGCCGCTAGAAGATCTCCTGATATCCC
EBV_C12_rev2	CTCTAGAACGGGAATATCGTAGCCTCC
EBV_C13_for1	TAGCGCTAGCGAGCAGCAGGCTTGTTCATGC
EBV_C13_rev1	TAGCTCTAGAGAAGGCTGGCAAAGATCCCC
pEYFP_for_1	TAGCAAGCTTGCCACCATGGTGTGAGCAAGG
pEYFP_rev_1	TAGCGGATCCTTACTTGTACAGCTCGTCC
5-pIRES2-HindIII	GATAAAGCTTATCCGCCCTCTCCCTC
3-pIRES2-HindIII	GATAAAGCTTGGTTGTGGCCATATTATC
5_BART_2	AGCGGATCCTCTCCGTTGCATTGACG
3_BART_2	CAAGAATTCTAGGAGAAGGAGCCTCGC
5_BART_5	CTAGGATCCGACACAAGGACTGCCAGCC
3_BART_5	CAAGAATTCTAAACAAGAGCACACACCC
5_BART_7	AGCGGATCCGCGAGCTACTTGACCTTTG
3_BART_7	CAAGAATTCATTGCACCGGCCAGTCAG
5_BART_10	AGCGGATCCAGGCGGTTGTACAGGTG
3_BART_10	CAAGAATTCCAAAGTGTCTGACCCAAC
5_BART_11	AGCGGATCCTGGAGTTGGCTGTGGTGC
3_BART_11	CAAGAATTCGCCAAAGGAGACACAAG
5_BART_13	AGCGGATCCTGGCATGAAGGCACAGCC
3_BART_13	CAAGAATTCATCGGCAGCGTAGGGTAC
5_BART_17	AGCGGATCCGTGTGTGCTCTTGTTTAAT
3_BART_17	TAGGAATTCAAGCCTATGGATTGGACC
5_BART_19	AGCGGATCCTACACGGTGCCAATAACC
3_BART_19	TAGGAATTCGTACGCAGGAATGAAGAC
5_BART_20	TAGGGATCCTTAAACATGTTTTGTTTGC
3_BART_20	CAAGAATTCACGAGCCACGAGCCGGTT
5_rL1-8	ACGGGATCCAAGGTCAGTGGGCTGTTTC
3_rL1-8	ACGGAATTC AAGGTCACACACCCACGC
5_rL1-20	AGCGGATCCTTCCCAGCCCTTCGATGC
3_rL1-20	CAAGAATTCAGATAAGAGAGCCCTCCC
JMHV_miR_PvuI_rev	CATCGATCGCGGGGTCTAACC
JMHV_miR_Not_for	CATGCGGCCGCCACATGGGATGACAACC

Table 2-4 Small RNA Cloning Linker Primer

Name	Sequence
5'-Linker	TGTTACGGCACCTCAGTTGATCAGAGCCCArGrGrG (purchased from Eurogentec)
3'-Linker	P-rUrUrUJCTGTAGGCACCATCAATGTCAAGTCGGAAAddC (purchased from Eurogentec)
5'-Linker_for_outer	TGTTACGGCACCTCAGTTG
5'-Linker_for_inner	AGTTGATCAGAGCCCAGG
3'-Linker_rev_outer	GTTCCGACTTGACATTG
3'-Linker_rev_inner	CATTGATGGTGCCTACAGAA

Table 2-5 Small RNA Cloning Primer rLCV

Name	Sequence
3p_MD274_rev	TTATTATGATGGAGAGG
3p_MD278_rev	AAGATGATGGGGAGGG
5p_MD1496_rev	AAGGTCACACACCCACG
5p_MD1502_rev	AATCAGGGTGCCGCTGTGAACCACACTAC
3p_MD1502_rev	CACTAAGGGAAGTTA
3p_MD1505_rev	AATTAGAATTGTGAGAAG
5p_MD1517_rev	GGATCCGGCGGACCAGG
3p_MD1517_rev	TTCCAGGTGCACCCGAC
3p_MD1551_rev	AATCAGGGTGCCATAATCGTGGGGATGAAA

Materials

5p_MD1555_rev	TCTTAGGTGCCAGCAC
3p_MD1555_rev	AATACTCTCCAGTGCAG
5p_MD1564_rev	CTGTATTGGAAATGAG
5p_MD1564_rev_2	TATTGCAAATGAGAAC
3p_MD1564_rev	GTATCAAGTCCTATCTC
3p_MD1564_rev_2	TCAAGTCCTATCTCCGA
3p_MD1579_rev	TGCTAAACCCGGAGAAT
3p_MD1583_rev	GCAACCACCTCCATGG
MD_3p_MR1588_rev	ACTACTAGACCCATTAA
3p_MD1593_rev	AATTCTAGAAGGCGGATAC
3p_MD1594_rev	ACTGCAGTCCCAAGCAAAC
3p_MD1601_rev	AATCAGGGTGCCGACAGCCGACCTTCGAA
5p_MD1604_rev	AATCAGGGTGCCGTTACGCGGTTCGGCGTA
3p_MD1604_rev	AATCAGGGTGCCCGGCTGCTTACGACGAC
5p_MD1610_rev	TGTAAAGCGGCAGTAGT
3p_MD1610_rev	ACGCCTACTACTGCTCGC
5p_MD1675_rev	ACGCAAGGGCAAATGAAG

Table 2-6 Small RNA Cloning Primer JMHV

Name	Sequence
cl_MR1259_5p_rev	GGAACGCACGTTAACTGCTC
cl_MR1259_3p_rev	CCTAGAAAGCAATTAACG
cl_MR1260_5p_rev	TACGATGTGCACACCTTTC
cl_MR1260_3p_rev	AATCGCAAAGGTTCGTAC
cl_MR1261_5p_rev	ACAATAGCGTTGTTGGTG
cl_MR1261_5p_rev_2	ATAGCGTTGTTGGTGACC
cl_MR1261_5p_rev_3	AATAGCGTTGTTGGTGAC
cl_MR1261_3p_rev	TACGATCACGAGCAACAC
cl_MR1265_5p_rev	CGGGCACGTGTCTTTGG
cl_MR1265_5p_rev_3	GGCACGTGTCTTTGGGTTTC
cl_MR1265_3p_rev	AAACGGAATCCAAAGAAC
cl_MR1267_5p_rev	GAGAATGTGTCTTTGGG
cl_MR1267_3p_rev	AAGCGGACCCAAAAAACC
cl_MR1270_5p_rev	AAGTAGCACACCAACTG
cl_MR1270_5p_rev_2	AAGTAGCACACCAACTGCAA
cl_MR1270_3p_rev	ACTAACTGCTGTGAGGTT
cl_MR1273_5p_rev	GGGAACGCGCGCTGACCAC
cl_MR1273_5p_rev_2	AACACGGGAACGCGCGCTG
cl_MR1273_3p_rev	TCGGGAGGACGGTTAACG
cl_MR1276_5p_rev	GTACCCAAGGCTTTCC
cl_MR1276_3p_rev	AAAAACAAAAAACCGT
cl_MR1281_5p_rev	CAACAGGGAGCACGAC
cl_MR1281_3p_rev	CAGTGTCCGTCGCAGACC
cl_MR1282_5p_rev	CGGAAATTGTCTTTAGTTC
cl_MR1282_3p_rev	TAGGGAATCTAAAAACGA
cl_MR1291_5p_rev	TACACGAATACGGGACG
cl_MR1291_3p_rev	CAACCGTGCAGCGCCGTA
cl_MR1291_3p_rev2	GCAACCGTGCAGCGCCG
cl_MR1295_5p_rev	ATGTGAACGGTCTATTC
cl_MR1295_3p_rev	TTCCCCAAACAAGGTAAAG
cl_MR1297_5p_rev	TATAATTTCAACCCTGTT
cl_MR1297_3p_rev	GATCCCCCTAACAAGATG
cl_MR1312_5p_rev	GCAGCGGTGTCAGCGGA
cl_MR1312_3p_rev	GTGATATGTTCTGATGAC
cl_MR1315_5p_rev	CGGCCGGCCAAAGGTGCG
cl_MR1315_3p_rev	TGACCGCATCCTCGGTGG
cl_MR1317_5p_rev	CAGGAAAGTGTGGCAAG
cl_MR1317_3p_rev	GGATGTCTTGAGCACT

Table 2-7 Luciferase Assay Primers

Name	Sequence
5_BA5_Luc_BanI	ACCTTGGGCACCTCATCTGATGCTCTGTG
3_BA5_Luc_BanI	ACCTTGGGTGCCTTCCAGCGATACGTCCG
5_Luc_CARD6	TAGACTAGTAGAGCTAACTCCAGAGATC
3_Luc_CARD6	TCGGCTAGCTGCCAAATGATTAATTTTATTGG
5_Luc_CASP3	TAGACTAGTAGAAATGGTTGGTTGGTG
3_Luc_CASP3	TAGAAGCTTAATTGTCACATAGAAACACAC
5_Luc_ELP4	TAGACTAGTGCCGCTCAAGCAAATGG
3_Luc_ELP4	TAGAAGCTTGACATTTTTTGGCGTTTATT
5_Luc_INPPL1	TAG-ACTAGT-TAGCGGAGGCACCACGAAG
3_Luc_INPPL1	TAG-AAGCTT-TTATTGAAGACATCACGCC
5_Luc_MX1	TAGACTAGTCCACACTCTGTCCAGCCC
3_Luc_MX1	TAGAAGCTTCTGCTAGAAATGAGTTTATTAC
5_Luc_NME3	TAGACTAGTCCCGGCAGATGCGCGTC
3_Luc_NME3	TAGAAGCTTGCCCTGTTCTGGGCCCAAATC
5_Luc_NVL	TAGACTAGTTGTCTCCAGCAGCCGGC
3_Luc_NVL	TCGAAGCTTATAGTCAAATAGTTCAAAG
5_Luc_PDCD2	TAGACTAGTAGGCATCTTAAAGCCTTG
3_Luc_PDCD2	TAGAAGCTTGTGGATGTACCAAATTT
PUMA_for_RHes_Hum_2	ACAAGCTTTCTCTGCACCATGTAGC
PUMA_rev_RHes_Hum_3	ACGAAGCTTCAGACTCCTCCCTCTTCC
5_Luc_TNKS2	TAG-ACTAGT-AACTAATCCACTGAACC
3_Luc_TNKS2	TAG-AAGCTT-AATGAGGGTATGGAATGTG
5_Luc_TCF4	TAGACTAGTAAGGGTCCAAGTTGCCAC
3_Luc_TCF4	TAGAAGCTTGCCGTTCACTCTCTGGGC
5_Luc_XPO1	TAGACTAGTAATCCAAATTCATGCTGT
3_Luc_XPO1	TAGGCTAGCAAATGTAAACCAAGTTTATTTTGC

Table 2-8 Standard Sequencing Primers

Name	Sequence
M13 for	TGTAACGACGCGCCAGT
M13 rev	GTTTTCCCAGTCACGAC
T7	TAATACGACTCACTATAGGG
SP6	ATTTAGGTGACACTATAG
pMIR-Report fw	TCCTCATAAAGGCCAAGAAG
pMIR-Report rev	TTCCCAGTCACGACGTTG
seq-GFP-3-fw	ATCACATGGTCTCTGCTGG
JMHV_miR_seq_1	TAACTCGACTCGGGTCCG
JMHV_miR_seq_2	TGGTTCTCCAGCCTGGTATCC
JMHV_miR_seq_3	TAGAACCTGTGCCACCC
JMHV_miR_seq_3b	TTGTCTTTAGTTCCCTACAGC
JMHV_miR_seq_4	TCAATGAGCAGTTAGTCTGTG
JMHV_miR_seq_5	AGTTAGTTGCACAGATGCC

Table 2-9 Real-time Primer

Name	Sequence
SL BA_5 TM	GTCGTATCCAGTGCAGGGTCCGAGGTATTTCGCACTGGATACGACCGATGG
SL BH1_3 TM	CTCGTATCCAGTGCAGGGTCCGAGGTATTTCGCACTGGATACGAGTGTGCT
SL BH1_3 TM 2	TCGTATCCAGTGCAGGGTCCGAGGTATTTCGCACTGGATACGAGTGTGC
SL miR21	GTCGTATCCAGTGCAGGGTCCGAGGTATTTCGCACTGGATACGACTCAACA
BA_5 SL for	cgaCAAGGTGAATATAGCTGC
BH1_3 SL for	cgaTAACGGGAAGTGTGTA
miR21 SL for	CGA TAG CTT ATC AGA CTG A
Uni-rev	GTG CAG GGt CCG AGG T
GAPDH TM rev	TGGTGGTGAAGACGCCAGTG
GAPDH TM for	AATCCCATCACCATCTTCCAGG
TM probe BA_5	(Vic TM)TGGATACGACCGATGGGC (MGB)
TM probe BH1_3	(Vic TM)TGGATACGAGTGTGCTT (MGB)
TM probe miR21	(6-Fam TM)TGGATACGACTCAACATC (MGB)
TM probe GAPDH	(ROX TM)GTGGCGCTGAGTACGTCTGGAGTC (MGB)

2.4.2. Probes

Table 2-10 EBV miRNA Probes

Name	Sequence
pBH_1-3	GTGTGCTTACACACTTCCCGTTA
pBA_2	GCAAGGGCGAATGCAGAAAATA
pBA_5	CGATGGGCAGCTATATTCACCTTG
pBA_7	CCCTGGACACTGGACTATGATG
pBA_10	ACAGCCAACCTCCATGGTTATGT
pBA_11-5p	ACAAC TAGCGCACCAAAC TGT C
pBA_11-3p	GGCAGTCAGCCTGGTGTGCGT
pBA_13	TCAGCCGTCCTGGCAAGTTACA
pBA_17-5p	CCTTGTATGCCTGCGTCCCTTT
pBA_17-3p	TAAGGGGACACCAGGCATACAA
pBA_19	GCATTCCCAAGCAAACAAAACA
pBA_20-5p	GGAATGAAGACATGCCTGCTAC
pBA_20-3p	GGTAACAGGCTGTGCCTTCATG
EBV_MD1411_5p	CGACGACCCAGGGCACAGATAGACACGTGG
EBV_MD1411_3p	ACCCACGCAAGGTCTGTACCGTAGACTGCC
EBV_MD1504_5p	GTGTTAGTTGCCTTCACTAGTGAATAC
EBV_MD1504_3p	CGGATAAACACCAGTGGGCACAAC TAGCAC
EBV_MD1511_5p	TGCCTAACCTCGTGATTTGGGACCCCAAC
EBV_MD1511_3p	TCTGGCTTAAGGGTCCCTCCTAAAGAGCCA
EBV_MD1524_5p	TGGTTCAACTCCAGGGTCTAGCACCTGTGA
EBV_MD1524_3p	TCACAAC TACTAGACCATGACTTTGTAAACC
EBV_MD1565_5p	AAATGACAGTCTACAAC TCGGGCACAA
EBV_MD1565_3p	TGCTGCGCCCGCGCTGTGGACCGCCCACT
EBV_MD1566_5p	CCAGGAGGCGGCGTGCGACCAATGGGTGCT
EBV_MD1566_3p	CCATCTCCAGGGCGGCACGCCCTCTCTCTG
EBV_MD1572_5p	CAGGTGGACAGGGCCGAGGAGGGCTGGGTG
EBV_MD1572_3p	CACGAGACGCAGCCTCCGGGTCCGTGCACC
EBV_MD1585_5p	AGCCGGCTGCTACCTACTGGCGGCAGTCCT
EBV_MD1585_3p	GGAAGGCCCCACCAAAGGCATGCACACGGC
EBV_MD1602_5p	TGCAGACACGCTGCCGGCGCGTGCTCGACC
EBV_MD1602_3p	GGGGTGGAGCTCGTCCGGAAGACGGCCTG

Table 2-11 rLCV miRNA Probes

Name	Sequence
LCV_MD274_5p	AGTGCACTTCCCCGCTGTCCATCAGAACAC
LCV_MD274_3p	TGTTATTATGATGGAGAGGGCGAAGCACCG
LCV_MD278_5p	AAGATACGCCGCCCAATCATCTAAACCC
LCV_MD278_3p	GGTGTCAAGATGATGGGAGGGGCTAACTT
LCV_MD1496_B16_5p	CAAGGTCACACACCCACGCTATCTA
LCV_MD1496_B16_3p	GGAAAGCAGACAGGGGGTGGTGTCTTTGT
LCV_MD1502_5p	AACTGCTGTGAACCACACTACCCTTTAAGG
LCV_MD1502_3p	GTTACACTAAGGGAAGTTAGATCCACAGGTT
LCV_MD1505_5p	AGAGCCCTCCCCCAATCAAAACTGCAC
LCV_MD1505_3p	TGTGAAATTAGAATTGTGAGAAGAGGCCTC
LCV_MD1517_5p	ATCCGGCGGACCAGGCCACCCGGACCGGA
LCV_MD1517_3p	CCTGCCTTCAGGTGCACCGGACCGGCGGA
LCV_MD1522_5p	GGACACACCTGCAGGTAACCCAACGGGCTA
LCV_MD1522_3p	CGTTAATCCCAATAGCATCACCTCCAGGTA
LCV_MD1529_5p	TCCTAAGGGCGGAGCACATGGATTAGCGGG
LCV_MD1529_3p	CGCCCTCTGGGTCCACGCTTCCGCCCTGG
LCV_MD1551_5p	CCAAAATCCACCGTTTTCCCCCACGAAT
LCV_MD1551_3p	AATCGTGGGGATGAAACGGTGAATAATA
LCV_MD1555_5p_2	CTTAGGTGCCAGCACTAGTGAATACCCAGC
LCV_MD1555_3p_2	AACCGAATACTCTCCAGTGCAGACAAC TAA
LCV_MD_MR1588_5p	TGTTTCCAATTTAGGGTCTAGCACCAGCAG
LCV_MD_MR1588_3p	ACTGCAACTACTAGACCCATTAATTGTCA
LCV_MD1564_B18_5p	AACTGTATTGGAAATGAGAACCTTGAG
LCV_MD1564_B18_3p	AACTGGTATCAAGTCTATCTCCGATACAA

LCV_MD1579_5p	CTGCTTCGAATCCCAGGTGTAGCGCCAGCG
LCV_MD1579_3p	GCGCAACTGCTAAACCCGGAGAATCGTAGC
LCV_MD1583_B10_5p	TGTGGACAGAACCAAGGAGCGGCTCCGGG
LCV_MD1583_B10_3p	CCGCAACCACCTCCATGGTTATGTGC
LCV_MD1593_5p	CAGCTGAAAGCAACGCCTTCCAAGACAGAC
LCV_MD1593_3p	AAGCCAATTCTAGAAGGCGATACTTTCCTC
LCV_MD1594_B19_5p	ACTGCAGTCCCAAGCAAACAAAACAC
LCV_MD1594_B19_3p	ATGTTTTGTCTGCTGGGACTGGTTTTAGGA
LCV_MD1601_5p	TGTTTCGTACCTCAAAGGACCGGTGCC
LCV_MD1601_3p	CTGACAGCCGACCTTCGAAAACGAAAC
LCV_MD1604_5p	GTTACGCGGTGCGCGTAAGCGACCGGGCAT
LCV_MD1604_3p	TCGCCCGGCTGCTTACGACGACACGCCTAA
LCV_MD1610_B14_5p	ATGTAAGCGGCAGTAGTAAGTTACA
LCV_MD1610_B14_3p	AGACGCCTACTACTGCTCGCATTAC
LCV_MD1675_B2_5p	ACGCAAGGGCAAATGAAGACAATGGT
LCV_MD1675_B2_3p	ACAGGCTATCCCCCATTTGCTCTTTGCA

Table 2-12 JMHV miRNA Probes

Name	Sequence
MR1255_5p	CCAGTCTGCGACTCATTATGGACAACCTTC
MR1255_3p	GCGGGTGTTCACACTAGAGACCTACACCT
MR1259_5p	GGAACGCACGTTAACTGCTCTCCACGGATCGCA
MR1259_3p	GATAGGATCCCTAGAAAGCAATTAACGTGCG
MR1260_5p	TACGATGTGCACACCTTCCGCGGTTACCGCC
MR1260_3p	TGGCGGTAAATCGCAAAAGTCTGTACATCG
MR1261_5p	ACAATAGCGTTGTTGGTGACCGCAAACGCAAATC
MR1261_3p	GCGGTTCTACGATCAGGACCAACACTATTGC
MR1265_5p	CGGGCACGTGCTTTGGGTTCCGGGGCGGTTACG
MR1265_3p	CATCGCAACGAAACGGAATCCAAGAACACGCC
MR1267_5p	GGAGAATGTGTCTTTGGGTCCCTTCCACGTGC
MR1267_3p	CGACATAACAAGCGGACCCAAAAAACACCCC
MR1270_5p	AAGTAGCACCAACTGCAATTAATTGCACTAA
MR1270_3p	ATCTGTGCAACTAACTGCTGTGACGTTACTACTC
MR1272_5p	CATAACCACACAAGTTTTTTAAACACAAATGC
MR1272_3p	ATTATAAACAAAAACATCGCAGTTAAATTG
MR1273_5p	GGGAACGCGCGCTGACCACCTCCCCAAATCACAAC
MR1273_3p	GCAGTAATCTCGGGAGGACGGTTAACGAGCG
MR1276_5p	CCAAGGCTTCCCTCAACTTTAAAACAGC
MR1276_3p	GCTAATTAAGAAAAAACAAAAACCGTTAG
MR1280_5p	CCCTGTTAGAACTCAAAACTCTATAGCAAA
MR1280_3p	ATAACAGCAACTTTAGGCAGCAAAACAGTG
MR1281_5p	CAACAGGGAGCACGACTAAACACAGACTAACT
MR1281_3p	GCAGCGAATCAGTGTCCGTGCGAGACCTGTTA
MR1282_5p	GGAAATTGTCTTTAGTTCCCTACAGCATTACAACA
MR1282_3p	CAATGCATTAGGGAATCTAAAAACGAAATCC
MR1291_5p	TACACGAATACGGGACGCGGCATGGTAGCGGG
MR1291_3p	GCCCCCAACCGTGCAGCGCCGTATATTGCA
MR1295_5p	ATGTGAACGGTCTATTCGGGGATTCCCAT
MR1295_3p	ACGGGGATTCCCCAAACAAGGTAAAGCCCACAT
MR1296_5p	TCAGCGGGACTGTAGGCTGGG
MR1296_3p	CCCATACCTCAGACCCGCCGA
MR1297_5p	TATATAATTTACCTGTTAGGGGAATCCCCGT
MR1297_3p	ACCGGGGATCCCCCTAACAAGATGTAATTAATA
MR1312_5p	GCAGCGGTGTCAGCGGAACATATTCTCCCC
MR1312_3p	GGGCGCGGGGGGTGATATGTTCTGATGACCGCC
MR1313_5p	ATCCCCGACCCCTTTAATGGTGCGGCTAGGC
MR1313_3p	CCCGAGTCGAGTTATTAAGCGACATTAGGG
MR1315_5p	CCGGCCAAAGGTGCGATCGCGGGTCTAACC
MR1315_3p	GGGTTGACCCATTGACCGCATCCTCGGTGGCC
MR1317_5p	CAGGAAAGTGCTGGCAAGACATCGACGGGGTT
MR1317_3p	GGCTCACCGGGGATGTCTTGTGAGCACTTCCC

2.5. Commercial Systems

Table 2-13 Kits

Name	Manufacturer
Luciferase Assay System with Reporter Lysis Buffer	Promega
peqGOLD Plasmid Miniprep Kit	peqLab
QIAGEN Plasmid Midi and Maxi Kit	QIAGEN
QIAquick [®] PCR Purification Kit, Gel Extraction Kit	QIAGEN
Quick Amp Labeling Kit	Agilent
Quant-iT [™] dsDNA BR Kit	Invitrogen
RNA Bee	Ambion
RNeasy Mini Kit	QIAGEN
TA cloning Kit	Invitrogen

Table 2-14 Transfection Components

Name	Manufacturer
PEI	Sigma
Fugene6	Roche
Lipofectamine [™] 2000	Invitrogen

Table 2-15 Real-time Components

Name	Manufacturer
Rotor Gene [™] Multiplex PCR Master Mix	Qiagen
SensiMixPlus SYBR	Quantace
Superscript III [™]	Invitrogen

Table 2-16 Western and Northern Blot

Name	Manufacturer
BAS-MP 2040P Imaging Plate Fuji Photo Film	Fuji Co.LTD
BioMax Transcreen HE Intensifying screen	Eastman Kodak Company
ExpressHyb Hybridization Solution	Clontech
G-25 Sephadex columns	GE Healthcare
Hyperscreen [™] Intensifying screens very fast speed RPN1669	Amersham Biosciences
Nytran [®] SuPerCharge Turbo Blotter [™]	Whatman [®] , Schleicher & Schuell
Radiographic cassettes	DR GOOS Supreme
RP New MedicalX-ray Screen Film Blue Sensitive	CEA AB
TurboBlotter [™]	Whatman [®]
UltraHyb [™]	Ambion
WESTRAN [®] S	Whatman [®] , Schleicher & Schuell
X-ray cassette 20x40	rego
γ -P ³² ATP	Hartmann Analytic
Zeta-Probe [®] GT Genomic Tested Blotting Membranes	Bio-Rad Laboratories

2.6. Instruments and Equipment

Table 2-17 Instruments and Equipment

Name	Manufacturer
Axon GenePix 4100A Scanner	GenePix
Phosphoimager BAS 2500	raytest
Biofuge fresco, Biofuge pico, Biofuge primoR	Heraeus Instruments
SubCell® GT	Bio-Rad Laboratories
Concentrator 5301	Eppendorf
Deluxe ProBlot™ 12S	Labnet International
FACSCalibur™, FACSScan™	B&D, Becton Dickinson, Immunocytometry Systems
E.O.S. processor	Agfa
Leica DFC 420C	Leica Camera AG
Mastercycler eppgradient s	Eppendorf
Microscope: Leica DM-IL	Leica Camera AG
Multifuge 3 S-R, Sorvall® RC-RC Plus	Sorvall GmbH
Model 700 Microarray oven	SciGene
NanoDrop1000	peqLab
Qubit™	Invitrogen
Rotor-Gene 6000™	Corbett Life Science
Spectral photometer Spectronic Genesys™ 10 Bio	Thermo Electron
Standard Polaroid Gel Documentation System	Bio-Rad Laboratories
Synergy Mx Microplate Reader	BioTek
Thermo-Cycler: GeneAmp® PCR System 9700	AB Applied Biosystems
UV-Transilluminator GelDoc 2000	Hartenstein
UV Stratalinker™ 1800	Stratagene

Table 2-18 Software

Name	Manufacturer
FACSDiva™	B&D, Becton Dickinson, Immunocytometry Systems
Gen5™	BioTek
GenePix	Molecular Devices
Genespring GX	Agilent Technologies
Rotor-Gene 6000™	Qiagen
CLC Workbench	CLC bio
AIDA Image Analyzer	raytest

2.7. Plasmids

Table 2-19 Purchased Plasmids

Name	Description	Reference
pcDNA3	standard cloning plasmid	Invitrogen
pCR2.1	TA cloning plasmid	Invitrogen
pMIR-Report Luciferase	Luciferase Reporter	Promega
pMIR-Report β -Galactosidase	β -Galactosidase expressing plasmid	Promega
pShuttle	transfer plasmid for Ad Easy System	Addgene
pAd Easy	Adenoviral Bacmid	Addgene

Table 2-20 Cloned Plasmids

Name	Description
pcDNA3-GFP	GFP expression vector
pcDNA3-GFP-BA2	GFP and single miRNA expression BART2
pcDNA3-GFP-BA5	GFP and single miRNA expression BART5
pcDNA3-GFP-BA7	GFP and single miRNA expression BART7
pcDNA3-GFP-BA10	GFP and single miRNA expression BART10
pcDNA3-GFP-BA11	GFP and single miRNA expression BART11
pcDNA3-GFP-BA13	GFP and single miRNA expression BART13
pcDNA3-GFP-BA17	GFP and single miRNA expression BART17
pcDNA3-GFP-BA19	GFP and single miRNA expression BART19
pcDNA3-GFP-rL1-8	GFP and single miRNA expression rL1-8
pcDNA3-GFP-rL1-20	GFP and single miRNA expression rL1-20
pcDNA3-GFP-EBV-BHRF-miR	GFP and all EBV BHRF miRNAs expression
pcDNA3-GFP-EBV-BART-miR	GFP and all EBV BART miRNAs expression
pcDNA3-GFP-EBV-miR	GFP and all EBV miRNAs expression
pcDNA3-IRES-GFP	GFP expression through IRES
pcDNA3-GFP-JMHV-miR (pcGJmiR)	GFP and all JMHV miRNAs expression
pcDNA3-GFP-JMHV-miR –polyA (pcGJmiRΔ)	GFP and all JMHV miRNAs expression without poly A site at the beginning
pShuttle BHRF	BHRF miRNA shuttle vector for AdEasy
pShuttle BART	BART miRNA shuttle vector for AdEasy
pShuttle EBV miRs	all EBV miRNA shuttle vector for AdEasy
pShuttle IRES GFP	IRES GFP shuttle vector for AdEasy
pMIR-Report-CO1	positiv control for luciferase assay, reporter for miR-BART5 1 binding site
pMIR-Report-CO4	positiv control for luciferase assay, reporter for miR-BART5 4 binding sites
pMIR-Report-CARD6	luciferase reporter for human CARD6 3' UTR
pMIR-Report-CASP3	luciferase reporter for human CASP3 3' UTR
pMIR-Report-ELP4	luciferase reporter for human ELP4 3' UTR
pMIR-Report-INPPL1	luciferase reporter for human INPPL1 3' UTR
pMIR-Report-MX1	luciferase reporter for human MX1 3' UTR
pMIR-Report-NME3	luciferase reporter for human NME3 3' UTR
pMIR-Report-NVL	luciferase reporter for human NVL 3' UTR
pMIR-Report-PDCD2	luciferase reporter for human PDCD2 3' UTR
pMIR-Report-Puma-hum	luciferase reporter for human PUMA 3' UTR
pMIR-Report-Puma-rhes	luciferase reporter for rhesus PUMA 3' UTR
pMIR-Report-TNKS2	luciferase reporter for human TNKS2 3' UTR
pMIR-Report-TCF4	luciferase reporter for human TCF4 3' UTR
pMIR-Report-XPO1	luciferase reporter for humanxPO1 3' UTR

2.7.1. Generation of Plasmids Encoding all EBV miRNAs and JMHV miRNAs

2.7.1.1. EBV miRNA Expression Vectors

All miRNAs encoded by EBV were cloned into one expression vector in five steps. First the BHRF miRNAs were amplified from Jijoye cells using the Primers BHRF1_1_for and BHRF1_1_rev for miR-BHRF1-1 (NC_007605: nt 41294-41729) and BHRF1_23_for and BHRF1_23_rev for miR-BHRF1-2 and -3 (NC_007605: nt 42643-43282), respectively. The amplified fragment for miR-BHRF1-1 was restricted with *Bam*HI and *Spe*I and the fragment for miR-BHRF1-2 and -3 with *Spe*I and *Eco*RI and both were ligated together into the vector via *Bam*HI and *Eco*RI and give rise to the pcDNA3-GFP-BHRF-miR vector.

Second the miRNA encoding BART cluster I (miRNAs -, NC_007605: nt 138803-140353) was cloned out of a previously established vector (pcDNA3-CII, Adam Grundhoff) with *Eco*RI and inserted into

the EcoRI site of the pcDNA3-GFP-BHRF-miR vector to generate the pcDNA3-GFP-BHRF-CII-miR vector.

Third miR-BART-2 was amplified from Raji cells with the primers miR-BART_2_for and _rev (NC_007605: nt 152510-153034) and cut with NheI and XbaI prior insertion into the XbaI site of the pcDNA3 vector to generate the pcDNA3-miR-BART-2 vector.

Fourth the miRNA encoding BART cluster II was amplified from Raji cells with the primers BART_CIII_for and _rev (NC_007605: nt 145332-149069) restricted with NotI and XhoI and inserted into the NotI and XhoI site of the pcDNA3-miR-BART-2 vector.

Finally the BART cluster II and miR-BART-2 were cut out of the pcDNA3-BART-CIII_CIIII vector with NotI and XbaI and inserted into the NotI and XbaI site of the pcDNA3-GFP-BHRF-CII-miR vector. The final vector was named pcDNA3-GFP-EBV-miR.

2.7.1.2. JMHV miRNAs Expression Vector

Cosmid #33 (from Scott Wong, Oregon Regional Primate Research Center) containing the region from about nt 83148 - 119569 of JMHV (NC_007016) was digestion restricted with *NotI*, *HindIII*, *XbaI*, *XhoI*, *NheI* and *PstI*. The fragment flanked by *HindIII* and *PstI* with a length of 5866 nt (JMHV nt 111105 - 116751) was subcloned into the *HindIII* and *PstI* site of the pBluescript (pBS) vector. Afterwards the fragment was cut out of pBS with *NotI* and *XhoI* and inserted into the *NotI* and *XhoI* site of the pcDNA3-GFP vector, that was named pcDNA3-GFP-JMHV-miR (pcGJmiR)

To get rid of a poly-A site at the beginning of the fragment, which might lead to a reduction in miRNA processing, a short part of the region ranging from nt 116283 - 116751 was PCR amplified from the cosmid with the primers JMHV-miR-*PvuI*-rev and JMHV-miR-*NotI*-for. In addition, the pcDNA3-GFP-JMHV-miR vector was restriction digested with *PvuI* and *XhoI*, to yield the rest of the JMHV cluster. The pcDNA3-GFP-vector was cut with *NotI* and *XhoI*. All three fragments, the PCR product, the linearized vector and the JMHV-miRNA cluster from the pcDNA3-GFP-vector, were ligated in one step to obtain the vector pcDNA3-GFP-JMHV-miR-polyA (pcGJmiRΔ).

2.8. Antibodies

Table 2-21 Antibodies

Name	Manufacturer
α-Argonaute 2 Rabbit mAb	Cell Signaling
Normal IgG Rabbit mAb	Upstate, #12-370
α-XPO-1 mouse mAb	BD Transduction Laboratories
α-ISG-15	Santa Cruz
α-Tubulin	Santa Cruz
α-rabbit-HRP	Santa Cruz
α-mouse-HRP	Santa Cruz
Dynabeads® M280 sheep-anti rabbit IgG	Invitrogen

3. Methods

3.1. DNA Techniques

3.1.1. Bacteria

3.1.1.1. Culture and Storage

Bacteria were grown in liquid culture containing Lysogeny Broth (LB) Medium (25 g/l dH₂O LB-Broth) or on LB-agar plates (40 g/l dH₂O LB-Agar). Media were sterilized by autoclaving.

Single colonies of *E. coli* (DH5 α) from agar plates or glycerol stocks were inoculated and grown in LB medium in the presence of antibiotics (Ampicillin (1 μ g/ml), Kanamycin (50 μ g/ml)). Bacteria were incubated over night at 30 °C (for adenoviral bacmids) or 37 °C under constant shaking at 220 rpm in an incubator shaker.

After transformation of *E. coli* with DNA, the bacteria were plated onto LB-Agar plates containing the appropriate antibiotics. Plates were incubated at 37 °C over night. Agar Plates were stored for several weeks at 4 °C.

For long time storage, single colonies were grown in sterile LB medium with antibiotics over night, cells were pelleted by centrifugation (3000 rpm, 5 min, Heraeus Biofuge pico[®]), resuspended in 0.5 ml LB medium and mixed with 0.5 ml sterile glycerine. Cultures were transferred into cryo tubes and stored at -80 °C.

3.1.1.2. Generation of Chemically Competent *E. coli*

Chemically competent *E. coli* were generated with the RbCl₂ method. *E. coli* were inoculated in LB medium and incubated over night at 37 °C under agitation at 220 rpm. Subsequently, the culture was diluted 1:100 in 500 ml LB medium containing 8 mM MgSO₄ and 10 mM CaCl₂. *E. coli* were continuously grown to an OD of 0.3-0.5. The optical density correlates with the concentration of bacteria and was determined photometrically using a wavelength of 600 nm against medium as reference (1 OD = 8x10⁸ cells/ml). Subsequently cells were chilled for 15 min on ice and pelleted by centrifugation (300 g, 5 min, 4 °C). The pellet was resuspended in 150 ml ice cold TFB1 buffer and incubated on ice for 60-90 min. Then, the bacteria were centrifuged (300 g, 5 min, 4 °C), resuspended in ice cold TFB2 buffer and aliquots of 210 μ l were frozen in liquid nitrogen and stored at -80 °C.

Table 3-1 TFB1 Buffer

Components	Concentration
RbCl ₂	100 mM
KAc	30 mM
CaCl ₂	10 mM
MnCl ₂	50 mM
Glycerol	15% (v/v)
Acetic Acid	to pH 5.8

Table 3-2 TFB2 Buffer

Components	Concentration
RbCl ₂	10 mM
MOPS	10 mM
CaCl ₂	75 mM
Glycerol	15% (v/v)

3.1.1.3. Transformation of *E. coli*

For the amplification of plasmids 1 µg DNA or 5-10 µl of a ligation were pipetted in an eppendorf tube. Chemically competent *E. coli* were thawed on ice, 100 µl of the cells were added to the DNA and careful mixing was performed by flicking the tube. The mixture was incubated on ice for 30 min. After flicking the tube again, cells were transferred to a water bath (42 °C) for 45 sec and immediately put on ice again for 2 min. Subsequently 900 µl LB medium was added and the sample was incubated for 45 min in a shaking incubator at 37 °C and 220 rpm. Afterwards the mixture was either diluted in 200 ml LB medium and grown over night at 37 °C and 220 rpm with antibiotics for amplification of a single plasmid or plated onto LB-agar plates and incubated over night at 37 °C for screening of different clones after transformation with ligated plasmid. Before plating the cells, the suspension was centrifuged (3000 rpm, 2 min, RT, Heraeus Biofuge pico) and resuspended in 100 µl LB medium.

3.1.1.4. Blue-White Screening of *E. coli* Colonies

Blue-white screening of growing colonies is based on the enzymatic activity of β-galactosidase. Bacteria harbouring a mutation in their lac Z-gene produce an enzymatic inactive protein (the Ω subunit), with 30 aa (α-region) missing at the N-terminus. The enzymatic activity can be recovered by transformation with a plasmid containing the missing α-region (e.g. the TA cloning vector pCR[®]2.1 from Invitrogen (see 3.1.6.1)). The lac repressor can be inactivated by binding of Isopropyl-β-D-Thiogalactopyranosid (IPTG) leading to expression of the Ω subunit. Together with the α subunit the β-galactosidase gets active and hydrolyzes the chromogenic substrate 5-Bromo-4-Chloro-3-indolyl-β-D-Galactopyranosid (XGal), which leads to blue staining of colonies. Blue colonies contain self-aligned vectors whereas white or light blue colonies contain vectors in which the sequence of the α-region is destroyed by insertion of an artificial DNA and hence indicate colonies containing vectors with an insert. For blue-white screening, the *E. coli* strain DH5α was used and grown on XGal and IPTG containing plates (2.5 µl of 0.1 M IPTG, 40 µl of 20 mg/ml XGal).

3.1.2. Preparation of Plasmid DNA from *E. coli*

Small amounts of plasmid DNA were isolated from 5 ml cultures whereas larger amounts were prepared from 200 ml over night cultures of plasmid DNA transformed *E. coli*. DNA was isolated with the peqGOLD Plasmid Miniprep Kit or with the QIAGEN Plasmid Mini or Maxi-Kit, respectively, according to the manufacturer's instructions.

3.1.3. Determination of DNA Concentration and Purity

DNA and RNA concentration and purity was determined photometrically at 260/280 nm with the NanoDrop 1000. Maximum absorption of DNA and RNA is given at a wavelength of 260 nm and the obtained absorption unit OD (optical density) can be used for calculating the concentration of DNA and RNA (Sambrook et al., 2001).

$$DNA \frac{\mu\text{g}}{\mu\text{l}} = OD \times \frac{50 \cdot 20}{1000} \rightarrow 1 \text{ OD}_{260} = 50 \mu\text{g}/\mu\text{l DNA}$$

$$ssDNA \frac{\mu\text{g}}{\mu\text{l}} = OD \times \frac{40 \cdot 20}{1000} \rightarrow 1 \text{ OD}_{260} = 40 \mu\text{g}/\mu\text{l ssDNA}$$

$$RNA \frac{\mu\text{g}}{\mu\text{l}} = OD \times \frac{33 \cdot 20}{1000} \rightarrow 1 \text{ OD}_{260} = 33 \mu\text{g}/\mu\text{l RNA}$$

For pure DNA and RNA, without protein contaminants, the ratio of OD 260 nm/OD 280 nm is 1.8 and 2, respectively. Solvent impurities like organic compounds absorb at 230 nm. The ratio OD 230 nm/OD 260 nm for pure DNA and RNA is 1.8 and 2, respectively.

Some experiments required very low and precise amounts of DNA (e.g. Luciferase Assay). In these cases, the DNA concentration was determined with the QubitTM fluorimeter. The measurements are more accurate and reproducible in comparison to the spectroscopical measurement of the NanoDrop. Fluorescence based dyes specifically binding to DNA, RNA and protein are used. Accordingly, discrimination between RNA and DNA in one sample is possible and measuring of very low amounts of DNA is accurate in contrast to spectroscopically methods. The Quant-iTTM dsDNA BR Kit was used for the preparation of DNA samples before measurement according to the manufacturer's instructions.

3.1.4. Restriction of DNA

Restriction endonucleases from NEB and Fast Digest enzymes from Fermentas were used according to the manufacturer's instructions. For analytic and preparative restrictions 0.5-1 μg and 1-2 μg DNA were restriction digested, respectively. Fragments were subsequently separated and analyzed by gel electrophoresis on a 1-2% agarose gel. For cloning approaches, DNA was isolated and consecutively used in ligation reactions.

3.1.5. Purification of DNA

To isolate DNA from ethidium-bromide containing agarose gels, the DNA bands were visualized by UV light, excised and purified with the QIAquick Gel Extraction Kit according to the manufacturer's instructions.

To purify DNA after enzymatic reactions from substances which might interfere with subsequent reactions such as enzymes, primers, nucleotides or salts the QIAquick PCR Purification Kit was used according to the manufacturer's instructions.

3.1.6. Ligation

Vector and insert DNA were restriction digested to generate compatible ligation ends. It is important to further dephosphorylate the vector prior ligation, to prevent self ligation of the vector. This was achieved using 1 U of Calf Intestine Phosphatase (CIP), which was added to the restriction mixture of vector DNA. Insert DNA was obtained through restriction of other plasmids or PCR products. The ligation was performed with T4-DNA Ligase. The standard composition of a ligation reaction is shown in table 3-3.

Table 3-3 Standard Ligation Reaction

Reagents	Amount
Vector DNA	20-100 ng
Insert DNA	5x molar amount of vector DNA
T4-Ligase reaction buffer [10x]	2 µl
T4-Ligase [1 U/µl]	1 µl
H ₂ O	to 10 µl

The amount of insert DNA was calculated using the following equation:

$$\frac{ng (Vector DNA) \times kbp (InsertDNA) \times 5}{kbp (Vector DNA)} = ng (Insert DNA)$$

The mixture was either incubated over night at 16 °C or for 2 h at 16 °C following incubation for 30 min at 22 °C and 20 min at 37 °C. Afterwards the whole ligation mixture was transformed into *E. coli* (see 3.1.1.3).

3.1.6.1. Ligation into a TA-vector

The ligation of DNA into the pCR[®]2.1 TA-vector was used for cloning approaches as a first step prior insertion of the fragment into the final vector and for sequencing PCR products from miRNA cloning (see chapter 3.2.3). The *Taq*-polymerase has a non-template dependent activity that adds a single

deoxyadenosine (A) to the 3' ends of PCR products. The linearized pCR[®]2.1 vector has 3' deoxythymidine (T) overhangs allowing PCR inserts to ligate efficiently with the vector.

By using thermostable polymerases containing extensive 3' to 5' exonuclease activity for proofreading (e.g. *Pfu*) no 3' A-overhangs are generated. Incubation with Taq polymerase was used subsequently to add 3' A-overhangs to *Pfu* amplified fragments.

The formula below was used to estimate the amount of PCR product needed to ligate with 50 ng of pCR[®]2.1 vector:

$$x \text{ ng PCR product} = \frac{(y \text{ bp PCR product}) \times (50 \text{ ng Vector})}{3900 \text{ bp (Vector)}}$$

In this formula, x ng is the amount of PCR product of y base pairs to be ligated for a 1:1 (vector:insert) molar ratio.

Since the DNA amount of the PCR products generated during the miRNA cloning was very low and not purified, a defined volume of insert DNA (shown in table 3-4) was used.

Table 3-4 Standard TA Ligation Reaction

Reagents	Amount
Vector DNA [25 ng/μl]	0.5 μl
Insert DNA (unpurified PCR Product)	2.5 μl
Ligation buffer [10x]	2 μl
T4-DNA Ligase [4 Weiss Units/μl]	1 μl
H ₂ O	4 μl

The ligation mixture was incubated for at least 4 h at 14 °C. Afterwards the whole reaction mixture was transformed into *E. coli* and blue white screening (see 3.1.1.4) was performed.

3.1.7. Agarose Gel Electrophoresis

Gel electrophoresis can be used for relative exact sizing of linear DNA fragments. Depending on the concentration of agarose, DNA can be separated over a broad size range. Corresponding to their lengths, DNA fragments have different velocities in an electrical field. For fragments between 0.3 and 10 kb a 1% agarose gel was used, fragments smaller than 0.3 kb were separated on an 1.5-2% gel. To prepare an 1% agarose gel 1 g agarose was dissolved in 100 ml of TAE (TRIS, Acetic acid, EDTA) buffer by boiling in a microwave at 800 W for 3 min. Then, 30 μg ethidium bromide were added and the gel was poured into a gel tray carrying a comb of appropriate size. After complete polymerization the gel was transferred in an electrophoresis chamber containing 1x TAE buffer. DNA was mixed with 6x loading dye (Fermentas), loaded into the pockets of the gel and the gel was run at 5-10 V/cm for an appropriate time depending on the size of the fragments. Since ethidium bromide, which is able to intercalate into DNA, was added to the gel, DNA bands can be visualized by UV light. Analytical gels

were analyzed on a UV transilluminator and documented with the Quantity One software. In preparative gels, bands were visualized with UV light of longer wave length (365 nm) to prevent DNA from UV induced damage and cut out with a scalpel to isolate the DNA.

3.1.8. Sequencing of Plasmids

The Sequencing Service from GATC or SeqLab was used.

3.1.9. Isolation of Genomic DNA

Genomic DNA was isolated from a sufficient amount of cells (10^5 - 10^7 cells). Cells were washed twice in PBS and pelleted by centrifugation (1200 rpm, 3 min, RT, Varifuge 3.0 R, Heraeus), then resuspended in either 500 μ l PBS for nuclei preparation or 20 μ l PBS for direct isolation of genomic DNA. For the nuclei preparation 500 μ l nuclei lysis buffer was added and mixed by inverting the tube several times. The mixture was incubated on ice for 10 min and further inverted every 2 min. The nuclei were then pelleted by centrifugation (1100 g, 10 min, 4 °C) and resuspended in 20 μ l PBS to isolate genomic DNA. 300 μ l of gDNA lysis buffer supplemented with Proteinase K was mixed with either 20 μ l of cells or nuclei and incubated over night at 55 °C. The DNA was then phenol chloroform isoamylalcohol (PCI) extracted using Phase Lock 2 ml tubes. The 300 μ l were loaded onto the pre spun Phase Lock tube, an equal amount of PCI was added, mixed by short vortexing, and centrifuged (13000 rpm, 5 min, 4 °C, centrifuge 5417 R, Eppendorf). This step was repeated once with PCI and once with chloroform. The upper aqueous phase (which is separated from the non aqueous phase through the gel of the phase lock tube) was transferred into a new Eppendorf tube and DNA was precipitated by adding 7 μ l 3 M NaAc pH 5.5 and 750 μ l EtOH, followed by mixing and centrifugation (13000 rpm, 10 min, 4 °C, centrifuge 5417 R, Eppendorf). The pellet was washed once with 1 ml 70% EtOH, centrifuged (13000 rpm, 10 min, 4 °C, Eppendorf) and dried in a DNA concentrator for 2 min after removing most EtOH with a pipet tip. Afterwards the DNA was desolved in an appropriate amount of TE buffer with 20 μ g/ml RNase A, incubated at 37 °C in a water bath and then stored at 4 or -20 °C. Genomic DNA was then used for the amplification of genomic regions via PCR.

Table 3-5 Nuclei Lysis Buffer

Reagents	Concentration
Sucrose	0.65 M
TRIS-Cl, pH 7.8	20 mM
MgCl ₂	10 mM
TritonX-100	2%

Table 3-6 gDNA Lysis Buffer

Reagents	Concentration
NaCl	100 mM
TRIS-Cl, pH 8	10 mM
EDTA, pH 8	25 mM
SDS	0.5%
Proteinase K (freshly added)	0.1 mg/ml

3.1.10. Polymerase Chain Reaction

Polymerase chain reaction (PCR) was used for the amplification of smallest amounts of specific DNA. It was first described by Mullis (Mullis et al., 1986) and consists of a cyclic progression of denaturing the DNA, annealing of specific primers to the DNA and synthesis of the complementary strand by polymerases, which leads in every cycle to a duplication of DNA. In this work PCR was used for the amplification of specific DNA for cloning, analytic testing of bacterial colonies (3.1.10.1), specific mutagenesis (3.1.10.2), sequencing (3.1.9) and relative quantitation of RNA transcripts by real-time PCR as well as for the detection of miRNAs by stem-loop RT-PCR (3.1.11).

Standard PCR conditions are shown below.

Table 3-7 Standard PCR Reaction

Reagents	Amount
DNA	100 ng-1 µg
fw Primer [10 µM]	1 µl
rev Primer [10 µM]	1 µl
dNTPS [10 nM]	1 µl
Buffer 10x	1 µl
Taq-Polymerase	1 Units
and/or Pfu-Polymerase	0.5 Units
dH ₂ O	to 50 µl

Amplification of DNA was carried out in a thermocycler. The standard program is listed in table 3-8.

Table 3-8 Standard PCR Program

Temperature	Time	Cycles
95 °C	5 min	1
95 °C	30 s	25 -30
45-60 °C	40 s	
72 °C	1 min/1000 bp	
72 °C	7 min	1
4 °C	∞	

The amplified DNA was analyzed on an agarose gel and if necessary eluted. DNA was either cloned directly into a TA vector or the products were purified, restriction digested according to the restriction sites of the primers used, then purified again and used in ligation.

3.1.10.1. Colony PCR

To screen for bacterial colonies containing the proper insertion of DNA fragment, PCR was performed. Either 2 µl of a liquid culture or 5 µl from a colony resuspended in 20 µl TE buffer were used for the PCR. Amplified DNA was then analyzed on an agarose gel.

3.1.10.2. Site-directed Mutagenesis

PCR amplified DNA can harbor false nucleotides particulare when *Taq* polymerases lacking proof reading activity are used. In some experiments (e.g. luciferase assays) a mutated sequence is required as a negative control. Mutagenesis was used to destroy seed matches (which are 6 bp sequences) of miRNAs in a 3'-UTR of a mRNA target by changing 2 nucleotides. Primer design is an essential step for site directed mutagenesis. They should have a length of 25-45 bp, with the mutated sequence located approximately in the middle and contain a melting temperature above 78 °C. The following formula was used to estimate the melting temperature:

$$T_M = 81.5 \times 0.41 \times (\%GC) - \frac{675}{\text{primer length}(nt)} \times \%mismatch$$

Importantly, the primer should be HPLC purified. Amplification was performed using *Pfu*-Turbo DNA polymerase, with a proof reading activity to avoid incorporation of false nucleotides. The contents of the PCR mixture is shown in table 3-9.

Table 3-9 Site-directed Mutagenesis PCR Components

Reagents	Amount
Template DNA	10 ng
Primer 1 and 2	each 125 ng
dNTPs [10 mM]	1 µl
Reaction Buffer for <i>Pfu</i> -Turbo [10x]	5 µl
dH ₂ O	ad 49 µl
<i>Pfu</i> -Turbo [2.5 U/µl]	1 µl

The cycling program was as follows:

Table 3-10 Site-directed Mutagenesis PCR Program

Temperature	Time	Cycles
95 °C	30 s	18x
95 °C	30 s	
60 °C	1 min	
68 °C	1 min	
68 °C	7 min	
4 °C	∞	

The non-mutated template DNA is methylated due to amplification in *E. coli* and can be specifically digested with the restriction enzyme *DpnI*. Therefore 1 µl *DpnI* [10 U/ µl] was added to the samples

and incubated for 1 h at 37 °C. Digested DNA was then used for transformation in *E. coli*, and clones were later sequenced to confirm successful mutation.

3.1.11. Real-time qPCR

Real-time quantitative PCR (qPCR) is a nucleic acid amplification method based on the principal of PCR that allows relative or absolute quantification of template DNA. The amplified DNA can be detected during amplification in real-time by measuring the intercalation of a fluorescence dye. Expression analysis can be further performed with real-time reverse transcriptase PCR (RT-PCR), for which transcription of RNA into cDNA is necessary. A more detailed explanation of this procedure is described in 3.1.11.3.

3.1.11.1. Real-time qPCR with SYBR Green

The asymmetrical cyanine dye SYBR Green, was used for these experiments unless otherwise noted. After intercalation of SYBR Green into dsDNA, the resulting DNA-dye-complex absorbs blue light ($\lambda_{\max} = 488 \text{ nm}$) and emits green light ($\lambda_{\max} = 522 \text{ nm}$). The PCR can be divided into three phases. The first phase is characterized by the limitation of template DNA and the fluorescence intensity is not detectable above the background signal. In the second phase, DNA is exponentially amplified and can be quantified, since the fluorescence intensity is proportional to the amount of PCR product. Fluorescence is then measured at the end of elongation. The third phase ends in a plateau where the fluorescence intensity of SYBR Green is at its maximum. The cycle, where the fluorescence is for the first time significantly higher than the background, is termed Cycle Threshold (CT).

Primers were carefully chosen to avoid primer dimers and side products. For mRNA analysis, amplicons should include introns and primers should be boundary spanning to exclude the amplification of genomic DNA.

Primers were designed according to the following criteria: They had a similar melting temperature of about 60 °C, with a length of 19-22 nt and a GC content of 40-60%. The desired length of the amplified PCR product was between 80-300 bp. Primers were furthermore optimized by the determination of the optimal annealing temperature in a gradient PCR and analysis of the amplified products on an agarose gel.

SYBR Green intercalates all dsDNA. Therefore a melting curve analysis is performed at the end of the real-time PCR to evaluate for the presence of primer dimers or side products among the real product. This is achieved by constantly increasing the temperature, allowing the DNA strands to dissociate depending on their specific melting point. The fluorescence of SYBR Green then gradually decreases, since it cannot intercalate dsDNA anymore.

For every primer pair a standard curve was generated to calculate the PCR efficiency to allow for an adequate determination of the relative amounts of unknown templates. Templates of higher

concentration (e.g. a transcript positive cell line) were serially diluted 5 times 1:10 and duplicates were measured to create a standard curve. The slope of the standard curve displays the efficiency of the PCR with these primer pairs. A slope of 1 represents a duplication of PCR product in each cycle and displays a perfect reaction. This standard curve was used to calculate the relative or absolute amount of template in a sample of interest by loading the curve into the same run. The absolute quantification is only possible, if the exact copy number or amount of a control is known.

A no template control and for expression analysis a -RT (cDNA synthesis reaction without reverse transcriptase) control were included into each run, to prove the absence of DNA contamination.

Table 3-11 Real-time SYBR Green Reaction

Reagents	Amount
fw Primer [10 μ M]	1 μ l
rev Primer [10 μ M]	1 μ l
template DNA	10 μ l
cDNA	1.5 μ l
DEPC-H ₂ O	7.3 μ l

Table 3-12 Real-time SYBR Green Program

Temperature	Time	Cycles
95 °C	7 min	1
95 °C	10 s	45
55 °C	30 s	
72 °C	7 s	

3.1.11.2. Real-time qPCR with TaqMan probes

More specificity can be gained using TaqMan probes for quantification of transcripts. In this work TaqMan probes were used for quantification of miRNA expression levels. The function of this type of probes is based on the Förster Resonance Energy Transfer (FRET). The probe contains a quencher (e.g. Dabcyl) on one end and a reporter fluorescence dye on the other (e.g. Fam, Vic). Additionally to its polymerase activity, the *Taq* polymerase harbors a 5'-3' exonuclease activity allowing the degradation of the probe from its 5'-end during complementary strand synthesis. This leads to a separation of quencher and reporter fluorescence dye and finally the loss of the FRET signal. Fluorescence was measured at the end of elongation.

The quantification of the amount of a template of interest was calculated using an intra assay control (e.g. a housekeeping gene) for normalization and the corresponding standard curve for the transcript. As general reference GAPDH from cDNA or genomic DNA was used for measurement of mRNA transcripts or DNA, respectively. The amount of miRNAs was related to the endogenous miR-21.

Using different TaqMan probes with different fluorescence dyes allows for the measurement of multiple templates in one PCR (multiplex PCR). Components of the reaction mixture and the program are listed in tables 3-13 and 3-14.

Table 3-13 Real-time Reaction with TaqMan Probes

Reagents	Amount
fw Primer	1 μ l
rev Primer	1 μ l
TaqMan probe	0.4 μ l
Mix	10 μ l
DEPC-H ₂ O	to 18.5 μ l
cDNA	1.5 μ l

Table 3-14 Real-time Program with TaqMan Probes

Temperature	Time	Cycles
95 °C	7 min	1
95 °C	10 s	45
55 °C	30 s	
72 °	7 s	

The real-time qPCR was performed in duplicate on the Rotor-Gene 6000™. Subsequent analysis was performed using the Rotor-Gene 6000™ software.

3.1.11.3. Reverse-Transcriptase PCR (RT-PCR)

To analyze RNA transcripts in a PCR reaction, the RNA has to be reverse transcribed to cDNA. The cDNA synthesis was done with the SuperScriptIII Reverse Transcriptase according to the manufacturer's instructions. If procurable, 1 μ g RNA was initially used. Both random primers and specific primers were used for the analysis of mRNA transcripts and stem-loop primers for the quantification of miRNA transcripts (see 3.1.11.4). The conditions used for the reverse transcription of mRNA are shown in table 3-15. First, RNA dNTPs and primers were mixed and heated to 65 °C for 5 min, then incubated on ice for 1 min and afterwards the remaining components were added. The synthesis of cDNA was accomplished by incubation at 50 or 55 °C for 1 h for random or specific primers, respectively. Synthesis was followed by inactivation of the reverse transcriptase at 70 °C for 15 min and incubation on ice prior further usage or storage. The program for using stem-loop primers is given in chapter 3.1.11.4.

Table 3-15 SuperScriptIII Reverse Transcription Reaction

Reagents	Amount
RNA	1 μ g
dNTPs [10 mM]	0.5 μ l
stem-loop primer [1 μ M] or random primer [250 ng/ μ l] or specific rev primer [2 μ M]	1 μ l
5x first strand-buffer	4 μ l
DTT [0.1 M]	2 μ l
RNaseOUT [40 units/ μ l]	0.1 μ l
SuperScript III RT [200 units/ μ l]	0.25-1 μ l
DEPC-H ₂ O	to 20 μ l

After cDNA synthesis 0.4 μ l RNase H [200 units/ μ l] was added and the mixture was incubated at 37 °C for 20 min. RNase H was inactivated by heating at 65 °C for 10 min and tubes were put on ice prior to use or stored in aliquots at -20 °C. Obtained cDNA was then directly used in real-time PCR applications or stored in aliquots at -20 °C.

3.1.11.4. Real-time Stem-loop PCR

A recently established method for the detection and quantification of miRNAs was described in 2005 (Chen et al., 2005a). In this method, a stem-loop primer is used for cDNA synthesis and afterwards the transcripts are measured by real-time PCR using TaqMan probes. Different stem loop primers harbor an equal 5'-end, which affords formation of a stem loop and differ in the last 6 nucleotides at their 3'-end, which is complementary to the 3' end of a specific miRNA. This method allows detection of very small amounts of mature miRNAs (~ 25 pg). Figure 3-1 shows a schematic overview.

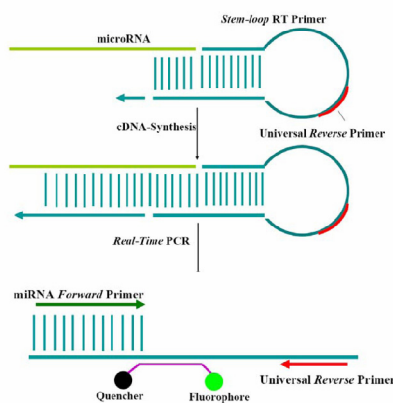


Figure 3-1 Schematic Overview of Stem-loop RT-PCR

cDNA Synthesis is performed using specific primers binding to the last 4-6 nt of a miRNA and fold into a stem-loop structure at the 5' end. Real-time PCR is performed using a specific primer for the miRNA and a universal reverse primer, binding to a region within the loop of the stem-loop primer. A TaqMan probe binding specifically to the miRNA can be used in real-time PCR to determine the relative amount of the amplified product (Christine Henning).

For detection of miRNAs expressed from the BHRF or BART clusters of EBV, exemplarily the miRNA BHRF1-3 and miRNA BART-5 were used, respectively.

Total RNA (1 μ g) was used for the cDNA synthesis with the corresponding stem loop primers. A stem-loop primer for miR-21 and a reverse primer for GAPDH were included as internal controls. cDNA synthesis was performed as described by Varkonyi-Gasic (Varkonyi-Gasic et al., 2007).

First, dNTPS were mixed with DEPC-H₂O and 1 pmole of each stem-loop primer and 2 pmole of GAPDH reverse primer. The mixture was heated to 65 °C for 5 min and incubated on ice for 2 min to allow primer binding. Then the remaining reagents listed in table 3-16 were added.

Table 3-16 Reverse Transcription Reaction for Stem-loop Primers

Reagents	Amount
First strand buffer [5x]	4 μ l
DTT [0.1 M]	2 μ l
RNAseOut [40 U/ μ l]	0.5 μ l
Superscript III RT [1 U/ μ l]	0.25 μ l
DEPC-H ₂ O	to 19 μ l

Subsequently 1 μ l RNA was added and a pulsed RT reaction was performed, shown in table 3-17.

Table 3-17 Reverse Transcription Program for Stem-loop Primers

Temperature	Time	Cycles
16 °C	30 min	1
30 °C	30 s	60
42 °C	30 s	
50 °C	1 s	
4 °C	∞	

After cDNA synthesis 0.4 μ l RNAse H [200 units/ μ l] was added and the mixture was incubated at 37 °C for 20 min. RNAse H was inactivated by heating at 65 °C for 10 min and tubes were put on ice prior to use or stored in aliquots at -20 °C.

3.2. RNA-Techniques

3.2.1. Isolation, Purification and Quantification of RNA

Total RNA was isolated with RNA Bee and poly A RNA with the Oligotex mRNA Mini Kit according to the manufacturer's instructions. RNA was purified with the RNeasy Mini Kit according to the manufacturer's instructions and quantified using the NanoDrop 1000.

3.2.2. Northern Blot

For RNA transcripts > 0.1 kb, 10 μ g of total RNA or 1 μ g of poly-A-RNA were separated on a 1,3% formaldehyde agarose gel. Therefore 1.2 g agarose were desolved in 67 ml DEPC H₂O by boiling in a microwave. Evaporated H₂O was then refilled and the solution was cooled down to 65 °C in a water bath. Then 13.5 ml of 37% formaldehyde and 10 ml of 1x MOPS buffer were added, mixed and the gel was prepared.

RNA was diluted in 14 μ l DEPC-H₂O, mixed with 5 μ l loading dye, heated for 5 min at 65 °C and chilled on ice for 2 min. Samples were supplemented with 1 μ l ethidium bromide (1 μ g) and loaded onto the gel as well as 3 μ l of a high range RNA ladder. The gel was run for 3-4 h at 65 mA in 1x MOPS buffer. Bands were analyzed by UV light for integrity.

RNA was subsequently transferred to a Nitran Nylon membrane with the TurboBlotter System. The transfer was performed in 2x SSC (Sodium chloride, Sodium Citrate)/0.5 M NaOH for 3 h. Hybridization of the membrane with oligonucleotide probes was done in a similar fashion to the small RNA Northern Blot (see 3.2.2.1). Probes < 100 bp synthesized by PCR were labeled with the DNA Labeling System and the blot was hybridized in UltraHyb hybridization buffer according to the manufacturer's instructions. The blots were developed for 1-3 days at -80 °C and the radioactivity was detected with X-ray films

Table 3-18 10x MOPS Buffer

Reagents	Amount
MOPS	200 mM
Sodium Acetate	50 mM
EDTA	10 mM
NaOH	to pH 7

Table 3-19 Loading Dye for Northern Blot Samples

Reagents	Amount
saturated aqueous bromophenol blue solution	4 µl
EDTA [500 mM], pH 8	20 µl
Formaldehyde [37%]	180 µl
Glycerol [100%]	500 µl
Formamide	771 µl
10x MOPS	1 ml
DEPC-H ₂ O	to 2,5 ml

3.2.2.1. Small RNA Northern Blot

The detection of small RNAs such as miRNAs was done by separating 14 µg total RNA on a 15% 8 M urea SDS gel. Components of the gel are listed in table 3-20. First urea was dissolved in buffer, acrylamide solution and buffer by warming the mixture to 37 °C and stirring. Then APS and TEMED were added and the gel was casted between to glass plates for polymerization.

Table 3-20 8 M Urea Gel for Small RNA Northern Blot

Reagents	Amount
Urea	12 g
10x TBE	2.5 ml
30% Acrylamid/Bisacrylamid (ratio 19/1)	12.5 ml
DEPC-H ₂ O	6.7 ml
APS	160 µl
TEMED	16 µl

The gel was pre run for 1 h at 45 mA. Samples were loaded after mixing 15 µl RNA with 15 µl formamide containing loading dye and heating the mixture for 2 min at 70 °C. RNA was then separated for 45 min at 35 mA. Afterwards the gel was stained in a 4% ethidium bromide solution and bands were evaluated for integrity by UV light. After washing the gel in 1x TBE (Tris, Borate, EDTA), RNA was transferred to a Zeta-Probe Membrane. The Semi-Dry-Transfer was performed in

1x TBE for 2 h at 2.26 mA/cm². The membrane was washed in 1x TBE, dried and cross-linked with UV light. Pre-hybridization was performed for 1 h at 37 °C in hybridization buffer in a rotating hybridization oven. At the same time the oligonucleotide probe was labeled for 1 h at 37 °C in a water bath.

Table 3-21 Labeling Reaction for Small Oligonucleotide Probes

Reagents	Amount
DEPC-H ₂ O	16 µl
10x PNK buffer	5 µl
Probe [10 mM]	2 µl
PNK [6 U/µl]	2 µl
P32-dATP [mCi]	25 µl

The PNK activity was inactivated by heating the probes for 10 min at 65 °C. Nucleotides which were not incorporated were separated from the probe using G-25 Sephadex columns according to the manufacturer's instructions.

The hybridization buffer was changed and the labeled probes were added. Membranes were then incubated over night at 37 °C under constant rotation. The next day membranes were washed twice in pre-heated wash buffer (2x SSC, 0.1% SDS), once at 37 °C for 1 min, once for 30 min at RT and twice for 30 min in RT wash buffer at RT. Membranes were then exposed to X-ray films or imaging plates for 1-3 d at -80 °C or at RT, respectively. X-ray films were developed on a E.O.S. processor and image plates were analyzed on the BAS-Reader. The evaluation was performed with the AIDA Software.

For multiple hybridization of the blot with different probes, the previously bound probes were removed by incubating the membrane in 0.5% SDS for 2 h at 60 °C in a rotator.

Table 3-22 TBE Buffer

Reagents	Concentration
TRIS base	89 mM
Boric Acid	89 mM
EDTA	20 mM, pH 8

Table 3-23 Formamide Loading Dye

Reagents	Concentration
Formamid	95% (v/v)
Bromphenol blue	0.09% (w/v)
Xylene cyanol FF	0.09% (w/v)

Table 3-24 20x SSC Buffer (Sodium Chloride, Sodium Citrate)

Reagents	Concentration
NaCl	3 M
Sodium citrate	0.3 M
HCl	to pH 7

Table 3-25 Northern Blot Wash Buffer

Reagents	Concentration
SSC	2x
SDS	0.1%

3.2.3. Cloning of Small RNAs

A cloning strategy for small RNAs was first described by Pfeffer et al. and was used for the identification of diverse small RNA species. In this work new miRNAs were predicted with the VMIR Programm and verified by small RNA Northern Blotting. To determine the exact 5'-ends of the confirmed miRNAs a modified protocol from Pfeffer (Pfeffer et al., 2005a) was used.

Total RNA (500 µg) from positive cell lines or transfected cells were separated on a 15% polyacrylamide gel containing 8 M Urea (see 3.2.2.1) and stained with ethidium bromide. RNA in the range of 18-26 nt was excised, crushed into small pieces in a 2 ml low bind Eppendorf tube and eluted rotating over night at 4 °C with 2-3 volumes of 0.3 M NaCl-solution. The next day gel pieces were centrifuged (2000 rpm, 4 °C, 5 min, Centrifuge 5417 R, Eppendorf) and the supernatant was transferred in a new tube. RNA was precipitated in the presence of 1 µl GlycoBlue or glycogen with 3-4 vol of 100% EtOH at -20 °C over night. The RNA was pelleted (16000 g, 4 °C, 10 min), dried in the SpeedVac and resolved in 30 µl DEPC-H₂O. For dephosphorylation, the components listed in table 3-26 were mixed and incubated at 50 °C for 30 min.

Table 3-26 Dephosphorylation Reaction Mixture for Small RNA Cloning

Reagents	Amount
RNA	27 µl
NEB buffer 3	1 µl
RNAseOut [40 U/µl]	1 µl
CIP [1 U/µl]	1 µl

RNA was then extracted with phenol-chloroform (see 3.1.9) and resolved in 11.5 µl DEPC-H₂O. Ligation of the 3'-linker was carried out by adding 1 µl of linkers [100 µM] to 10 µl RNA. The mixture was heated to 65 °C for 3 min. Then components listed in table 3-27 were added.

Table 3-27 Linker Ligation Reaction Mixture for Small RNA Cloning

Reagents	Amount
ATP [10 mM]	2 µl
RNase Out [40 U/µl]	1 µl
10x RNA-Ligase Buffer	2 µl
BSA	2 µl
T4-RNA-Ligase	1 µl

The ligation was performed at 16 °C over night. To get rid of unbound 3'-linker, the ligated RNA was separated on a 8.5 cm 15% polyacrylamide gel containing 8 M Urea. RNA in the range of 52-58 nt was excised, eluted, precipitated and resolved in 11.5 µl DEPC-H₂O as described above. For 5'-linker

ligation the isolated RNAs have to be phosphorylated at their 5' end. Therefore, reagents listed in table 3-28 were added to 10 μ l RNA and the mixture was incubated at 37 °C for 30 min.

Table 3-28 Phosphorylation Reaction Mixture for Small RNA Cloning

Reagents	Amount
10x PNK buffer	2 μ l
ATP [100 mM]	0.4 μ l
PNK	0.5 μ l
DEPC H ₂ O	7.1 μ l

Following this, 37 μ l DEPC-H₂O and 3 μ l 5 M NaCl solution were added and RNA was extracted with PCI (see 3.1.9). Ligation of the 5'-linker was done in the same way as the ligation of the 3'-linker with subsequent purification on a 8.5 cm 15% polyacrylamide gel containing 8 M Urea. RNA in the range of 85-91 nt was cut out and isolated as described above. The RNA was then reverse transcribed to cDNA using the 3'-outer primer (see also 3.1.11.3). For unspecific amplification of the ligated small RNAs a PCR was carried out with the 5'- and 3'-outer primers (3.1.10). If the yield was too low a second PCR was performed by using the 5'- and 3'-inner primers. To sequene the 5'-ends of single cloned small RNAs, products were PCR amplified with a specific 3'-primer for each identified miRNA and the 5'-outer or -inner primer. Products were purified on 2% agarose gels, extracted, cloned into a TA-cloning vector (3.1.6.1) and then sequenced (3.1.8).

3.3. Protein Techniques

3.3.1. Isolation of Protein from Cultured Cells

Protein analysis was performed using Western Blotting. To obtain protein from cultured cells, the cells were trypsinized (adherent cells), resuspended in PBS and pelleted by centrifugation (1000 rpm, 3 min, RT, Biofuge pico, Heraeus). The cells were then washed twice in PBS, transferred into a 1.5 ml Eppendorf tube and pelleted again by centrifugation (12000 rpm, 2 min, RT, Biofuge pico, Heraeus). The pellet was then resuspended in Laemmli buffer (Laemmli, 1970), heated for 5 min at 100 °C and placed on ice or stored at -20 °C.

3.3.2. Determination of Protein Yield

Protein yield was quantified using the 2-D Quant Kit (GE Healthcare) according to the manufacturer's instructions. The quantification assay is based on the specific binding of copper ions to proteins. Precipitated proteins are resuspended in a copper-containing solution and unbound copper is measured with a colorimetric dye. The color intensity is inversely related to the protein concentration. This assay can be used for quantifying protein concentrations in the range of 0-50 μ g/ μ l.

3.3.3. SDS-Polyacrylamide Gel Electrophoresis (SDS-PAGE)

For western blotting 10-50 μg protein were loaded per lane of an SDS-gel. To separate proteins electrophoretically, they were dissolved in Laemmli buffer containing negatively charged SDS, which compensates the positive charge on denatured proteins. Within a SDS-gel the proteins move towards the anode in an electric field. The velocity of a protein through the pores of a gel is determined by its size. To increase the separation of proteins, a lower concentrated gel (collecting gel) is polymerized above a higher concentrated gel (separating gel) to concentrate proteins at the boundary before separation (Laemmli, 1970). The gel Components are shown in table 3-30 and 3-31.

Table 3-29 Collecting Gel Buffer (10x)

Reagents		Concentration
TRIS base		0.47 M
H ₃ PO ₄		to pH 6.7

Table 3-30 Separating Gel Buffer (10x)

Reagents		Concentration
TRIS base		3 M
HCl		to pH 8.9

Table 3-31 SDS-Polyacrylamide Collecting Gel

Reagents	Amount
Acrylamide Stock (Roti30)	1 ml
Collecting gel buffer (10x)	1.25 ml
SDS [10%]	100 μl
APS	100 μl
TEMED	25 μl
H ₂ O	to 10 ml

Table 3-32 SDS-Polyacrylamide Separating Gel [14%]

Reagents	Amount
Acrylamide Stock	9.3 ml
Separating gel buffer (10x)	2.5 ml
SDS [10%]	200 μl
APS	70 μl
TEMED	12.5 μl
H ₂ O	to 20 ml

Table 3-33 TGS Buffer (Tris Glycine SDS) (1x)

Reagents	Concentration
TRIS base	25 mM
Glycine	192 mM
SDS	0.1%
pH 8.3	

Table 3-34 Laemmli Sample Buffer (5x)

Reagents	Concentration
SDS	10% (w/v)
Glycerol	50%
DTT	10% (w/v)
Bromo phenol blue	0.05% (w/v)

Samples were first resuspended in an appropriate volume of H₂O (e.g. 10 µl for 1-2x 10⁶ cells) and mixed with an equal amount of 5x Laemmli buffer. The mixture was heated to 95 °C for 5 min and stored on ice before loading. Samples were loaded onto the gel and run at 80 V for 20 min in 1x TGS. After the dye front reached the boundary to the separating gel the voltage was increased to 160 V for another 40-60 min until the blue front reached the end of the gel. Proteins were then blotted onto a nitrocellulose membrane.

3.3.4. Western Blot

The separated proteins on the SDS gel were transferred to a nitrocellulose membrane. The positively charged membrane binds and immobilizes negatively charged proteins. The membranes can then be probed for the detection of different proteins with specific antibodies.

The transfer was performed using a semi-dry set up. Whatman papers (3 mm) and a cellulose membrane were cut to the same size as the gel. The Whatman paper as well as the membrane and the gel were immersed in 1x TGS buffer with 20% Ethanol. In a Phase Transfer System the Components were stacked as follows: three Whatman papers, then the gel, the membrane and 4 Whatman papers. Air bubbles were carefully squeezed out. The transfer was performed with a current of 0.8 mA/ cm² for 2 h.

Complete transfer of proteins was analyzed using Ponceau S solution, to stain proteins on the membrane. Ponceau stain is reversible and was performed for 5 min under agitation. Afterwards the membrane was washed for 10 min in 1x TBS (Tris Buffered Saline) before continuing.

To minimize unspecific binding of the antibodies to the membrane, the membrane was first blocked by incubation in 10% milk powder in TBS (MTBS) for 30 min under agitation. Afterwards the 1st antibody was diluted in 5% milk powder in TBST (TBS, Tween) (MTBST) and the membrane was incubated for 2 h at RT or over night at 4°C under constant agitation. Membranes were then washed 5 times for 5 min in 1x TBST and pre blocked in 10% MTBS for 15 min before incubating with the 2nd antibody in 5% MTBST for 2 h at RT. Subsequently membranes were washed again 5 times in 1x TBST for 5 min, twice in 1x TBS and once in H₂O.

Since the secondary antibodies are coupled to horseradish peroxidase the detection of protein bands was accomplished by adding chemiluminescent substrates and measuring the resulting signal. Therefore ECL solution A and B were mixed in equal amounts, membranes were incubated in the solution for 2 min and the chemiluminescent signal was detected on an X-ray film.

Table 3-35 Blotting Buffer (1x)

Reagents	Concentration
TRIS base	25 mM
Glycine	192 mM
SDS	0.01% (v/v)
Ethanol	20%
	to pH 8.6

Table 3-36 TBS Buffer (1x)

Reagents	Concentration
TRIS base	100 mM
NaCl	0.9% (w/v)
HCl	to pH 7.5

Table 3-37 TBST Buffer (1x)

Reagents	Concentration
TRIS base	100 mM
NaCl	0.9% (v/v)
HCl	to pH 7.5
Tween 20	0.1% (v/v)

Table 3-38 ECL Solution A

Reagents	Concentration
TRIS-HCl, pH 8.5	100 mM
Cumaric acid	0.4 mM
Luminol	2.5 mM

Table 3-39 ECL Solution B

Reagents	Concentration
TRIS-HCl, pH8.5	100 mM
H ₂ O ₂	0.18%

3.3.5. Immunoprecipitation RIP-ChIP

The RIP-ChIP was performed after a protocol previously described (Keene et al., 2006). Cells (1-2x 10⁷) were infected with adenovirus (Ad-IRES or Ad-BART) at an MOI of 500. After 2 days, the cells were collected by scraping in ice cold PBS and pelleted by centrifugation (1000 g, 3 min, 4°C). Cells were washed three times with ice cold PBS and pelleted as described above. Cells were then lysed in one pellet volume of polysome lysis buffer (table 3-40) supplemented with RNase inhibitors (RNaseOut and Vanadyl ribonucleoside complexes (VRC)) as well as protease inhibitors. The mRNP lysate was incubated on ice for 5 min and immediately frozen at -80 °C for at least 30 min or until further needed. Magnetic beads (50 µl per IP reaction) were washed with 200 µl PBS, pelleted and blocked in 200 µl NT2 buffer (table 3-41) supplemented with 5% BSA for 10 min. The beads were then pelleted and the blocking step was repeated. Next 200 µl NT2 buffer containing 5% BSA and antibody were added to the bead slurry and incubated over night at 4 °C under rotation.

The next day the lysate was thawed on ice and centrifuged (15000 g, 15 min, 4 °C). The supernatant was transferred into a new tube and stored on ice until needed. The lysate was pre-cleared with 25 µl beads, which were washed and blocked in a similar fashion as the beads for antibody incubation, resuspended in 850 µl ice cold NT2 buffer containing 200 U RNaseOut, 400 µM VRC, 1 mM DTT and 20 mM EDTA and incubated for 30 min at 4 °C under rotation.

The antibody coated beads were gently washed 5 times with ice-cold NT2 buffer. The beads were then resuspended in 950 µl of pre-cleared lysate and 100 µl was saved as an input control. The beads were incubated for 4 h at 4 °C under rotation. The beads were then pelleted, the supernatant was removed and they were washed 5 times with ice cold NT2 buffer as described above. Following this, the beads were resuspended in 100 µl NT2 buffer containing 30 µg Proteinase K and incubated at 55 °C for 30 min. The tubes were occasionally agitated. Then 1 ml of RNA Bee was directly added and RNA isolation was performed as described in chapter 3.2.1. For precipitation, 20 µg of glycogen were added in the precipitation step. RNA was solubilized in 5-10 µl DEPC-H₂O.

Table 3-40 Polysome Lysis Buffer

Reagents	Amount [for 5 ml]
KCl [1 M]	500 µl
MgCl ₂ [1 M]	25 µl
HEPES [1 M]	50 µl
NP40	25 µl
DTT [0.1 M]	50 µl
RNaseOut [40 U/µl]	12.5 µl
Vanadyl ribonucleoside complexes [200 mM]	10 µl
Protease inhibitors	200 µl

Table 3-41 NT2 Buffer

Reagents	Amount [for 50 ml]
TRIS-HCl [1 M], pH 7.4	2.5 ml
NaCl [1 M]	7.5 ml
MgCl ₂ [1 M]	50 µl
NP40	25 µl

3.4. Cell Biological Methods

3.4.1. Culture of Adherent Mammalian Cell Lines

Adhesive mammalian cells HEK-293, HEK-293T, SLK, Beas-2b and C666-1 were cultured in polystyrene cell culture flasks or dishes in Dulbecco's Modified Eagle Medium (DMEM) supplemented with 10% fetal calf serum (FCS, PAA), 1% Penicillin/Streptomycin and 1% sodium pyruvate. Cells were cultured at 37 °C with 5% CO₂. Cells were split in a 1:10 ratio every 3-5 days when they reached a cell density of 90%.

The primary cells Human Nasal Epithelial primary Cells (HNEpC) were cultivated in medium without antibiotics and split weekly.

Cells were split by washing once with Trypsin/EDTA and then incubating them with Trypsin/EDTA for 1-5 min at RT or 37 °C until the cells detached from the bottom of the flask and from each other. Cells were then resuspended in DMEM and 1/10 was reseeded with fresh medium.

3.4.2. Culture of Suspension Mammalian Cell Lines

The non adherent cell lines BJAB, Jijoye, Raji, B95.8, 211-98 and 260-98 were cultured in RPMI 1640 containing 10% FCS (or 20% for 211-98 and 260-98) and 1% Penicillin/Streptomycin at 37 °C and 5% CO₂. Cells were grown to a density of 1-2x 10⁶ cells/ml and then split 1:5 in fresh medium.

3.4.3. Cryo-freezing of Cell Lines

For long time storage of cells, sub-confluent cells were resuspended in cell culture medium, pelleted by centrifugation (1000 rpm, 3 min, RT, Heraeus) and resuspended in FCS containing 10% DMSO. The mixture was aliquotted in CryoPure tubes and slowly frozen to -80 °C in an isopropanol containing box. The cells were then transferred and stored in liquid nitrogen.

To bring cells back into culture from a frozen stock, the cells were thawed at 37 °C in a water bath and immediately added to 10 ml of cell culture medium, centrifuged (1000 rpm, 3 min, RT, Heraeus) and resuspended in fresh medium in a new flask.

3.4.4. Transfection

The transfection of cells was performed using different components depending on the cell line. In general, cells were seeded one day prior to transfection. Cells were counted in a Neubauer counting chamber. To identify the amount of living cells, these were stained with Trypan Blue by mixing 1 volume Trypan Blue with 1 volume cell suspension for an incubation time of 5 min. Damaged cells were stained blue. Cells were counted under the microscope and cell number was determined using the following formula.

$$cell\ number = \frac{cells\ (in\ 4\ large\ squares)}{4} \times 10000$$

The next day cells achieved a density of about 60-80%. The number of seeded cells and amount of transfected DNA is shown in table 3-42.

Table 3-42 Cell Seeding

Plate	Density	Amount
96 Well	2*10 ⁴ /Well	0.1-0.2 µg
24 Well	2*10 ⁵ /Well	0.3-0.5 µg
6 Well	1*10 ⁶ /Well	1-2 µg
10 cm dish	5*10 ⁶ /dish	5-10 µg

3.4.4.1. Transfection with Polyethyleneimine (PEI)

Polyethylenimine (PEI) is a basic and branched molecule. It was dissolved in ddH₂O at a concentration of 1 mg/ml and neutralized to pH 7.2 with HCl. The solution was then filter sterilized (0.22 µm), aliquoted and stored at -80 °C. The working solution was stored at -20 °C.

For transfection, DNA was resuspended in Opti-MEM[®] cell culture medium and PEI was added afterwards. The solution was shortly vortexed and incubated for 10-15 min at RT. Cells were washed once with DMEM without supplements and covered with Opti-MEM[®]. The DNA-PEI mixture was added slowly in a dropwise fashion to the cells. The amounts of PEI and Opti-MEM[®] are listed in table 3-43.

Table 3-43 Transfection Mixture for PEI Transfection

Plate	Opti-MEM [®] (cells)	Opti-MEM [®] (DNA)	PEI
96 Well	0.075 ml	0.025 ml	1 µl
24 Well	0.5 ml	0.05 ml	2 µl
6 Well	1 ml	0.1 ml	5-10 µl
10 cm dish	4 ml	1 ml	40 µl

After 6 or 24 h the medium was changed to DMEM with supplements.

3.4.4.2. Transfection with FuGene[®]6

FuGene[®]6 (Roche) is a lipid based transfection reagent. First, FuGene was mixed in medium without supplements. After 10 min incubation, the mixture was slowly added to the DNA, mixed and further incubated at RT for 15 min. Then the mixture was added slowly and dropwise to the cells containing fresh medium with supplements. It was not necessary to change the medium after transfection. The amount of FuGene[®]6 used is listed below.

Table 3-44 Transfection Mixture for Fugene Transfection

Format	DMEM (on cells)	DMEM without suppl. (DNA)	FuGene [®] 6
6 Well	1 ml	0.1 ml	2 µl
10 cm dish	4 ml	1 ml	10 µl

3.4.4.3. Transfection with Lipofectamine[™]2000

Lipofectamine[™]2000 is a liposome based transfection reagent and is suitable for cotransfecting DNA and synthetic small RNAs like siRNAs. Lipofectamine[™]2000 and DNA were diluted separately in the same volume of Opti-MEM[®] cell culture medium and incubated for 5 min at RT. Both were then mixed together and further incubated for 20 min at RT. Then the mixture was added slowly and dropwise to the cells containing Opti-MEM[®] cell culture medium. Prior to adding cell culture medium, cells were washed once in DMEM without supplements. After 4-6 h post transfection, the medium

was changed and fresh DMEM with supplements was added. The amount of Lipofectamine™2000 and DNA used is listed below.

Table 3-45 Transfection Mixture for Lipofectamine Transfection

Format	Opti-MEM® (cells)	Opti-MEM® (DNA)	Opti-MEM® (Lipof.)	Lipof.
6 Well	1 ml	0.05 ml	0.05 ml	2 µl
10 cm dish	4 ml	0.5 ml	0.5 ml	10 µl

3.4.4.4. Electroporation

Electroporation was used to transfer DNA into non adherent cells in order to generate stable cell lines. Cells (1×10^7) were washed and resuspended in RPMI (0.5 ml) without supplements. Linearized purified DNA (20 µg) was pipetted into a electroporation cuvette, then 480 µl cell suspension were added and the components were mixed. The cells and DNA were incubated for 20 min at room temperature and resuspended again. The cuvette was then transferred into the electroporation chamber and electroporated. The electroporation conditions varied slightly according to the cell line and size of the cuvette. In general, BJAB cells were electroporated at 250 V, 975 µF, $\infty \Omega$. After electroporation, cell debris were removed carefully with a pipet tip and cells were transferred in a new culture flask (T75) with fresh supplemented RPMI medium. The cells were grown under selection (G418) for several weeks.

3.4.5. Generation of Stable Cell Lines

Constitutive EBV miRNAs stable cell lines were generated as model system to analyze latent infection of EBV. Either BJAB or Beas-2b cells were used to generate EBV miRNA stable cell lines. DNA was transferred by electroporation (see 3.4.4.4) or by transfection (see 3.4.4.3), respectively.

The DNA (pcDNA3-GFP-miR or control vector (pcDNA3-GFP, pcDNA3-IRES-GFP)) was linearized with *PvuI*, a restriction enzyme which leaves the resistance gene and the gene of interest intact, to facilitate and direct insertion into the cellular DNA. This was further achieved through antibiotal selection with G418. Inserted vector DNA leads to the expression of a neomycin resistance gene and accordingly to neomycin resistance. After a few weeks of selection > 90% of cells were GFP positive, which was increased to 100% by FACS-sorting.

3.4.6. Fluorescence Activated Cell Sorting (FACS)

Cells can be distinguished by their specific properties, such as volume and granularity. Furthermore it is possible to separate cells after staining them with fluorescent antibodies directed toward different proteins or after transfection with fluorescent proteins. In principle a beam of light (usually laser light) of a single wavelength is directed onto a hydrodynamically-focused stream of fluid, which contains

the cells. Different detectors analyze each passing cell, since each particle passing through the beam scatters the ray, depending on its properties. One detector is located in line with the light beam to measure the forward scatter (FSC) and others are perpendicular to it to detect the sideward scatter (SSC) and fluorescence signals. The FCS is correlated with the cell volume, the SSC with the granularity and the different light sources can excite different fluorescence dyes.

Fluorescence Activated Cell Sorting (FACS) was used to selectively collect GFP positive cells from transfected cells after G418 selection, to further increase the amount of cells that have stably and functional inserted the transfected plasmid (see chapter 3.4.5) (FACS was performed in the HPI by Arne Düsedau). Furthermore, flow cytometry was used to quantitate the amount of transfected or infected cells.

Prior to flow cytometry analysis or FACS, the cells were collected and pelleted (1200 rpm, 3 min, RT; Multifuge 3 S-R). Cells were afterwards resuspended in an appropriate volume of FACS buffer (PBS with 3% FCS) for sorting or in PBS for analysis without sorting. Sorting was performed on FACSaria and analysis was performed on the FACSCanto using the FACSDiva Software.

3.4.7. Induction of Interferon Signaling

Interferons are produced upon diverse stimuli like viral infections. Binding to their receptor on cell membranes lead to signal cascades and transcription of a set of genes, which are important in antiviral defense. To analyze the activation of interferon induced genes and to analyze, if EBV-encoded miRNAs are interacting with this pathway, stable cell lines were incubated with 100 or 1000 U IFN- β for 6 or 24 h, prior to protein extraction and Western blotting (see 3.3.1. and 3.3.4.).

3.4.8. Adenovirus

Adenoviruses were generated to obtain viruses infecting primary cells with a high efficiency. Different viruses were produced expressing either IRES-GFP, BHRF-miRNAs or BART-miRNAs.

The AdEasy™ system was developed by He et al. (He et al., 1998) and utilizes *E. coli's* efficient recombination machinery for generation of adenoviruses, thereby circumventing restriction and ligation of the large adenovirus genome. Briefly, the DNA of either IRES-GFP, BHRF-miRNAs or BART-miRNAs was first cloned into a transfer vector (pShuttle-CMV). The resulting plasmid was then linearized with *PmeI* and transformed into *E. coli* together with the viral DNA plasmid (pAd-Easy-1). Recombinants were screened by restriction digestion and positive constructs were further cleaved with *PacI* to expose the Inverted Terminal Repeats (ITR). The linearized bacmid was then transfected into 293 cells for virus production.

Adenoviruses were generated in cooperation with Peter Groitl (Department Molecular Virology, Heinrich-Pette-Institute) and are a part of the diploma thesis of our diploma student Ina Kowalski

(Title: Charakterisierung der MicroRNAs des Epstein-Barr-Virus (EBV), 2008, University Rostock, Germany).

3.4.8.1. Generation of Virus from DNA

The bacmid containing the viral DNA was first linearized by *PacI* digestion and purified by precipitation with 1/10 vol 3 M NaOAc and 1 vol isopropanol. Then the pellet was washed in 75% ethanol and 5 µg of DNA were transfected into E2E cells by lipofectamine transfection. The medium was changed after 16 h and replaced with DMEM containing supplements. After 5 days the cells were harvested (1000 rpm, 3 min, RT, Heraeus). The cells were then subjected to three freeze-thaw cycles by freezing in liquid nitrogen and thawing in a 37 °C water bath to release the virus from the cells. Afterwards cell debris were pelleted (4500 rpm, 5 min, RT, Multifuge 3S Heraeus) and the supernatant was sterile filtrated (0.22 µm).

3.4.8.2. Propagation and Storage of Adenovirus Stocks

To generate high titer virus stocks, several 10 cm dishes containing 293 cells were infected with an MOI of 20 for 2 h. The medium was then changed to DMEM containing supplements and the cells were harvested after 4 days. Cells were initially pelleted by centrifugation (1000 rpm, 3 min, RT, Heraeus) and resuspended in DMEM without supplements. Virus was released as described above and pelleted. Virus-containing supernatant was transferred into a new tube and mixed with 87% Glycerol in a 1:1 ratio for long term storage at -80 °C

3.4.8.3. Titration of Virus Stocks

293 cells were seeded one day prior transfection in a 6 well plate at a density of 1×10^6 cells per well. The next day cells were infected with different dilutions of adenoviral stocks ranging from 10^{-2} to 10^{-7} . After 24 h the cells were fixed with 1 ml of ice cold methanol and incubating for 20 min at -20 °C. Afterwards methanol was removed and cells were air dried for 5 min. Then the cells were washed once with 1x TBS supplemented with BSA and Glycin (TBS-BG) for 10 min and the first antibody against the E1A protein was added in 1ml of 1x TBS-BG. Cells were incubated on a rocking plate for 2 h at RT. The first antibody solution was removed and cells were washed 3 times for 5 min with 1x TBS-BG. Subsequently the secondary antibody was added in 1x TBS-BG and cells were incubated for 2 h with light exclusion and under constant slow agitation. The cells were washed again 3 times with 1x TBS-BG and coated with 1 ml PBS prior analysis by microscope. Positive cells were counted to determine the titer, which was calculated with the following formula.

$$Titer = Cells \times Microscope\ Factor \times Dilution$$

Table 3-46 Microscope Factors for Calculating Adenoviral Titer

Magnification	Factor Microscope
10x 10	389
20x 10	1600
40x 10	6399

Table 3-47 TBS BG Buffer 10x

Component	Concentration
TRIS-HCl pH 7.6	20 mM
NaCl	137 mM
KCl	3 mM
MgCl ₂	1.5 mM
Tween 20	0.05%
Na-acid	0.05%
Glycin	5 mg/ml
BSA	5 mg/ml

3.4.8.4. Infection with Adenovirus

The specific MOI of adenovirus infection to obtain 100% infection was determined for each cell line used. The MOI was calculated using the following equation:

$$Virus[\mu l] = \frac{cell - number}{Titer} \times MOI \times dilution$$

Cells were seeded 1 day prior to infection and the next day washed once in DMEM without supplements. Subsequently fresh DMEM without supplements was added containing the diluted virus. After 1 h twice of the initial volume of DMEM with supplements was added and the cells were grown for 24 h up to several days.

3.4.9. Luciferase Assay

To confirm a direct binding of a miRNA to a target mRNA the luciferase assay system was used with the pMIR-ReportTM miRNA Expression Vector System.

In the pMIR-Report vector the firefly luciferase is expressed as a reporter gene. The 3' UTR of a mRNA of interest can easily be cloned behind the open reading frame of the luciferase. This leads to a potential target mRNA for a specific miRNA. Binding of the miRNA to the target site in the 3'UTR should then lead to translational repression and according to this, the luciferase should be decreased in expression level and activity.

The firefly luciferase is a monomeric 61 kDa protein which catalyzes luciferin oxidation using ATP•Mg²⁺ as a co-substrate. Light is produced by converting the chemical energy of luciferin oxidation through an electron transition, forming the product molecule oxyluciferin.

One day prior to transfection 2×10^4 293T cells were seeded in each well of a 96 well plate. Cells were then transfected with the pMIR-report construct (expressing the luciferase including the 3' UTR of interest), the pcDNA3-GFP-miRNA construct (expressing the miRNA of interest) and a β -Gal expressing vector for normalization. The transfection set up is shown in table 3-48.

Table 3-48 Transfection Mixture for Luciferase Assay

Material	Amount
Luciferase Reporter vector	5 ng
β -Gal vector	50 ng
miRNA expression vector	50 ng
Opti-MEM	ad 25 μ l
PEI	1 μ l

Transfections were done in duplicate or triplicate. Lysates were prepared 24 h post transfection for the measurement of luciferase and β -galactosidase activity. Cells were washed once in 50 μ l PBS and then lysed in 100 μ l 1x RLB (Renilla Lysis Buffer). To completely destroy the cells, the plate was frozen once at -80 °C for at least 30 min. Before measuring the luciferase activity, the lysates were thawed at RT for 30 min and homogenized by pipetting.

The galactosidase activity was measured by transferring 50 μ l lysate in a new 96 well plate and mixing with 50 μ l 2x Z-buffer (table 3-49) with o-nitrophenyl- β -D-galactopyranoside (ONPG) and freshly added β -mercaptoethanol (7 μ l/ml). Depending on the concentration of β -galactosidase the plate was incubated at RT or 37 °C for a few minutes up to 1 h. As soon as a faint yellow color was observed, the reaction was stopped with 150 μ l of 1 M NaCO_3 . Immediately afterwards the absorption at 420 nm with a reference at 650 nm was measured with the microplate reader Synergy Mx using the Gen5 data analysis software.

Luminescence was measured by transferring 20 μ l of lysate into a flat bottom white 96 well plate and adding 100 μ l of the Renilla Assay Substrate solution. Luminescence was measured over 10 ms. The obtained light units were subsequently normalized to the absorption of β -galactosidase activity.

Table 3-49 Z-buffer with ONPG 2x

Reagents	Concentration
Sodium Phosphate Buffer, pH 7.3	200 mM
MgCl_2	2 mM
ONPG	1.33 mg/ml
β -Mercaptoethanol (freshly added)	100 mM

3.4.9.1. Cloning of Controls for the Luciferase Reporter Assays

A control luciferase reporter was generated containing a binding site for miR-BART-5. The site was amplified with three different primer pairs: 5' _Luc_BA5_HindIII and 3' _Luc_BA5_BanI, 5' _Luc_BA5_BanI and 3' _Luc_BA5_BanI and 5' _Luc_BA5_BanI and 3' _Luc_BA5_SpeI. All three fragments were restricted with BanI and ligated with a ratio 1:5:1. Afterwards, the fragments were

amplified again with the primers 5' _Luc_BA5_HindIII and 3' _Luc_BA5_SpeI, restricted with HindIII and SpeI and ligated into the same sites of the pMIR-Report vector. Clones were analyzed and two clones containing an insert of appropriate size for one, as well as four binding sites were sequenced.

3.5. DNA Microarrays

MiRNAs can regulate gene expression post transcriptionally by binding imperfectly to the 3'-UTR of their target mRNAs, thus leading subsequently to a destabilization of the corresponding mRNA. To identify miRNA target mRNAs, whole genome expression arrays (Agilent 4x44K) were performed from stable cell lines (BJAB or Beas-2b, see 3.4.5) expressing all EBV miRNAs and GFP or only GFP. Additionally Human Nasal Epithelial primary Cells (HNEpC) were infected with adenoviruses containing all BART miRNAs or IRES-GFP. RNA (1 µg) was labeled using the Quick Amp Labeling Kit. Figure 3-2 shows the work scheme for performing a dual color gene expression array.

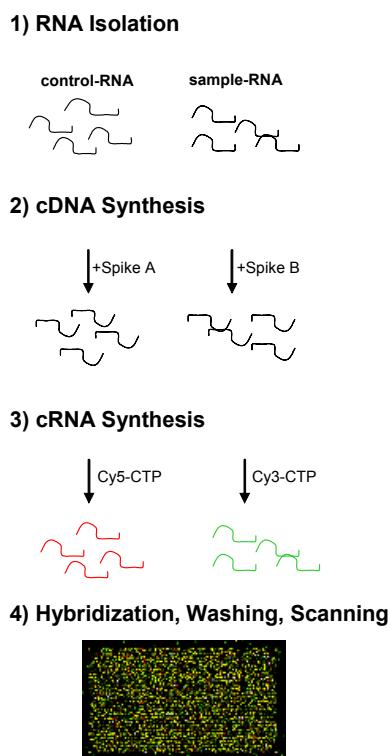


Figure 3-2 Schematic Workflow of Gene Expression Microarrays

Control and sample RNA are first reverse transcribed to cDNA. Concomitant a promotor for T7 RNA polymerase is added. Second, the cDNA is transcribed in cRNA with T7 RNA Polymerase, incorporating Cy5 or Cy3 labeled CTP for control or sample RNA, respectively. Third, RNA is purified and the same amount of control and sample amount is hybridized to one array.

Initially RNA was purified with the RNeasy Kit and loaded onto a formaldehyde agarose gel (3.2.2) to prove integrity.

3.5.1. cDNA Synthesis with Spike-in Controls

Control RNA and sample RNA including spike in controls (one for each dye: spike A for Cy3, spike B for Cy5) were transcribed into cDNA. Spike in RNAs were first diluted according to the manufacturer's instructions 1:20 and afterwards to 1:40. From the last dilution 2 µl were mixed with 1.2 µl T7 promotor primer and 1 µg sample RNA in 8.3 µl DEPC-H₂O, heated to 65 °C for 10 min and incubated on ice for 5 min. Subsequently 8.5 µl of a cDNA mix were added.

Table 3-50 cDNA Synthesis for Expression Arrays

Reagents	Amount
5x FS Buffer	4 µl
DTT [0.1 M]	2 µl
dNTPs [10 mM]	1 µl
MMLV-RT	1 µl
RNaseOut	0.5 µl

The cDNA synthesis was performed at 40 °C for 2 h. Afterwards the reverse transcriptase was inactivated by heating the samples to 65 °C for 15 min and incubated on ice for 5 min.

3.5.2. cRNA Synthesis with Fluorescence Dye Incorporation

After cDNA synthesis, 60 µl of transcription master mix (listed in table 3-51) were added.

Table 3-51 cRNA Synthesis and Labeling of RNA for Expression Arrays

Reagents	Amount
DEPC-H ₂ O	15.3 µl
4x Transcription buffer	20 µl
DTT [0.1 M]	6 µl
NTP-Mix	8 µl
50% PEG	6.4 µl
Anorganic Phosphatase	0.5 µl
T7-RNA Polymerase	0.6 µl
RNaseOut	0.8 µl
Cyanine 3-CTP or Cyanine 5-CTP	2.4 µl

The cRNA synthesis was carried out at 40 °C for 2 h. Samples were purified with the RNeasy Kit and purity and dye incorporation were measured spectrophotometrically. The total amount of RNA was calculated with the following formula.

$$\frac{(\text{Concentration of cRNA}) \times 30 \mu\text{l (elution volume)}}{1000} = \mu\text{g of cRNA}$$

The specific activity was calculated with the following formula:

$$\frac{(\text{Concentration of Cy3 or Cy5})}{(\text{Concentration of cRNA})} \times 1000 = \text{pmol Cy3 or Cy5 per } \mu\text{g cRNA}$$

Only if the reaction yielded more than 825 ng cRNA and if the specific activity was greater than 8 pmole per μg cRNA, the samples were hybridized to the array. Otherwise the labeling reaction was repeated.

3.5.3. Hybridization of DNA Microarrays

The same amount of labeled Cy3 and Cy5 cRNA were mixed with the reagents listed in table 3-52.

Table 3-52 Hybridization Mixture for Expression Arrays

Reagents	Amount
Cy-3 labeled cRNA	825 ng
Cy-5 labeled cRNA	825 ng
10x Blocking solution	11 μl
DEPC-H ₂ O	ad 52.8 μl
25x Fragmentation buffer	2.2 μl

The mixture was incubated for 30 min at 60 °C, immediately mixed with one volume of 2x GEx Hybridization Buffer HI-RPM and loaded onto the array. Incubation of the array was performed for 17 h at 65 °C and 10 rpm in a hybridization oven slowly rotating.

3.5.4. Washing of DNA Microarrays

After disassembling the chamber and dissociating the gasket slide, the array was washed in a glass container filled with wash buffer 1. The array was transferred carefully with tweezers in a second glass container with a holder for the array filled with wash buffer 1. A magnetic stir bar under the holder was slowly rotating for 1 min. Afterwards the holder containing the array was transferred into a third glass container with magnetic stir bar and prewarmed wash buffer 2 and incubated for 1 min under stirring. Then the holder was taken out carefully and very slowly (10 s) allowing the array to dry and then was shortly centrifuged on a cell culture dish holder (300 rpm, 2 min, RT, Heraeus). The array was immediately scanned on a GenePix reader 4100A.

3.5.5. Scanning and Evaluation of DNA Microarrays

3.5.5.1. Scanning

The GenePix 4100A uses a high-sensitivity, low-noise photo multiplier tube (PMT) to detect the emitted light.

A preview scan with 40 μm resolution was performed to automatically determine the PMT gain for each wavelength. After that the first scan was performed using a 5 μm spatial resolution with the calculated optimal PMTs and then 2-3 further scans were done using higher and lower PMTs. The

dynamic range of a detection is the range of signal values over which the instrument can accurately measure changes and is often considered in conjunction with its detection limit. The detection limit is defined as the dye concentration for which the signal to noise ratio is 3. The signal to noise ratio is calculated with the following formula:

$$\text{Signal to Noise Ratio} = \frac{(\text{Signal} - \text{Background})}{\text{Standard deviation of Background}}$$

3.5.5.2. Evaluation

To get more reliable results, two different analysis softwares, the GenePix software and the Feature Extraction software in combination with GeneSpring GX10 were used.

For GenePix analysis, the image and grid file were opened simultaneously in the program. After placing the grid exactly over the spots, features in a selected block were aligned and analyzed. Integrated settings like “fair features” were further used to flag spots as “good” when fulfilling the fair feature criteria. All “good” flagged spots were included for normalization and control spots were excluded. Normalization was performed using the ratio of medians of all normalization features to yield an overall ratio of 1. Results were exported as .txt or .gpr file for further analysis. The cut off was calculated using the genome browser. Multiple spots of the same substance were averaged. This was performed with Microsoft Excel for either one or two arrays. For biological duplicate experiments a standard deviation was calculated for each substance.

Feature Extraction (FE) consists of two major processes, first the image analysis to place the grid and locate spots and second the data analysis to define and measure spot features for gene expression. FE automatically detects the array barcode and loads the corresponding grid template and an extraction protocol. The grid template was automatically fitted to the spots and the FE extraction protocol was applied to carry out data analysis.

During data analysis FE removes outlier pixels and calculates statistics of inlier pixels of features and background. The software subtracts the background from the features. It also estimates the error at this point. With the 2-color experiments, it performs dye normalization and for gene expression calculates a p-value, that is a confidence measure of differential gene expression.

Gene Spring GX10 was afterwards used to analyze the FE data from the Agilent expression arrays. Arrays were treated as duplicates or triplicates by giving them just one parameter in the experiment grouping step (e.g. Adeno infected = yes). Probe sets were then filtered by their flag values (analyzed by Feature Extraction) P(present), M(marginal) and A(absent). Only entities having the present and marginal flags in at least two or all samples are displayed in a profile plot. The significance analysis was performed afterwards using the T-test against 0 without correction. Fold change analysis was finally used to identify genes with expression ratios or differences between miRNA expressing cells and control cells, that are outside of a given cut off or threshold. The cut off was arbitrarily set to 1.2 fold.

3.6. Computational Methods

3.6.1. Prediction of Pre-miRNA Hairpins with VMir

The VMir program was established to predict pre-miRNA hairpins in a given sequence. Therefore the program moves a window of adjustable size (here 500 nt in length) with a given step size (here 10 nt) over the sequence of interest and predicts the secondary structure of the corresponding sequence using the RNAFold algorithm (Schuster et al., 1994). Hairpins with a size above a certain threshold are then identified and scored (Grundhoff et al., 2006). The hairpins detected in each of the windows are classified as Main, Subsidiary or Repeated Hairpins (MHPs, SHPs or RHPs), respectively to reduce the complexity of the prediction. Then, these hairpins are grouped into local families, which include hairpins at the same genomic location and identical core region but differing flanking regions or repeat families, in which hairpins of identical sequence and structure but different genomic location are pooled. In local families, the longest hairpin is designated MHP and the others SHPs, whereas the MHP of a repeat family is the 5'-proximal hairpin and all others are classified as RHPs. The results of the analysis can be visualized using a graphical user interface.

VMir scores are calculated for hairpins with a trimmed length of 120 nt. Each paired nucleotide in the hairpin gets 2 points. If the terminal loop includes more than 17 nt, for each additional nucleotide 1 point is subtracted from the score. Bulges are implemented in the score depending on their symmetry and size. Symmetric bulges ≤ 4 nt were subtracted (1 point per nucleotide), bulges > 4 nt were multiplied with a factor 1.5 for each nt and also subtracted. For each nt in an asymmetric bulge 2 points are subtracted. The resulting basic score is then multiplied with a factor I_p , that represents a value that a given hairpin is probably a pre-miRNA. Two data sets were used for the development of an algorithm that calculates I_p , a reference set of 175 known miRNAs and a training set of 5500 unrelated hairpins. For more details see (Grundhoff et al., 2006)

3.6.2. Prediction of Target mRNAs

3.6.2.1. Genome Browser

The Genome Browser is a program written by Adam Grundhoff and enables the prediction and visualization of potential miRNA binding sites on an RNA of interest. The program predicts target sites for miRNAs using the TargetScan algorithm. All mRNAs listed in the UCSC database are screened and every binding site gets a certain score.

TargetScan predicts generally mRNA targets by searching for the presence of conserved 8mer and 7mer sites that match the seed region of each miRNA (Lewis 2005). It is however also possible to predict nonconserved sites, which is important for the prediction of viral miRNA targets. In the newest release of the program, sites with mismatches in the seed region are also identified, when they are compensated by conserved 3' pairing (Friedman, 2009). Context scores are calculated displaying the predicted efficacy of targeting (Grimson, 2007). Additionally to the seed match are other criteria,

which are also considered in the calculation of target efficacy. Positive factors, that increase efficacy are AU-rich nucleotide composition near the site, the proximity to sites for coexpressed miRNAs, that may have cooperative action, additional residue pairing at miRNA nucleotides 13-16, the positioning within the 3'-UTR at least 15 nt away from the stop codon, and the positioning afar from the center of long UTRs.

Data from gene expression arrays (.gpr files) can be loaded into the genome browser. The standard deviation of the array data is automatically calculated and diverse statistics are listed in a separate window. The program also calculates the average 3'UTR length and analyzes the abundance of miRNA binding sites in the down or upregulated gene fraction. Each gene from the array data can be analyzed by visualizing the mRNA with possible miRNA binding sites and the picture of the corresponding spot. The further investigation of a putative target mRNAs was assisted by the genome browser, since good scoring binding sites can be easily visualized.

4. Results

4.1. Identification of Novel miRNAs Within the γ -Herpesvirus Family

4.1.1. Sequence Conservation Among γ -Herpesviruses

To date, more than 200 viral miRNAs have been identified. At the beginning of this work, the miRNA registry release v13.0 listed 146 viral miRNAs. These are mainly encoded by polyomaviruses and herpesviruses. Polyomaviruses encode for only one miRNA, whereas members of the herpesvirus family have been shown to encode for multiple miRNAs.

Since miRNAs are abundantly expressed by γ -herpesviruses compared to other DNA viruses it was suggested that the ability to encode miRNAs is a conserved feature of herpesviruses. Furthermore, a conservation of miRNA sequences might translate into conserved functions, by regulating the same sets of genes. Nevertheless, only two viruses have been shown to encode for conserved miRNAs, the γ -herpesviruses Epstein-Barr virus (EBV) and the related rhesus lymphocryptovirus (rLCV). These had been previously reported to encode 23 and 16 miRNAs, respectively, seven of them being partially conserved (Cai et al., 2006; Grundhoff et al., 2006; Pfeffer et al., 2005b). It was suggested that there are more examples of conservation. Therefore, a detailed analysis of miRNAs encoded by the γ -herpesvirus family was performed.

The aim of this work was to get a better insight into γ -herpesvirus miRNA conservation and function. Assuming that miRNAs are functionally important, their sequences should be more conserved than adjacent regions. The closer two viruses are related the more background conservation will occur and thus discrimination between false positives and true positives will increase with evolutionary distance. However, pre-miRNAs that are predicted within coding regions might either be conserved due to protein conservation or due to their own importance. Additionally, viral miRNAs are primarily encoded within intergenic and non-coding regions. Thus, to facilitate the analysis and to minimize the number of false positives, only non-coding regions were analyzed.

First, pre-miRNA hairpins were predicted in all fully sequenced γ -herpesvirus genomes using the VMir program. VMir is a previously designed algorithm for the *ab initio* prediction of pre-miRNA hairpins and uses the RNAFold algorithm for prediction (Hofacker and Stadler, 2006). Four γ -herpesviruses belonging to the lymphocryptovirus genus and ten from the rhadinovirus genus were analyzed (see table 4-1).

Table 4-1 γ -Herpesviruses Analyzed in This Work

Genus	Name	Abbreviation	Genbank
lymphocryptovirus	Callithricine herpesvirus-1	CaHV-3	NC_004367
	Epstein-Barr virus type I	EBV type I	NC_007605
	Epstein-Barr virus type II	EBV type II	NC_009334
	Rhesus lymphocryptovirus	rLCV	NC_006146
rhadinovirus	Equidherpesvirus-2	EHV-2	NC_001650
	Ovine herpesvirus-2	OvHV-2	NC_007646
	Alcelaphine herpesvirus-1	AHV-1	NC_002531
	Bovine herpesvirus-4	BoHV-4	NC_002665
	Saimiriine herpesvirus-2	HVS	NC_001350
	Kaposi's sarcoma associated herpesvirus type M	KSHV type M	NC_003409
	Kaposi's sarcoma associated herpesvirus type P	KSHV type K	NC_009333
	Rhesus rhadinovirus	RRV	NC_003401
	Japanese monkey herpesvirus	JMHV	NC_007016
	Murine herpesvirus-68	MHV-68	NC_001826

Several potential pre-miRNA hairpins were predicted for all viruses and passed the filter criteria, which are described in detail in 3.6.1. A total number of 42,356 hairpins were predicted. Out of these, 810 passed the filter criteria. Due to the partially inverted nature of the RNA sequences able to form stem-loop structures, these 810 hairpins included stem-loops that are predicted for both strands of the genome. In general only one strand is transcribed *in vivo* and produces a *bona fide* miRNA. The only known exceptions so far are mouse cytomegalovirus (MCMV) and herpes simplex virus type 1 (HSV-1), in which miRNAs are transcribed from bidirectional loci (Buck et al., 2007; Dolken et al., 2007; Umbach 2008). Excluding hairpins from the reverse strand that is not suggested to produce miRNAs *in vivo* decreases the number to 607 hairpin loci.

The sensitivity of the analysis was demonstrated by considering previously identified miRNAs. In the initial prediction, all 68 known miRNAs were predicted and 64 of them were retained after filtering. This elimination was performed to circumvent identification of miRNAs conserved, due to the fact that they are contained within overlapping coding regions, which generally show a higher conservation between viruses. For miRNAs encoded within ORFs, it is impossible to distinguish if miRNA conservation is due to conservation of the coding regions or due to the importance of the miRNA itself. On the basis of that, the number of predicted pre-miRNAs was further reduced to 61 miRNAs. In conclusion 548 novel pre-miRNA hairpin loci were predicted.

To identify conserved pre-miRNAs, pairwise BLAST alignments were performed for all combinations. The resulting sequence identity is shown in figure 4-1 A. A conserved pre-miRNA had to fulfill different requirements. These were:

- alignment to at least one putative orthologue pre-miRNA hairpin,
- conservation of six consecutive nt in one of the hairpin arms, and
- a second BLAST alignment of the two orthologues resulted in an expect value ≤ 0.01 .

The results of this analysis are depicted in figure 4-1 B. Figure 4-1 highlights the overall low sequence identity of γ -herpesviruses except for high identity between strain variants of a given virus (e.g. KSHV type P and M; EBV type I and II). Only two pairs show a significantly higher sequence identity, rhesus

Results

rhadinovirus (RRV) and Japanese monkey herpesvirus (JMHV), as well as Epstein-Barr virus (EBV) and rhesus lymphocryptovirus (rLCV). They had an overall sequence identity of about 88% and 60%, respectively. Interestingly, rLCV is the next related virus to EBV, infecting rhesus macaques. RRV and JMHV infect also rhesus macaques and are the related viruses to KSHV. So the question arises if these viruses express conserved miRNAs.

As depicted in figure 4-1, a correlation between the overall sequence conservation and the prediction of putative conserved pre-miRNAs was found. In accordance with the low sequence identity, in only two cases (apart from strain variants) the conservation of putative pre-miRNA hairpins was predicted. Indeed, these were RRV and JMHV and EBV and rLCV.

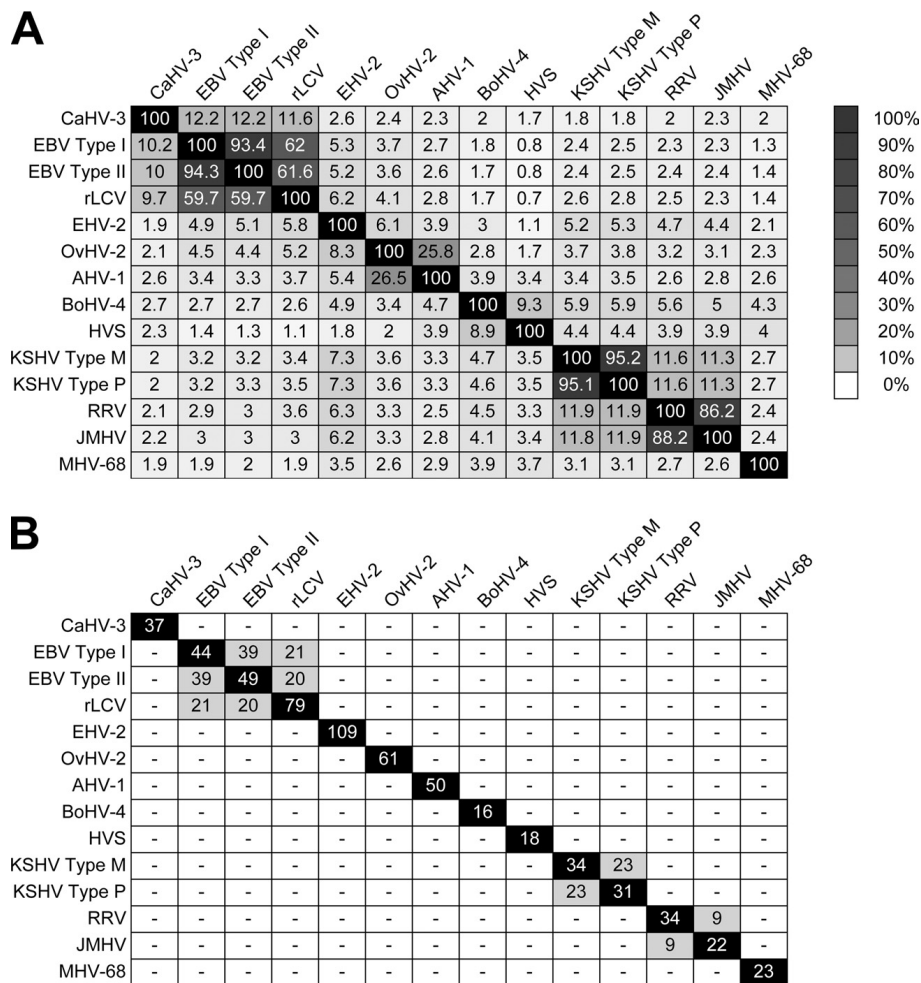


Figure 4-1 Sequence Identity and Pre-miRNA Hairpin Conservation of γ -Herpesvirus Genomes

All fully sequenced γ -herpesviruses were subjected to pairwise BLAST alignments. The sequence identity is given as percentage and additionally indicated by shading (A). Vmir prediction of pre-miRNA hairpins identified several putative pre-miRNAs in all tested genomes (white numbers on black background) and few conserved pre-miRNA hairpin loci (black numbers on grey background) (B) (Walz et al., 2010). (figure: Copyright © American Society for Microbiology, [J Virol, 84, 716-728, 2010])

4.1.2. VMir Prediction of Pre-miRNA Hairpins

A detailed analysis of the predicted pre-miRNA hairpin loci revealed that miRNAs are often located at similar positions in the genome. Some examples are shown in figure 4-2. The VMIR analysis of the closely related lymphocryptoviruses EBV and rLCV as well as the rhadinoviruses RRV and JMHV are depicted in figure 4-1 A and B, respectively. Both examples display conserved hairpins at the same genomic loci. While EBV and rLCV harbor two loci encoding for miRNAs, RRV and JMHV were predicted to encode conserved miRNAs only at one position.

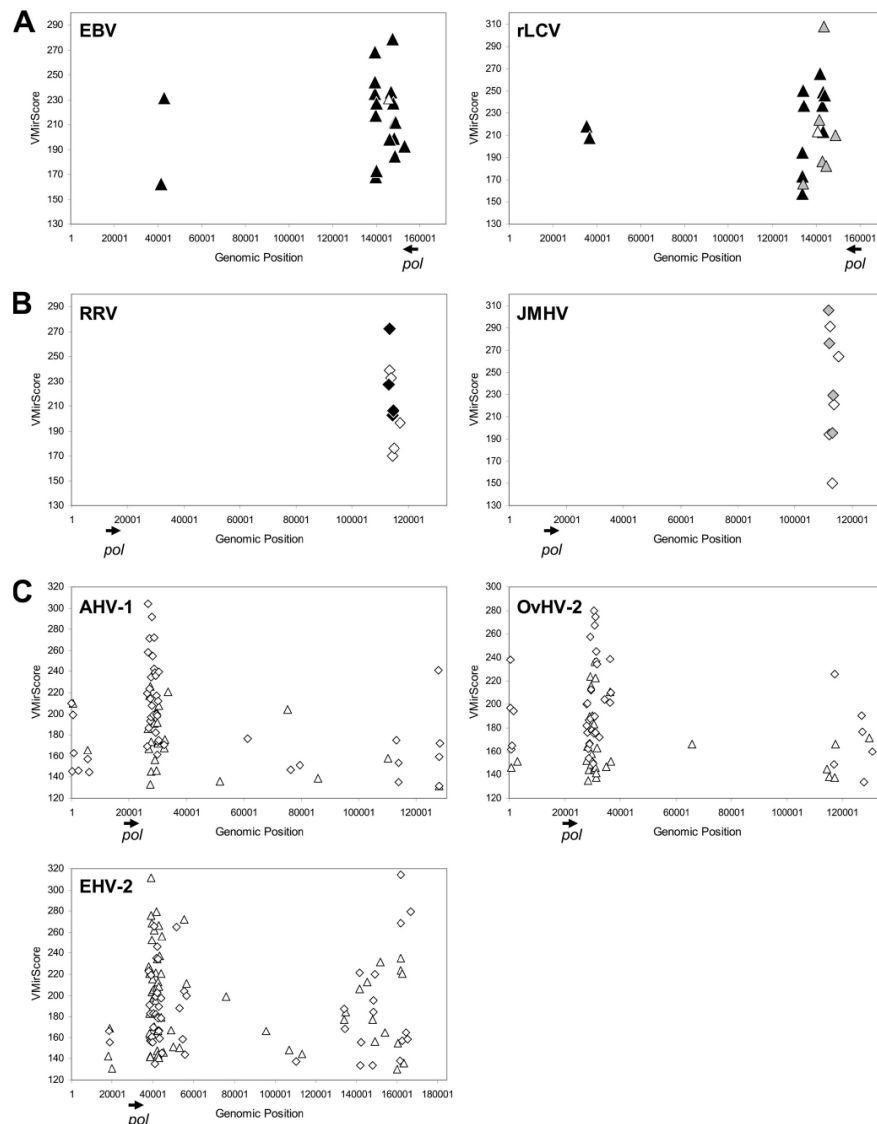


Figure 4-2 VMir Prediction of Pre-miRNA Hairpins Within γ -Herpesvirus Genomes

Shown are the VMir predictions for the conserved pre-miRNA hairpin loci between EBV and rLCV (A), RRV and JMHV (B) as well as non conserved pre-miRNA hairpin loci of AHV-1, OvHV-2 and EHV-2 (C). The genomic position is given on the x-axis, the VMir score on the y-axis. The location of the polymerase is marked with an arrow underneath the graph. Triangles and diamonds show miRNAs encoded in direct and reverse orientation, respectively. Dark, grey and white symbols depict known pre-miRNAs, novel predicted orthologues of known pre-miRNAs and novel predicted orthologues of unknown pre-miRNAs, respectively (Walz et al., 2010). (figure: Copyright © American Society for Microbiology, [J Virol, 84, 716-728, 2010])

In addition to the predicted conserved hairpin loci found in EBV and rLCV (4-2 A) and RRV and JMHV (4-2 B), the distantly related γ -herpesviruses AHV-1, OvHV-2 and EHV-2 were also predicted to encode for miRNAs at the same genomic location (4-2 C). Despite this fact, they were not conserved in sequence.

In this work miRNAs that are encoded by EBV, rLCV as well as RRV and JMHV were analyzed in detail. The following chapters include data from both analyses, since the methods that are used are identical.

4.1.2.1. Proof of Principle: VMir Prediction of Novel and Known Pre-miRNA Hairpins

The prediction of EBV pre-miRNA hairpins includes all 23 already known pre-miRNAs. Additionally, another conserved 16 pre-miRNA hairpin loci were predicted. Different analyses using a wide variety of methods for identification of miRNAs including cloning, Northern blot analysis and microarrays, were not successful in identifying any of the 16 (Cai et al., 2006; Grundhoff et al., 2006; Pfeffer et al., 2005b) suggesting that most of them are false positive predictions. A total of 21 and 20 conserved pre-miRNA hairpin loci were predicted for rLCV in comparison to EBV type I and II, respectively. The seven previously identified conserved pre-miRNAs were retained within the prediction (Cai et al., 2006). As mentioned in the beginning, due to a higher sequence conservation of closely related viruses (as for EBV type I and II) the prediction of pre-miRNAs is suggested to reveal a high number of false positives. Unlike the high conservation between EBV type I and II, the lower sequence identity of EBV versus rLCV should therefore reduce the amount of false positive predictions. Thus, it was assumed that the amount of conserved rLCV pre-miRNAs was significantly higher than previously thought.

KSHV encodes 12 miRNA hairpins, one encoded within the open reading frame of a latency gene. Only nine miRNAs were retained in the analysis, since two had a low VMir score due to folding in limited sequence context and one miRNA was missed due to its location within a coding region. In addition to the already known pre-miRNA hairpins, 14 novel conserved pre-miRNA hairpin loci were identified within the region that encodes for miRNAs. As mentioned above, these seem to be false positive predictions, since again several studies were not able to identify miRNAs arising from these precursors (Cai et al., 2006; Grundhoff et al., 2006; Pfeffer et al., 2005b; Samols et al., 2005). The detection limit of the methods used could just as well be a reason for missing these candidates.

RRV is a distantly related virus to KSHV and has also been shown to encode for seven miRNAs. Both viruses share only 12% sequence identity and no pre-miRNA hairpin was predicted to be conserved between the two viruses. Nevertheless, the viruses encode for pre-miRNA hairpins at the same genomic location. Interestingly, JMHV, another very closely related rhadinovirus to RRV, was predicted to share nine pre-miRNA hairpins with RRV. Out of these, four were predicted to be orthologues to known RRV pre-miRNAs (Schafer et al., 2007) and the remainder were novel predicted orthologues in both viruses. An overview of hairpin locations is given in figure 4-2B.

A detailed analysis showed that EBV and rLCV as well as RRV and JMHV are more divergent in the predicted regions encoding pre-miRNA hairpins compared to the miRNA encoding regions of EBV type I and II or KSHV type M and P. Therefore, it can be assumed that the predicted pre-miRNA hairpins are less likely false positives than the predicted for different subtypes. The results from global alignment analyses are given in figure 4-3.

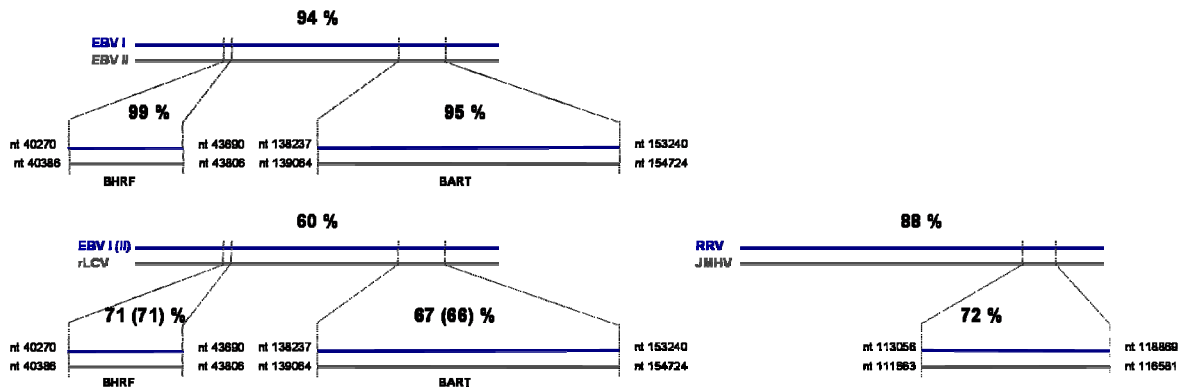


Figure 4-3 Global Alignment of miRNA-encoding Regions of EBV, rLCV, RRV and JMHV

Global Blast alignments were performed using Needleman-Wunsch Global sequence Alignment Tool (NCBI). Location of aligned sequences is shown by enlargement of genomic areas, and nt positions are indicated for each virus. Percentage of identical nucleotides is given above each alignment.

Whereas the closely related viruses EBV type I and II as well as RRV and JMHV show a higher or equal sequence identity within the miRNA encoding regions compared to the overall sequence identity (figure 4-3), the sequence identity between EBV and rLCV is higher within the miRNA encoding regions compared to the overall sequence identity. This strengthens the hypothesis that pre-miRNAs predicted in EBV and rLCV are less likely false positives than pre-miRNAs predicted in RRV and JMHV. However, all viruses were suggested to encode more miRNAs than identified so far.

4.1.3. Confirmation of Novel miRNAs of EBV, rLCV and JMHV by Northern Blot

The predicted precursor of putative miRNAs that passed the threshold ((min. score: 135, min. window count: 25, min. stem-loop length: 50, max. stem-loop-length: 220) (for details see 3.6.1)) were further analyzed in confirmatory Northern blots. The confirmation was performed by using RNA derived from cell lines latently infected with the corresponding virus and expressing the miRNAs (EBV and rLCV). For JMHV no latently infected cell lines were available and therefore confirmation of miRNAs was performed using transfected cells. A vector expressing all miRNAs encoded by JMHV was generated (see below and 2.7.1.2). The prediction of pre-miRNA hairpins in general allows a good estimation where the mature miRNA is located. The location of mature miRNA sequences is estimated to comprise 21 nt adjacently to the terminal loop. Probes were designed for either 5p and 3p arm of the predicted precursor and positioned adjacent to the terminal loop with a length of about 30

nt. However, secondary structure prediction is not accurate, especially for the size of the terminal loop and therefore exact shape and processing by Drosha and Dicer is not known.

EBV miRNAs

All hairpins of EBV type I and II that passed the threshold, were analyzed in Northern hybridization to either confirm novel pre-miRNA hairpins or to exclude false positive predictions. Since it has been shown that miRNA expression varies between cell lines and also differs based on the hairpin structures, RNA from different EBV positive B-cell lines Raji and Jijoye and an EBV positive epithelial cell line the nasopharyngeal carcinoma cell line C666-1, were used. The EBV negative B-cell line BJAB was used as negative control.

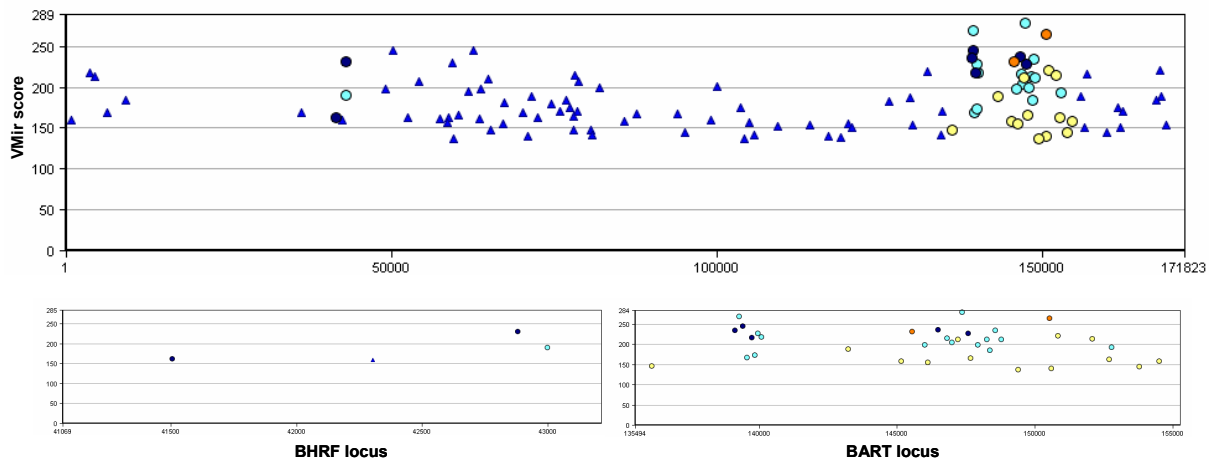


Figure 4-4 VMir Prediction of EBV Pre-miRNA Hairpins

The upper graph shows all predicted pre-miRNA hairpins, that passed filter criteria. The VMir score is given on the y-axis, the genomic position on the x-axis. The graphs below depict the enlarged BHRF and BART loci. Hairpins are shown as blue triangles and are encoded in the direct orientation of the genome. Dark blue circles display known conserved pre-miRNAs, and light blue circles display known non-conserved pre-miRNAs. Analyzed pre-miRNAs in this work are highlighted as orange and yellow circles for putative conserved and non-conserved pre-miRNAs, respectively.

The latency genes are encoded in direct orientation. According to this, the pre-miRNAs investigated are also predicted in the direct orientation. From the 15 novel predicted BART miRNA precursors, only two could be confirmed to be processed into mature miRNAs by Northern blotting (figure 4-4). They were named miR-BART-21, for which miRNAs from both arms of the hairpin could be detected, and miR-BART-22, which is shown to express just the 5p miRNA at detectable levels.

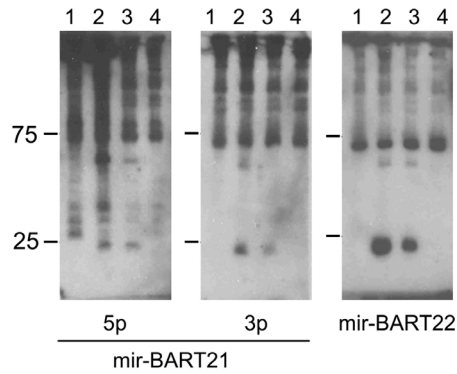


Figure 4-5 Confirmatory Northern Blot for Novel EBV miRNAs.

Four different cell lines were used: EBV negative B cell line BJAB (1) and three EBV positive cell lines, the epithelial cell line C666-1 (2), and two B cell lines Jijoye (3) and Raji (4) (Walz et al., 2010, modified). (figure: Copyright © American Society for Microbiology, [J Virol, 84, 716-728, 2010])

In all Northern blots, the epithelial cell line C666-1 showed the highest expression of mature miRNAs. The two miRNAs were also abundantly expressed in the B-cell line Jijoye but were not detectable in the B-cell line Raji. This is in good correlation with previous findings for other EBV miRNAs (Cai et al., 2006). The identification of two novel EBV miRNAs, which were missed in diverse previous analysis, argues for the high probability to detect novel miRNAs also in rLCV and JMHV.

rLCV miRNAs

The pre-miRNA hairpins predicted at the BHRF and BART loci of rLCV were investigated. Beneath several putative conserved pre-miRNA hairpins, non-conserved good candidates were also found. The analysis was therefore extended, to include all good performing pre-miRNA hairpins.

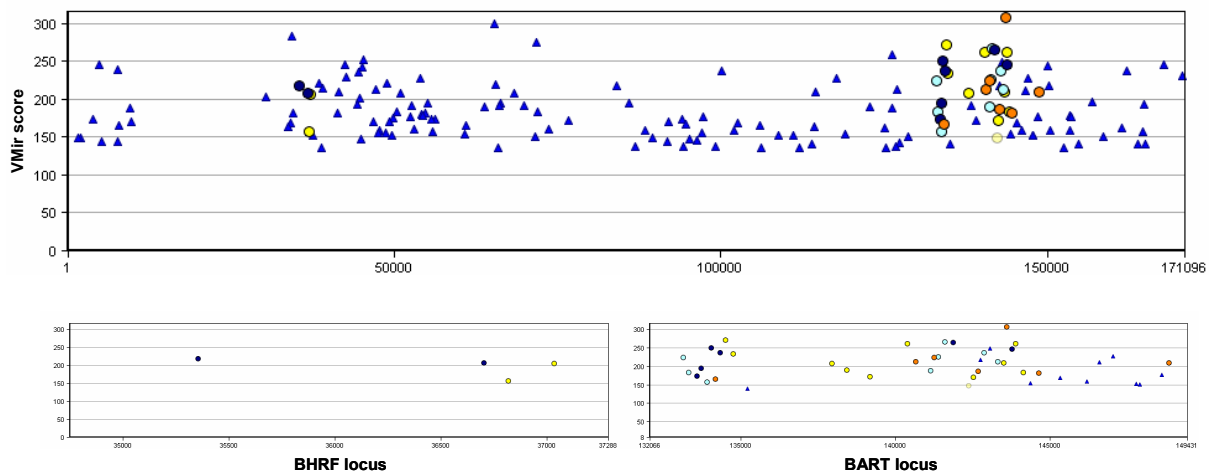


Figure 4-6 VMir Prediction of rLCV Pre-miRNA Hairpins

The upper graph shows all predicted pre-miRNA hairpins, that passed filter criteria. The VMir score is given on the y-axis, the genomic position on the x-axis. The graphs below depict the enlarged BHRF and BART loci. Hairpins are shown as blue triangles and are encoded in the direct orientation of the genome. Dark blue circles display known conserved pre-miRNAs, and light blue circles display known non-conserved pre-miRNAs. Analyzed pre-miRNAs in this work are highlighted as orange and yellow circles for putative conserved and non-conserved pre-miRNAs, respectively.

Altogether 20 pre-miRNA hairpins were analyzed by Northern blotting including one candidate found to be located in reverse direction and being conserved to miR-BART-9. On closer inspection, a hairpin was folded in reverse orientation to the gene product, but failed to pass the threshold. But a suboptimal folding with a slightly lower energy of 0.5 kcal/mol represents a good hairpin and so this one was included in the analysis.

RNA from EBV and rLCV negative B-cell line BJAB was used as a negative control and two rLCV positive B-cell lines, 211-98 and 260-98, were used to confirm rLCV miRNAs. In addition the EBV positive and rLCV negative cell line C666-1 was integrated to show cross reactivity of probes for conserved miRNAs. 17 out of 20 predicted precursors could be confirmed to be processed to mature miRNAs. Overall 22 novel mature miRNAs were identified (fig. 4-7).

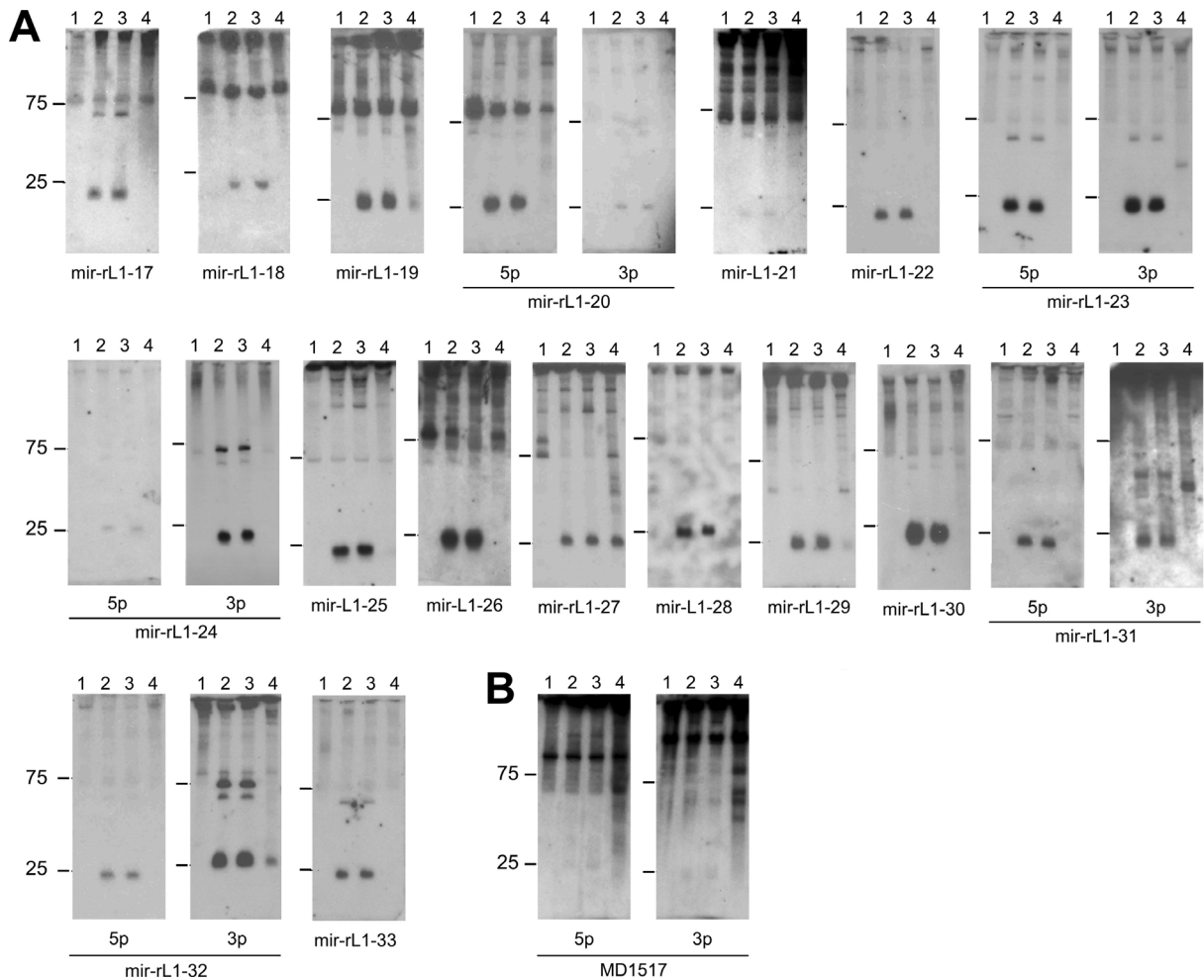


Figure 4-7 Confirmatory Northern Blots of Novel rLCV miRNAs.

Different cell lines were used for the detection: rLCV negative B cell line BJAB (1), rLCV positive B cell lines 211-98 (2) and 260-98 (3) and a rLCV negative but EBV positive epithelial cell line C666-1 (4). miRNAs which were further sequenced are shown in A, whereas a Northern Blot with a potential miRNA band for hairpin MD1517, which failed to be sequenced, is shown in B (Walz et al., 2010, modified). (figure: Copyright © American Society for Microbiology, [J Virol, 84, 716-728, 2010])

In some cases, i.e. hairpins rL1-19, rL1-27 and rL1-32 3p, the degree of conservation is represented by the cross-reaction of probes in the EBV positive cell line C6661-1 (fig. 4-7 A). The expression level varies for the different miRNAs. EBV and rLCV encoded miRNAs are expressed from one primary transcript, suggesting an equal expression level. Since the hairpins are different in structure, processing through Drosha and Dicer is affected. Therefore, some hairpins are more efficiently processed than others. One pre-miRNA hairpin (MD1517) leads to a faint reproducible band in the Northern blots, but further analysis (see below) could not confirm the existence of that miRNA. Nevertheless, it was included for completeness (fig. 4-7 B).

JMHV miRNAs

The Vmir prediction for JMHV miRNAs revealed only novel, putative, conserved pre-miRNA hairpins (figure 4-8), since the virus has been shown to be highly conserved to RRV (figure 1-1) and no viral miRNAs have been identified from JMHV so far. As for EBV and rLCV, the miRNAs are oriented in the same direction as the latent gene products (figure 4-8).

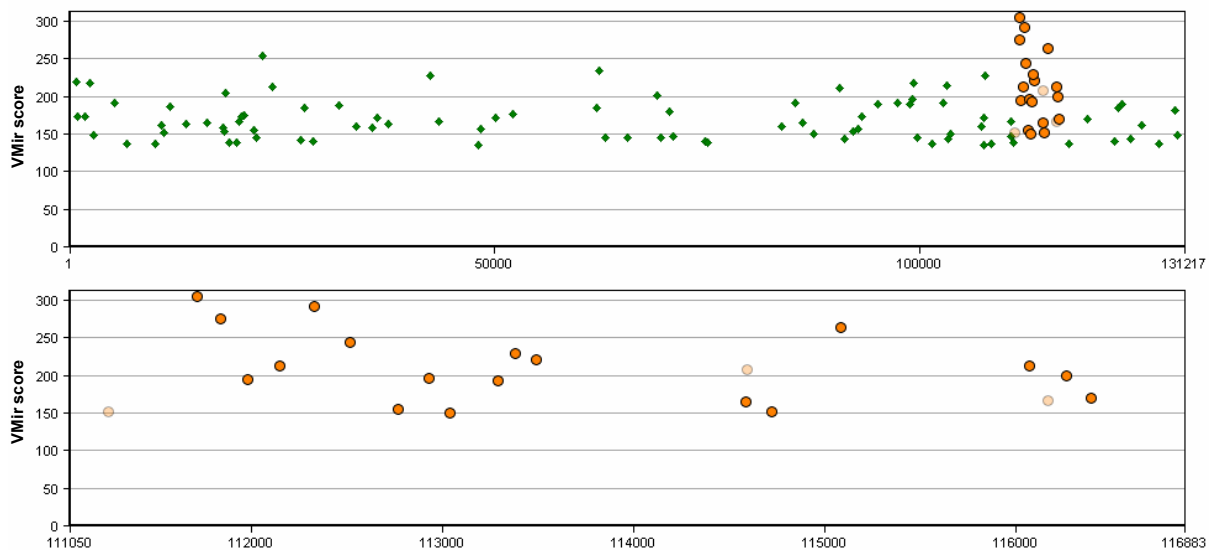


Figure 4-8 VMir Prediction of JMHV Pre-miRNA Hairpins

The upper graph shows all predicted pre-miRNA hairpins, that passed filter criteria. The VMir score is given on the y-axis, the genomic position on the x-axis. The graphs below depict the enlarged miRNA encoding region between ORF69 and ORF 71. Hairpins are shown as green diamonds and are encoded in the reverse orientation of the genome. Analyzed pre-miRNAs in this work are highlighted as orange circles for putative conserved pre-miRNAs.

Two circumstances hampered the further identification of JMHV miRNAs. First, no stably infected established cell lines were available for JMHV and, secondly, the amount of RNA from primary rhesus fibroblast infected with JMHV was restricted. To obtain sufficient amount of RNA, $1 \cdot 10^8$ primary cells had to be infected with JMHV, which makes the procedure very expensive. For that reason, the genomic region probably encoding for miRNAs was subcloned into the pcDNA3-GFP vector and used for transfection of 293T cells.

Two vectors were generated, pcGJmiR and pcGJmiR Δ containing the regions ranging from nt 111105 - 116751 and nt 111105 - 116283, respectively. The first contained a poly-A site at the beginning of the miRNA encoding region that was excluded in the second expression plasmid (see also chapter 2.7.1.2). The vector contains a CMV promoter that is Pol II driven and encodes for gfp and miRNAs. If the poly-A site is functional, some or all transcripts might be shortened by restriction and polyadenylation 10-30 nt behind this site and that would lead to a lower expression of the miRNAs. However, miRNAs were expressed from both vectors, but indeed the vector pcGJmiR Δ expresses miRNAs at a higher level (figure 4-9).

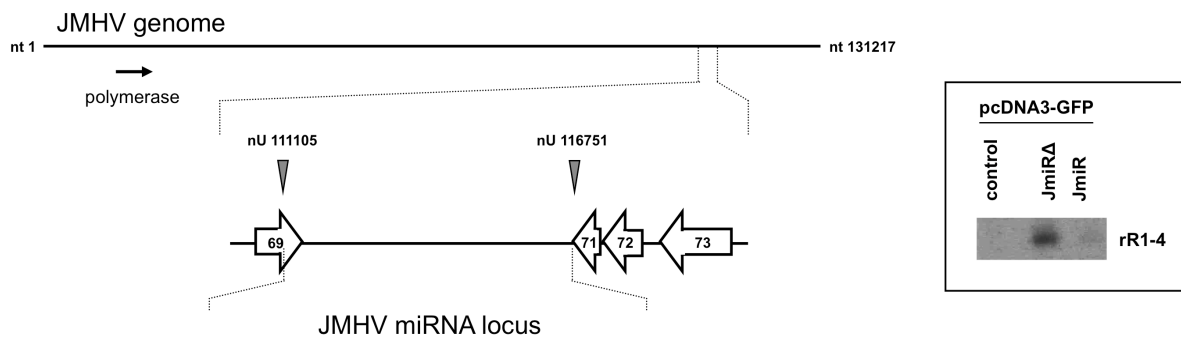


Figure 4-9 miRNA Locus of JMHV

The JMHV genome is shown at the top, location of polymerase gene is indicated by an black arrow. The miRNA locus is enlarged below the genome and open reading frames of adjacent genes are highlighted as large arrows. The region cloned into an expression vector is given by the nt positions of the miRNA locus. Northern blot analysis of transfected 293T cells with control, pcGJmiR Δ and pcGJmiR for one miRNA is shown on the right.

To confirm the predicted JMHV miRNAs, 293T cells were either transfected with the vector pcGJmiR Δ or the control vector pcDNA3-GFP. Twenty μ g RNA was used for Northern Blots.

A total of 21 different pre-miRNA hairpins were tested and 14 of them were shown to express mature miRNAs detectable in the Northern blot. Out of these 14 pre-miRNAs at least 9 expressed mature miRNAs from both arms as seen in figure 4-10. For miRNAs miR-rJ1-4, -7, -9, -10 and -14, only one mature miRNA could be detected in the Northern blot.

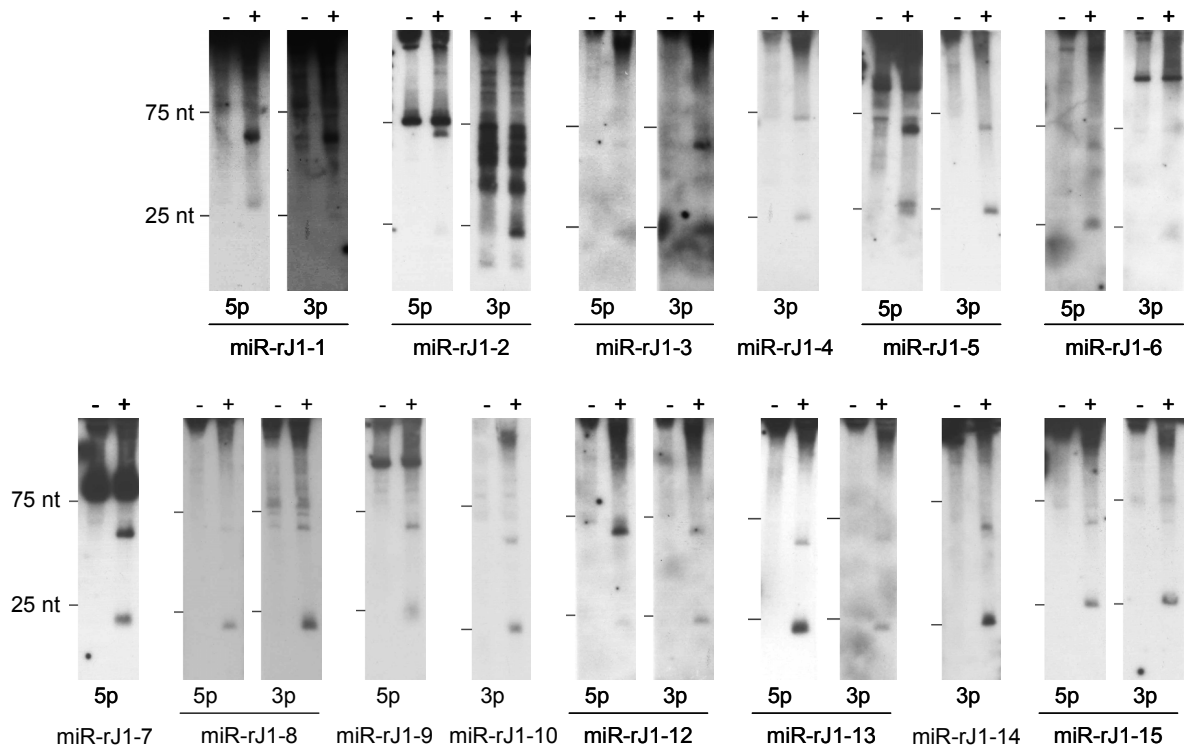


Figure 4-10 Confirmatory Northern Blots for JMHV miRNAs

293T cells were transfected with either pcDNA3-GFP (-) or pcGJmiRΔ (+) plasmid. RNA was isolated 48 h post transfection and 20 µg RNA were used and blots were exposed to autoradiographic films for 4 d.

Viral miRNAs encoded by RRV have been shown to increase in expression upon lytic replication. As mentioned before, no stably latent infected cell lines are available for JMHV. Infection of rhesus primary fibroblast cells with JMHV, however, results in lytic replication. Therefore it was tested, if miRNAs can be detected in JMHV infected rhesus primary fibroblast cells. A Northern blot containing 14 µg RNA of rhesus primary fibroblast cells infected with JMHV for 24, 48 and 72 h was probed with two different and abundantly expressed miRNAs (figure 4-11).

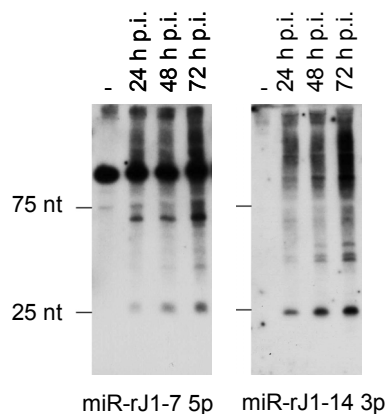


Figure 4-11 Confirmatory Northern Blot for miRNAs in JMHV Infected Rhesus Primary Fibroblast Cells

Rhesus primary fibroblast cells were either mock or JMHV infected for 24, 48 and 72 h, respectively. Shown are two miRNAs. For miR-7 5p and miR-14 3p, 14 and 10 µg RNA were used, respectively.

Both tested miRNAs miR-rJ7-5p and miR-rJ14-3p were abundantly expressed and expression increased over the time of infection.

4.1.4. Cloning of novel miRNAs from rLCV and JMHV

Isolation and cloning of mature miRNAs from cell lines or transfected cells was necessary to determine the exact 5'-sequence of the miRNAs, since the 5'-end contains the most important region for target mRNA binding, the seed region. This information is crucial for the computational prediction of target mRNAs. A schematic overview of the cloning approach is shown in figure 4-12.

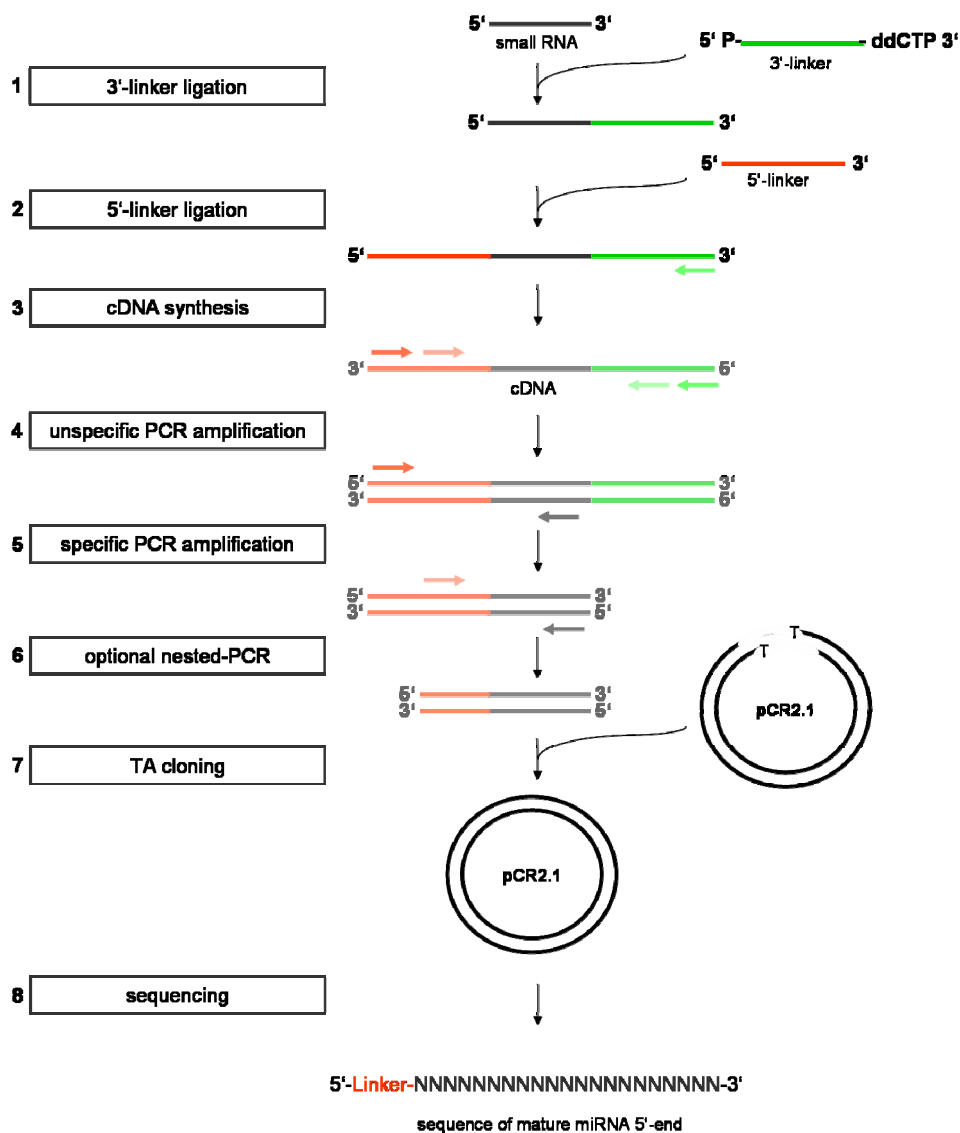


Figure 4-12 Schematic Overview of the miRNA Cloning Procedure.

Small RNAs are electrophoretically separated and ligated in several steps to 3'- and 5'-linkers (1-2). After cDNA synthesis (3), unspecific PCR with linker specific primers allows amplification of the pool of different DNAs (4). The specific PCR with one primer binding in the 5'-linker and a primer specific for each 3'-end of different miRNAs allows amplification of specific miRNA sequences (5, 6). Obtained PCR products are subjected to TA cloning (7) and sequenced to identify the 5'-end (8).

EBV and rLCV miRNAs

The cloning of novel EBV and rLCV miRNAs was performed using EBV and rLCV positive cell lines (C666-1 and 211-98 or 260-98, respectively). During this analysis the novel miRNAs from EBV were published (Zhu et al., 2009). Deep Sequencing of small RNAs identified the two novel pre-miRNAs (figure 4-5) and therefore the EBV miRNAs were not sequenced in this work. In contrast, rLCV miRNA sequences were investigated. The B-cell lines 211-98 and 260-98 were initially used in the cloning protocol, but all sequences were obtained in the end from the 211-98 cell line (table 4-2).

Table 4-2 rLCV miRNA Sequences
(Walz et al., 2010, modified)

miRNA	Sequence	Clones
rlcv-miR-rL1-17	UGCUUCGCCUCUCAUCAA	4
rlcv-miR-rL1-18	UUAGCCCCUCCCAUCAUCUUG UAGCCCCUCCCAUCAUCUUG	4 2
rlcv-miR-rL1-19	UAUAGAUAGCGUGGGUGUGUGA AUAGAUAGCGUGGGUGUGUGA	6 2
rlcv-miR-rL1-20-5p	UAAAGGGUAGUGUGUUCACAG	4
rlcv-miR-rL1-20-3p	UGUGGAACUAAUCCCUUAGU	3
rlcv-miR-rL1-21	AGGCCUCUUCACAAUUCUAA GCCUCUUCACAAUUCUAAU	3 1
rlcv-miR-rL1-22	UCACCGUUUCAUCCCCACGAUU	3
rlcv-miR-rL1-23-5p	UCACUAGUGCUGGCACCUAAGA	3
rlcv-miR-rL1-23-3p	UUAGUUGUCUGCACUGGAGAGU	3
rlcv-miR-rL1-24-5p	CUCAAGUUCUCAUUCCAUAUC	4
rlcv-miR-rL1-24_3p	UAUCGGAGAUAGGACUUGAUAC	4
rlcv-miR-rL1-25	UGACAAUUUAAUGGGUCUAGUA	3
rlcv-miR-rL1-26	UACGAUUCUCGGGUUAGCAG	3
rlcv-miR-rL1-27	CACAUAACCAUGGAGGUGGUUG ACAUAACCAUGGANGUGGUUG	4 1
rlcv-miR-rL1-28	GAGGAAAGUAUCGCCUUCUAGA	3
rlcv-miR-rL1-29	UUUUGUUUGCUUGGGACUGCAG	3
rlcv-miR-rL1-30	UUUCGUUUUCGAAGGUCGGCUG UUCGUUUUCGAAGGUCGGCUG	3 1
rlcv-miR-rL1-31-5p	UCGCUUACGCCGACCGCUAAC CUCGCUUACGCCGACCGCUAAC	3 1
rlcv-miR-rL1-31-3p	UAGGCGUGUCGUGUAAGCAGC	3
rlcv-miR-rL1-32-5p	UAACUUACUACUGCCGCUUAC GUAACUUACUACUGCCGCUUAC	3 1
rlcv-miR-rL1-32-3p	UAAUUGCGAGCAGUAGUAGGCG	3
rlcv-miR-rL1-33	CAUUGUCUUCUUUGCCCUUGC	3

(figure: Copyright © American Society for Microbiology, [J Virol, 84, 716-728, 2010])

The novel rLCV miRNAs identified by small RNA cloning are listed in table 4-2. For all miRNAs confirmed in Northern blotting, mature sequences could be obtained. No sequences were obtained for the miRNA MD1517 shown in figure 4-7 B and thus it appears likely that the Northern blot shows a cross reactivity to cellular fragments of RNAs. But it might also be a problem to generate sequences because of their high GC content.

5' end variabilities were found for many mature miRNAs (30%) of the cloned sequences, while always one miRNA end was predominant. However, the exact distribution of 5' end variabilities could not be investigated with this approach. In addition the less important 3' end was not determined. Given the fact that the average length of mature miRNAs is 21 nt the 3' end was estimated.

Results

The location of the cloned miRNA sequences within the predicted hairpin structures is given in the following figure. The location of mature sequences is as expected positioned adjacent to the terminal loop.

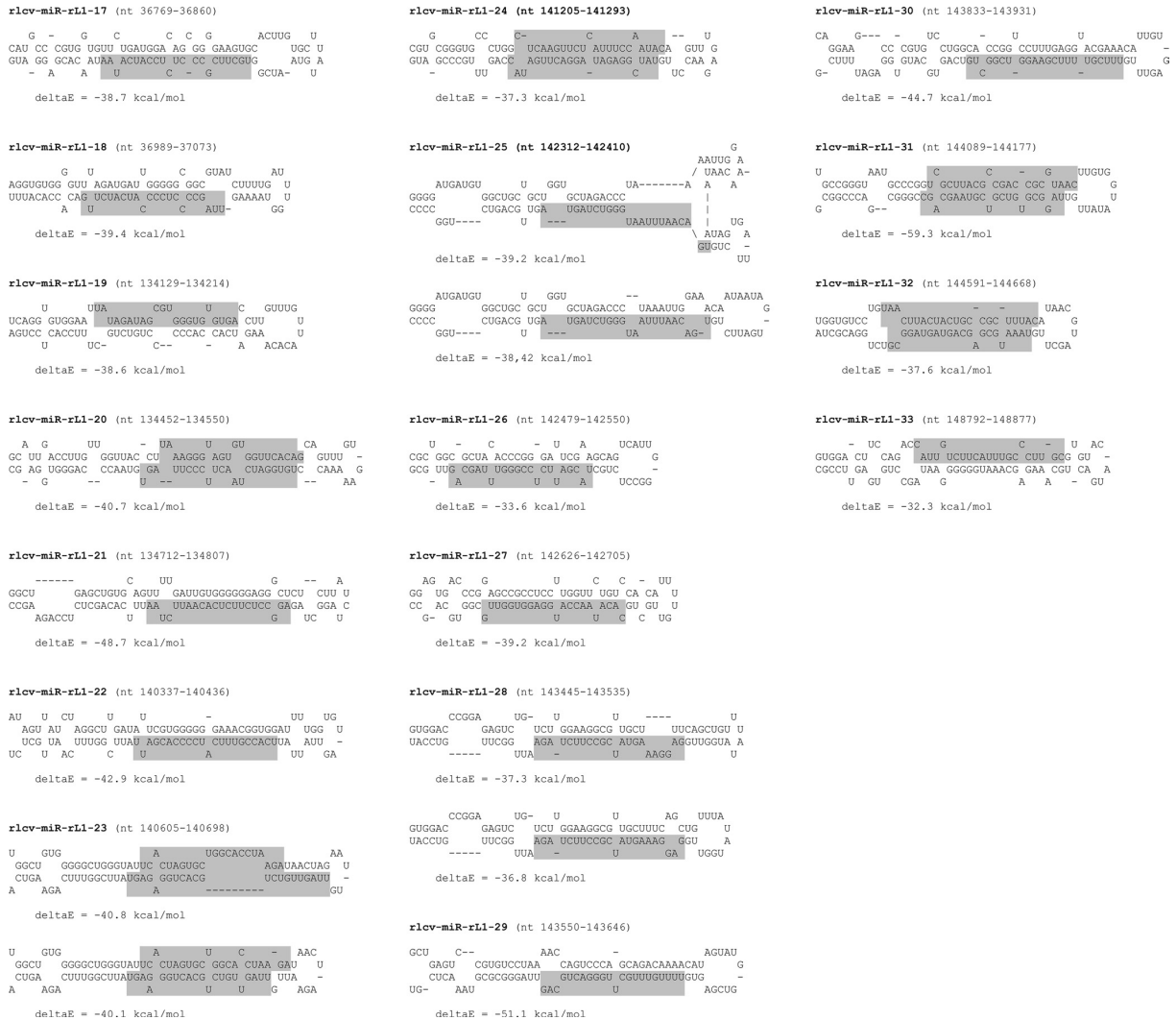


Figure 4-13 Pre-miRNA Hairpins of Novel rLCV-miRNAs

The secondary structures of novel identified pre-miRNA hairpins are shown. The folding with the lowest free energy is displayed. In cases where a folding with higher free energy is more likely to represent the real structure, both are shown. Mature miRNA sequences are marked in grey. Notably the 5' ends are sequenced, whereas the 3' ends are estimated by the average length of miRNAs of 21 nt (Walz et al., 2010). (figure: Copyright © American Society for Microbiology, [J Virol, 84, 716-728, 2010])

For some miRNAs (rL1-23, -25 and -28), it was found that the predicted structure with the lowest free energy might not resemble the probable pre-miRNA hairpin, since the predicted terminal loop seemed to be either too small or too big for Drosha processing. A structure with a slightly lower free energy reveals a more likely structure, supported by the location of the mature miRNA sequences within the predicted structure.

JMHV miRNAs

To obtain a sufficient amount of RNA for cloning of JMHV miRNAs, 1×10^7 293T cells were transfected with pcGJmiR and pcGJmiR Δ in a 15 cm dish. Two to three days post transfection, RNA was isolated. Usually an amount of 300 μ g RNA from one 15 cm dish was used. Both vectors, pcGJmiR and pcGJmiR Δ were used in parallel for the small RNA cloning approach. All retained sequences are listed in the table below.

Table 4-3 JMHV miRNA Sequences

miRNA	Sequence	Clones
jmhv-miR-rJ-1-5p	CGAUCGCACCUUUGGCCGGCC	4
jmhv-miR-rJ-1-3p	GGCCACCGAGGAUGCGGUCAA	3
jmhv-miR-rJ-2-5p	UACCAUGCCCGUCCCGUAUU	4
jmhv-miR-rJ-2-3p	UAUACGGCGCUGCAGCGGUUG	3
jmhv-miR-rJ-3-5p	GUGUUUAGUCGUGCUCUCCUGU	4
jmhv-miR-rJ-3-3p	CAGGGUCUGCGACGGACACUG	3
jmhv-miR-rJ-4-5p	UGGGGAGGGUGUCAGCGCGC	4
jmhv-miR-rJ-4-3p	CUCGUUAACCGUCCUCCGAG	3
jmhv-miR-rJ-5-5p	ACCCAAAGACACGUGCCCGUG	1
jmhv-miR-rJ-5-3p	GGCGUGUUCUUUGGAUUCCGU	5
	GCGUGUUCUUUGGAUUCCGU	1
	CGUGUUCUUUGGAUUCCGUUU	2
jmhv-miR-rJ-6-5p	CCGCGGAAAGGUGUGCACAUC	4
jmhv-miR-rJ-6-3p	CGAUGUACNACCUUUUGCGAU	3
jmhv-miR-rJ-7-5p	UGGAGAGCAGUUAACGUGCGU	3
jmhv-miR-rJ-7-3p	CGCACGUUAAUUGCUUUCUAG	4
	CCGGCGCACGUUAAUUGCUUUCUAG	1
	CACGUUAAUUGCUUUCUAG	1
jmhv-miR-rJ-8-5p	GAUGUCUUGCCAGCACUUUC	4
jmhv-miR-rJ-8-3p	AAAGUGCUCACAAAGACAUCCC	3
jmhv-miR-rJ-9-5p	AAUAUGUUCCGCUGACACCGC	1
	GAAUAUGUUCCGCUGACACCGC	4
jmhv-miR-rJ-9-3p	GCGGUCAUCAGAACAUAUCAC	2
	CGGGGUCUACAGAACAUAUCAC	2
jmhv-miR-rJ-10-3p	AUUACAUCUUGUUAGGGGGAU	4
jmhv-miR-rJ-11-5p	GACCCAGCCUACAGUCCCGCU	2
jmhv-miR-rJ-12-5p	UAGGGAACUAAAGACAUUUC	3
jmhv-miR-rJ-12-3p	UUUCGUUUUAGAUUCCCUA	1
	UCGUUUUAGAUUCCCUA	1
	AUUUCGUUUUAGAUUCCCUA	4
jmhv-miR-rJ-13-5p	UAAUUGCAGUUGGUGUGCUAC	4
	AAUUGCAGUUGGUGUGCUAC	1
jmhv-miR-rJ-13-3p	GUAACCUGACAGCAGUUAGU	1
	AGUAACCUGACAGCAGUUAGU	1
	UAGUAACCUGACAGCAGUUAGU	4
jmhv-miR-rJ-14-3p	GGUGUUUUUUGGGUCCGCUU	3
jmhv-miR-rJ-15-5p	UGCGGUCACCAACAACGCUAU	1
jmhv-miR-rJ-15-3p	UAGUGUUGCUCUGAUUCGUAG	3

Sequences were retained for all miRNAs shown in the Northern blot (figure 4-10). In most cases of pre-miRNAs, only one miRNA is predominantly expressed, while the other was cloned at very low levels. This miRNA is often designated as miRNA *. In addition to the confirmed miRNAs in the Northern blot, sequences for the miRNA* of miR-rJ1-7 3p as well as miR-10 3p were obtained. In four sequences (without the miRNA* moieties), slightly differing 5' ends (miR-rJ1-5, -13, -12, -9) were obtained, otherwise only one sequence was identified.

Cloning of miR-rJ1-12-3p was hindered due to sequence overlap of the specific reverse primer with the 3' end of the 5'-linker and the amplicons contained only linker sequences. The use of different 3' reverse primers lead to two different sequences. In one third of all pre-miRNA hairpins, 5' end variations were found, mainly with one sequence being the dominant form. In figure 4-14 the mature sequences of miRNAs within the predicted hairpins are shown. The sequence locations are in good correlation with the predicted stem-loop structures.

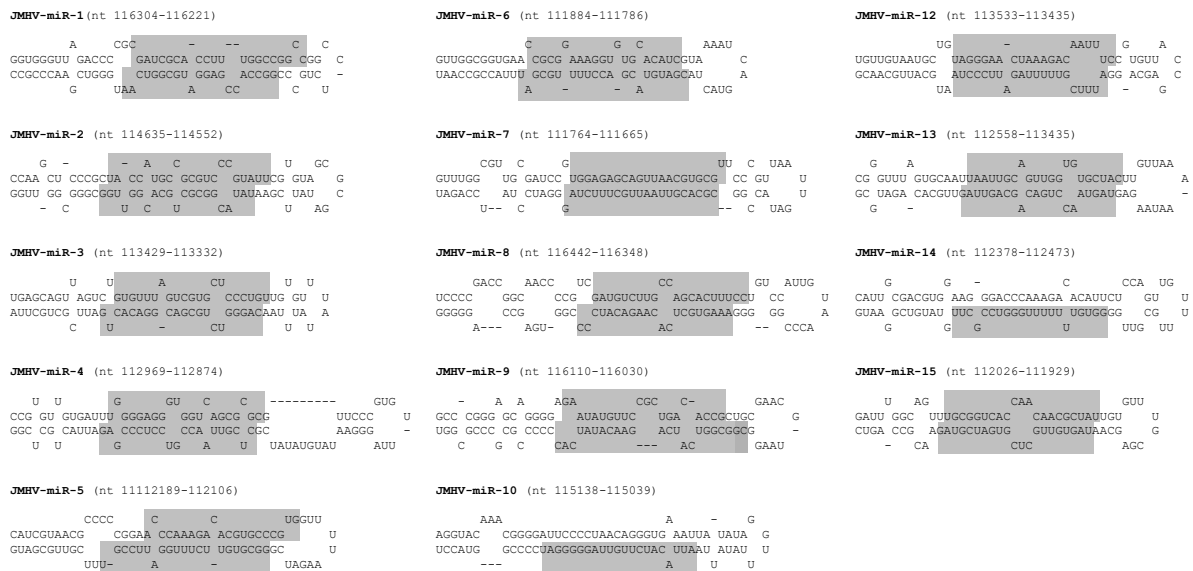


Figure 4-14 Pre-miRNA Hairpins of Novel JMHV miRNAs

The secondary structures of novel identified pre-miRNA hairpins are shown. The folding with the lowest free energy is displayed. In cases where a folding with higher free energy is more likely to represent the real structure, both are shown. Mature miRNA sequences are marked in grey. Notably the 5' ends are sequenced, whereas the 3' ends are estimated by the average length of miRNAs of 21 nt.

4.1.4.1. Conservation Analysis of Known and Novel Pre-miRNAs from EBV and rLCV

Next, the conservation state of the novel identified miRNAs was analyzed. The conservation of the seed region could translate into an important conserved function of the miRNA. Figure 4-15 shows the alignment of the mature miRNAs for EBV and rLCV.

In addition to the seven identified mature miRNAs that are conserved between EBV and rLCV, eight novel mature rLCV miRNAs have conserved seed regions to their EBV counterparts, increasing significantly the number of conserved miRNAs between the two viruses. In four cases of novel conserved pre-miRNAs, alternative 5' ends were identified. Consequently only one of the sequences can have a conserved seed region. Interestingly, this does not have to be the more frequently sequenced miRNA. For miR-rL1-19, the miRNA with an additional 5' nt was cloned three times more frequently than the other sequence, which harbors the conserved seed region. In summary, a total of 16 miRNAs have conserved seed regions. This represents approximately 35% of all miRNAs encoded by EBV and rLCV.

Results

rlcv-miR-rL1-1	<u>UAACCUAGUCAGCCCGGGGUU</u> *	rlcv-miR-rL1-19	<u>UAUAGAUACCGUGGUGUGAGCCU</u>	rlcv-miR-rL1-14-5p	<u>UCGGACGGUCUGGUGCGCUUGAUG</u>
ebv-miR-BHRF1-1	<u>UAACCUAGUCAGCCCGGGGUU</u>	ebv-miR-BART16	<u>UAUAGAUAGUGGUGUGUGUCUCU</u>	ebv-miR-BART11-5p	<u>UCAGACAGUUUGGUGCGCUAGUUG</u>
rlcv	AAAUUCUGCCACAGAAUAUAGC	rlcv	UAAGAGGGGGCCUCACGCCGAG	rlcv-miR-rL1-14-3p	<u>UCGCACAUCAGGCUGAACGAC</u>
ebv-miR-BHRF1-2*	<u>AAAUUCUGUGCAGCAGAUAGC</u>	ebv-miR-BART17-5p	<u>UAAGAGGACG-CAGGCAUAC-AAG</u>	ebv-miR-BART11-3p	<u>ACGCACACCAGGCUGACUGCC</u>
rlcv-miR-rL1-2	<u>UAUCUUUUGCGGGAAUUUCCA</u> *	rlcv-miR-rL1-9	<u>UCGAUCAGUGGCCCCUUAGU</u>	rlcv-miR-rL1-15	<u>UCCUGUAGAGUAUGGGUGUGUUU</u>
ebv-miR-BHRF1-2	<u>UAUCUUUUGCGGGAAUUUCCA</u>	ebv-miR-BART17-3p	<u>UGUAGCCUGGUGGCCUUAGU</u>	ebv-miR-BART12	<u>UCCUGUGUGUUUGG-UGUGUUU</u>
rlcv	UGAUGGACAGCGGGAAUGCA	rlcv-miR-rL1-20-5p	<u>UAAAGGGUAGUGGUUACACAG-</u>	rlcv	CCAGUCCCAGCAGACAAAACAUA
ebv-miR-BHRF1-3	<u>UAACGGGAAGUGUGUAAGCA</u>	ebv-miR-BART6-5p	<u>UAAAGGUUGGUCACAUCCAUAGG</u>	ebv-miR-BART19-5p	<u>ACAUUCCCCCAACAGUAGCAUG</u>
rlcv-miR-rL1-17	<u>UGCUUGCCCUUCCUCAUAAUA</u>	rlcv-miR-rL1-20-3p	<u>UGUGAUUCAACUCCUUAGU</u>	rlcv-miR-rL1-29	<u>UUUUUUUUUGUGGGACUGGAC</u>
ebv	UGCUUCACGCUCUCGUAAAAUA	ebv-miR-BART6-3p	<u>CGGGAGUCGACUAGCCUUAGA</u>	ebv-miR-BART19-3p	<u>UUUUUUUUUGUGGGAAAGGUC</u>
rlcv-miR-rL1-5-5p	<u>AACCUAGUGCCGGUGUGUCU</u> *	rlcv-miR-rL1-23-5p	<u>UCACUAGUGUGGACCCUAGA</u>	rlcv-miR-rL1-16-5p	<u>AGCAGGGCAUGUUCUAUUC</u>
ebv-miR-BART3-5p	<u>AACCUAGUGUGUGUGUGUCU</u>	ebv-miR-BART21-5p	<u>UCACUAGUGAAGGACUAACA</u>	ebv-miR-BART20-5p	<u>UAGCAGGCAUGUUCUAUUC</u>
rlcv-miR-rL1-5-3p	<u>CGCACCAUUUUCACUAGGUGU</u> *	rlcv-miR-rL1-23-3p	<u>UUAGUUUGUCAGUCAGAGAGU</u>	rlcv-miR-rL1-16-3p	<u>CAUGAACACAUUGCCUGUUCU</u>
ebv-miR-BART3-3p	<u>CGCACCAUAGUACACAGGUGU</u>	ebv-miR-BART21-3p	<u>CUAGUUUGCCACUGGUGUUU</u>	ebv-miR-BART20-3p	<u>CAUGAAG-GCACGCCUGUUAUC</u>
rlcv-miR-rL1-5-5p	<u>AACCUAGUGCCGGUGUGUCU</u>	rlcv-miR-rL1-24-5p	<u>CUACAGUUCUUAUCCAAUAGA</u>	rlcv-miR-rL1-32-5p	<u>UAACUUACUACGCCUUUACA</u>
ebv-miR-BART4	<u>GAUCUAGUGUGUGUGUGUCU</u>	ebv-miR-BART18-5p	<u>CUACAGUUCGCAUCCUUAUACA</u>	ebv-miR-BART14*	<u>GUACCCUAC-GCUGCCGAUUACA</u>
rlcv-miR-rL1-5-3p	<u>CGCACCAUUUUCACUAGGUGU</u>	rlcv-miR-rL1-24-3p	<u>UAUCGGAGUA-GGACUUGUAGC</u>	rlcv-miR-rL1-32-3p	<u>UAUUUGGAGCAGUAGGCGGU</u>
ebv-miR-BART4*	<u>CACAUCACGUAGCCACAGGUGU</u>	ebv-miR-BART18-3p	<u>UAUCGGAGUUUGGCUUCGUCC</u>	ebv-miR-BART14	<u>UAUUUGCU-GCAGUAGGGAU</u>
rlcv-miR-rL1-6-5p	<u>UUUUAGUGGAAGUGACGUGUGUG</u> *	rlcv	CCUGGGCAGUGGCUAUGAAACA	rlcv-miR-rL1-33	<u>CAUUGUCUUAUUUGCCUUGC</u>
ebv-miR-BART1-5p	<u>UCUUAGUGGAAGUGACGUGUGUG</u>	ebv-miR-BART7*	<u>CCUGGACCUUAGUAGAAACA</u>	ebv-miR-BART2-5p	<u>UAUUUUUGCUAUGGCCUUGC</u>
rlcv-miR-rL1-6-3p	<u>UAGCACCGCUAUCACUAUGUC</u> *	rlcv-miR-rL1-13	<u>GAUCAUAG-CCAGUGCCAGGGA</u> *	rlcv	AAAGAGCAAAU-GGGGGAAUAGC
ebv-miR-BART1-5p	<u>UAGCACCGCUAUCACUAUGUC</u>	ebv-miR-BART7	<u>CAUCAUAGUCCAGUGCCAGGGA</u>	ebv-miR-BART2-3p	<u>AAAGAGCAAAUUGGAAAAUAAA</u>
rlcv-miR-rL1-7	<u>CGAGGUAACAUCGGCUUACUG</u>	rlcv	UGCUAGACCCUAAAUUGGAAAC		
ebv	GGAGGGAAACAU-GACCACCG	ebv-miR-BART9*	<u>UACUGGACCCUAGAAUUGGAAAG</u>		
rlcv	GUCAGUGGGCCUUUCCUCA	rlcv-miR-rL1-25	<u>UGACAAUUUAAUGGGUCUAGUAGU</u>		
ebv-miR-BART15	<u>GUCAGUGGUUUUUUUCCUUGA</u>	ebv-miR-BART9	<u>UAACACUUA-UGGGUCCCGUAGU</u>		
rlcv-miR-rL1-8	<u>UAAGGUAUAUAGCUGCCCAUUG</u> *	rlcv	GCCGCCUCCUUUGGUUCUGUCA		
ebv-miR-BART5	<u>CAAGGUAUAUAGCUGCCCAUUG</u>	ebv-miR-BART10*	<u>GCCACCUUUUGGUUCUGUACA</u>		
rlcv	GUGGGCCGAGUUCACCU	rlcv-miR-rL1-27	<u>CACAUAAACUAGGAGGUGUUC</u>		
ebv-miR-BART5*	<u>GUGGGCCGUGUUCACCU</u>	ebv-miR-BART10	<u>UAACAUAAACUAGGAGUUGGUGU</u>		

Figure 4-15 Sequence Alignment of EBV and rLCV Mature miRNAs

Shown are all mature EBV and rLCV miRNA sequences, that map to orthologous miRNAs. In cases where no mature miRNA is derived from the homologous sequence, the genomic sequence was used for alignment. Mature miRNAs are highlighted in grey, whereas dark grey shading represents sequence variations. Sequences with an asterisk represent conserved miRNAs identified in a previous study (Walz et al., 2010). (figure: Copyright © American Society for Microbiology, [J Virol, 84, 716-728, 2010])

An alignment of the pre-miRNA hairpins to each other was also performed to obtain a more complete overview of EBV and rLCV miRNA conservation. These data are provided in the appendix. A summary of all data for the EBV and rLCV miRNA conservation state is depicted in figure 4-16.

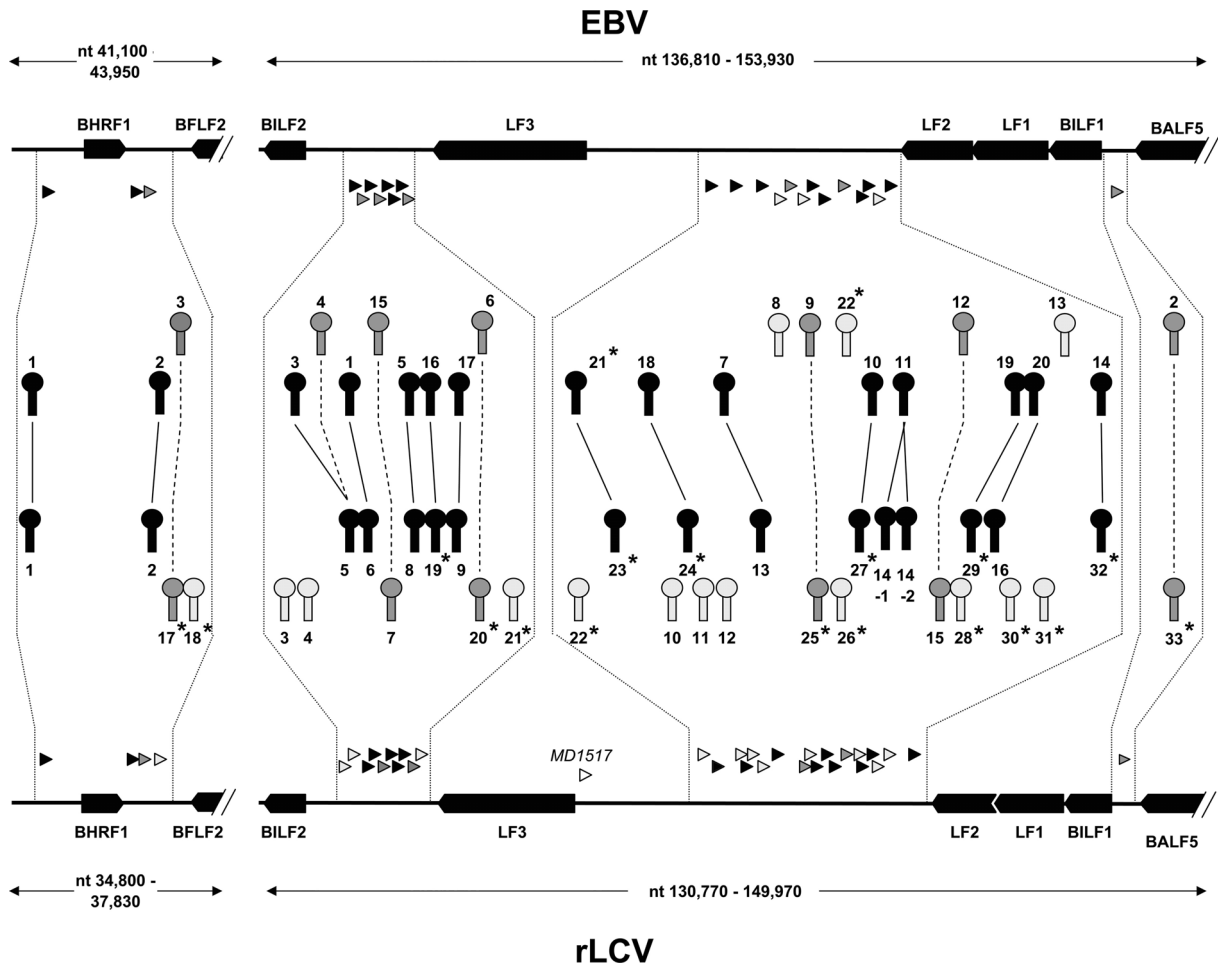


Figure 4-16 Location Map of Novel and Known Pre-miRNA Hairpins from EBV and rLCV

Shown are the miRNA containing regions of the EBV and rLCV genomes. Open reading frames are depicted as black arrows, pre-miRNA hairpins are given as triangles below and above the genomes for EBV and rLCV, respectively. In the middle is a close up of the pre-miRNA hairpin locations. Light gray hairpins drawn proximal to the backbone symbolize non-conserved pre-miRNAs, and dark gray or black hairpins depict homologous hairpins. Solid lines connecting black hairpins indicate pairs in which the seed region of at least one mature miRNA has been conserved, whereas dark gray hairpins connected by dotted lines indicate orthologues in which the seed regions have diverged. Novel miRNAs identified in this study are marked with an asterisk (Walz et al., 2010). (figure: Copyright © American Society for Microbiology, [J Virol, 84, 716-728, 2010])

In figure 4-16, dark hairpins connected with solid lines indicate orthologous pre-miRNAs in which at least one mature miRNA has a conserved sequence. A connection with dotted lines indicates orthologous pre-miRNAs, in which the seed sequences have diverged. Initially, 20 pre-miRNAs were predicted to be conserved (figure 4-1 B). A detailed analysis of the pre-miRNA hairpins revealed that two more pre-miRNAs show homologous sequences, which were missed in the first stringent BLAST analysis. These were rL1-17 and rL1-20 which show a common ancestry to BHRF1-3 and BART6, respectively. Interestingly, next to BART3, which is an orthologue of rL1-5, BART4 also has sequence conservation to rL1-5, which might be due to duplication and diversification of a common ancestor. This mechanism is nicely represented by the probable recent duplication of pre-miRNA14, which differ only in two nucleotides within the terminal loop. Thus, the pre-miRNA hairpins could give rise to the same mature miRNAs.

In conclusion, EBV and rLCV encode for 44 and 43 mature miRNAs, produced from 25 and 34 pre-miRNA stem-loop structures, respectively. The analysis of pre-miRNA stem-loops, revealed that 39 (~85%) of all mature EBV and 31 (~72%) of all mature rLCV miRNAs located in 22 pre-miRNA hairpins show signs of conservation. Out of these 22 pre-miRNA hairpins, 14 harbor at least one mature miRNA with a conserved seed sequence.

4.1.4.2. Conservation Analysis of Known and Novel miRNAs from RRV and JMHV

As for EBV and rLCV, the pre-miRNA hairpins and mature miRNA sequences from JMHV were analyzed in detail and compared to the RRV miRNAs. Figure 4-17 highlights the sequence alignments of mature miRNAs encoded by RRV and JMHV.



Figure 4-17 Sequence Alignment of Conserved Mature RRV and JMHV miRNAs

Shown are all mature RRV and JMHV miRNA sequences, that map to orthologous miRNAs. In cases where no mature miRNA is derived from the homologous sequence, the genomic sequence was used for alignment. Mature miRNAs are highlighted in gray, whereas dark gray shading represents sequence variations.

At the time of this analysis, another group identified eight novel pre-miRNAs from RRV in viral induced tumors from infected rhesus macaques, increasing the total number of RRV miRNAs to 15 (Umbach 2010). Therefore, a conservation alignment of all miRNAs encoded by RRV and JMHV was performed. In analogy to the high sequence conservation of both viruses, all hairpins are highly conserved and 19 out of 27 mature miRNAs have retained their seed sequence.

4.2. Target Identification of EBV miRNAs

A big challenge in the work with miRNAs is the target identification. Different algorithms were developed to predict miRNA binding sites on mRNAs. The most important criteria for target identification is the binding of the seed-match to the mRNA, which is in most cases required, but not sufficient for a functional target site. This minimal requirement leads to prediction of numerous potential binding sites on mRNAs and furthermore to large numbers of false positive candidates. Experimental strategies are necessary to minimize the vast majority of false positive predictions or, strictly speaking, the predictions can be better used to confirm the experimental data. Another problem affects especially viral miRNAs. The overall conservation is very low and thus the implementation of conservation criteria into the target prediction not expedient. Therefore different experimental strategies were used to allow miRNA target identification next to computational predictions.

4.2.1. EBV miRNA Delivery Systems

In order to analyze effects of miRNAs in cell culture without additional effects of viral proteins the generation of a delivery system was necessary. Two strategies were used to generate delivery systems for EBV miRNAs. On the one hand an expression vector encoding for all EBV miRNAs was generated and on the other hand a adenoviral vector system encoding for the BHRF and BART miRNAs was used.

4.2.1.1. Design of Vectors Encoding EBV miRNAs

The first approach to investigate functions of EBV-encoded miRNAs was to establish stable cell lines that express all EBV miRNAs. Therefore all EBV miRNAs (sequences: NC_007605: nt 41294-41729, nt 42643-43282, nt 138803-140353, nt 152510-153034, nt 145332-149069) were cloned into the pcDNA3-GFP vector (see 2.7.1.1).

The expression of miRNAs from the designed vector was confirmed by Northern blot analysis. Therefore, one miRNA from each cloned cluster of BHRF1- and BART-miRNAs was used. (e.g. BHRF1-3, BART-5, -10 and -2). In figure 4-18 RNA isolated from stable Beas-2b cells, which were transfected with the linearized vector or the control vector pcDNA3-IRES-GFP and selected with neomycin for several weeks, was analyzed in Northern blots.

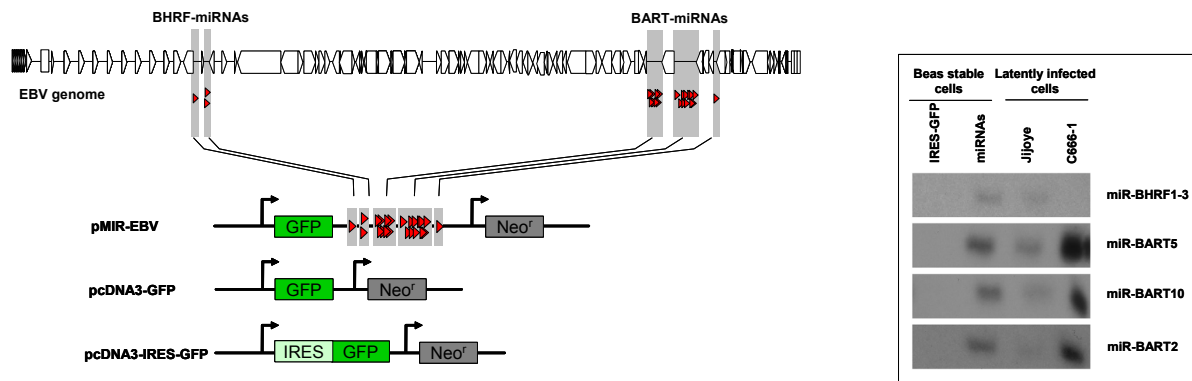


Figure 4-18 miRNA Expression Vector and Expression of miRNAs in Stable Cell Lines.

The pcDNA3 vector was used to design control as well as miRNA expressing constructs. As controls, the GFP or the IRES-GFP were cloned behind the CMV promoter of pcDNA3. MiRNAs of the BHRF as well as the BART locus were cloned behind GFP (left). RNA from stable cell lines was analyzed for different EBV miRNAs, one of each locus cloned. Expression level was compared to latently infected Jijoye and C666-1 cells. In all cases the miRNA expression was higher than in Jijoye, but lower as in the C666-1 cells (right).

The ectopic expression of miRNAs in all cells of a population was one essential criteria. Since the efficiency in transient transfections is very different, the generation of stable cell lines was performed. They not only express miRNAs in every cell but also at a stable amount over the time and thus resemble a good model system for latently infected cells.

4.2.1.2. EBV-miRNA Encoding Adenoviruses

Transfection of cell lines with vectors expressing miRNAs has the disadvantage that not every cell can be transfected, especially when using large vectors as the generated pcDNA3-GFP-EBV-miR. Furthermore, to generate stable cells, the cells must be maintained for a long time in culture under selection until all cells express the resistance gene. This might lead to compensatory effects of the host cell mRNA or miRNA expression to repress EBV miRNA function. In addition, the expression level can not be modulated. Another delivery system was needed to infect primary cells and to modulate miRNA expression levels. For this purpose an adenoviral vector system was used. (Adenoviruses were generated by a diploma student Ina Kowalski under my supervision with the help of Peter Groitl) The AdEasy System was used to generate different adenoviruses (figure 4-19) (Luo et al., 2007).

The adenoviruses were initially tested on established cell lines to proof their functionality. Beas-2b and SLK cells were infected at different MOI and RNA was isolated 2 days after infection for Northern blot analysis. As shown in Figure 4-19, the expression of miRNAs is dependent on the MOI and can be further adjusted to reach levels comparable to latently infected cells.

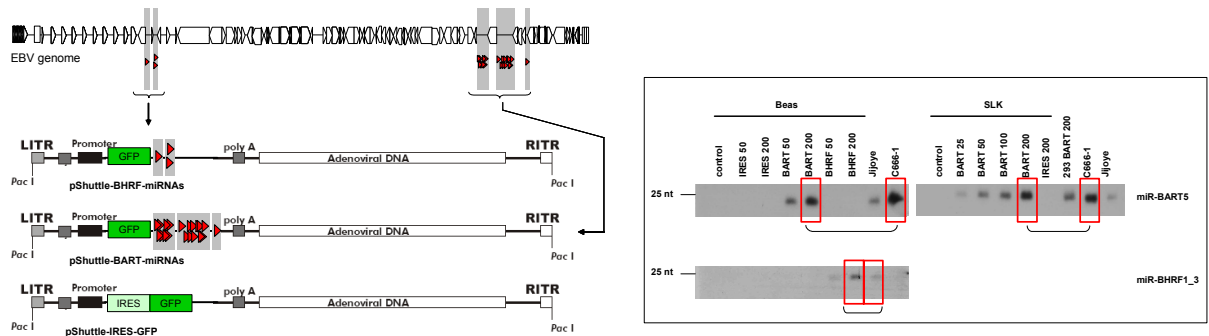
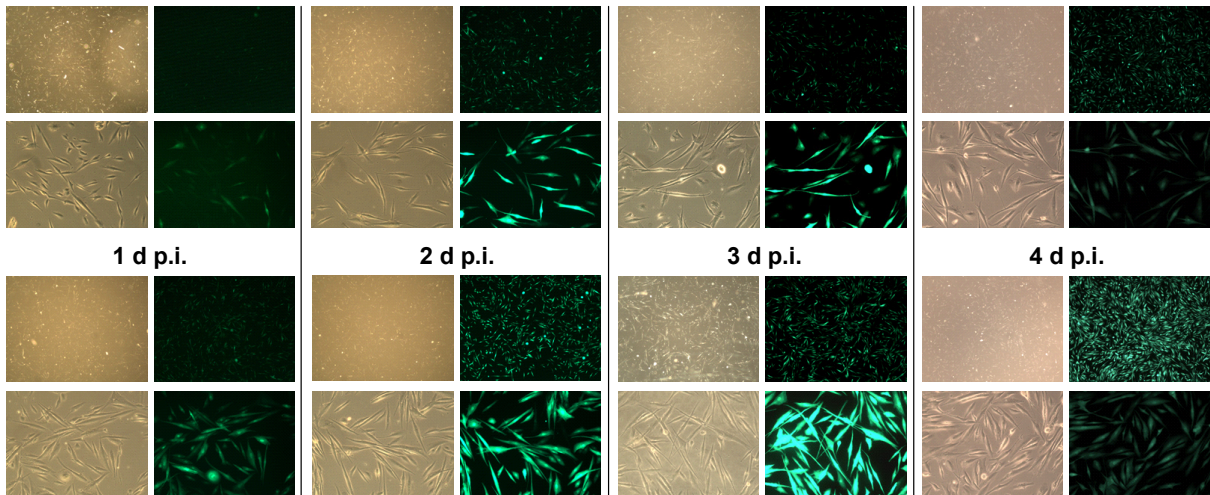


Figure 4-19 pShuttle Vectors for miRNA Expressing Adenovirus Production.

As control IRES GFP was introduced behind the promoter of pShuttle. Two miRNA expressing vectors were designed, one for the BHRF-miRNAs and another for the BART miRNAs. In both cases GFP was inserted behind the promoter followed by the miRNAs (left). Epithelial or endothelial derived cell lines (Beas-2b or SLK) were infected with adenovirus expressing IRES-GFP, BHRF-miRNAs or BART-miRNAs at different MOIs for 2 days. Northern Blots for miR- BART-5 and miR-BHRF1-3 are shown. As controls served the B-cell line Jijoye and the nasopharyngeal carcinoma cell line C666-1 cells (right).

Adenoviruses were mainly established to infect primary cells, since these are difficult to transfect or even cultured for longer periods to generate stable cell lines. Human nasal primary epithelial cells (HNEpC) were infected at different MOIs. Infection studies revealed an MOI of 500 being optimal for achieving 100% infection. Cells were then infected and monitored for several days, to control phenotypic changes.

Ad-IRES MOI 500



Ad-BART MOI 500

Figure 4-20 Adenovirus Infected HNEpC

Light and fluorescence microscopic pictures of Human Nasal Epithelial primary Cells (HNEpC), infected with adenoviruses for 1-4 d at an MOI of 500. Infection with Ad-IRES-GFP and Ad-BART is shown in the upper and lower panel, respectively. Magnification is 100 x and 200 x in each upper and lower row, respectively.

Results

The infection of HNEpC was successful and reproducible. Furthermore cells were phenotypically unchanged as shown in figure 4-20 for at least 4 days. Another important point was the expression level of miRNAs in the infected cells. Preferably the expression level should be in the same range as for latently infected cells (e.g. C666-1). Since the culture of HNEpC was very expensive and the amount of isolated RNA very low as compared to established cell lines, the need for another quantitation method next to Northern blotting was obvious. A novel quantitation method for miRNAs (stem-loop RT-PCR see) uses stem-loop primers for cDNA synthesis, which bind to specific mature miRNAs. Afterwards the cDNA can be analyzed in real time PCR. To compare the expression levels of infected HNEpC with latently infected C666-1 cells or Jijoye, the same amount of RNA was reverse transcribed with a stem-loop primer specific for EBV miRNAs (miR-BART-5) and for normalization with a stem-loop primer specific for an endogenous miRNA (miR-21) and a specific reverse primer for GAPDH. After cDNA synthesis, a multiplex real-time PCR with different specific probes for miR-BART-5, miR-21 and GAPDH was performed. The raw data of an exemplarily run are shown in figure 4-21.

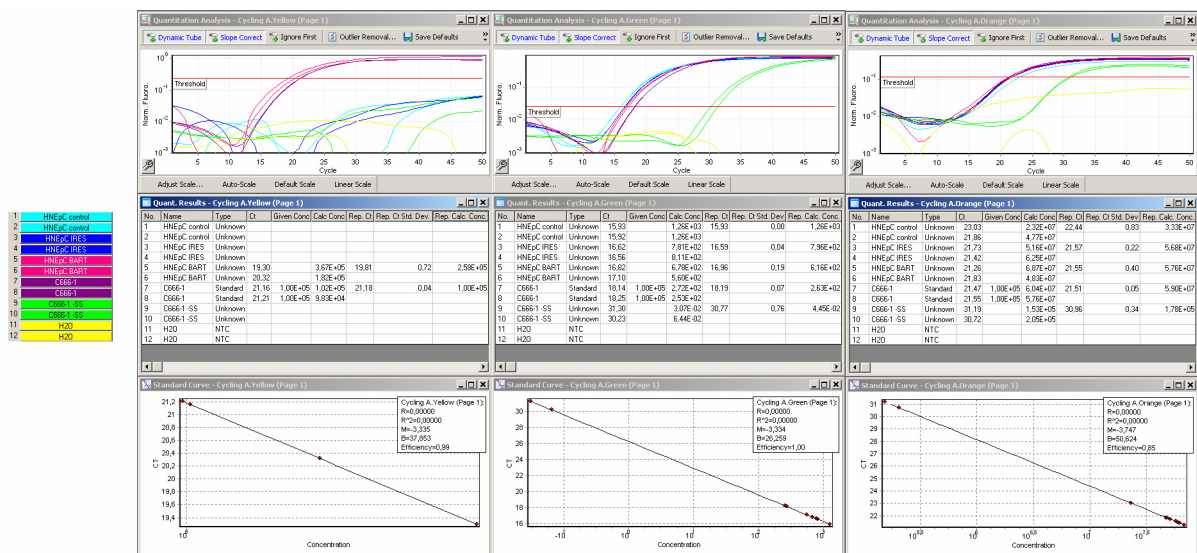


Figure 4-21 Stem-loop RT-PCR of Adenoviral Infected HNEpC

HNEpC were infected with an MOI of 500 for 24 h. RNA was isolated and samples were analyzed in a multiplex RT-PCR using different TaqMan probes. Expression level of miR-BART5 was compared to 500 ng C666-1 cell line used in RT. Shown are the real time curves for miR-BART5, miR-21 and GAPDH. All of them were analyzed using the corresponding standard curve for each primer pair shown below and calculated relative concentrations are given in the middle. Samples are colored and the legend is given on the left.

The normalization to miR-21 and / or GAPDH showed that the expression levels of latently infected cells are indeed comparable to the amount of HNEpC cells infected with an MOI of 500 for 1 d. In comparison to an amount of 100 a.u. of C666-1 miRNA an amount of 110 a.u. of infected HNEpC miRNA-BART5 was found. This leads to the assumption, that this approach is a good model system to study functions of EBV-encoded miRNAs in primary epithelial cells.

4.2.2. Target Identification on mRNA Level - DNA Microarrays

DNA microarrays are widely used in diverse applications. DNA microarrays containing the whole human genome (genes and transcripts), synthesized on glass slides as 60mers were used. Labeling of two probes with different fluorescence dyes allows identification of differences between RNA derived from the two samples. Due to the fact that binding of miRNAs to their target mRNAs destabilize the mRNA, expression arrays were used to identify putative miRNA targets.

To identify putative miRNA targets in B-cells, mRNA expression profiling was performed under three sets of conditions. Stable B-cell lines expressing all EBV miRNAs were analyzed compared to three different controls; either BJAB cells or BJAB stable cell lines expressing GFP or IRES-GFP. In the following the different sets of conditions were named BJAB set-up, BJAB-IRES set-up and BJAB-GFP set-up. The BJAB-GFP set-up was performed in biological duplicate.

For the identification of miRNA targets in epithelial cells, two distinct approaches were used. First, the Beas-2b stable cell line expressing all EBV miRNAs were analyzed compared to Beas-2b stable cell line expressing IRES-GFP (Beas-IRES set-up). Second, the Human Nasal Epithelial primary Cells (HNEpC) were either infected with adenovirus encoding for all BART miRNAs or adenovirus expressing IRES GFP: The HNEpC were infected either for 4 or 6 d before RNA isolation (HNEpC 4 d p.i. set-up and HNEpC 6 d p.i. set-up, respectively). The Beas-IRES set-up was performed in biological duplicate. The HNEpC 4 d p.i. set-up was also performed in biological duplicate, whereas the HNEpC 6 d p.i. set-up was performed singularly.

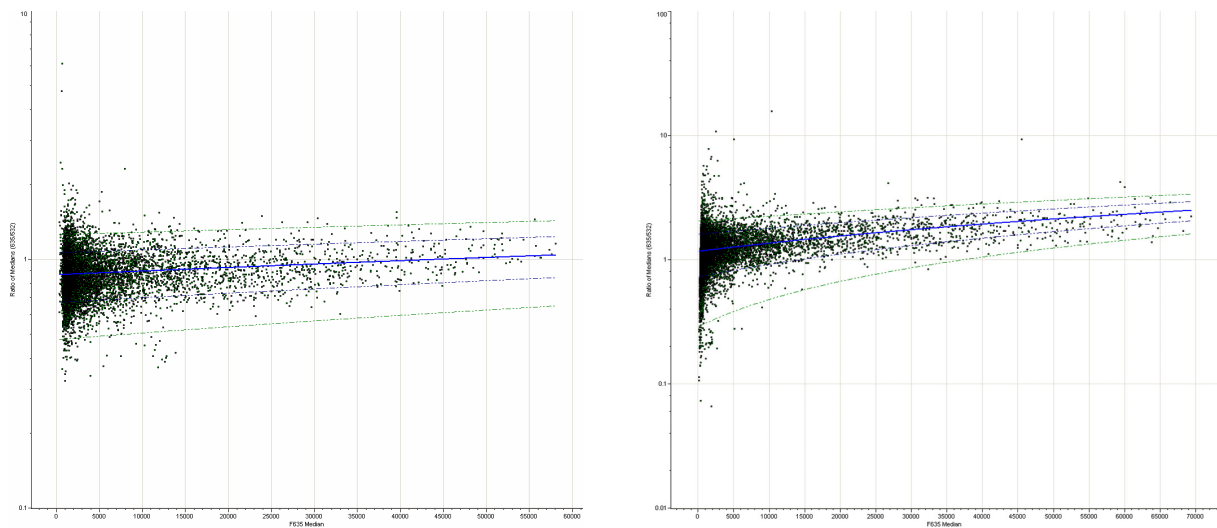


Figure 4-22 Scatter Plots of DNA Microarrays.

The distribution of all spots included in normalization is shown in two scatter plots, exemplarily. The mean fluorescence intensity of F635 nm is given on the x-Axis, the log ratio of medians (635 nm/532 nm) on the y-axis. BJAB-GFP set-up (left), HNEpC 4 d p.i. set-up (right).

Results

Arrays were analyzed with the Genepix software and the standard deviation (stdv) of all spots for each array was calculated. Array analyses revealed approximately 100-200 mRNAs in every experiment being down-regulated. While these 100-200 mRNAs pass the threshold of 2x stdv, approximately 1000-2000 down-regulated mRNAs pass the 1x stdv threshold (table 4-4).

Table 4-4 Statistics of Regulated Genes of DNA Microarrays

Set-up	All Genes	Down 2xStdv	Down 1xStdv	Up 2xStdv	Up 1xStdv
BJAB	9796	173	1251	280	1300
BJAB-IRES	7967	215	1232	135	1107
BJAB-GFP-1	10741	214	1294	362	1527
BJAB-GFP-2	9787	91	1199	366	1450
Beas-IRES-1	12909	395	1960	228	1797
Beas-IRES-2	14803	528	2263	189	1614
HNEpC 4 d p.i.1	10708	143	1080	319	824
HNEpC 4 d p.i.2	12742	420	1688	1198	175
HNEpC 6 d p.i.	4936	82	602	122	551

Further statistic analyses revealed that putative target sites for the EBV-encoded miRNAs are in most set-ups more enriched in the down-regulated than in the upregulated fraction. Exeptions are the BJAB set-up and the HNEpC 6 d p.i. array. At the same time the average length of 3'-UTR shows a similar distribution in the up- and down-regulated gene fractions compared to predicted binding sites. These data are summarized in table 4-5.

Table 4-5 Statistics of Regulated Genes of DNA Microarrays

Array Set-up	Average 3' UTR Length				miRNA Target Sites	
	up mean [nt]	down stdv	up mean [nt]	down stdv	up [%]	down [%]
BJAB-GFP 1	533	869	1139	1147	55.4	109.0
BJAB-GFP 2	756	1112	930	920	74.9	105.6
BJAB	1087	980	1044	926	108.7	103.3
BJAB-IRES	961	1184	1048	1077	101.7	103.7
Beas-IRES 1	968	962	1664	1633	90.6	141.0
Beas-IRES 2	707	792	1572	1404	66.4	136.6
HNEpC 4 d p.i.1	1044	1157	1122	1241	95.7	109.4
HNEpC 4 d p.i.2	963	969	1397	1481	91.4	123.2
HNEpC 6 d p.i.	1456	1288	901	943	134.3	104.0

The overlap of down-regulated targets should result in a list of more probable novel targets of EBV miRNAs. To gain a significant set of putative genes, the overlap of all set-ups was generated initially to include all regulated genes above the threshold of 2x stdv. In the end, only one gene was left: zinc finger, CCHC domain containing 17 (ZCCHC17) that was regulated in all three BJAB array set-ups passing the threshold. This gene does not harbor good binding sites for any of the EBV miRNAs (data not shown) and was not investigated further. A less stringent analysis was necessary. Therefore, all genes above a threshold of 1x stdv were considered. A schematic overview of the down-regulated genes is shown in figure 4-23.

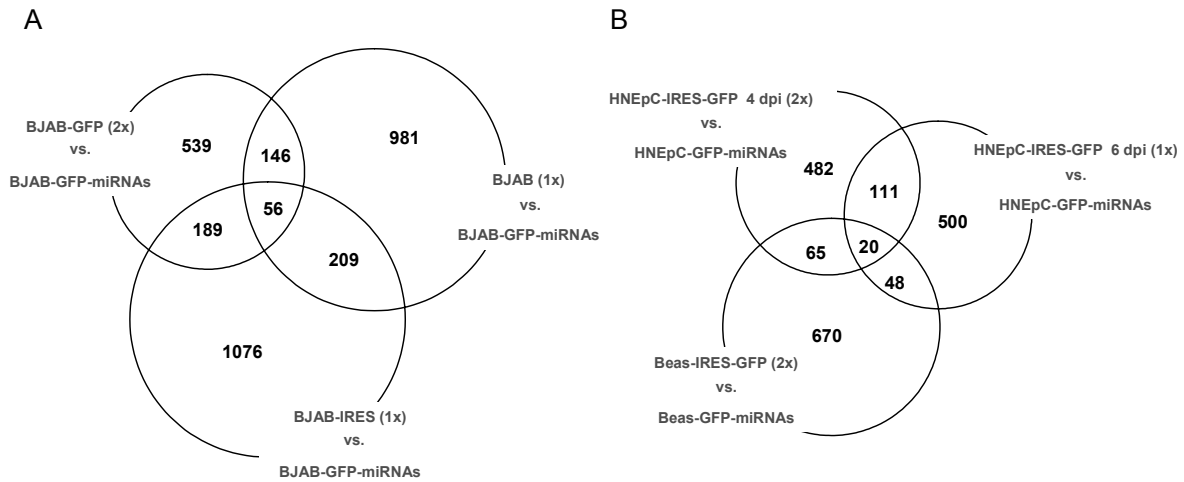


Figure 4-23 Overlap of Down-regulated Genes Derived from BJAB or Epithelial mRNA Expression Arrays.

Shown are all down-regulated genes passing a threshold of 1x standard deviation of all arrays performed. The number of down regulated genes is represented by circles for indicated set ups. The overlap of the set-ups is given by numbers in the intersection of the circles. A: BJAB cell line set-ups, B: epithelial cell line and primary cell set-ups.

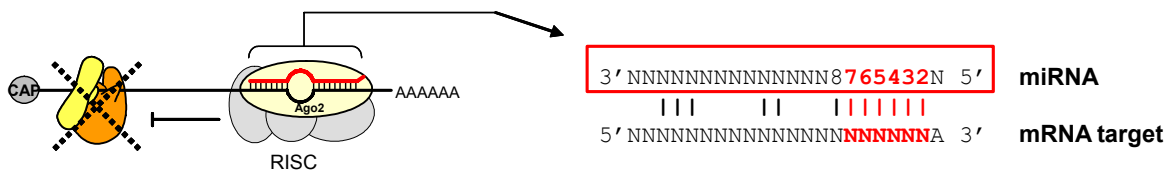
In total 56 genes are down-regulated in all three set-ups. As shown in figure 4-23 the overlap between these three set-ups was even lower (20 genes) as for the BJAB arrays. This is not astonishing, since very different systems were analyzed: stable cell lines compared to adenovirus infected primary cells. Interestingly, some down-regulated mRNAs are found in all three set-ups. The mRNA expression data obtained from the primary cells were analyzed in more detail. The lists of overlapping mRNAs are given in supplementary table 1. Additionally DNA microarrays of RNA from infected HNEpC were analyzed using Genespring GX software. These data were investigated in more detail (supplementary table 2).

4.2.3. Computational Target Prediction

4.2.3.1. Genome Browser

The overlap of the gene expression data still provided a huge number of possible target mRNAs. To extract the most interesting candidates, all genes were analyzed for their amount and quality of putative miRNA binding sites within their 3'UTR. The genome browser uses the UCSC database and the TargetScan algorithm to predict miRNA target sites within all genes. The program then visualizes and lists all possible binding sites for all miRNAs that are selected. Since the binding of a miRNA to its target mRNA is in general imperfect, the prediction of putative target sites is hindered. Nevertheless, a lot of research has revealed some important aspects of miRNA target binding. One general feature is the need for perfect binding to the seed region of the miRNA. Furthermore additional base pairing at the 3'-end of the miRNA facilitates binding. An AU rich region in the

adjacent sequence is also favoured, as well as an A at position 1 of the mRNA (figure 4-24). Putative binding sites at the beginning or end of an mRNA are favoured over sites lying in the middle.



Translational inhibition of target mRNAs

Figure 4-24 miRNA Target Recognition

miRNAs inhibit translation of target mRNAs. A schematic close up highlighting some important features of a miRNA binding to its mRNA is shown. The seed regions, the most important requirement for target recognition is marked in red. A adenine (A) at position one and additional base pairing within the 3' end of the miRNA are additional features that might help in the target recognition (figure: Dr. Adam Grundhoff, modified).

These and other criteria were included in different algorithms and each binding site received a score. For further investigations different mRNAs from each overlap list were selected for at least one or mostly two criteria. The gene needs at least one good target site and should be interesting due to its biological function. For example, genes involved in apoptosis, tumorigenesis, cell cycle control, interference with virus or miRNA regulation were preferentially examined. A list with all analyzed genes is given in the appendix. Some examples are presented in the next chapters.

4.2.4. Confirmation of miRNA Targets

4.2.4.1. Luciferase Reporter Assay

To confirm the direct binding of a miRNA to a 3'UTR, luciferase reporter assays were performed. The 3'UTRs of interest were cloned behind the luciferase into the pMIR-Report vector. Together with a β -Gal vector for normalization and the miRNA of interest, the pMIR-Report was transfected into 293T cells. After 24 h lysates were prepared and β -Gal, as well as luciferase activity was measured. The system is very sensitive to changes in the DNA amount either of the luciferase reporter or the miRNA expressing plasmid. Therefore, the DNA concentration of the single plasmids was measured fluorometrically instead of spectrometrically.

4.2.4.2. Design of Controls for Luciferase Reporter Assays

A control luciferase reporter was generated containing a binding site for miR-BART-5 (see 3.4.9.1). Two control reporters were generated containing one and four binding sites and were named CO1 and CO4, respectively. Both were tested in the luciferase assay using different miRNAs. As negative controls the empty vector pcDNA3-GFP or pcDNA3-GFP-rL1-20 (containing a rLCV miRNA that should not bind to the target site) were used. Binding, in contrast, should be measurable with either

pcDNA3-GFP-BART-5 or pcDNA3-GFP-rL1-8 (the conserved miRNA from rLCV). To analyze each EBV miRNA, all miRNAs were separately amplified with primers listed in table 2-3 and cloned into the pcDNA3-GFP. Expression of miRNAs was verified in Northern blots.

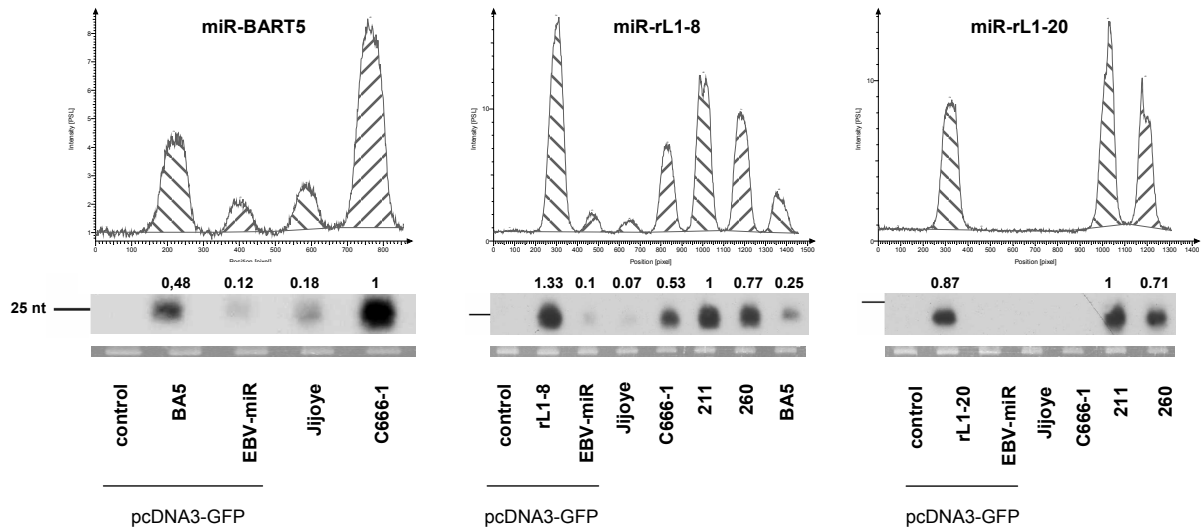


Figure 4-25 Quantitative Northern Blots of miRNA Expressing Transfected Cells.

293T cells were transfected with pcDNA3-GFP expressing either one specific EBV or rLCV or all EBV miRNAs for 1 d. MiRNA expression of EBV-miR-BART5, rLCV-miR-rL1-8 and -20 were compared to latently infected cells. Shown are the quantification graphs obtained from the AIDA software after scanning at the BAS-Reader. Northern blots are shown below the graphs and a low molecular weight RNA from the ethidium bromide stained gels of the Northern blots are given as loading controls. The latently infected cell lines C666-1 and 211 was set to 1 for EBV and rLCV miRNA, respectively. The relative fold changes of miRNA expression are depicted above the Northern blots.

Expression levels of transfected 293T cells with single miRNAs were compared to a vector encoding all EBV miRNAs and latently infected cells. For miRNA-BART5 the expression was significantly higher when expressed alone than with all miRNAs, as well as higher compared to the expression of latently infected B-cells (Jijoye). The latently infected epithelial cell line (C666-1) in contrast showed a higher expression compared to Jijoye and miRNA-BART5. The conserved miRNA-rL1-8 was expressed at higher level in the single transfected cells than in the latently infected rhesus macaque cell lines 211 and 260, and showed even a higher expression compared to latently infected human epithelial cells (C666-1), which express miR-BART5. The third miRNA tested, miR-rL1-20, was expressed at equal amounts in the single transfected 293T cells and the latently infected rhesus macaque cells (211, 260). Since this miRNA is not conserved in EBV, there was no crossreaction seen in the EBV positive cell lines as well as the transfected 293T cells expressing all EBV miRNAs. At the single cell level, the expression of the specific miRNAs should be even higher than depicted in the Northern blots, depending on transfection efficiency, represented here.

All luciferase assays were performed by co-transfection of three different plasmids. The luciferase reporter pMIR-Report™ including the 3'UTR of interest, the β -galactosidase expressing vector pMIR-Report™ Beta-gal for normalization and a miRNA of interest expressing vector pcDNA3-GFP-

miRNA. Either a control miRNA or the putative binding miRNA were used in two different transfection. Cells were transfected for 24 h prior to lysate preparation and each transfection was performed in duplicate. First, the efficiency of down-regulation of the luciferase activity of the control reporters CO1 and CO4, containing one and 4 perfectly complement binding sites to miR-BART5, was investigated. The reporter CO4 showed a higher regulation (figure 4-26) and so this vector was further used in every experiment as an internal control.

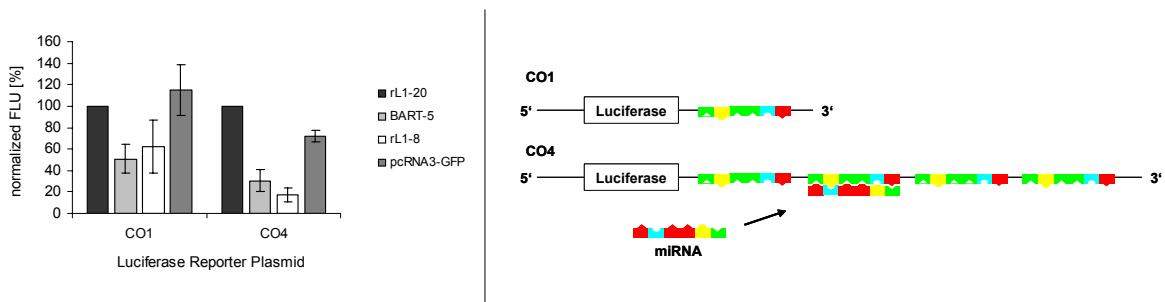


Figure 4-26 Luciferase Assay of Control Reporters.

Luciferase reporter CO1 and CO4 containing one and four perfect complementary binding sites for miR-BART5, respectively, (right) were analyzed in luciferase assay. Results are from two independent experiments. Expression of miR-rL1-20 serves as negative control and was set to 100%. miR-BART5 and the conserved miRNA of rlcv miR-rL1-8 were analyzed. In addition a control vector without miRNA expression was included. The reporter harboring 4 binding sites is more affected in regulation (left).

Another finding was that the transfection of a plasmid expressing only the miR-BART-5 was more efficient as the vector expressing all miRNAs of EBV. Even in higher concentration of the pcDNA3-GFP-EBV-miRs vector, no down-regulation of the control vector could be detected. Other experiments were done to further optimize the assay conditions, e.g. usage of different cell lines, different amounts of luciferase reporter and miRNA containing vectors or usage of adenovirus containing all miRNAs, but the best results were obtained using 293T cells, an amount of 5 ng luciferase reporter and at least an amount of 100 ng miRNA expressing vector. The normalization vector β -Gal was used with 50 ng per transfection.

Due to the fact that regulation of the luciferase reporter only is measurable with a very high amount of miRNAs, all EBV miRNAs used in the luciferase assay were cloned individually into the pcDNA3-GFP vector by usage of primers listed in table 2-3. To screen different target mRNAs with different miRNAs, the assay was performed in 96 well plates. Putative targets were selected from the array data. Triplicate biological repeats were performed with two replicates. Supplementary table 1 and 2 list regulated genes from the diverse DNA microarrays and different evaluations of these data. Genes analyzed in luciferase assay are highlighted in red (if they are shown here) or in yellow (if they are still under investigation) However, supplementary table 2 gives an overview about the amplitude of differentially regulated genes that is typical for the analysis of miRNA dependent regulation (and mainly between 1-2 fold regulation).

4.2.4.3. PUMA from Rhesus Macaques is Not Regulated by the Conserved miRNA rL1-8

PUMA has been shown to be regulated by EBV miR-BART-5 in nasopharyngeal carcinoma (Choy, 2005). Interestingly, this miRNA is highly conserved in rLCV, including the seed region. Furthermore, the 3'UTR of rhesus PUMA is also widely conserved and harbors a potential binding site for the miRNA. Therefore, both 3'UTRs from human and rhesus cell lines were cloned and the luciferase activity in presence of a control or the putative binding miRNA was tested. The results are depicted in (figure 4-27).

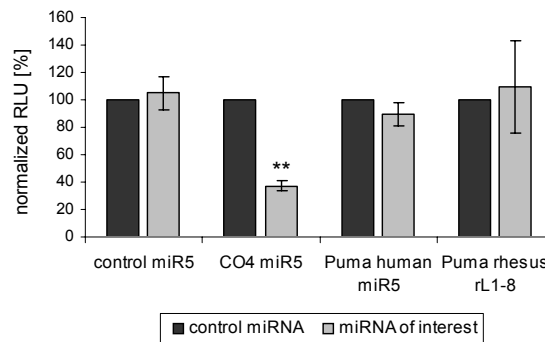


Figure 4-27 Luciferase Assay for Puma 3'UTR

The 3'UTR of PUMA from human and rhesus macaques were analyzed for binding of miR-BART5 and miR-rL1-8, respectively. Results are derived from three independent experiments. pMIR-Report without additional 3'UTR as well as pMIR-Report-CO4 were included as negativ and positive controls, respectively. PUMA from humans showed a marginal regulation through miR-BART-5, whereas PUMA from rhesus was not reproducibly regulated by rL1-8. Regulation of the control was significant (T-test $p \leq 0.01$).

Neither the luciferase activity of pMIR-Rep-PUMA-hum nor pMIR-Rep-PUMA-rhes was decreased in presence of the corresponding miRNA. Although the luciferase activity of pMIR-Rep-PUMA-hum was down-regulated slightly in three independent experiments, this regulation was not significant.

4.2.4.4. MX-1 and PDCD2 Might be Regulated by miR-BART11 and -19, Respectively

Three interesting candidates for miRNA targets from BJAB gene expression data were analyzed in the luciferase assay. myxovirus resistance 1 (MX-1) is an interferon induced GTP-binding protein, which has been shown to inhibit replication of large dsDNA virus (Netherton et al., 2009). Caspase recruitment domain 6 (CARD6) is a modulator of NF- κ B (Dufner et al., 2006; Stehlik et al., 2003) and has been shown to be up-regulated in different types of cancers (Kim et al., 2010). Programmed cell death 2 (PDCD2) has recently been shown to be involved in the induction of apoptosis (Baron et al., 2010). The next figure highlights exemplarily the target analysis using the Genome Browser. All mRNAs identified within the overlap of the arrays were analyzed for good scoring target sites within the 3' UTRs.

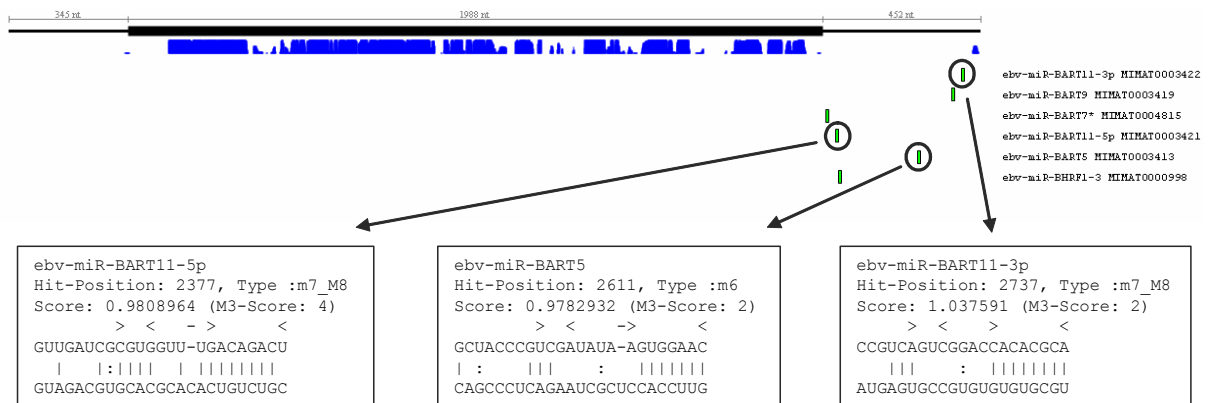


Figure 4-28 Genome Browser Analysis of miRNA Binding Sites Within the MX-1 3'UTR

The mRNA of MX-1 is shown at the top, subdivided in 5' UTR, ORF and 3' UTR. Sequence conservation is marked in blue below the mRNA. miRNA binding sites are listed below at the corresponding position in the 3' UTR as green bars. The binding sites are enlarged in the boxes below. Given are the miRNA name, position of the binding site, seed match type and score.

The Genome Browser shows the mRNA separated into 5' UTR, open reading frame and 3' UTR, the conservation state compared to other species as blue histogram under the mRNA, miRNA target sites marked as green bars and lists seed match type and score (implemented from TargetScan).

Two EBV miRNAs were tested for their ability to bind to the 3' UTR of MX-1, miR-BART11 and miR-BART5. A significant down-regulation of an average of 22% was measured for miR-BART11, whereas miR-BART5 showed no effect. The CARD6 3' UTR was also tested with two miRNAs, miR-BART19 and miR-BART2. Neither were able to reduce luciferase activity. The luciferase activity of the luciferase containing the PDCD2 3' UTR was only slightly but significantly reduced (13%) ($P \leq 0.01$). The expression level of tested miRNAs was between latently infected Jijoye and C666-1 cells. For miR-BART-11 a expression level comparable to C666-1 cells was detected.

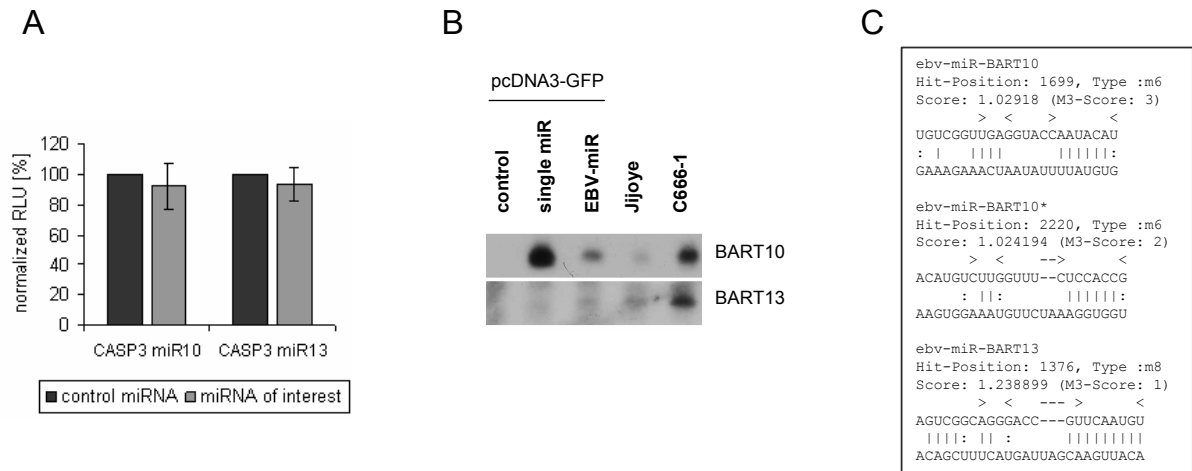


Figure 4-30 Luciferase Assay for CASP3

The 3'UTR of CASP3 was analyzed. Results are derived from three independent experiments with duplicates for each experiment. CASP3 was not reproducibly down regulated neither through miR-BART-10 nor miR-BART 13. Northern blots for single miRNAs are given in B. 293T cells were transfected with pcDNA3-GFP expressing either one or all EBV-miRNAs and expression level was compared to latently infected cells (Jijoye and C666-1). Investigated target sites derived from the Genome Browser are given in C.

Neither BART-10 nor BART-13 showed a significant down-regulation of luciferase activity as depicted in figure 4-30. Expression level of miRNAs showed a very low expression of miR-BART 13 in the single miRNA expressing vector. Therefore, a regulation might still be possible, if expression levels are higher. But at least miRNA-BART10 is not responsible for the down-regulation of mRNA levels found in the epithelial arrays. If other miRNAs are doing so, has to be further investigated.

4.2.4.6. Evaluation of Putative Targets identified in Adenovirus-infected Primary Cells

Different regulated genes identified in the infected HNEpC were investigated (supplementary table 2). Elongator complex 4 (ELP4) acts as a subunit of the RNA polymerase II complex, which is a histone acetyltransferase component of RNA polymerase II (Hawkes et al., 2002; Kim et al., 2002).

Inositol polyphosphate phosphatase-like protein 1 (INPPL-1) negatively regulates the phosphoinositide 3-kinase (PI3K) pathway. The human miRNA miRNA-205 has been shown to downregulate SH2-containing phosphoinositide 5'-phosphatase 2 (SHIP2). miR-205 enhances keratinocyte survival by negatively regulating SHIP2. This effect is antagonized by another human miRNA, miRNA-184, in corneal keratinocytes (Yu et al., 2008).

Non-metastatic cells 3 (NME3) has a major role on the synthesis of nucleoside triphosphates other than ATP. It might play a role in normal hematopoiesis by inhibition of granulocyte differentiation and induction of apoptosis (Desvignes et al., 2009; Venturelli et al., 1995).

Nuclear vcp like (NVL) belongs to the ATPases associated with diverse cellular activities (AAA-ATPases) and might have a role in ribosome biogenesis, as well as development and apoptosis (Nagahama et al., 2004).

The transcription factor 4 (TCF4) targets, amongst others, receptor tyrosine kinase EPHB2, which controls the intestinal epithelial architecture and has been shown to be lost in human colorectal cancers (Fu et al., 2009). In general, deregulation of transcription factors is often found in tumors; they might act as tumor suppressors as well as oncogenes.

Exportin-1 (XPO1) is a nuclear export factor exporting cellular proteins harboring a nuclear export signal (NES) and RNAs. Viruses like HIV or Influenza A uses XPO-1 to transport their unspliced or incompletely spliced RNAs out of the nucleus (Askjaer et al., 1998; Fornerod et al., 1997; Ossareh-Nazari et al., 1997). Recent studies revealed that XPO-1 might also be involved in shuttling of mature miRNA (Castanotto et al., 2009).

All this genes were found to harbor good scoring binding sites for different EBV-encoded miRNAs and were analyzed in luciferase assays.

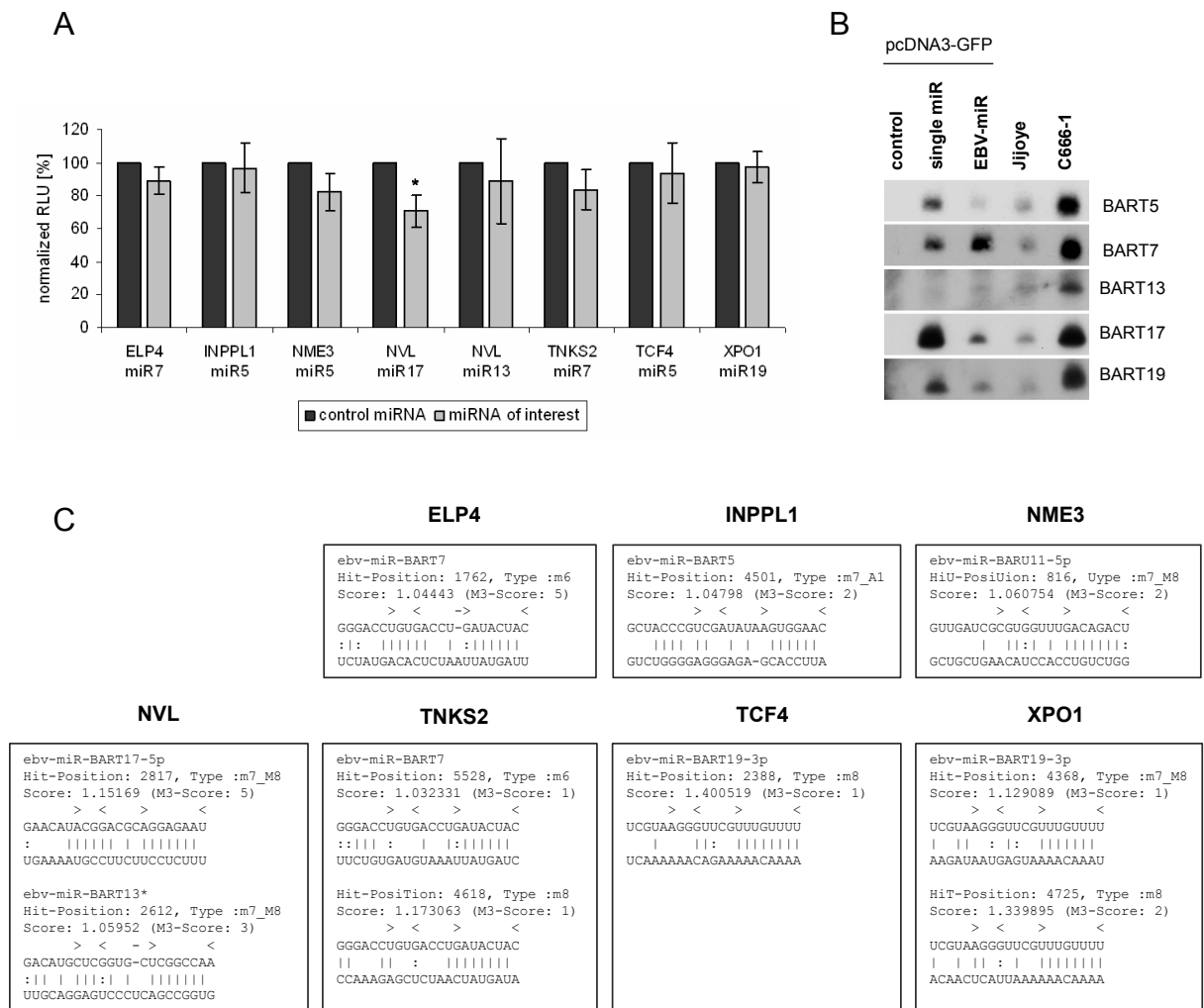


Figure 4-31 Luciferase Assay of Down-regulated Genes from HNEpC Gene Expression Arrays

The 3'UTR of diverse genes identified in HNEpC gene expression arrays were analyzed. Results are derived from three independent experiments with duplicates for each experiment. Significant regulation is marked with an * (T-Test $p \leq 0.05$) Northern blots for single miRNAs are given in B. 293T cells were transfected with pcDNA3-GFP expressing either one or all EBV-miRNAs and expression level was compared to latently infected cells (Jijoye and C666-1). Investigated target sites derived from the Genome Browser are given in C.

Significant down-regulation of luciferase activity was found for miR-BART17 targeting NVL 3'UTR. In contrast, less regulation was shown for the miRNA-BART13. For ELP4, NME3 and TNKS2, a down-regulation through miR-BART7, miR-BART 5 and miR-BART7, respectively, was detected, but were not significant. The miRNAs tested for INPPL1, TCF4 and XPO1 were not able to down regulate luciferase activity.

For all investigated 3'UTRs further confirmatory luciferase assays have to be done. Mutating the putative binding sites should compensate the down-regulation. In addition, other EBV-encoded miRNAs might be tested for their ability to regulate the 3'UTRs. Western Blot analysis then might confirm the regulation on protein level to translate the finding into biological relevant mechanisms.

4.2.4.7. Gene Ontology of Gene Lists Derived From DNA Microarrays

The output of the array experiments led to a huge list of regulated genes. Another possibility to translate the derived data into biological relevant mechanisms is to analyze them functionally using algorithms from gene ontology databases available online. The database for annotation, visualization and integrated discovery (DAVID) (Dennis et al., 2003) was used to extract biological features associated with large gene sets. The arrays, which were performed in duplicate were analyzed (BJAB-GFP, Beas-2b, HNEpC4 d p.i.). Therefore, the overlap of both arrays passing a threshold of 2-fold standard deviation were submitted. Some interesting gene ontology (GO) terms, which were significantly enriched ($p \leq 0.05$) are depicted in tables 4-6 to 4-8.

For all array set-ups, genes involved in different mechanisms like apoptosis, cell death, immune response or cell cycle were enriched leading to the assumption that indeed important cell modulating functions might be regulated by EBV miRNAs.

Table 4-6 Gene Ontology Categories Enriched in BJAB-GFP Arrays

Term	Count	%	PValue
GO:0045580~regulation of T cell differentiation	3	10.0	0.0036
GO:0001817~regulation of cytokine production	4	13.3	0.0039
GO:0045619~regulation of lymphocyte differentiation	3	10.0	0.0055
GO:0006927~transformed cell apoptosis	2	6.7	0.0071
GO:0051094~positive regulation of developmental process	4	13.3	0.0126
GO:0050863~regulation of T cell activation	3	10.0	0.0181
GO:0006915~apoptosis	5	16.7	0.0203
GO:0012501~programmed cell death	5	16.7	0.0213
GO:0051249~regulation of lymphocyte activation	3	10.0	0.0280
GO:0006955~immune response	5	16.7	0.0316
GO:0008284~positive regulation of cell proliferation	4	13.3	0.0358
GO:0010033~response to organic substance	5	16.7	0.0363

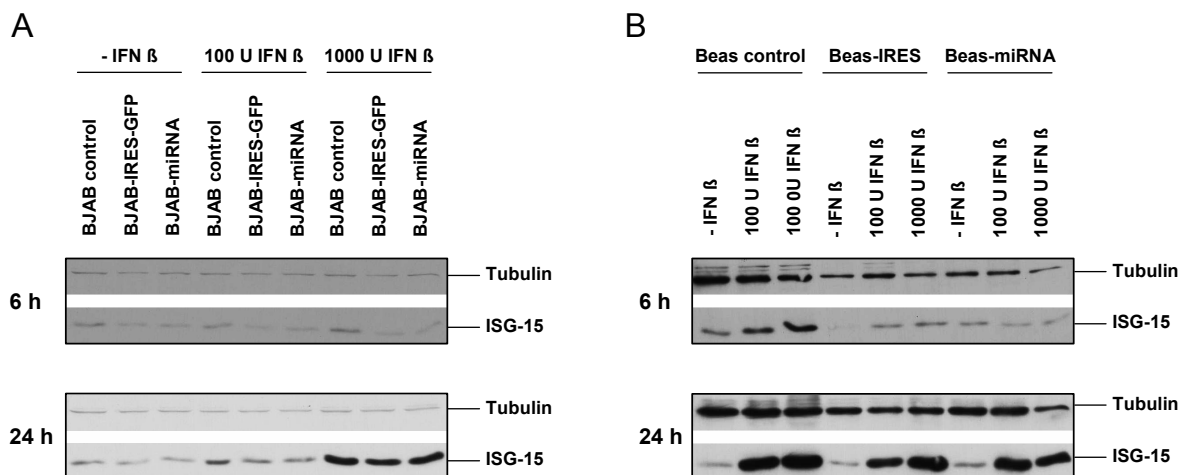
Table 4-7 Gene Ontology Categories Enriched in Beas-2b Arrays

Term	Count	%	PValue
GO:0045580~regulation of T cell differentiation	3	10.0	0.0036
GO:0001817~regulation of cytokine production	4	13.3	0.0039
GO:0045619~regulation of lymphocyte differentiation	3	10.0	0.0055
GO:0006927~transformed cell apoptosis	2	6.7	0.0071
GO:0051094~positive regulation of developmental process	4	13.3	0.0126
GO:0050863~regulation of T cell activation	3	10.0	0.0181
GO:0006915~apoptosis	5	16.7	0.0203
GO:0012501~programmed cell death	5	16.7	0.0213
GO:0051249~regulation of lymphocyte activation	3	10.0	0.0280
GO:0006955~immune response	5	16.7	0.0316
GO:0008284~positive regulation of cell proliferation	4	13.3	0.0358
GO:0010033~response to organic substance	5	16.7	0.0363

Table 4-8 Gene Ontology Categories Enriched in HNEpC 4 d p.i. Arrays

Term	Count	%	PValue
GO:0010033~response to organic substance	15	13.3	0.0002
GO:0006915~apoptosis	12	10.6	0.0018
GO:0012501~programmed cell death	12	10.6	0.0020
GO:0008219~cell death	13	11.5	0.0023
GO:0043123~positive regulation of I-kappaB kinase/NF-kappaB cascade	5	4.4	0.0037
GO:0009719~response to endogenous stimulus	9	8.0	0.0048
GO:0010647~positive regulation of cell communication	8	7.1	0.0056
GO:0007049~cell cycle	12	10.6	0.0117
GO:0009967~positive regulation of signal transduction	7	6.2	0.0124
GO:0040008~regulation of growth	7	6.2	0.0237

Triggering the immune response (see table 4-6 and 4-7) seems to be a beneficial way for miRNAs to facilitate episome maintenance. To further test this aspect, the aim was to investigate differences in interferon signaling of cells expressing EBV-encoded miRNAs or GFP only. Stable cell lines and the adenovirus infected HNEpC were treated with IFN- β to induce interferon signaling and subsequently analyzed in Western blots for the expression of an interferon-stimulated gene (ISG-15) (figure 4-32).

**Figure 4-32 Western Bot Analysis of IFN- β Treated BJAB and Beas-2b Stable Cell Lines**

BJAB or Beas-2b stable cell lines (A and B, respectively) were incubated either without or with 100 U or 1000 U IFN- β for indicated time. Western Blot was performed using α -ISG-15 and α -Tubulin antibodies. ISG-15 production was increased depending on both concentration and time.

ISG-15 production was induced upon stimulation in correlation to amount of IFN- β and time elapsing before lysate preparation. No obvious difference was detectable between control stable cell lines or miRNA expressing cell lines. Nevertheless a miRNA dependent inhibition of interferon pathways might be possible. Due to long cultivation and selection with G418, the stable cell lines might have diminished the potential of miRNAs to inhibit interferon stimulation through adaption of cellular genes involved in this pathway. Nevertheless an effect in primary cells upon infection with adenoviruses regarding IFN response might be detectable. Therefore lysates from adenoinfected HNEpC used in gene expression arrays, were analyzed for ISG-15 expression.

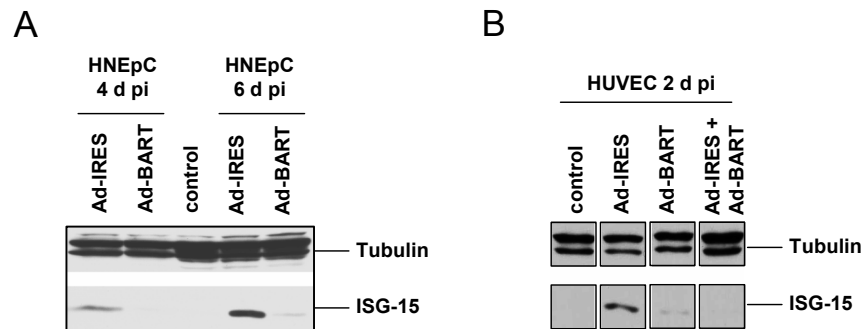


Figure 4-33 Western Blot Analysis of HNEpC or HUVEC Cells Infected With Adenovirus

HNEpC, that were used in microarray analysis were analyzed for their expression of ISG-15 (A). HUVEC cells were infected with either Ad-IRES, Ad-BART or both to evaluate miRNA dependent inhibition of ISG-15 expression (B). Western blot was performed using α -ISG-15 and α -Tubulin antibodies.

The Western blotting showed that ISG-15 was more induced in Ad-IRES infected cells than in Ad-BART infected cells. To analyze this in more detail, HUVEC cells were used as model system, to perform adenoviral infections. The cells were infected with either Ad-IRES or Ad-BART alone or together to investigate if the miRNAs are able to inhibit the interferon response of Ad-IRES. Indeed a first analysis demonstrated that infection with Ad-IRES leads to the production of ISG15, whereas Ad-BART, as well as the double infection, only slightly activated expression. These data are very promising to further investigate a potential regulation of the interferon answer by EBV-encoded miRNAs.

5. Discussion

More than 90% of adults are estimated to be infected with EBV. EBV is not only the aetiologic agent of Infectious Mononucleosis (IM), but is also associated with different kinds of tumors like Burkitt's lymphoma or Nasopharyngeal carcinoma. The precise contribution of EBV to tumorigenesis is however, only partially understood. The virus usually remains as a benign latent infection throughout the host's lifetime. The gene expression in latency is strictly limited to very few genes, whereas all viral miRNAs are expressed. When this work was started the miRNA registry listed 146 viral miRNAs, with the vast majority being encoded by herpesviruses. Since miRNAs require minimal coding capacity and are non-immunogenic, they are a useful tool for herpesviruses to modulate host cell gene expression. Thus, it was proposed that miRNAs have an important function in the herpesviral life cycle. There is little evidence for evolutionary conservation, except for seven miRNA hairpins shared between EBV and its next related rhesus lymphocryptovirus (rLCV). It was postulated that γ -herpesviruses encode many more miRNAs and with the assumption that miRNAs are functionally important, they may be more conserved than adjacent sequences without coding capacity. Therefore, the conservation state of all known and predicted γ -herpesvirus encoded miRNAs was investigated.

Beside the analysis of miRNA conservation, EBV miRNA targets were investigated. Very little was known about the functions and mRNA targets of EBV-encoded miRNAs. Therefore, different vector systems were generated to investigate functions of all EBV-encoded miRNAs. Additionally, different biological systems were established to identify miRNA targets. Taken together, the global identification of viral miRNAs and their conservation as well as their target identification should lead to a better understanding of viral miRNA function and EBV pathogenesis.

5.1. Identification and Conservation of γ -herpesvirus miRNAs

5.1.1. VMir Analysis to Identify Conserved Pre-miRNA Hairpins

To date, different methods have been used for the identification of miRNAs. Next to conventional cloning approaches and Northern blotting, different computational predictions support miRNA identification.

Several bioinformatic techniques use diverse definitions for the identification of miRNAs, including size, structure, conservation and function. Distinctive properties include structural features as well as sequence features. Some examples are listed in table 5-1 (Bentwich, 2005).

Table 5-1 Features Implemented in Algorithms to Predict Pre-miRNA Hairpins

Structural Features	Sequence Features
Hairpin length, Loop- length	Nucleotide content
Base pairing	Nucleotide location (introns, exons, intergenic)
Amount location and size of bulges	Sequence complexity
Thermodynamic stability	Repeat elements
Location of the miRNA within the hairpin	Internal and inverted repeats

Whereas programs for cellular miRNAs often use evolutionary conservation as a criterion for minimizing false positive predictions, known orthologs of viruses are often evolutionary distant. VMir was established a few years ago as an *ab initio* prediction for viral miRNAs. Its sensitivity was demonstrated by its ability to identify more than 50 viral miRNAs (Grundhoff et al., 2006; Sullivan and Ganem, 2005; Sullivan et al., 2009; Walz et al., 2010). Nevertheless, as with all computational predictions an appropriate balance between accuracy and sensitivity needs to be considered. VMir uses the RNAFold Algorithm (Hofacker and Stadler, 2006; Schuster et al., 1994) and was designed to over-rather than under-predict candidate pre-miRNAs to ensure a high sensitivity. The assumption for conserved miRNAs was that the hairpins should be more conserved than the background. Proteins of herpesviruses are also more conserved than intergenic regions and thus it is impossible to decide, if the conservation of pre-miRNAs located in coding regions is due to conservation of miRNA function or to conservation of protein sequence. Based on this detail and to minimize the amount of false positives, all pre-miRNA hairpins predicted within open reading frames (ORF) were excluded in the analysis. Although this might lead to the loss of some pre-miRNAs, it can be assumed, that the amount would be rather low, since only three of all experimentally verified viral miRNAs are located within ORFs (Cai et al., 2005; Schafer et al., 2007).

5.1.2. Identification of Novel Pre-miRNA Hairpins in γ -Herpesvirus Genomes

In this work novel pre-miRNA for EBV (2), rLCV (17) and JMHV (14), were identified from 9, 20 and 21 predicted pre-miRNAs were confirmed, representing a manageable amount of false positives.

Since there are very few structural features that allow one to distinguish between *bona fide* pre-miRNA hairpins and other hairpin structures, a lot of false positive candidates are expected on the one hand, while on the other hand some *bona fide* pre-miRNA hairpins will be missed since the program considers only the lowest free energy structure, which does not always represent the most probable folding of a hairpin. A few mature miRNAs were in fact identified that were not derived from the lowest free energy prediction, like rlcV-miR-23 and 25 (figure 4-13) as well as JMHV-rJ1-4 (figure 4-14), but from a structure with a slightly higher free energy.

Two studies of direct relevance supported the data of this work analyzing the whole small RNA content of different cell lines by next generation sequencing (deep sequencing). Here, two novel EBV miRNAs were identified and confirmed by Northern blotting (figure 4-5). In 2009, Zhu and colleagues published deep sequencing data from EBV positive nasopharyngeal carcinoma cells C666-1, including

the same miRNAs (Zhu et al., 2009). Since no other pre-miRNAs were identified in this and in the work of Zhu and colleagues, it may be assumed that all EBV-encoded miRNAs have now been identified.

In this work, 17 novel rLCV encoded pre-miRNAs with 22 novel mature miRNAs were identified and confirmed in Northern hybridization (figure 4-7). Out of each pre-miRNA hairpin, two mature sequences are processed. In most cases, one is more rapidly degraded and represents the minor mature miRNA, which is designated miRNA*. Here, a very stringent strategy for the identification of novel miRNAs was used. First, secondary structures were predicted. Second, good scoring candidates were analyzed using Northern blotting to identify novel mature miRNAs. Third, positive candidates from Northern blotting were subjected to a cloning approach specific for each sequence. Thereby mature sequences with very low expression were missed, due to the detection limit of Northern blotting. Another problem arises due to cross reactivity of probes in Northern blotting. If a band was detectable also in control cells that are not encoding the miRNA of interest, the predicted miRNA was not investigated further. Nevertheless, this approach was reliable and productive in comparison to the deep sequencing data of a study analyzing another rLCV positive cell line (Riley et al., 2010). Recently after publication of the data shown in this work (Walz et al., 2010), Riley and colleagues identified two additional, novel pre-miRNAs and 21 additional, novel mature miRNAs, which were missed in all previous analyses (Cai et al., 2006; Walz et al., 2010). One was not even producing mature miRNAs at sufficient levels for detection in Northern hybridization. The other novel mature miRNAs were missed in our study due to their expression levels and the absence in Northern blots. The current opinion is that star miRNAs are not biologically active or play only a minor role in target recognition, due to their faster degradation and statistical lower abundance in RISC complexes. It is, however, possible that in some cases the star miRNA is incorporated into RISC as efficiently as the more abundant mature miRNA (Riley et al., 2010).

The identification of JMHV miRNAs was more challenging, since a latently infected cell line was not available. JMHV is highly homologous to RRV and in particular the region encoding RRV miRNAs is at the same genomic location in JMHV. Therefore, the region flanked by ORF69 and ORF71 was cloned into an expression vector and used to transfect cell lines. Although this approach does not reflect physiological expression levels in latently infected cells, sufficient amounts of RNA for Northern blot analysis were produced. Out of 14 novel identified pre-miRNA hairpins, 26 mature sequences were identified in Northern hybridization and sequencing analyses. Additionally, mature miRNA* moieties were cloned and sequenced (e.g. miR-rJ-4 5p, miR-rJ-7 3p, miR-rJ-9 3p, see figure 4-10 and table 4-3) even without a detectable band in Northern blots.

Interestingly, a high sequence variability was shown for the mature miRNA sequences (table 4-2 and 4-3). The different 5'ends, sequenced in this work, were consistent with the deep sequencing data and abundance of mature sequences (Riley et al., 2010). This further underlines the efficacy of this approach. The sequence variability determined by deep sequencing was significantly higher at the

3' end matching the knowledge that the 5' end is more relevant for target recognition and therefore should be less diverse.

It has been shown for different rhadinoviruses it was shown, that infection of primary cells leads to lytic replication and increased levels of miRNA expression. Based on these findings, the miRNA expression of JMHV infected rhesus primary fibroblast cells was analyzed by Northern hybridization using two JMHV miRNAs (figure 4-11). Consistent with other rhadinoviruses, JMHV replicates lytically in primary cells and miRNA expression was found to increase over time.

Although diverse analysis have been performed to analyze and identify γ -herpesvirus miRNAs, in this work a very reliable and sensitive strategy was established allowing the identification of all viral encoded miRNAs.

5.1.3. Conservation State of Predicted Pre-miRNA Hairpins

The conservation of miRNAs is discussed in the next section. Different terms that are used in the following part are explained to clarify their meaning. The pre-miRNAs of viruses analyzed in this work are homologous pre-miRNAs, since they are encoded at the same genomic regions. Orthologous pre-miRNAs are believed to be derived from the same evolutionary ancestor. Sequence identity is used as a term to describe conservation between two orthologous pre-miRNAs. Both the pre-miRNA and the mature miRNAs are analyzed for their sequence identity.

To identify novel pre-miRNAs and further analyze the conservation state, pre-miRNA hairpins of all fully sequenced γ -herpesvirus genomes were predicted and the sequences of all viruses were aligned with each other. Candidate hairpins were predicted for all viruses, but only in two cases conserved pre-miRNA hairpins were predicted, indicating that indeed the conservation of viral miRNAs is rare. This analysis showed no evidence that viruses having less than 60% sequence conservation encode for evolutionarily conserved miRNAs. Interestingly, high numbers of miRNAs were predicted for all analyzed viruses especially in AHV-1, OvHV-2 and EHV-2. Whereas AHV-1 and OvHV-2 share about 25% sequence conservation the conservation to EHV-2 was less than 10%. Strikingly, the location of predicted pre-miRNA hairpins was identical in all viruses, although they lack higher sequence conservation. Hairpins were generally located in one of two regions. The first of these was a region downstream of the DNA polymerase gene, which is equivalent to the location of the BART miRNA of EBV and miRNAs from rLCV, and which is furthermore devoid of open reading frames. Moreover, the position of BHRF miRNAs of EBV and rLCV was equivalent to that of the known and predicted miRNAs from KSHV, RRV and JMHV. The prediction of pre-miRNA hairpins of CaHV-3, BoHV-4, HVS and MHV-68 lead to fewer candidates, these were also located at similar positions of the EBV and / or KSHV encoded miRNAs.

After prediction of putative novel conserved pre-miRNAs, a detailed analysis of all predicted (conserved and non-conserved) miRNAs from EBV, rLCV and JMHV was performed and all high scoring hairpins were analyzed in Northern hybridization. Following sequencing of the 5' ends the

analysis of conservation was performed. By comparing all rLCV and EBV miRNAs it was shown that 22 pre-miRNAs display signs of evolutionary conservation (figure 4-15 and supplementary figure 1). This number is about three times higher than previously known. A seed region conservation of one third of all mature miRNAs was detected, which likely is the most important criteria for target conservation and function. The conservation of the miRNA* moieties was lower. Although they map to pre-miRNA hairpins with evolutionary conservation, their seed tended not to be conserved, whereas the corresponding mature miRNA from the other arm of the hairpin are conserved in their seed region, indicating that they are subject to higher evolutionary pressure and have more important biological functions. One example is miR-BART14, which is homologous to rlcv-miR-rL1-32 and is depicted below (figure 5-1).

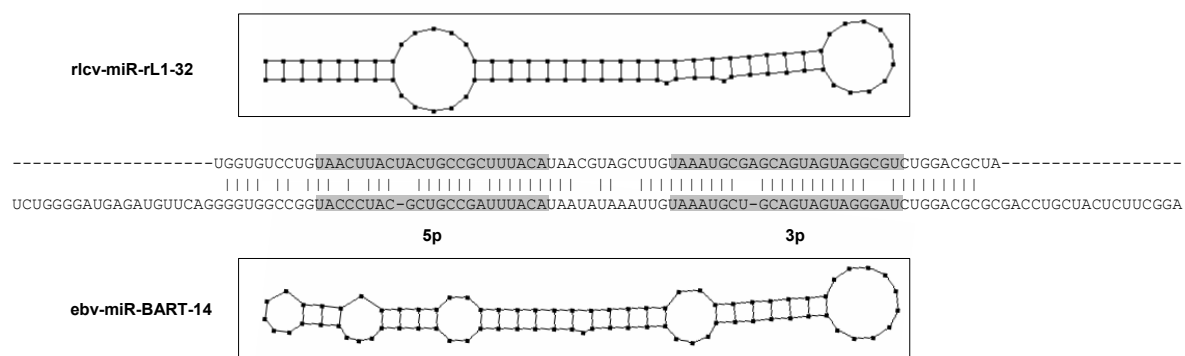


Figure 5-1 Alignment of Pre-miRNA Hairpins of rlcv-miR-rL1-32 and ebv-miR-BART14

Alignment of rlcv-miR-rL1-32 and ebv-miR-BART14 pre-miRNA sequences are aligned. Identical nucleotides are connected with lines. Hairpin structures are shown above and below the alignment. Mature miRNA sequences are highlighted in grey (dark grey shading highlights an alternative start of the miRNA, that was sequenced). The mature miRNA representing the minor moiety is marked with an *. The seed sequence ranging from nt 2-7 of the mature miRNA is not conserved for the 5p* miRNA but for the 3p miRNA.

Changes in the pre-miRNA hairpin sequence and structure could lead to different start sites of procession and processing efficiency by Drosha and Dicer. Accordingly, mature miRNAs from homologous hairpins without seed conservation may arise due to either no mature miRNA being produced at all, or an alternative start of the mature sequence being used in one of the orthologous hairpins. Examples for the first observation are BHRF1-3/rlcv-miR-17 and ebv-miR-BART-15/rlcv-miR-rL1-7, producing mature miRNAs from opposite strands of the EBV and rLCV hairpins (figure 4-15). The orthologous mature sequence to ebv-miR-BART16, rlcv-miR-rL1-6 has been shown in 6 out of 8 sequences to have an additional nucleotide in position 1 leading to a different seed match, whereas the other two sequences have the same seed as the EBV miRNA (figure 4-15, table 4-2). This raises the possibility that the altered seed sequence of one miRNA moiety may have evolved additional or different targets.

The recently identified novel mature miRNAs (Riley et al., 2010) did not increase the number of conserved miRNAs between EBV and rLCV. Four novel mature sequences from previously identified

pre-miRNA hairpins all represented less abundant miRNAs that had no conservation in their seed. The other novel mature miRNAs that were identified from non-conserved pre-miRNA hairpins or from conserved hairpins in which the homologous EBV miRNA has not been identified so far.

At the time of this work another group identified eight novel pre-miRNAs from RRV in viral induced tumors from infected rhesus macaques, increasing the total number of RRV miRNAs to 15 (Umbach et al., 2010). Five novel pre-miRNAs were also included in our previous prediction, the remaining ones were encoded within ORFs (rJ1-5, -9, -1, -8) and thus had evaded our analysis. Only one pre-miRNA hairpin was missed, due to its low window count (rJ1-11). An alignment of the novel identified RRV and JMHV pre-miRNAs illustrates the high conservation between the closely related viruses (figure 4-17, supplementary figure 2). In this work 14 novel pre-miRNAs were identified in JMHV, a virus very closely related to RRV, infecting the same host. Due to the high sequence conservation all identified miRNAs show conservation to their counterparts. Of the 26 mature miRNAs 19 have conserved seed sequences, mirroring the overall high sequence conservation and probably the high functional importance of these miRNAs (see also supplementary table).

Although the primary sequence conservation was very high, as in the case of EBV and rLCV, some pre-miRNAs seem to be differentially processed leading to different mature miRNA sequences. Table 5-2 summarizes the findings.

Table 5-2 Differences of Mature miRNA Sequences of JMHV and RRV

miRNA	JMHV miRNA compared to RRV
miR-rJ1-1 3p	mature miRNA sequence 1 nt different
miR-rJ1-2	JMHV 5p and 3p, RRV only 3p mature miRNA
miR-rJ1-6 5p	mature miRNA sequence 1 nt different
miR-rJ1-9 5p	mature miRNA sequence 1 nt different
miR-rJ1-9 3p	mature miRNA sequence 1 nt different
miR-rJ1-10 3p	mature miRNA sequence 2 nt different
miR-rJ1-11	Northern blot negativ, 5p miRNA sequenced
miR-rJ1-14	JMHV 3p miRNA, RRV 5p miRNA

Most of the differences in mature miRNA sequences are likely due to nucleotide changes that lead to slightly different hairpin secondary structures assuming a different procession by Drosha and Dicer (table 5-2, hairpins miR-rJ1-2, -6p, -9 5p, 10-3p, -14). Some other sequences had a very low abundance and thus it might be suggested that the sequences are not representing the correct end (table 5-2, miR-rJ1-1 3p, -9 3p). The hairpin encoding for miR-rJ1-11 was missed in the first analysis probably due to a low window count (2) and a Vmir score near the threshold (135.8). Northern hybridization, accordingly, failed to detect a mature sequence. The hairpin of the identified miRNA from RRV miR-rJ1-11, in contrast, folds in 6 windows and has a greater Vmir score (194.1), displaying a secondary structure, that is more probable to for being processed by Drosha and Dicer into mature miRNAs. Nevertheless, a sequence for the 5p miRNA from this predicted hairpin of JMHV was obtained. Due to that, the hairpin might produce mature miRNAs at an expression level below the Northern blot detection limit. Interestingly, the 3p mature miRNA from rJ1-14 was identified in this work, whereas deep sequencing identified the 5p miRNA from the orthologous

hairpin (miR rR1-14 5p) (Umbach et al., 2010). The pre-miRNA hairpins differ only in 2 nt, one at the 5' end and one near the terminal loop, leading to a slightly differing hairpin structure. It might be possible that thermodynamic differences in the resulting miRNA duplexes lead to the different expression of 5p or 3p mature miRNA.

Mature miRNAs are the functional part of the pre-miRNA hairpin. Assuming that they have important functions, the mature miRNAs should be more conserved than the overall conservation of the hairpin. Furthermore, mature miRNAs that are derived from an orthologous hairpin but are only expressed from either one of two viruses should be more diverse due to a lower evolutionary pressure. Table 5-3 summarizes the analysis of hairpin conservation between EBV and rLCV as well as JMHV and RRV.

Table 5-3 Sequence Identity of Orthologous Hairpins

Virus	Mature miRNA Conserved	Mature miRNA Non-conserved	Pre-miRNA conserved
EBV vs. rLCV	77%	72%	71%
JMHV vs. RRV	95%	91%	88%

The overall sequence conservation of orthologous pre-miRNA hairpins and mature miRNAs is lower for EBV and rLCV as they are evolutionary more distant than JMHV and RRV. As expected, the sequence conservation of the pre-miRNAs is higher than the overall sequence conservation of the miRNA encoding regions as shown in figure 4-3. The BHRF and BART locus of EBV has a sequence identity of 71 and 67% and the region between ORF 67 and 71 of RRV has a sequence identity of 72%. Mature miRNAs, that are found in both viruses are more conserved than the conserved pre-miRNAs. Furthermore, mature miRNAs that are derived from an orthologous pre-miRNA, but are only found in one virus are less conserved as the mature miRNAs found in both viruses. This argues for a higher selection of the mature miRNA sequence in comparison to the pre-miRNA. A detailed analysis of mature miRNAs that are only expressed in one of the viruses showed that they are the less abundant star miRNAs of the pre-miRNA. Thus the more abundant mature miRNA are under higher evolutionary pressure. The higher evolutionary sequence conservation of pre-miRNAs and mature miRNAs compared to the overall sequence conservation argues for important functions of these miRNAs.

To date, no targets of RRV miRNAs have been identified. However, considering the conservation of mature miRNA sequences it will be interesting to see, if miRNA sequences have evolved co-linearly with their viral or host mRNA targets since JMHV was isolated only from Japanese monkeys, whereas RRV was identified in diverse other rhesus macaques.

The identification of conserved miRNAs in related viruses may help in the computational target identification in different ways. Conserved mature miRNAs, especially those in which the seed sequence is conserved are suggested to regulate the same mRNAs. This was demonstrated for the miR-K11 of KSHV and the human cellular miRNA miR-155. The mature miRNAs share the same seed sequence and regulate the same set of target mRNAs (McClure and Sullivan, 2008). A first prediction of potential target sites in the human genome for conserved miRNAs of EBV revealed

147748 sites. A comparable search for corresponding sequences in the rhesus genome was performed in order to narrow down the amount of potential target sites. Subsequently the ability of conserved rLCV miRNAs to bind to the corresponding sites was conducted and revealed 105482 hits, reducing the number of potential sites by approximately 1/3rd. The other way around, non-conserved miRNAs might either have non-conserved targets or more interestingly might have co-evolved with their host to target the same mRNA. A target site prediction for non-conserved miRNAs revealed 340971 possible target sites. Out of these, 1108 are targeted by different miRNAs. This approach led to a dramatic reduction of predicted potential conserved target sites as depicted in figure 5-2.

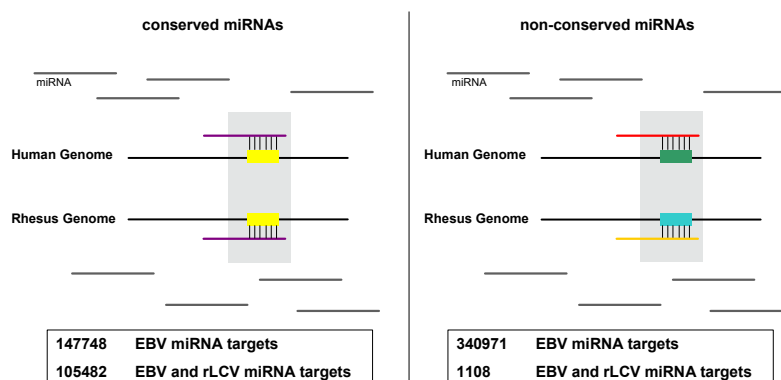


Figure 5-2 Implementation of Conserved and Non-conserved miRNAs Into Target Prediction

Conserved miRNAs might target conserved mRNAs (left). Non-conserved miRNAs targeting the same sites of the corresponding mRNA can highly reduce the list of putative mRNA target sites (right). miRNAs are indicated as short, gray lines, and colored to display conserved or non-conserved miRNAs. Target sites on mRNAs are highlighted as colored boxes, indicating the same or non-conserved sequences (left and right, respectively).

Whether targets identified using this approach are more relevant or more probable to be regulated by miRNAs has to be experimentally confirmed.

5.2. Target Identification

This work was started shortly after the first viral miRNAs were identified (Cai et al., 2005; Grundhoff et al., 2006; Pfeffer et al., 2005b). Nothing was known about the targets of viral miRNAs and also the techniques to identify miRNA targets were not well established. Nevertheless, it was clear that viral miRNAs are thought to have important functions, based on the fact that they are non-immunogenic and require few coding capacity. Due to their imperfect complementary binding to target mRNAs they are able to regulate large amounts of targets to modulate either viral or cellular mRNAs. The fact that EBV miRNAs are expressed in all types of latency and found in EBV associated tumors lead to the assumption that they may play an important role in latency, in modulating the cellular environment and in tumorigenesis. To address some of these questions and to elucidate the putative functions of EBV miRNAs different computational and analytical approaches were applied in this work.

5.2.1. Conserved Targets

Although herpesviruses encode for large numbers of miRNAs, their conserved functions are widely unknown. In contrast, the polyomaviruses are known to encode for only one miRNA, which is expressed late during infection to autoregulate early gene expression. Polyomavirus miRNAs have evolved a conserved function, however, their sequences are not conserved. The miRNA dependent down-regulation of the immunogenic early transcripts enables polyomaviruses to evade immune surveillance (Seo et al., 2009; Seo et al., 2008; Sullivan et al., 2005; Sullivan et al., 2009).

The global analysis of miRNAs encoded by EBV and rLCV revealed the existence of 17 mature miRNAs with a conserved seed region. Thus, the miRNAs might target the same mRNAs in different host species, if these targets are conserved as well. During this work, some EBV miRNA targets have been published (see chapter 1.3.7.4, table 1-2) and are discussed below.

BALF5, the polymerase encoded by EBV, has been shown to be regulated by miR-BART2, a miRNA that is perfectly complementary to the 3'UTR of BALF5 (Furnari et al., 1992). BALF5 lacks a canonical poly A signal and has a very long 3'UTR. miR-BART2 is encoded at a position within this 3'UTR but on the other strand of the EBV dsDNA genome. Thus miR-BART2 has a perfectly matching sequence and can act as a siRNA on the BALF5 mRNA. The direct binding of the miR-BART2 to the 3'UTR of BALF5 was confirmed in *in vitro* experiments and the cleaved BALF5 transcript was detected by Northern blotting (Barth et al., 2008; Furnari et al., 1992). In this work, a homologous miRNA was identified at the same genomic position in the rLCV genome. In line with the EBV-encoded BALF5 no canonical poly-A signal was found in the BALF5 gene of rLCV. Northern hybridization failed to detect both, the RNA of the polymerase BALF5 and the degradation products (data not shown). Thus a conserved function was not confirmed. The relevance *in vivo*, however, is controversial. BALF5 is a lytic gene product, while miR-BART2 is latently expressed. A proposed involvement in the switch from the lytic cycle to latency (Barth et al., 2008) is not likely, since latency is also established in systems lacking miRNAs (Seto et al., 2010).

The 3'UTRs of other published viral miRNA targets like LMP-1 and LMP-2A (Lo et al., 2007; Lung et al., 2009) are not conserved. Additionally, the miRNAs shown to regulate these mRNAs are only partially conserved for LMP-1 or not conserved in the case of LMP-2A. A conserved function would only be possible, if alternative binding sites and viral miRNAs exist.

The p53 upregulated modulator of apoptosis (PUMA) has been shown to be regulated by miR-BART5. The expression of PUMA was found to be significantly decreased in about 60% of NPC tissues, where the expression of BART5 is high. Furthermore, depletion of miR-BART5 or the induction of PUMA expression leads to a higher susceptibility of NPC cells to apoptotic stimuli. Thus, it was suggested that miR-BART5 facilitates the establishment of latent infection by promoting host cell survival (Choy et al., 2008). rLCV encodes a nearly 100% identical mature miRNA rL1-8. The 3'UTR of PUMA is also conserved in rhesus macaques with only two nucleotide changes in the area of miRNA binding. Nevertheless, the analysis in the luciferase assay did not confirm the target

conservation of this miRNA. Whereas a marginal effect was observed for human PUMA regulated by BART5, no effect was detected for rhesus PUMA and rL1-8.

PUMA-human	5' UGGUGGGCAUGCCUGCCUCACCUUC 3'	PUMA-human	5' UGGUGGGCAUGCCUGCCUCACCUUC 3'
PUMA-rhesus	5' UGGUGGGUGUGCCUGCCUCACCUUC 3'	ebv-miR-BART5	3' GCUACCCGU-CGAUUAAGUGGAAC 5'
ebv-miR-BART5	5' CAAGGUGAAUAUAGCUGCCCAUCG 3'	PUMA-rhesus	5' UGGUGGGUGUGCCUGCCUCACCUUC 3'
rLcv-miR-rL1-8	5' UAAGGUGAAUAUAGCUGCCCAUUG 3'	rLcv-miR-rL1-8	3' GUUACCCGUCGAUUA-AGUGGAU 5'

Figure 5-3 Sequence Comparison of Conserved PUMA Target Site and Conserved miRNAs

The conserved PUMA target site and the conserved miRNAs postulated to bind the site are depicted in the left box. In the right box, the binding of the miRNAs to the corresponding target site is shown.

This unexpected negative finding may be due to different 3'UTRs used in this work and by Choy et al. (Choy et al., 2008). Although the target site was included in the construct used here, a slightly shorter sequence was generated, due to amplification difficulties, compared to the work of Choy and colleagues. It is possible that sequence differences can cause secondary structures making it impossible for the miRNA to bind to the mRNA target site. It was postulated that the two nucleotide changes in the miRNA binding site may disrupt the efficient binding of the miRNA by changing Watson Crick base pairs into GU pairs (figure 5-3). Similarly another group also investigated the potential of PUMA being a conserved target and could not confirm a regulation of rhesus PUMA 3'UTR by rL1-8 (Riley et al., 2010). In conclusion, it is likely that PUMA is not a conserved functional target.

For the published cellular targets of miR-BHRF1-3 and miR-BART6, CXCL-11 and Dicer, respectively (Iizasa et al., 2010; Xia et al., 2008b), no convincing direct regulation of the miRNA was shown. Additionally, although the 3'UTR of CXCL-11 is highly conserved between human and rhesus, there is no conserved miRNA (miR-BHRF1-3, figure 4-16). The same is true for the miRNA targeting Dicer (miR-BART6), which displays no seed match conservation making a conservation is not likely.

MHC class I chain-related molecule B (MICB) has been identified to be a target of diverse viral miRNAs. MICB is one of several stress induced molecules upregulated at the cell surface due to different processes such as viral infections, tumor transformation or DNA damage (Boissel et al., 2006; Groh et al., 1996). It is recognized by a NK-cell activating receptor (NKG2D) (Raulet, 2003) and is for obvious reasons a conceivable target of viral miRNAs. It has been shown that HCMV, EBV and KSHV encode miRNAs that reduce mRNA expression. Although the various viral miRNAs share no sequence conservation, they are functionally similar and target MICB at adjacent sites within the 3'UTR (Nachmani et al., 2009). Interestingly, MICB is targeted by ebv-miR-BART2 5p, which was shown here, to be conserved in rLCV (rlcv-miR-33 5p) (figure 4-15, supplementary figure 1). Despite the fact, that the mature miRNAs are derived from an orthologous hairpin, the seed region of the mature miRNA is not identical in both miRNAs (figure 4-15). If the function is conserved, it would be likely that the rlcV-miR-rL1-33 5p has co-evolved with the mRNA of MICB, suggesting that

differences in the seed sequences are compensatory to the MICB mRNA sequence in rhesus macaques. However, the binding site for ebv-miR-BART2 5p is conserved in the rhesus genome and thus it is unlikely that rlcv-miR-rL1-33 regulates MICB. Nevertheless, it can not be excluded that rlcv-miR-rL1-33 might bind to another site or that another rlcv miRNA may have evolved the ability to regulate MICB.

Two novel EBV miRNA targets have been identified by immunoprecipitation of Ago2 complexes following DNA array analysis (Dolken et al., 2010). Mitochondrial import receptor subunit TOM 22 homolog (TOMM22) and Importin 7 (IPO7) were enriched in the Ago IP and luciferase assays verified the direct binding of miR-BART 16 and -3, respectively (Dolken et al., 2010). TOMM22 is involved in the import of proteins from the cytoplasm into the mitochondria (Saeki et al., 2000; Yano et al., 2000) and is able to prevent BAX induced apoptosis (Bellot et al., 2007). IPO7 is a nuclear import factor (Gorlich et al., 1997) that may play a role in the innate immunity. Knockout of IPO7 in macrophages for instance reduces IL-6 production upon lipopolysaccharide (LPS) challenge (Yang et al., 2009). The importance and exact function of TOMM22 and IPO7 regarding EBV infection has not been demonstrated so far. Both miRNAs are conserved, but the mature sequence homologous to miR-BART16 has been shown to have two different 5'ends. One exactly representing the seed of miR-BART16, the other having an additional nucleotide at position 1. These candidate targets may be regulated by rLCV miRNAs and will be investigated in the near future.

5.2.2. Expression Systems for miRNAs and Phenotypic Analysis

EBV-encoded miRNAs are expressed simultaneously in all types of latency. Therefore it can be proposed, that they act as unit to modulate virus as well as host gene expression. This might be done by either targeting of the same mRNA by different miRNAs or by regulating different mRNAs leading to a global alteration of different mechanisms to generate an advantageous environment for the virus. In addition, the miRNAs might act independently of each other. To gain a better understanding of how EBV-encoded miRNAs co-operate, all EBV miRNAs were cloned into an expression vector driven by a CMV promoter and following GFP as a marker gene. MiRNAs were cloned behind *gfp*. We reasoned that, although miRNA processing is expected to destabilize the transcript, enough mRNA should escape Drosha processing to achieve detectable GFP expression. Indeed, transfected cells were producing less GFP when miRNA hairpins were introduced. Fluorescence activated cell sorting (FACS) of GFP-positive cells and Northern blotting showed, that miRNAs were abundantly expressed at comparable levels comparable to latently infected cells (figure 4-18). Although miRNAs are all derived from one transcript, expression levels are different in latently infected cells as well as within the transfected cells. This likely occurs due to different secondary structures of hairpins and thereby resulting processing efficiencies (Zeng and Cullen, 2005; Zhang and Zeng, 2010)

Using this expression construct the first analyses were performed in transfected cell lines (293T, HeLa) to investigate if miRNA expression leads to any observable phenotypic changes. Different

pathways and functions were investigated including cell cycle distribution, growth (MTT Assay), survival (after treatment with cisplatin, UV induced damage, γ -irradiation), differences in interferon signaling (Fas, IFN- β) as well as Western blotting for key cellular proteins involved in apoptosis and survival like cMyc, p53 and Bax. Unfortunately no significant differences were identified (data not shown). To exclude the possibility of false negative results, cells were sorted by FACS to generate miRNA expressing stable cell lines (BJAB and Beas-2b). The cellular assays were then repeated which yielded no profound differences to the unselected transiently expressing cells. Based on these findings it was concluded that EBV miRNAs display no detectable phenotypic changes in these established cell lines. Alternatively, the miRNAs might regulate genes or pathways that are not functional in transformed cell lines (e.g. interferon responses) or that were compensated by other mechanisms. Another possibility is that miRNA target regulation may be a time dependent event, occurring exclusively shortly after expression of miRNAs, which would be missed in this approach due to the long time selection of the cell lines (e.g. BJAB and Beas-2b stable cells).

To either confirm or negate these later possibilities, a viral approach was employed to allow infection of cell lines at a high infection rate and to infect primary cells. Therefore to have a more sensitive and more relevant model system to study miRNA functions, we tried to generate retro- and lentiviral vectors. This proved to be unsuccessful as only few virus particles were produced. This can be explained by a potential destruction of the retro- or lentiviral genome mediated by the secondary structure of the inserted pre-miRNA sequence. In a single stranded RNA genome, as found in retro- and lentiviruses, the pre-miRNA sequence might fold into their hairpin structures, when novel RNA is generated in the nucleus, and might be recognized and processed by Drosha leading to a fragmentation of virus genomes (Liu et al., 2010; Poluri and Sutton, 2008). Accordingly, no complete genome is packaged into novel virus particles. Although there are diverse systems available that use hairpins to generate miRNAs or siRNAs from lentiviral vectors (Ventura et al., 2004), these are limited and dependent on the number of miRNAs. In our group pre-miRNA encoding vectors producing infectious viral particles were established encoding fewer miRNAs. However the efficiency of these viruses is remarkably lower compared to control viruses. In order to circumvent this problem and to prevent pre-miRNA processing in the virus producing cells, it is possible to down-regulate Drosha (Liu et al., 2010). Another alternative is to use adenoviral vector systems, since these are DNA viruses the pre-miRNA hairpins do not interfere with the production of novel viruses. Additionally, they highly infect most cell types.

Based on the favourable features of the adenoviral system and on the availability of human nasal epithelial primary cells (HNEpC) it was opted for this approach. Since only BART miRNAs are expressed in this carcinoma, it was decided to generate three different adenoviruses expressing either only IRES-GFP as a negative control, the BHRF miRNAs or the BART miRNAs. The resulting adenoviruses efficiently infected cell lines as well as in HNEpCs (figures 4-19 and 4-20, respectively). The expression levels of the miRNAs could be further modulated using different multiplicity of infection (MOI) titers (figure 4-19). Infection rates of nearly 100% and expression levels comparable

to latently infected cells. This was shown by Northern blots for cell lines or by stem-loop RT PCR for primary cells (figure 4-19 and 4-21, respectively).

No obvious phenotypic changes were observed in the adenoviral infected cell lines during cultivation for more than 4 days. Both miRNA expressing primary cells as well as control cells changed slightly in shape and appearance. Growth may have been slightly increased in the miRNA expressing cells (figure 4-20), but this finding was not reproduced until now.

The global phenotypic consequences of EBV miRNAs were very difficult to analyze, since they are not pronounced in cell lines. Further complicating this analysis is the fact that primary cells are difficult to handle due to their slow growth, restricted passaging time and expensive maintenance.

To analyze the effects of viral miRNAs in an infection system, different virus mutants were generated. A recombinant version of the prototypic EBV genome derived from EBV strain B95.8 was used as control. Based on this control, different mutants were established. EBV encodes miRNAs in two clusters BHRF- and BART-miRNAs. The prototypic strain B95.8 has a 12 kb deletion within the BART region and thus encodes only for 5 BART-miRNAs. To obtain a virus lacking the BHRF- or BART- or all miRNAs, the corresponding miRNA sequences were altered to scrambled sequences that maintain the nucleotide composition and the overall genomic architecture, but destroy the specific hairpin structure, so that these are not processed by Drosha. To generate a virus encoding all EBV miRNAs, I generated a plasmid containing a CMV promotor and all EBV BART-miRNAs that were PCR amplified from Jijoye. The cloning procedure was similar to the constructs used in this work (see 2.7.1.1). Our collaborators introduced the expression cassette from this generated plasmid into the BALF1 gene of the control virus. BALF1 is located directly downstream of the BART region. It is furthermore a redundant gene and therefore dispensable for EBV's transforming functions. Previous analyses have shown that viral miRNAs are implicated in maintaining herpesviral latency by inhibiting induction of the lytic cycle (Bellare and Ganem, 2009; Murphy et al., 2008). However the deletion of all miRNAs did not lead to a higher amount of spontaneous induction of the lytic cycle in infected primary B-cells, suggesting that these are dispensable for the establishment and maintenance of latency.

While virus mutants lacking all EBV miRNAs show only a slight increase in the amount of cells in G0/G1 and a reduction in S phase in established LCLs, they showed a slightly prolonged doubling time in freshly infected primary B-cells. Additionally, early infected primary B-cells were rescued from spontaneous apoptosis when miRNAs were expressed. Furthermore, they also found that under conditions of low cell density and MOI that the BART-miRNAs of EBV promoted proliferation of primary human B cells early after infection (Vereide et al., unpublished correspondence). This data underline the challenges of using the right system to analyze miRNA functions. In most cases, the effects of miRNAs are very mild and only function to fine tune different target genes and pathways. Due to all of this obstacles in analyzing miRNA function, very few relevant data have been published so far. Nevertheless, there are other promising high-throughput methods available to identify novel miRNA targets. Some of them were also employed in this work.

5.2.2.1. High Throughput Methods for the Identification of miRNA Targets

Besides analyzing the functions and consequences of miRNAs, different high throughput methods for the identification of miRNA targets were evaluated. The translational inhibition of target mRNAs by miRNAs is thought to be their main mode of action. Therefore a method capable of analyzing large numbers of different proteins in one assay should be quite informative for target identification. The approaches that were used to achieve this were either 2-D-gelelectrophoresis in combination with Mass spectrometry (MS) or differential in gel electrophoresis (DIGE). In these experiments protein was obtained from either stable cell lines (BJAB and Beas-2b) or from adenovirus infected HNEpC. Although 2-D-gels were highly reproducible, very few differentially regulated proteins were identified. A disadvantage of this approach was that the spots that were analyzed by MS were often contaminated with GFP degradation products. Furthermore, 2-D-gels are also limited in one dimension by a pH range and in the second dimension by molecular weight meaning that all cellular proteins cannot be analyzed simultaneously. Another drawback of this technique is that the expression level has to be high enough to be detected in the gel. Finally, it gives a result about overall protein changes but does not distinguish between primary miRNA binding effects and secondary ones. Accordingly, based on the limited data output obtained from this approach it was not utilized further.

5.2.2.2. DNA Microarrays

At the beginning of this work little was known about the miRNA dependent effects on mRNA levels. The current opinion is that miRNAs primarily repress protein levels with little effect on mRNA levels (Olsen and Ambros, 1999; Wightman et al., 1993). Nevertheless, translational repression also leads to a slight destabilization of mRNA transcripts, that can be detected in microarrays. DNA microarrays are used to analyze changes in mRNA levels globally across the whole genome. Indeed, several studies using DNA microarrays to analyze miRNA targets have been previously performed (Giraldez et al., 2006; Krutzfeldt et al., 2005; Lim et al., 2005; Rehwinkel et al., 2006). Detailed analysis of miRNA mediated mRNA destabilization demonstrated that mRNA decrease is associated with poly(A)-tail shortening, de-capping and higher mRNA turnover (Behm-Ansmant et al., 2006; Eulalio et al., 2009; Giraldez et al., 2006; Wu et al., 2006).

In this work dual color whole human expression arrays from Agilent were used to analyze transcriptomes of miRNA expressing cells in comparison to control cells. To analyze the effects of all EBV miRNAs, BJAB and Beas-2b stable cell lines as well as adenovirus infected HNEpC were analyzed by transcriptome microarrays. The first analysis was performed with BJAB stable cell lines and with BJAB stable cells expressing only GFP as a control. Technical duplicates were performed and resulted in a large number of regulated genes being identified. One minor technical problem that was encountered was that GFP expression was higher in the control cells than in the miRNA expressing cells. To minimize false positives due to this, two additional arrays were performed using

BJAB stable cells expressing IRES-GFP or just BJAB cells as controls. The common overlap of all experiments was interpreted as the most probable miRNA targets.

Analysis of array data was performed using the Genepix program and the Genome browser, a program written by Adam Grundhoff. Genepix allows identification of stained spots, mapping to the genomic region and normalization of all data. The genome browser then includes standard deviations and cut off values to be calculated. Normally 2x standard deviation is used to define the cut off for minimizing false positive signals resulting from fluctuations of background. The identification of genes passing this criteria from the three independent BJAB stable cell line set-ups was then evaluated. Furthermore, with the 2x stdv. cut off genes were enriched that were very strong differently expressed. It is frequently believed that mRNA levels are directly correlated with protein levels. A study investigating protein and mRNA expression from freshly isolated human monocytes for example displayed a good correlation for all studied genes (Guo et al., 2008). In contrast, other studies investigating protein and mRNA expression from arabidopsis or human prostate tissues were unable to identify a significant correlation (Greenbaum et al., 2003; Pascal et al., 2008). Therefore it remains disputed if miRNA and protein levels must correlate. The lack of correlation in the forementioned studies may be due to diverse reasons. For example, post-translational modifications, protein half-lives or even methodical difficulties could explain the very different findings. Independent from general correlations between mRNA and protein levels, several other publications investigating miRNA dependent decrease of mRNA levels detected a wide range of regulation including a great amount of possible target mRNAs only slightly regulated (Guo et al., 2010; Hendrickson et al., 2008). The assumption that miRNA primarily inhibit translation and that mRNA destabilization is a secondary effect and not very pronounced, lead to the decision to set the cut off to 1x stdv. This was on the one hand believed to increase false positives, but on the other hand to also increase sensitivity. But since three independent controls were used, it was suggested to obtain a manageable list of putative target mRNAs, which then could be further investigated experimentally. The overlap lead to 56 and 20 genes regulated in BJAB arrays and in epithelial arrays, respectively (4-23).

A detailed look at the genes regulated in my experiments identified some of the previously published targets (table 1-2), however they were to a large extent found close to the background. For example, PUMA is a published miRNA target that was identified in all of my microarray experimentes, but was only considered to be significantly down regulated in the BJAB-IRES arrays. Therefore it was identified in all experiments but only passed the threshold in one type of experimental set-up. Another example is MICB, which was previously shown by Nachmani and colleagues (Nachmani et al., 2009) to be a target of different miRNAs. In my studies it was also regulated but it was found to be slightly upregulated. This is surprising and inconsistent with the published literature, because if MICB is a target of EBV miRNAs then one would assume that it should be down regulated. Perhaps one of the best matching targets I found was TOMM22, which was identified recently in co-immunoprecipitation of RISC complexes and confirmed to be targeted by miRNA-BART-16 (Dolken et al., 2010) TOMM22 was consistent and reproducible down regulated in all experimental set-ups arguing strongly that it is a target of EBV miRNAs. Although this observation was reproducible, due to the

stringent criteria, in two set ups BJAB-GFP and HNEpC 4 d p.i., TOMM22 did not pass the threshold. Similar to TOMM22, IPO7 was also identified as a miRNA target in co-IP (Dolken et al., 2010). In three of my array set-ups it was identified to be down regulated, but not in all of the experimental set-ups. The lack of IPO7 regulation in these other arrays may be due to technical difficulties such as bad spot performance or it may be related to the abundance of the IPO7 mRNA making it difficult to see modest changes. Dicer is another published target of EBV-miRNA-BART-6 (Iizasa et al., 2010), which was found in the epithelial array set-ups but not in the BJAB set-ups. Lastly CXCL11 was found by to be a target of EBV-miRNA-BHRF1-3 but it was not confirmed in any of my arrays. Together these findings demonstrate that the identification of host target genes regulated by miRNAs may fluctuate or be entirely different depending on the source of the miRNA and the cell line / cell type analyzed.

In general, DNA microarrays are useful in the global analysis of miRNA targets but should be very stringently controlled. Replicates are essential to reduce the amount of false positives even at the expense of increasing false negatives. In this work different controls were used in the BJAB set-ups leading to partially different transcriptomes of the analyzed cells. One challenge in analyzing targets that are only marginally regulated is that it increases the amount of false positives, which can be reduced again by replicate experiments. The controls should also be carefully chosen to compensate for changes only due to slight differences in the samples. For example, using antagomirs (miRNAs that are 100% complementary to mature miRNAs) which inhibit the function of a certain miRNA and therefore to rescue the effect of a given miRNA or scrambled miRNA (a miRNA consisting of the same set of nucleotides randomly ordered), which should lose the function of the real miRNA, are alternative experiments. Of course it is also possible that your control miRNAs have unwanted cellular effects and therefore it is wise to incorporate several controls into the design of the DNA microarray. Using a very stringent approach, Ziegelbauer and colleagues were able to identify several miRNA targets of KSHV miRNAs (Ziegelbauer et al., 2009). In this study, they transfected BJAB B-cells with single miRNAs, they stably transduced cells with retroviruses expressing clusters of KSHV miRNAs, they infected primary endothelial cell lines with KSHV and they inhibited single miRNAs in latently infected B-cell line (Bcbl-1). For each miRNA 10-30 mRNAs were consistently identified that passed all sets of conditions. As a proof of principle for the functionality of this high throughput screening they confirmed the mRNA target of miR-K5 using luciferase reporter assay and Western blot analysis. A very recent study investigated the molecular consequences of miRNA repression by ribosome profiling (Guo et al., 2010), a procedure, which determines the positions of ribosomes on cellular mRNAs with sub-codon resolution. The data were analyzed by deep sequencing of ribosome-protected mRNA fragments and provided quantitative data on thousands of genes. With that approach it was demonstrated that lowered mRNA levels account for most of the decreased protein production and additionally that changes in mRNA levels closely reflected the impact of miRNAs on gene expression. The implementation of data resulting from SILAC (stable isotope labeling with amino acids in cell culture) allowed comparison of miRNA dependent changes on protein level with the mRNA data and revealed that miRNAs do not repress less expressed targets more efficiently than they do highly

expressed targets. This is the first experimental proof pointing towards destabilization of target mRNA as the predominant reason for reduced protein output. However, as to be expected, there are also exceptions where translational repression is coupled with mRNA destabilization (Coller and Parker, 2004). Guo and colleagues argued that even if destabilization is a secondary effect, it is the mRNA destabilization that would exert the greatest impact on protein level.

5.2.3. Gene Ontology of DNA Microarrays

The first analysis of the gene lists obtained from the DNA microarrays was performed using DAVID (Dennis et al., 2003). A large number of interesting GO terms were enriched (p value ≤ 0.05) in all of the microarrays analyzed comprising genes involved in many relevant processes like apoptosis, cell death, immune response, differentiation or cell proliferation (table 4-6 to 4-8).

The interferon system is one of the mechanisms used by cells to trigger an immune protective defense against pathogens like viruses. Therefore, the interferon system is a feasible and meaningful target for viral miRNAs. Some viral miRNAs have already been shown to modulate genes important for cellular defense such as MICB (see above) or KSHV miRNAs, which target thrombospondin (THBS) a protein that is involved in TGF- β activation (Samols et al., 2007). Similarly, several cellular miRNAs have been shown to regulate parts of the innate immunity. Recently, Witwer and colleagues investigated the role of cellular miRNAs (miR-26a, -34a and let-7b) in the regulation of IFN- β directly (Witwer et al., 2010). They showed that these miRNAs are upregulated upon IFN- β induction and are able to down-modulate a luciferase reporter containing the 3'UTR of IFN- β , generating a negative feedback loop presumably for fine tuning the IFN- β signaling. Consistently stimulation with polyinosinic polycytidylic acid (poly(I:C)), a component mimicking dsRNA, activates an immune response and type I IFNs, similar to the miRNA expression. Another study demonstrated the ability of miR221 and miR-222 to attenuate phosphorylation of STAT1 and -2 in response to IFN- α (Zhang et al., 2010). Interestingly, adenosine deaminase acting on RNA 1 (ADAR-1) is upregulated by IFN- α and - β and is capable of deaminating cellular and viral mRNAs as well as miRNAs. Editing of pri-miR-BART6 has been shown to abrogate regulation of DICER activity. Regardless of the point of view, interfering with the interferon signaling pathway might be a relevant mode of action for viral miRNAs.

Therefore, based on these findings and assumptions, IFN signaling was analyzed in further detail. In addition to the genes involved in immune defense and as a confirmation and read out of IFN- β signaling the expression of ISG-15 was analyzed by Western blotting. Interferon stimulated gene 15 (ISG-15) is expressed upon IFN signaling and therefore served as an appropriate control for IFN- β stimulation. In this way it can be evaluated if the miRNA dependent regulation of immune defense genes directly act on this pathway and if it had any consequences. Using the stable cell lines (BJAB and Beas-2b) the interferon response was induced by addition of IFN- β and analyzed for the expression of ISG-15. This experiment did not reveal any significant differences in ISG-15 expression

between control cells and miRNA expressing cells (figure 4-32) suggesting that in these cell lines the level of miRNAs were not sufficient to trigger an interferon response. It is possible that when the cells were maintained a long time in culture develop an antagonistic response to the miRNAs. Another possibility is that the level of miRNA expression needed to be higher to result in an effect on interferon signaling.

In contrast to the immortalized cell lines (BJAB and Beas-2b) the primary cells (HNEpC) did show a significant decrease in ISG-15 expression when challenged in adenoviruses expressing BART miRNAs. It was shown, that infection with the adenoviral control (IRES-GFP) stimulated IFN signaling whereas Ad-BART lead to a reduction in ISG-15 and therefore interfered with IFN signaling (figure 4-33). To reproduce this result and to confirm this effect was not due to differences in the viruses ability to stimulate an IFN response co-infected HUVEC cells with both viruses to see if the BART miRNAs would reduce the induction of ISG-15 by Ad-IRES-GFP (figure 4-33 B). In these experimetns Ad-BART was capable of inhibiting the adenoviral (Ad-IRES-GFP) activation of IFN signaling, suggesting that a protective function of miRNAs may be to down-regulate interferon signaling. These results are very interesting and require further investigation to ensure an accurate interpretation. The differences in IFN signaling between the two approaches may be explained by the fact that there is a higher level of expression of the miRNA in the adenoviral infected cells implying a dose dependent effect or may be due to cellular differences between primary cells and immortalized cell lines, which ever situation is the case can be experimentally clarified by titration with different MOI in the HUVEC cells or by adenoviral infection in Beas-2b cells.

5.2.4. Target Confirmation

High throughput analysis generates large lists of putative regulated mRNAs or proteins that must be subjected to detailed analysis to determine direct regulation. Data sets can be minimized by performing replicates and using different controls for one question, like control vectors or antagomirs, or in case of IP data, input and control IP. The mRNA data from microarrays must be reproduced using alternative approaches such as real-time analysis of mRNA levels. Furthermore, the effect on protein level should also be analyzed to evaluate biological relevant mechanisms. The standard test currently for evaluating direct binding of a miRNA to its target mRNA is the luciferase reporter assay. This assay is very sensitive, and it is necessary that the conditions are established very carefully. Different strategies were employed to control these experiments including the generation of control vectors containing one or four binding sites for miR-BART5 (4-26). Transfection of the single miRNA miR-BART5 resulted in reproducible regulation of the control vectors. The control reporter constructs containing one or four binding sites for miR-BART5 were repressed to 40 - 60% and 20 - 40% of activity, respectively. Binding of a miRNA with the RISC complex to one site might interfere with the binding of another miRNA to the adjacent site due to steric hinderance and can potentially explain why a complete repression was not observed. Since it is possible that the genes identified in the DNA

microarrays are co-regulated by more than one EBV-encoded miRNA, the luciferase reporter assays were performed using a vector expressing all EBV miRNAs. It was speculated that the combined expression of EBV miRNAs should result in a similar reduction of the control reporter constructs. However, only a modest reduction of around 10% which was not even reproducible in all experiments was observed (figure 4-25, 4-29 - 4-31). This unexpected result is likely due to the dilution of the miR-BART5 with other EBV miRNAs reducing the concentration of the specific miRNA. Furthermore, the construct co-expressing all miRNAs expresses less efficiently transfectable due to its size, further reducing the amount of available miR-BART5. To achieve a higher efficiency of cells expressing all miRNAs imultaneously, SLK cells (an endothelial cell line) were infected with adenoviruses prior to or after transfection with the luciferase reporter. Unfortunately this also yielded non-reproducible results, which is also most likely due to lower miRNA expression in comparison to 293T cells. Since 293T cells are permissive for adenovirus replication they could not be used for luciferase assays. Therefore, it will be important in the future to identify other cell lines that are not permissive for adenoviral replication, capable of expressing all EBV miRNAs simultaneous and have a high transfection ability. A dual luciferase system could minimize the variability of control plasmid to luciferase plasmid, since two different luciferase genes are encoded on one plasmid. Another possibility that might be investigated in the future would be a FACS based assay using GFP constructs with specific miRNA binding sites and measuring the decrease in fluorescence signal.

Finally, it was decided to test single miRNAs in transient transfections and to analyze their functions on luciferase activity.

Good scoring target sites for all EBV miRNAs were selected using the genome browser. The results from this in silico analysis determined which 3' UTRs were investigated. Different algorithms are available for the prediction of miRNA binding sites using different criteria. TargetScan was used, because it has a low stringency in identifying miRNA binding sites (the only criteria needed is the seed match), but additionally it calculates scores for each binding site regarding different aspects that have been shown to have positive and negative effects on binding efficiency, like location of a site within the 3'UTR, nucleotide composition of the surrounding sequence or additional base pairing at the 3' end of a miRNA (Grimson et al., 2007). The higher the score, the more probable it is that a site will be affected by miRNA binding. Although this is helpful in analyzing mRNA-3'UTR regions, confirmatory analyses have to be done. TargetScan was implemented into the genome browser program to combine, analyze and visualize the binding sites of miRNAs in potential mRNA targets from the gene expression arrays. All mRNAs obtained in the overlap of the two array set ups were analyzed regarding their potential binding sites for EBV miRNAs. As mentioned above, transcripts having good scoring sites were then further subjected to cloning of the 3'UTRs.

In some cases, it was very difficult to amplify the correct mRNA, due to either low PCR efficiency, missing knowledge about the ends of a 3'UTR or the amplification of several products due to highly spliced genomic region. Some interesting candidates were identified among the positive products, which are potentially directly regulated by EBV miRNAs.

Inhibition of apoptotic pathways is a mechanism used by miRNAs to preserve viral health, as has been shown for BART5, which targets PUMA. Programmed cell death 2 (PDCD2), a protein involved in the induction of apoptosis (Baron et al., 2010), is a candidate target of miR-BART19 (figure 4-29). A significant reduction in mRNA level was observed ($P \leq 0.01$), but only resulted in a decrease of 10-15%. Analysis of PDCD2 on the protein level still has to be performed, but it is possible that it will be difficult to detect such a modest reduction. This will depend on the specificity and sensitivity of the antibody as well as what a 10-15% reduction at the mRNA level translates to at the protein level.

Caspase 3 was the only gene analyzed from the overlap of epithelial cell and has independently been predicted (Lagana et al., 2010), but a direct regulation by the two highest scoring miRNAs could not be reproduced and therefore it seems unlikely to be a direct target of a single EBV-encoded miRNA (figure 4-30).

Luciferase assays have been successfully used to show miRNA regulation (figure 4-31). Elongator complex 4 (ELP4) is for example, a subunit of the RNA polymerase II complex that has a histone acetyltransferase activity (Hawkes et al., 2002; Kim et al., 2002). ELP4 might be regulated by miR-BART7, however, since the regulation was not very pronounced, alternative analysis must be performed to confirm a regulatory effect. Non-metastatic cells 3 (NME3) is important for the synthesis of nucleoside triphosphates other than ATP and is suggested to play a role in normal hematopoiesis by inhibiting granulocyte differentiation and inducing apoptosis (Desvignes et al., 2009). Nuclear vcp like (NVL) belongs to the ATPase associated with diverse cellular activities AAA-ATPase and might have a role in ribosome biogenesis as well as development and apoptosis (Nagahama et al., 2004). NVL, in contrast, was more efficiently regulated by miR-BART17 but not -13, suggesting that one would be able to see an effect at the protein level as well. The biological relevance for the targeting of ELP4, NME3 and NVL remains unclear and therefore, if there is a link to EBV pathogenesis still needs to be determined.

It was easier to infer the biological relevance of two other regulated genes identified in this work. myxovirus resistance 1 (MX1) was identified in the BJA1 arrays and has been previously linked to defense against virus infections like influenza and hepatitis B virus (Haller et al., 2007). It has also been shown to inhibit replication of large dsDNA viruses (Netherton et al., 2009). For EBV infection, the inhibition of an antiviral function is for obvious reasons a useful function, however, the inhibition of replication might be controversial, since the virus generally establishes latency and therefore would favor replication. A physical interaction with the nucleoprotein components of nucleocapsids was demonstrated for the orthomyxoviruses and MX1 (Kochs and Haller, 1999). However, a correlation between EBV pathogenesis and MX1 has not been shown to date.

Tankyrase 2 (TNKS2) was regulated in the HNEpC set-ups and has been shown to down-modulate EBV replication in a poly-ADP ribose polymerase (PARP)-dependent manner by binding to EBNA-1 (Deng et al., 2005; Tempera et al., 2010). Based on this it is tempting to speculate that a downregulation of TNKS2 might support the maintenance of viral episomes and its ability to be replicated once per cell cycle. In this work, miR-BART7 was shown to regulate TNKS2 mRNA. However, since the 3'UTR has many different target sites for different miRNAs, an additional

regulation by other viral miRNAs is possible and needs to be investigated further. To confirm a biologic function, it is planned to investigate the protein levels of TNKS2 by Western blotting and to perform a replication assay. TNKS2 is therefore a promising candidate to be regulated by viral miRNAs to allow latent replication and ensure maintenance.

It will be very interesting to analyze, if the potential investigated mRNA targets display conserved targets. For MX1 and TNKS2 the identified miRNAs (miR-BART11 and miR-BART7, respectively) that are regulating the mRNAs are derived from conserved miRNAs (see 4-16). The conservation analyses of regulated genes derived from DNA microarrays is currently under investigation and might further help in the identification of miRNA targets and functions.

5.3. Outlook

In this work a global analysis of miRNA conservation within the γ -herpesvirus family was performed, showing that the overall sequence conservation is low. However, EBV and rLCV have been shown to encode a significantly higher number of conserved miRNAs than previously thought. Furthermore, the more closely related rhadinoviruses RRV and JMHV conserved nearly all viral miRNAs. Another closely related virus to RRV and JMHV and also infects rhesus macaques is MneRV. It is planned to investigate in the future MneRV for the expression of miRNAs. Next generation sequencing will be used for this purpose. This analysis will lead to a better understanding of miRNA evolution and conservation.

Several approaches will be combined and optimized to identify miRNA targets. Putative targets derived from DNA microarrays and the luciferase assays will provide the basis for candidates that will be further investigated. Next it needs to be determined how much regulation on the mRNA level is needed to reduce the protein and result in a relevant biological consequence. To analyze this questions, the proposed target sites can be mutated to see if a reverse effect can be observed in luciferase activity. We have already performed successfully such analysis for a KSHV miRNA target. Importantly an analysis on the protein level, Western blotting of target proteins will be investigated. Depending on the confirmed targets, functional assays will be ultimately used to analyze the functional consequences in more detail like a replication assay for the TNKS2 target.

It is further planned to optimize the high-throughput methods. For example a broader range of proteins can be analyzed using stable isotope in-gel electrophoresis (SILAC) in comparison to 2-D-gel electrophoresis. In a cooperation with Prof. Dr. Schlüter (UKE) this will be performed using the stable cell lines expressing all EBV miRNAs.

Currently, novel methods are being established to enrich the relevant miRNA targets prior to DNA microarrays or deep sequencing technology. One approach is the immunoprecipitation of RISC complex components, e.g. Ago2. Enrichment of miRNAs and mRNAs incorporated or associated with RISC should allow identification of direct targets more easily, because all other mRNAs that are only changed secondary would be excluded. Recently, as mentioned above, two novel EBV miRNA targets

were identified using Ago2-IP in combination with subsequent microarray analysis (Dolken et al., 2010). These experiments can be controlled with a non-specific IgG antibody from the same species or Hypoxanthine-guanine phosphoribosyltransferase (HPRT) as well as a comparison to the input. Diverse correlations of the samples reveal a small list of probable target that can be validated by following assays. An initial IP was already performed in this work using adenoviral infected Beas-2b cells. It was possible to enrich the miRNA-BART5 by Ago2 immunoprecipitation, but the efficiency of IP was relatively low and in comparison to the controls they only showed a slight enrichment. Therefore, like many co-immunoprecipitations this procedure has to be optimized. Nevertheless, this approach seems promising and will be further investigated in the future.

Another method that will be adapted in our future studies, is high throughput sequencing of RNA isolated by crosslinking immunoprecipitation (HITS-CLIP). With this method not only miRNAs associated with Ago proteins but also mRNAs located within the complex can be enriched and analyzed by deep sequencing (Chi et al., 2009). Comparable to this method, Photoactivatable-Ribonucleoside-Enhanced Crosslinking and Immunoprecipitation (PAR-CLIP) has also recently been established in another lab (Hafner et al., 2010). In this cases, the photoactivatable nucleoside 4-thiouridine (4SU)-labeled transcripts are crosslinked by UV with RNA binding proteins (RBPs) and partially RNase-digested. RNA-protein complexes can then be immunopurified, size fractionated, and after protein digestion the RNA can be isolated and converted into cDNA to generate a cDNA library, that can then be deep sequenced. An advantage of PAR-CLIP in comparison to HITS-CLIP is that cross-linking with photoactivatable nucleosides is more efficient and allows identification of RBP binding sites in the sequenced cDNA due to thymidine to cytidine transitions. These methods are more sensitive and probably allow the direct identification of target sites, since these sequences are protected within the RISC complex.

With the knowledge of phenotypic differences in primary infected B cells (Seto et al., 2010), it is now interesting to further analyze the targets that are responsible for the changes. One possible mechanism of miRNAs promoting cell cycle progression might be dependent on the regulation of relevant cell cycle dependent cyclins. The G1 to S transition for example is dependent on two cyclins, D-Cdk4,6 and E-CDK2. A recent work by Wang and colleagues showed the direct regulation of p21, an inhibitor of the cyclin E-Cdk2 complex, by cellular miRNAs. This regulation leads to a faster G1-S transition, and cellular proliferation is promoted (Wang et al., 2008b).

With the novel recombinant viruses that were produced by our collaborators (Seto et al., 2010), it is possible to analyze primary infected cells in combination with the different methods established in this work, like DNA microarrays, 2-D-Gelelectrophoresis or novel methods that are under investigation like immunoprecipitations. Furthermore, infection of primary epithelial cells can be established to get a detailed insight into miRNA function in these cells. However, the data will lead to a clearer understanding of viral miRNA function and herpesvirus pathogenesis.

6. Indices

6.1. Abbreviations

AAA-ATPase	ATPase associated with diverse cellular activities
ADAR	adenosine deaminase acting on RNA 1
AIDS	acquired immunodeficiency disease syndrome
Amp	ampicillin
Ago	Argonaute
ATP	adenosine triphosphate
a.u.	arbitrary units
BALF5	viral encoded DNA-dependent DNA polymerase
BART	BamHI-A region rightward transcripts
BCL2	B-cell lymphoma 2
BCBL	body cavity-based lymphoma
BCR	B-cell receptor
BHRF	<i>Bam</i> HI rightward open reading frame
BL	Burkitt's lymphoma
BSA	bovine serum albumin
bp	base pairs
cDNA	complementary DNA
CMV	cytomegalovirus
CNS	central nerve system
d	day
Dam	DNA adenin methylase
dH ₂ O	distilled water
ddH ₂ O	double distilled water
DGCR	DiGeorge syndrome critical region
DMEM	Dulbeccos's modified Eagle medium
DMSO	dimethyl sulfoxide
DNA	deoxyribonucleic acid
dNTP	deoxyribonucleotide-mix
d p.i.	days post infection
ds	double stranded
DTT	dithiothreitol
EA	early antigen
EBER	EBV-encoded RNAs
EBNA	EBV nuclear antigen
EBV	Epstein-Barr virus
<i>E. coli</i>	<i>Escherichia coli</i>
EDTA	ethylendiaminetetra acetic acid
EM	electron microscopy
ELP4	elongator complex 4
EtOH	ethanol
FACS	fluorescence associated cell sorting
FCS	fetal calf serum
FITC	fluorescein isothiocyanate
° C	degree Celsius
G	gram
g	gravity
GAPDH	glyceraldehyd 3-phosphate dehydrogenase
GFP	green fluorescent protein
h	hour(s)
HCV	hepatitis C virus
HD	Hodkin's disease
HEK	human embryonic kidney
HEPES	2-(4-(2-hydroxyethyl)-1-piperazinyl)-ethanesulfonic acid
HHV	human herpesvirus

HIV	human immunodeficiency virus
HNEpC	human nasal primary epithelial cells
HSV	herpes simplex virus
HTLV	human T-cell leukemia virus
HVS	herpesvirus saimiri
IE	immediate early gene
IM	infectious mononucleosis
IFN	interferon
IPO7	importin 7
IR	internal repeats
IRES	internal ribosome entry site
ISG	interferon stimulated gene
JMHV	Japanese monkey herpesvirus
Kan	kanamycin
kb	kilo base
kDa	kilo Dalton
KS	Kaposi's sarcoma
KSHV	Kaposi's sarcoma-associated herpesvirus
l	liter
L	late gene
LANA	latency associated nuclear antigen
LB	Lysogeny broth
LCV	lymphocryptovirus
LFs	left end genes
LMP	latent membrane protein
LCL	lymphoproliferative cell line
mA	milliampere
M	molar
MCMV	mouse cytomegalovirus
MDV	Marek's disease virus
min	minute
miRNA	microRNA
miRNP	miRNA containing ribonucleoprotein complexes
ml	milliliter
mM	millimolar
mmol	millimol
MOI	multiplicity of infection
mRNA	messenger RNA
MS	multiple sclerosis or mass spectrometry
MW	molecular weight
m	micro
mg	microgram
MHC	major histocompatibility complex
miRISC	RISC with incorporated miRNA
MTT	3-(4,5-Dimethylthiazol-2-yl)-2,5-diphenyltetrazolium bromide
ml	mikroliter
nm	nanometer
MX1	myxovirus resistance 1
NME3	non-metastatic cells 3
NPC	nasopharyngeal carcinoma
NVP	nuclear vcp like
OD	optical density
OHL	oral hairy leukoplakia
ORG	origin-recognition complex
ORF	open reading frame
oriP	origin of plasmid replication of EBV
PABP	poly(A)-binding protein
PARP	poly-ADP ribose polymerase
PAZ	Piwi/ Argonaute/ Zwillig
PB	processing body
PDCD2	programmed cell death 2
PFA	paraformaldehyde
PIWI	P-element induced wimpy testis

poly-A	polyadenylation signal
pre-miRNA	precursor miRNA
pri-miRNA	primary mirRNA
PBS	phosphate buffered saline
PCR	polymerase chain reaction
PTLD	post transplant lymphoproliferative disease
PUMA	p53 up-regulated modulator of apoptosis
Qp	promoter Qp of EBV
R	resistance
RDV	rhadinovirus
RFs	right end genes
RNA	ribonucleic acid
RNAi	RNA interference
RISC	RNA-induced silencing complex
rLCV	rhesus lymphocryptovirus
RRV	rhesus rhadinovirus
RT	room temperature
RT-PCR	reverse transcription PCR
rpm	rounds per minute
<i>S. cerevisiae</i>	<i>Saccharomyces cerevisiae</i>
SDS	sodium dodecyl sulfate
SIV	simian immunodeficiency virus
stdv	standard deviation
s	second
siRNA	small interfering RNA
TRBP	transactivating response RNA-binding protein
TNF	tumor necrosis factor
TOMM22	mitochondrial import receptor subunit TOM 22 homolog
TNKS	tankyrase, TRF1-interacting ankyrin-related ADP-ribose polymerase
TR	terminal direct repeats
U	unit
UTR	untranslated region
V	Volt
vol	volume
v/v	volume/volume
VZV	varizella-zoster virus
wt	wildtype
w/v	weight/volume

6.2. Figure Index

Figure 1-1 Phylogenetic Tree of Herpesviruses	1
Figure 1-2 EBV Structure	3
Figure 1-3 EBV Life Cycle	6
Figure 1-4 Latency Genes and Programs	9
Figure 1-5 miRNA Biogenesis	15
Figure 1-6 Mechanisms of miRNA Target Regulation	17
Figure 1-7 <i>Bam</i> HI-A rightward Transcripts	20
Figure 1-8 miRNA Location within EBV and rLCV Genomes	21
Figure 3-1 Schematic Overview of Stem-loop RT-PCR	48
Figure 3-2 Schematic Workflow of Gene Expression Microarrays	65
Figure 4-1 Sequence Identity and Pre-miRNA Hairpin Conservation of γ -Herpesvirus Genomes	73
Figure 4-2 VMir Prediction of Pre-miRNA Hairpins Within γ -Herpesvirus Genomes	74
Figure 4-3 Global Alignment of miRNA-encoding Regions of EBV, rLCV, RRV and JMHV	76
Figure 4-4 VMir Prediction of EBV Pre-miRNA Hairpins	77
Figure 4-5 Confirmatory Northern Blot for Novel EBV miRNAs.	78
Figure 4-6 VMir Prediction of rLCV Pre-miRNA Hairpins	78
Figure 4-7 Confirmatory Northern Blots of Novel rLCV miRNAs.	79
Figure 4-8 VMir Prediction of JMHV Pre-miRNA Hairpins	80
Figure 4-9 miRNA Locus of JMHV	81
Figure 4-10 Confirmatory Northern Blots for JMHV miRNAs	82
Figure 4-11 Confirmatory Northern Blot for miRNAs in JMHV Infected Rhesus Primary Fibroblast Cells	82

Figure 4-12 Schematic Overview of the miRNA Cloning Procedure.	83
Figure 4-13 Pre-miRNA Hairpins of Novel rLCV-miRNAs	85
Figure 4-14 Pre-miRNA Hairpins of Novel JMHV miRNAs	87
Figure 4-15 Sequence Alignment of EBV and rLCV Mature miRNAs	88
Figure 4-16 Location Map of Novel and Known Pre-miRNA Hairpins from EBV and rLCV	89
Figure 4-17 Sequence Alignment of Conserved Mature RRV and JMHV miRNAs	90
Figure 4-18 miRNA Expression Vector and Expression of miRNAs in Stable Cell Lines.	92
Figure 4-19 pShuttle Vectors for miRNA Expressing Adenovirus Production.	93
Figure 4-20 Adenovirus Infected HNEpC	93
Figure 4-21 Stem-loop RT-PCR of Adenoviral Infected HNEpC	94
Figure 4-22 Scatter Plots of DNA Microarrays.	95
Figure 4-23 Overlap of Down-regulated Genes Derived from BJAB or Epithelial mRNA Expression Arrays.	97
Figure 4-24 miRNA Target Recognition	98
Figure 4-25 Quantitative Northern Blots of miRNA Expressing Transfected Cells.	99
Figure 4-26 Luciferase Assay of Control Reporters.	100
Figure 4-27 Luciferase Assay for Puma 3'UTR	101
Figure 4-28 Genome Browser Analysis of miRNA Binding Sites Within the MX-1 3'UTR	102
Figure 4-29 Luciferase Assay for mRNAs Down-regulated in BJAB Arrays	103
Figure 4-30 Luciferase Assay for CASP3	104
Figure 4-31 Luciferase Assay of Down-regulated Genes from HNEpC Gene Expression Arrays	105
Figure 4-32 Western Bot Analysis of IFN- β Treated BJAB and Beas-2b Stable Cell Lines	107
Figure 4-33 Western Blot Analysis of HNEpC or HUVEC Cells Infected With Adenovirus	108
Figure 5-1 Alignment of Pre-miRNA Hairpins of rlcv-miR-rL1-32 and ebv-miR-BART14	113
Figure 5-2 Implementation of Conserved and Non-conserved miRNAs Into Target Prediction	116
Figure 5-3 Sequence Comparison of Conserved PUMA Target Site and Conserved miRNAs	118

6.3. Table Index

Table 1-1 Functions of Cellular miRNAs	23
Table 1-2 Targets of EBV-encoded miRNAs	25
Table 2-1 Bacterial Strain	27
Table 2-2 Cell Lines	27
Table 2-3 General Cloning Primers	28
Table 2-4 Small RNA Cloning Linker Primer	28
Table 2-5 Small RNA Cloning Primer rLCV	28
Table 2-6 Small RNA Cloning Primer JMHV	29
Table 2-7 Luciferase Assay Primers	30
Table 2-8 Standard Sequencing Primers	30
Table 2-9 Real-time Primer	30
Table 2-10 EBV miRNA Probes	31
Table 2-11 rLCV miRNA Probes	31
Table 2-12 JMHV miRNA Probes	32
Table 2-13 Kits	33
Table 2-14 Transfection Components	33
Table 2-15 Real-time Components	33
Table 2-16 Western and Northern Blot	33
Table 2-17 Instruments and Equipment	34
Table 2-18 Software	34
Table 2-19 Purchased Plasmids	34
Table 2-20 Cloned Plasmids	35
Table 2-21 Antibodies	36
Table 3-1 TFB1 Buffer	37
Table 3-2 TFB2 Buffer	38
Table 3-3 Standard Ligation Reaction	40
Table 3-4 Standard TA Ligation Reaction	41
Table 3-5 Nuclei Lysis Buffer	42
Table 3-6 gDNA Lysis Buffer	43
Table 3-7 Standard PCR Reaction	43
Table 3-8 Standard PCR Program	43
Table 3-9 Site-directed Mutagenesis PCR Components	44

Table 3-10 Site-directed Mutagenesis PCR Program	44
Table 3-11 Real-time SYBR Green Reaction	46
Table 3-12 Real-time SYBR Green Program	46
Table 3-13 Real-time Reaction with TaqMan Probes	47
Table 3-14 Real-time Program with TaqMan Probes	47
Table 3-15 SuperScriptIII Revere Transcription Reaction	47
Table 3-16 Reverse Transcription Reaction for Stem-loop Primers	49
Table 3-17 Reverse Transcription Program for Stem-loop Primers	49
Table 3-18 10x MOPS Buffer	50
Table 3-19 Loading Dye for Northern Blot Samples	50
Table 3-20 8 M Urea Gel for Small RNA Northern Blot	50
Table 3-21 Labeling Reaction for Small Oligonucleotide Probes	51
Table 3-22 TBE Buffer	51
Table 3-23 Formamide Loading Dye	51
Table 3-24 20x SSC Buffer (Sodium Chloride, Sodium Citrate)	51
Table 3-25 Northern Blot Wash Buffer	52
Table 3-26 Dephosphorylation Reaction Mixture for Small RNA Cloning	52
Table 3-27 Linker Ligation Reaction Mixture for Small RNA Cloning	52
Table 3-28 Phosphorylation Reaction Mixture for Small RNA Cloning	53
Table 3-29 Collecting Gel Buffer (10x)	54
Table 3-30 Separating Gel Buffer (10x)	54
Table 3-31 SDS-Polyacrylamide Collecting Gel	54
Table 3-32 SDS-Polyacrylamide Separating Gel [14%]	54
Table 3-33 TGS Buffer (Tris Glycine SDS) (1x)	54
Table 3-34 Laemmli Sample Buffer (5x)	55
Table 3-35 Blotting Buffer (1x)	56
Table 3-36 TBS Buffer (1x)	56
Table 3-37 TBST Buffer (1x)	56
Table 3-38 ECL Solution A	56
Table 3-39 ECL Solution B	56
Table 3-40 Polysome Lysis Buffer	57
Table 3-41 NT2 Buffer	57
Table 3-42 Cell Seeding	58
Table 3-43 Transfection Mixture for PEI Transfection	59
Table 3-44 Transfection Mixture for Fugene Transfection	59
Table 3-45 Transfection Mixture for Lipofectamine Transfection	60
Table 3-46 Microscope Factors for Calculating Adenoviral Titer	63
Table 3-47 TBS BG Buffer 10x	63
Table 3-48 Transfection Mixture for Luciferase Assay	64
Table 3-49 Z-buffer with ONPG 2x	64
Table 3-50 cDNA Synthesis for Expression Arrays	66
Table 3-51 cRNA Synthesis and Labeling of RNA for Expression Arrays	66
Table 3-52 Hybridization Mixture for Expression Arrays	67
Table 4-1 γ -Herpesviruses Analyzed in This Work	72
Table 4-2 rLCV miRNA Sequences	84
Table 4-3 JMHV miRNA Sequences	86
Table 4-4 Statistics of Regulated Genes of DNA Microarrays	96
Table 4-5 Statistics of Regulated Genes of DNA Microarrays	96
Table 4-6 Gene Ontology Categories Enriched in BJAB-GFP Arrays	106
Table 4-7 Gene Ontology Categories Enriched in Beas-2b Arrays	107
Table 4-8 Gene Ontology Categories Enriched in HNEpC 4 d p.i. Arrays	107
Table 5-1 Features Implemented in Algorithms to Predict Pre-miRNA Hairpins	110
Table 5-2 Differences of Mature miRNA Sequences of JMHV and RRV	114
Table 5-3 Sequence Identity of Orthologous Hairpins	115
Table 8-1 R and S clauses for chemicals	I

7. Literature

- Ackermann, M. (2006). Pathogenesis of gammaherpesvirus infections. *Vet Microbiol* *113*, 211-222.
- Adamson, A. L., Wright, N., and LaJeunesse, D. R. (2005). Modeling early Epstein-Barr virus infection in *Drosophila melanogaster*: the BZLF1 protein. *Genetics* *171*, 1125-1135.
- Alba, M. M., Das, R., Orengo, C. A., and Kellam, P. (2001). Genomewide function conservation and phylogeny in the Herpesviridae. *Genome Res* *11*, 43-54.
- Alwine, J. C., Steinhart, W. L., and Hill, C. W. (1974). Transcription of herpes simplex type 1 DNA in nuclei isolated from infected Hep-2 and KB cells. *Virology* *60*, 302-307.
- Aparicio, O., Razquin, N., Zaratiegui, M., Narvaiza, I., and Fortes, P. (2006). Adenovirus virus-associated RNA is processed to functional interfering RNAs involved in virus production. *J Virol* *80*, 1376-1384.
- Asangani, I. A., Rasheed, S. A., Nikolova, D. A., Leupold, J. H., Colburn, N. H., Post, S., and Allgayer, H. (2008). MicroRNA-21 (miR-21) post-transcriptionally downregulates tumor suppressor Pcd4 and stimulates invasion, intravasation and metastasis in colorectal cancer. *Oncogene* *27*, 2128-2136.
- Askjaer, P., Jensen, T. H., Nilsson, J., Englmeier, L., and Kjems, J. (1998). The specificity of the CRM1-Rev nuclear export signal interaction is mediated by RanGTP. *J Biol Chem* *273*, 33414-33422.
- Banchereau, J., Bazan, F., Blanchard, D., Briere, F., Galizzi, J. P., van Kooten, C., Liu, Y. J., Rousset, F., and Saeland, S. (1994). The CD40 antigen and its ligand. *Annu Rev Immunol* *12*, 881-922.
- Baron, B. W., Hyjek, E., Gladstone, B., Thirman, M. J., and Baron, J. M. (2010). PDCD2, a protein whose expression is repressed by BCL6, induces apoptosis in human cells by activation of the caspase cascade. *Blood Cells Mol Dis* *45*, 169-175.
- Bartel, D. P. (2004). MicroRNAs: genomics, biogenesis, mechanism, and function. *Cell* *116*, 281-297.
- Barth, S., Pfuhl, T., Mamiani, A., Ehse, C., Roemer, K., Kremmer, E., Jaker, C., Hock, J., Meister, G., and Grasser, F. A. (2008). Epstein-Barr virus-encoded microRNA miR-BART2 down-regulates the viral DNA polymerase BALF5. *Nucleic Acids Res* *36*, 666-675.
- Bashkirov, V. I., Scherthan, H., Solinger, J. A., Buerstedde, J. M., and Heyer, W. D. (1997). A mouse cytoplasmic exoribonuclease (mXRN1p) with preference for G4 tetraplex substrates. *J Cell Biol* *136*, 761-773.
- Bayliss, G. J., and Wolf, H. (1980). Epstein-Barr virus-induced cell fusion. *Nature* *287*, 164-165.
- Beaufils, P., Choquet, D., Mamoun, R. Z., and Malissen, B. (1993). The (YXXL/I)2 signalling motif found in the cytoplasmic segments of the bovine leukaemia virus envelope protein and Epstein-Barr virus latent membrane protein 2A can elicit early and late lymphocyte activation events. *Embo J* *12*, 5105-5112.
- Behm-Ansmant, I., Rehwinkel, J., and Izaurralde, E. (2006). MicroRNAs silence gene expression by repressing protein expression and/or by promoting mRNA decay. *Cold Spring Harb Symp Quant Biol* *71*, 523-530.
- Bellare, P., and Ganem, D. (2009). Regulation of KSHV lytic switch protein expression by a virus-encoded microRNA: an evolutionary adaptation that fine-tunes lytic reactivation. *Cell Host Microbe* *6*, 570-575.
- Bellot, G., Cartron, P. F., Er, E., Oliver, L., Juin, P., Armstrong, L. C., Bornstein, P., Mihara, K., Manon, S., and Vallette, F. M. (2007). TOM22, a core component of the mitochondria outer membrane protein translocation pore, is a mitochondrial receptor for the proapoptotic protein Bax. *Cell Death Differ* *14*, 785-794.
- Bentwich, I. (2005). Prediction and validation of microRNAs and their targets. *FEBS Lett* *579*, 5904-5910.
- Bernstein, E., Denli, A. M., and Hannon, G. J. (2001). The rest is silence. *Rna* *7*, 1509-1521.
- Bhende, P. M., Seaman, W. T., Delecluse, H. J., and Kenney, S. C. (2004). The EBV lytic switch protein, Z, preferentially binds to and activates the methylated viral genome. *Nat Genet* *36*, 1099-1104.
- Black, M. M. (1970). Tumor immunity in patients with Burkitt lymphoma. *Lancet* *1*, 1393.
- Bodescot, M., Perricaudet, M., and Farrell, P. J. (1987). A promoter for the highly spliced EBNA family of RNAs of Epstein-Barr virus. *J Virol* *61*, 3424-3430.
- Boese, Q., Leake, D., Reynolds, A., Read, S., Scaringe, S. A., Marshall, W. S., and Khvorova, A. (2005). Mechanistic insights aid computational short interfering RNA design. *Methods Enzymol* *392*, 73-96.
- Bohnsack, M. T., Czaplinski, K., and Gorlich, D. (2004). Exportin 5 is a RanGTP-dependent dsRNA-binding protein that mediates nuclear export of pre-miRNAs. *Rna* *10*, 185-191.
- Boissel, N., Rea, D., Tieng, V., Dulphy, N., Brun, M., Cayuela, J. M., Rousselot, P., Tamouza, R., Le Bouteiller, P., Mahon, F. X., *et al.* (2006). BCR/ABL oncogene directly controls MHC class I chain-related molecule A expression in chronic myelogenous leukemia. *J Immunol* *176*, 5108-5116.
- Bornstein, P. (2001). Thrombospondins as matricellular modulators of cell function. *J Clin Invest* *107*, 929-934.
- Brady, G., MacArthur, G. J., and Farrell, P. J. (2007). Epstein-Barr virus and Burkitt lymphoma. *J Clin Pathol* *60*, 1397-1402.
- Brennecke, J., and Cohen, S. M. (2003). Towards a complete description of the microRNA complement of animal genomes. *Genome Biol* *4*, 228.
- Brennecke, J., Stark, A., Russell, R. B., and Cohen, S. M. (2005). Principles of microRNA-target recognition. *PLoS Biol* *3*, e85.

- Buck, A. H., Santoyo-Lopez, J., Robertson, K. A., Kumar, D. S., Reczko, M., and Ghazal, P. (2007). Discrete clusters of virus-encoded microRNAs are associated with complementary strands of the genome and the 7.2-kilobase stable intron in murine cytomegalovirus. *J Virol* *81*, 13761-13770.
- Burkitt, D., and Wright, D. (1966). Geographical and tribal distribution of the African lymphoma in Uganda. *Br Med J* *1*, 569-573.
- Burnside, J., Bernberg, E., Anderson, A., Lu, C., Meyers, B. C., Green, P. J., Jain, N., Isaacs, G., and Morgan, R. W. (2006). Marek's disease virus encodes MicroRNAs that map to meq and the latency-associated transcript. *J Virol* *80*, 8778-8786.
- Cai, X., Hagedorn, C. H., and Cullen, B. R. (2004). Human microRNAs are processed from capped, polyadenylated transcripts that can also function as mRNAs. *Rna* *10*, 1957-1966.
- Cai, X., Lu, S., Zhang, Z., Gonzalez, C. M., Damania, B., and Cullen, B. R. (2005). Kaposi's sarcoma-associated herpesvirus expresses an array of viral microRNAs in latently infected cells. *Proc Natl Acad Sci U S A* *102*, 5570-5575.
- Cai, X., Schafer, A., Lu, S., Bilello, J. P., Desrosiers, R. C., Edwards, R., Raab-Traub, N., and Cullen, B. R. (2006). Epstein-Barr virus microRNAs are evolutionarily conserved and differentially expressed. *PLoS Pathog* *2*, e23.
- Calado, A., Treichel, N., Muller, E. C., Otto, A., and Kutay, U. (2002). Exportin-5-mediated nuclear export of eukaryotic elongation factor 1A and tRNA. *Embo J* *21*, 6216-6224.
- Caldwell, R. G., Wilson, J. B., Anderson, S. J., and Longnecker, R. (1998). Epstein-Barr virus LMP2A drives B cell development and survival in the absence of normal B cell receptor signals. *Immunity* *9*, 405-411.
- Calin, G. A., Dumitru, C. D., Shimizu, M., Bichi, R., Zupo, S., Noch, E., Aldler, H., Rattan, S., Keating, M., Rai, K., *et al.* (2002). Frequent deletions and down-regulation of micro-RNA genes miR15 and miR16 at 13q14 in chronic lymphocytic leukemia. *Proc Natl Acad Sci U S A* *99*, 15524-15529.
- Calin, G. A., Liu, C. G., Sevignani, C., Ferracin, M., Felli, N., Dumitru, C. D., Shimizu, M., Cimmino, A., Zupo, S., Dono, M., *et al.* (2004a). MicroRNA profiling reveals distinct signatures in B cell chronic lymphocytic leukemias. *Proc Natl Acad Sci U S A* *101*, 11755-11760.
- Calin, G. A., Sevignani, C., Dumitru, C. D., Hyslop, T., Noch, E., Yendamuri, S., Shimizu, M., Rattan, S., Bullrich, F., Negrini, M., and Croce, C. M. (2004b). Human microRNA genes are frequently located at fragile sites and genomic regions involved in cancers. *Proc Natl Acad Sci U S A* *101*, 2999-3004.
- Cantalupo, P., Doering, A., Sullivan, C. S., Pal, A., Peden, K. W., Lewis, A. M., and Pipas, J. M. (2005). Complete nucleotide sequence of polyomavirus SA12. *J Virol* *79*, 13094-13104.
- Carel, J. C., Myones, B. L., Frazier, B., and Holers, V. M. (1990). Structural requirements for C3d,g/Epstein-Barr virus receptor (CR2/CD21) ligand binding, internalization, and viral infection. *J Biol Chem* *265*, 12293-12299.
- Carmell, M. A., Xuan, Z., Zhang, M. Q., and Hannon, G. J. (2002). The Argonaute family: tentacles that reach into RNAi, developmental control, stem cell maintenance, and tumorigenesis. *Genes Dev* *16*, 2733-2742.
- Castanotto, D., Lingeman, R., Riggs, A. D., and Rossi, J. J. (2009). CRM1 mediates nuclear-cytoplasmic shuttling of mature microRNAs. *Proc Natl Acad Sci U S A* *106*, 21655-21659.
- Cen, H., Breinig, M. C., Atchison, R. W., Ho, M., and McKnight, J. L. (1991). Epstein-Barr virus transmission via the donor organs in solid organ transplantation: polymerase chain reaction and restriction fragment length polymorphism analysis of IR2, IR3, and IR4. *J Virol* *65*, 976-980.
- Cha, T. A., Tom, E., Kemble, G. W., Duke, G. M., Mocarski, E. S., and Spaete, R. R. (1996). Human cytomegalovirus clinical isolates carry at least 19 genes not found in laboratory strains. *J Virol* *70*, 78-83.
- Chang, Y., Tung, C. H., Huang, Y. T., Lu, J., Chen, J. Y., and Tsai, C. H. (1999). Requirement for cell-to-cell contact in Epstein-Barr virus infection of nasopharyngeal carcinoma cells and keratinocytes. *J Virol* *73*, 8857-8866.
- Chaudhuri, B., Xu, H., Todorov, I., Dutta, A., and Yates, J. L. (2001). Human DNA replication initiation factors, ORC and MCM, associate with oriP of Epstein-Barr virus. *Proc Natl Acad Sci U S A* *98*, 10085-10089.
- Chen, C., Ridzon, D. A., Broomer, A. J., Zhou, Z., Lee, D. H., Nguyen, J. T., Barbisin, M., Xu, N. L., Mahuvakar, V. R., Andersen, M. R., *et al.* (2005a). Real-time quantification of microRNAs by stem-loop RT-PCR. *Nucleic Acids Res* *33*, e179.
- Chen, H., Huang, J., Wu, F. Y., Liao, G., Hutt-Fletcher, L., and Hayward, S. D. (2005b). Regulation of expression of the Epstein-Barr virus BamHI-A rightward transcripts. *J Virol* *79*, 1724-1733.
- Chendrimada, T. P., Gregory, R. I., Kumaraswamy, E., Norman, J., Cooch, N., Nishikura, K., and Shiekhattar, R. (2005). TRBP recruits the Dicer complex to Ago2 for microRNA processing and gene silencing. *Nature* *436*, 740-744.
- Chi, S. W., Zang, J. B., Mele, A., and Darnell, R. B. (2009). Argonaute HITS-CLIP decodes microRNA-mRNA interaction maps. *Nature* *460*, 479-486.
- Child, S. J., Hakki, M., De Niro, K. L., and Geballe, A. P. (2004). Evasion of cellular antiviral responses by human cytomegalovirus TRS1 and IRS1. *J Virol* *78*, 197-205.
- Choy, E. Y., Siu, K. L., Kok, K. H., Lung, R. W., Tsang, C. M., To, K. F., Kwong, D. L., Tsao, S. W., and Jin, D. Y. (2008). An Epstein-Barr virus-encoded microRNA targets PUMA to promote host cell survival. *J Exp Med* *205*, 2551-2560.

- Cimmino, A., Calin, G. A., Fabbri, M., Iorio, M. V., Ferracin, M., Shimizu, M., Wojcik, S. E., Aqeilan, R. I., Zupo, S., Dono, M., *et al.* (2005). miR-15 and miR-16 induce apoptosis by targeting BCL2. *Proc Natl Acad Sci U S A* *102*, 13944-13949.
- Cohen, J. I. (2000). Epstein-Barr virus infection. *N Engl J Med* *343*, 481-492.
- Cohen, J. I., Wang, F., Mannick, J., and Kieff, E. (1989). Epstein-Barr virus nuclear protein 2 is a key determinant of lymphocyte transformation. *Proc Natl Acad Sci U S A* *86*, 9558-9562.
- Coller, J., and Parker, R. (2004). Eukaryotic mRNA decapping. *Annu Rev Biochem* *73*, 861-890.
- Countryman, J., Jenson, H., Seibl, R., Wolf, H., and Miller, G. (1987). Polymorphic proteins encoded within BZLF1 of defective and standard Epstein-Barr viruses disrupt latency. *J Virol* *61*, 3672-3679.
- Countryman, J., and Miller, G. (1985). Activation of expression of latent Epstein-Barr herpesvirus after gene transfer with a small cloned subfragment of heterogeneous viral DNA. *Proc Natl Acad Sci U S A* *82*, 4085-4089.
- Covarrubias, S., Richner, J. M., Clyde, K., Lee, Y. J., and Glaunsinger, B. A. (2009). Host shutoff is a conserved phenotype of gammaherpesvirus infection and is orchestrated exclusively from the cytoplasm. *J Virol* *83*, 9554-9566.
- Cui, C., Griffiths, A., Li, G., Silva, L. M., Kramer, M. F., Gaasterland, T., Wang, X. J., and Coen, D. M. (2006). Prediction and identification of herpes simplex virus 1-encoded microRNAs. *J Virol* *80*, 5499-5508.
- Dalla-Favera, R., Bregni, M., Erikson, J., Patterson, D., Gallo, R. C., and Croce, C. M. (1982). Human c-myc onc gene is located on the region of chromosome 8 that is translocated in Burkitt lymphoma cells. *Proc Natl Acad Sci U S A* *79*, 7824-7827.
- Damania, B. (2004). Oncogenic gamma-herpesviruses: comparison of viral proteins involved in tumorigenesis. *Nat Rev Microbiol* *2*, 656-668.
- Damania, B., and Pipas, J. M. (2009). DNA tumor viruses (New York: Springer Science + Business Media), pp. xxvi, 794 p., [794] p. of plates.
- Dambaugh, T., Hennessy, K., Chamnankit, L., and Kieff, E. (1984). U2 region of Epstein-Barr virus DNA may encode Epstein-Barr nuclear antigen 2. *Proc Natl Acad Sci U S A* *81*, 7632-7636.
- de Jesus, O., Smith, P. R., Spender, L. C., Elgueta Karstegl, C., Niller, H. H., Huang, D., and Farrell, P. J. (2003). Updated Epstein-Barr virus (EBV) DNA sequence and analysis of a promoter for the BART (CST, BARF0) RNAs of EBV. *J Gen Virol* *84*, 1443-1450.
- Deng, Z., Atanasiu, C., Zhao, K., Marmorstein, R., Sbodio, J. I., Chi, N. W., and Lieberman, P. M. (2005). Inhibition of Epstein-Barr virus OriP function by tankyrase, a telomere-associated poly-ADP ribose polymerase that binds and modifies EBNA1. *J Virol* *79*, 4640-4650.
- Deng, Z., Lezina, L., Chen, C. J., Shtivelband, S., So, W., and Lieberman, P. M. (2002). Telomeric proteins regulate episomal maintenance of Epstein-Barr virus origin of plasmid replication. *Mol Cell* *9*, 493-503.
- Denli, A. M., Tops, B. B., Plasterk, R. H., Ketting, R. F., and Hannon, G. J. (2004). Processing of primary microRNAs by the Microprocessor complex. *Nature* *432*, 231-235.
- Dennis, G., Jr., Sherman, B. T., Hosack, D. A., Yang, J., Gao, W., Lane, H. C., and Lempicki, R. A. (2003). DAVID: Database for Annotation, Visualization, and Integrated Discovery. *Genome Biol* *4*, P3.
- Desrosiers, R. C., Sasseville, V. G., Czajak, S. C., Zhang, X., Mansfield, K. G., Kaur, A., Johnson, R. P., Lackner, A. A., and Jung, J. U. (1997). A herpesvirus of rhesus monkeys related to the human Kaposi's sarcoma-associated herpesvirus. *J Virol* *71*, 9764-9769.
- Desvignes, T., Pontarotti, P., Fauvel, C., and Bobe, J. (2009). Nme protein family evolutionary history, a vertebrate perspective. *BMC Evol Biol* *9*, 256.
- Dhar, S. K., Yoshida, K., Machida, Y., Khaira, P., Chaudhuri, B., Wohlschlegel, J. A., Leffak, M., Yates, J., and Dutta, A. (2001). Replication from oriP of Epstein-Barr virus requires human ORC and is inhibited by geminin. *Cell* *106*, 287-296.
- Di Bartolo, D. L., Cannon, M., Liu, Y. F., Renne, R., Chadburn, A., Boshoff, C., and Cesarman, E. (2008). KSHV LANA inhibits TGF-beta signaling through epigenetic silencing of the TGF-beta type II receptor. *Blood* *111*, 4731-4740.
- Doench, J. G., Petersen, C. P., and Sharp, P. A. (2003). siRNAs can function as miRNAs. *Genes Dev* *17*, 438-442.
- Dolken, L., Malterer, G., Erhard, F., Kothe, S., Friedel, C. C., Suffert, G., Marcinowski, L., Motsch, N., Barth, S., Beitzinger, M., *et al.* (2010). Systematic analysis of viral and cellular microRNA targets in cells latently infected with human gamma-herpesviruses by RISC immunoprecipitation assay. *Cell Host Microbe* *7*, 324-334.
- Dolken, L., Perot, J., Cognat, V., Alioua, A., John, M., Soutschek, J., Ruzsics, Z., Koszinowski, U., Voinnet, O., and Pfeffer, S. (2007). Mouse cytomegalovirus microRNAs dominate the cellular small RNA profile during lytic infection and show features of posttranscriptional regulation. *J Virol* *81*, 13771-13782.
- Donati, D., Espmark, E., Kironde, F., Mbidde, E. K., Kanya, M., Lundkvist, A., Wahlgren, M., Bejarano, M. T., and Falk, K. I. (2006). Clearance of circulating Epstein-Barr virus DNA in children with acute malaria after antimalaria treatment. *J Infect Dis* *193*, 971-977.
- Dufner, A., Pownall, S., and Mak, T. W. (2006). Caspase recruitment domain protein 6 is a microtubule-interacting protein that positively modulates NF-kappaB activation. *Proc Natl Acad Sci U S A* *103*, 988-993.

- Dunn, W., Trang, P., Zhong, Q., Yang, E., van Belle, C., and Liu, F. (2005). Human cytomegalovirus expresses novel microRNAs during productive viral infection. *Cell Microbiol* 7, 1684-1695.
- Edwards, R. H., Marquitz, A. R., and Raab-Traub, N. (2008). Epstein-Barr virus BART microRNAs are produced from a large intron prior to splicing. *J Virol* 82, 9094-9106.
- Eis, P. S., Tam, W., Sun, L., Chadburn, A., Li, Z., Gomez, M. F., Lund, E., and Dahlberg, J. E. (2005). Accumulation of miR-155 and BIC RNA in human B cell lymphomas. *Proc Natl Acad Sci U S A* 102, 3627-3632.
- Elbashir, S. M., Harborth, J., Lendeckel, W., Yalcin, A., Weber, K., and Tuschl, T. (2001). Duplexes of 21-nucleotide RNAs mediate RNA interference in cultured mammalian cells. *Nature* 411, 494-498.
- Enright, A. J., John, B., Gaul, U., Tuschl, T., Sander, C., and Marks, D. S. (2003). MicroRNA targets in *Drosophila*. *Genome Biol* 5, R1.
- Epstein, M. A., Achong, B. G., and Barr, Y. M. (1964). Virus Particles in Cultured Lymphoblasts from Burkitt's Lymphoma. *Lancet* 1, 702-703.
- Eulalio, A., Huntzinger, E., Nishihara, T., Rehwinkel, J., Fauser, M., and Izaurralde, E. (2009). Deadenylation is a widespread effect of miRNA regulation. *Rna* 15, 21-32.
- Fabian, M. R., Sonenberg, N., and Filipowicz, W. (2010). Regulation of mRNA translation and stability by microRNAs. *Annu Rev Biochem* 79, 351-379.
- Faggioni, A., Zompetta, C., Grimaldi, S., Barile, G., Frati, L., and Lazdins, J. (1986). Calcium modulation activates Epstein-Barr virus genome in latently infected cells. *Science* 232, 1554-1556.
- Farrell, P. J. (2005). Epstein-Barr Virus Genome. Epstein-Barr Virus, E. S. Robertson (eds.), Chapter 15, 263-287.
- Fields, B. N., Knipe, D. M., and Howley, P. M. (2007). *Fields' virology*, 5th edn (Philadelphia: Wolters Kluwer Health/Lippincott Williams & Wilkins).
- Filipowicz, W. (2000). Imprinted expression of small nucleolar RNAs in brain: time for RNomics. *Proc Natl Acad Sci U S A* 97, 14035-14037.
- Fingerroth, J. D., Weis, J. J., Tedder, T. F., Strominger, J. L., Biro, P. A., and Fearon, D. T. (1984). Epstein-Barr virus receptor of human B lymphocytes is the C3d receptor CR2. *Proc Natl Acad Sci U S A* 81, 4510-4514.
- Fire, A., Xu, S., Montgomery, M. K., Kostas, S. A., Driver, S. E., and Mello, C. C. (1998). Potent and specific genetic interference by double-stranded RNA in *Caenorhabditis elegans*. *Nature* 391, 806-811.
- Fornerod, M., Ohno, M., Yoshida, M., and Mattaj, I. W. (1997). CRM1 is an export receptor for leucine-rich nuclear export signals. *Cell* 90, 1051-1060.
- Fortin, K. R., Nicholson, R. H., and Nicholson, A. W. (2002). Mouse ribonuclease III. cDNA structure, expression analysis, and chromosomal location. *BMC Genomics* 3, 26.
- Fu, H., Cai, J., Clevers, H., Fast, E., Gray, S., Greenberg, R., Jain, M. K., Ma, Q., Qiu, M., Rowitch, D. H., *et al.* (2009). A genome-wide screen for spatially restricted expression patterns identifies transcription factors that regulate glial development. *J Neurosci* 29, 11399-11408.
- Furnari, F. B., Adams, M. D., and Pagano, J. S. (1992). Regulation of the Epstein-Barr virus DNA polymerase gene. *J Virol* 66, 2837-2845.
- Ganem, D. (2006). KSHV infection and the pathogenesis of Kaposi's sarcoma. *Annu Rev Pathol* 1, 273-296.
- Gerner, C. S., Dolan, A., and McGeoch, D. J. (2004). Phylogenetic relationships in the Lymphocryptovirus genus of the Gammaherpesvirinae. *Virus Res* 99, 187-192.
- Gilligan, K. J., Rajadurai, P., Lin, J. C., Busson, P., Abdel-Hamid, M., Prasad, U., Tursz, T., and Raab-Traub, N. (1991). Expression of the Epstein-Barr virus BamHI A fragment in nasopharyngeal carcinoma: evidence for a viral protein expressed in vivo. *J Virol* 65, 6252-6259.
- Giraldez, A. J., Mishima, Y., Rihel, J., Grocock, R. J., Van Dongen, S., Inoue, K., Enright, A. J., and Schier, A. F. (2006). Zebrafish MiR-430 promotes deadenylation and clearance of maternal mRNAs. *Science* 312, 75-79.
- Gong, M., and Kieff, E. (1990). Intracellular trafficking of two major Epstein-Barr virus glycoproteins, gp350/220 and gp110. *J Virol* 64, 1507-1516.
- Gorlich, D., Dabrowski, M., Bischoff, F. R., Kutay, U., Bork, P., Hartmann, E., Prehn, S., and Izaurralde, E. (1997). A novel class of RanGTP binding proteins. *J Cell Biol* 138, 65-80.
- Gottwein, E., and Cullen, B. R. (2008). Viral and cellular microRNAs as determinants of viral pathogenesis and immunity. *Cell Host Microbe* 3, 375-387.
- Gottwein, E., Mukherjee, N., Sachse, C., Frenzel, C., Majoros, W. H., Chi, J. T., Braich, R., Manoharan, M., Soutschek, J., Ohler, U., and Cullen, B. R. (2007). A viral microRNA functions as an orthologue of cellular miR-155. *Nature* 450, 1096-1099.
- Granzow, H., Klupp, B. G., Fuchs, W., Veits, J., Osterrieder, N., and Mettenleiter, T. C. (2001). Egress of alphaherpesviruses: comparative ultrastructural study. *J Virol* 75, 3675-3684.
- Greenbaum, D., Colangelo, C., Williams, K., and Gerstein, M. (2003). Comparing protein abundance and mRNA expression levels on a genomic scale. *Genome Biol* 4, 117.
- Gregory, R. I., Yan, K. P., Amuthan, G., Chendrimada, T., Doratotaj, B., Cooch, N., and Shiekhattar, R. (2004). The Microprocessor complex mediates the genesis of microRNAs. *Nature* 432, 235-240.

- Grey, F., Antoniewicz, A., Allen, E., Saugstad, J., McShea, A., Carrington, J. C., and Nelson, J. (2005). Identification and characterization of human cytomegalovirus-encoded microRNAs. *J Virol* 79, 12095-12099.
- Griffiths-Jones, S. (2004). The microRNA Registry. *Nucleic Acids Res* 32, D109-111.
- Griffiths-Jones, S., Grocock, R. J., van Dongen, S., Bateman, A., and Enright, A. J. (2006). miRBase: microRNA sequences, targets and gene nomenclature. *Nucleic Acids Res* 34, D140-144.
- Griffiths-Jones, S., Saini, H. K., van Dongen, S., and Enright, A. J. (2008). miRBase: tools for microRNA genomics. *Nucleic Acids Res* 36, D154-158.
- Grimson, A., Farh, K. K., Johnston, W. K., Garrett-Engele, P., Lim, L. P., and Bartel, D. P. (2007). MicroRNA targeting specificity in mammals: determinants beyond seed pairing. *Mol Cell* 27, 91-105.
- Grishok, A., Pasquinelli, A. E., Conte, D., Li, N., Parrish, S., Ha, I., Baillie, D. L., Fire, A., Ruvkun, G., and Mello, C. C. (2001). Genes and mechanisms related to RNA interference regulate expression of the small temporal RNAs that control *C. elegans* developmental timing. *Cell* 106, 23-34.
- Groh, V., Bahram, S., Bauer, S., Herman, A., Beauchamp, M., and Spies, T. (1996). Cell stress-regulated human major histocompatibility complex class I gene expressed in gastrointestinal epithelium. *Proc Natl Acad Sci U S A* 93, 12445-12450.
- Grossman, S. R., Johannsen, E., Tong, X., Yalamanchili, R., and Kieff, E. (1994). The Epstein-Barr virus nuclear antigen 2 transactivator is directed to response elements by the J kappa recombination signal binding protein. *Proc Natl Acad Sci U S A* 91, 7568-7572.
- Grundhoff, A., Sullivan, C. S., and Ganem, D. (2006). A combined computational and microarray-based approach identifies novel microRNAs encoded by human gamma-herpesviruses. *Rna* 12, 733-750.
- Guo, H., Ingolia, N. T., Weissman, J. S., and Bartel, D. P. (2010). Mammalian microRNAs predominantly act to decrease target mRNA levels. *Nature* 466, 835-840.
- Guo, S., and Kemphues, K. J. (1995). par-1, a gene required for establishing polarity in *C. elegans* embryos, encodes a putative Ser/Thr kinase that is asymmetrically distributed. *Cell* 81, 611-620.
- Guo, Y., Xiao, P., Lei, S., Deng, F., Xiao, G. G., Liu, Y., Chen, X., Li, L., Wu, S., Chen, Y., *et al.* (2008). How is mRNA expression predictive for protein expression? A correlation study on human circulating monocytes. *Acta Biochim Biophys Sin (Shanghai)* 40, 426-436.
- Hafner, M., Landthaler, M., Burger, L., Khorshid, M., Hausser, J., Berninger, P., Rothballer, A., Ascano, M., Jungkamp, A. C., Munschauer, M., *et al.* (2010). PAR-CLIP--a method to identify transcriptome-wide the binding sites of RNA binding proteins. *J Vis Exp*.
- Haller, O., Staeheli, P., and Kochs, G. (2007). Interferon-induced Mx proteins in antiviral host defense. *Biochimie* 89, 812-818.
- Hamilton, A. J., and Baulcombe, D. C. (1999). A species of small antisense RNA in posttranscriptional gene silencing in plants. *Science* 286, 950-952.
- Hammerschmidt, W., and Sugden, B. (1988). Identification and characterization of oriLyt, a lytic origin of DNA replication of Epstein-Barr virus. *Cell* 55, 427-433.
- Hammond, S. M., Bernstein, E., Beach, D., and Hannon, G. J. (2000). An RNA-directed nuclease mediates post-transcriptional gene silencing in *Drosophila* cells. *Nature* 404, 293-296.
- Han, J., Lee, Y., Yeom, K. H., Kim, Y. K., Jin, H., and Kim, V. N. (2004). The Drosha-DGCR8 complex in primary microRNA processing. *Genes Dev* 18, 3016-3027.
- Haque, T., Thomas, J. A., Falk, K. I., Parratt, R., Hunt, B. J., Yacoub, M., and Crawford, D. H. (1996). Transmission of donor Epstein-Barr virus (EBV) in transplanted organs causes lymphoproliferative disease in EBV-seronegative recipients. *J Gen Virol* 77 (Pt 6), 1169-1172.
- Harada, S., Yalamanchili, R., and Kieff, E. (2001). Epstein-Barr virus nuclear protein 2 has at least two N-terminal domains that mediate self-association. *J Virol* 75, 2482-2487.
- Hawkes, N. A., Otero, G., Winkler, G. S., Marshall, N., Dahmus, M. E., Krappmann, D., Scheidereit, C., Thomas, C. L., Schiavo, G., Erdjument-Bromage, H., *et al.* (2002). Purification and characterization of the human elongator complex. *J Biol Chem* 277, 3047-3052.
- He, L., Thomson, J. M., Hemann, M. T., Hernando-Monge, E., Mu, D., Goodson, S., Powers, S., Cordon-Cardo, C., Lowe, S. W., Hannon, G. J., and Hammond, S. M. (2005). A microRNA polycistron as a potential human oncogene. *Nature* 435, 828-833.
- He, T. C., Zhou, S., da Costa, L. T., Yu, J., Kinzler, K. W., and Vogelstein, B. (1998). A simplified system for generating recombinant adenoviruses. *Proc Natl Acad Sci U S A* 95, 2509-2514.
- He, X., He, L., and Hannon, G. J. (2007). The guardian's little helper: microRNAs in the p53 tumor suppressor network. *Cancer Res* 67, 11099-11101.
- Hendrickson, D. G., Hogan, D. J., Herschlag, D., Ferrell, J. E., and Brown, P. O. (2008). Systematic identification of mRNAs recruited to argonaute 2 by specific microRNAs and corresponding changes in transcript abundance. *PLoS One* 3, e2126.
- Hensbergen, P. J., Wijnands, P. G., Schreurs, M. W., Scheper, R. J., Willemze, R., and Tensen, C. P. (2005). The CXCR3 targeting chemokine CXCL11 has potent antitumor activity in vivo involving attraction of CD8+ T lymphocytes but not inhibition of angiogenesis. *J Immunother* 28, 343-351.

- Hildebrand, J., Rutze, M., Walz, N., Gallinat, S., Wenck, H., Deppert, W., Grundhoff, A., and Knott, A. (2010). A Comprehensive Analysis of MicroRNA Expression During Human Keratinocyte Differentiation In Vitro and In Vivo. *J Invest Dermatol*.
- Hofacker, I. L., and Stadler, P. F. (2006). Memory efficient folding algorithms for circular RNA secondary structures. *Bioinformatics* 22, 1172-1176.
- Hsieh, J. J., and Hayward, S. D. (1995). Masking of the CBF1/RBPJ kappa transcriptional repression domain by Epstein-Barr virus EBNA2. *Science* 268, 560-563.
- Hutvagner, G., McLachlan, J., Pasquinelli, A. E., Balint, E., Tuschl, T., and Zamore, P. D. (2001). A cellular function for the RNA-interference enzyme Dicer in the maturation of the let-7 small temporal RNA. *Science* 293, 834-838.
- Hwang, H. W., and Mendell, J. T. (2006). MicroRNAs in cell proliferation, cell death, and tumorigenesis. *Br J Cancer* 94, 776-780.
- Iizasa, H., Wulff, B. E., Alla, N. R., Maragkakis, M., Megraw, M., Hatzigeorgiou, A., Iwakiri, D., Takada, K., Wiedmer, A., Showe, L., *et al.* (2010). Editing of Epstein-Barr virus-encoded BART6 microRNAs controls their dicer targeting and consequently affects viral latency. *J Biol Chem* 285, 33358-33370.
- Imai, S., Nishikawa, J., and Takada, K. (1998). Cell-to-cell contact as an efficient mode of Epstein-Barr virus infection of diverse human epithelial cells. *J Virol* 72, 4371-4378.
- Jakymiw, A., Lian, S., Eystathioy, T., Li, S., Satoh, M., Hamel, J. C., Fritzler, M. J., and Chan, E. K. (2005). Disruption of GW bodies impairs mammalian RNA interference. *Nat Cell Biol* 7, 1267-1274.
- Jenkins, P. J., Binne, U. K., and Farrell, P. J. (2000). Histone acetylation and reactivation of Epstein-Barr virus from latency. *J Virol* 74, 710-720.
- Kang, M. S., Hung, S. C., and Kieff, E. (2001). Epstein-Barr virus nuclear antigen 1 activates transcription from episomal but not integrated DNA and does not alter lymphocyte growth. *Proc Natl Acad Sci U S A* 98, 15233-15238.
- Kapoor, P., Lavoie, B. D., and Frappier, L. (2005). EBP2 plays a key role in Epstein-Barr virus mitotic segregation and is regulated by aurora family kinases. *Mol Cell Biol* 25, 4934-4945.
- Keene, J. D., Komisarow, J. M., and Friedersdorf, M. B. (2006). RIP-Chip: the isolation and identification of mRNAs, microRNAs and protein components of ribonucleoprotein complexes from cell extracts. *Nat Protoc* 1, 302-307.
- Kennedy, G., Komano, J., and Sugden, B. (2003). Epstein-Barr virus provides a survival factor to Burkitt's lymphomas. *Proc Natl Acad Sci U S A* 100, 14269-14274.
- Ketting, R. F., Fischer, S. E., Bernstein, E., Sijen, T., Hannon, G. J., and Plasterk, R. H. (2001). Dicer functions in RNA interference and in synthesis of small RNA involved in developmental timing in *C. elegans*. *Genes Dev* 15, 2654-2659.
- Kilger, E., Kieser, A., Baumann, M., and Hammerschmidt, W. (1998). Epstein-Barr virus-mediated B-cell proliferation is dependent upon latent membrane protein 1, which simulates an activated CD40 receptor. *Embo J* 17, 1700-1709.
- Kim, J. H., Lane, W. S., and Reinberg, D. (2002). Human Elongator facilitates RNA polymerase II transcription through chromatin. *Proc Natl Acad Sci U S A* 99, 1241-1246.
- Kim, S. S., Ahn, C. H., Kang, M. R., Kim, Y. R., Kim, H. S., Yoo, N. J., and Lee, S. H. (2010). Expression of CARD6, an NF-kappaB activator, in gastric, colorectal and oesophageal cancers. *Pathology* 42, 50-53.
- Kim, V. N. (2005). MicroRNA biogenesis: coordinated cropping and dicing. *Nat Rev Mol Cell Biol* 6, 376-385.
- Kiriakidou, M., Nelson, P. T., Kouranov, A., Fitziev, P., Bouyioukos, C., Mourelatos, Z., and Hatzigeorgiou, A. (2004). A combined computational-experimental approach predicts human microRNA targets. *Genes Dev* 18, 1165-1178.
- Kloosterman, W. P., Wienholds, E., Ketting, R. F., and Plasterk, R. H. (2004). Substrate requirements for let-7 function in the developing zebrafish embryo. *Nucleic Acids Res* 32, 6284-6291.
- Knight, S. W., and Bass, B. L. (2001). A role for the RNase III enzyme DCR-1 in RNA interference and germ line development in *Caenorhabditis elegans*. *Science* 293, 2269-2271.
- Knox, P. G., and Young, L. S. (1995). Epstein-Barr virus infection of CR2-transfected epithelial cells reveals the presence of MHC class II on the virion. *Virology* 213, 147-157.
- Kochs, G., and Haller, O. (1999). Interferon-induced human MxA GTPase blocks nuclear import of Thogoto virus nucleocapsids. *Proc Natl Acad Sci U S A* 96, 2082-2086.
- Kovalchuk, A. L., Qi, C. F., Torrey, T. A., Taddesse-Heath, L., Feigenbaum, L., Park, S. S., Gerbitz, A., Klobeck, G., Hoernagel, K., Polack, A., *et al.* (2000). Burkitt lymphoma in the mouse. *J Exp Med* 192, 1183-1190.
- Krek, A., Grun, D., Poy, M. N., Wolf, R., Rosenberg, L., Epstein, E. J., MacMenamin, P., da Piedade, I., Gunsalus, K. C., Stoffel, M., and Rajewsky, N. (2005). Combinatorial microRNA target predictions. *Nat Genet* 37, 495-500.
- Krutzfeldt, J., Rajewsky, N., Braich, R., Rajeev, K. G., Tuschl, T., Manoharan, M., and Stoffel, M. (2005). Silencing of microRNAs in vivo with 'antagomirs'. *Nature* 438, 685-689.
- Laemmli, U. K. (1970). Cleavage of structural proteins during the assembly of the head of bacteriophage T4. *Nature* 227, 680-685.

- Lagana, A., Forte, S., Russo, F., Giugno, R., Pulvirenti, A., and Ferro, A. (2010). Prediction of human targets for viral-encoded microRNAs by thermodynamics and empirical constraints. *J RNAi Gene Silencing* 6, 379-385.
- Lagos-Quintana, M., Rauhut, R., Lendeckel, W., and Tuschl, T. (2001). Identification of novel genes coding for small expressed RNAs. *Science* 294, 853-858.
- Lai, E. C. (2002). Notch cleavage: Nicastrin helps Presenilin make the final cut. *Curr Biol* 12, R200-202.
- Lai, E. C., Burks, C., and Posakony, J. W. (1998). The K box, a conserved 3' UTR sequence motif, negatively regulates accumulation of enhancer of split complex transcripts. *Development* 125, 4077-4088.
- Lai, E. C., and Posakony, J. W. (1997). The Bearded box, a novel 3' UTR sequence motif, mediates negative post-transcriptional regulation of Bearded and Enhancer of split Complex gene expression. *Development* 124, 4847-4856.
- Lai, E. C., Tam, B., and Rubin, G. M. (2005). Pervasive regulation of Drosophila Notch target genes by GY-box-, Brd-box-, and K-box-class microRNAs. *Genes Dev* 19, 1067-1080.
- Laichalk, L. L., and Thorley-Lawson, D. A. (2005). Terminal differentiation into plasma cells initiates the replicative cycle of Epstein-Barr virus in vivo. *J Virol* 79, 1296-1307.
- LaJeunesse, D. R., Brooks, K., and Adamson, A. L. (2005). Epstein-Barr virus immediate-early proteins BZLF1 and BRLF1 alter mitochondrial morphology during lytic replication. *Biochem Biophys Res Commun* 333, 438-442.
- Landgraf, P., Rusu, M., Sheridan, R., Sewer, A., Iovino, N., Aravin, A., Pfeffer, S., Rice, A., Kamphorst, A. O., Landthaler, M., et al. (2007). A mammalian microRNA expression atlas based on small RNA library sequencing. *Cell* 129, 1401-1414.
- Landthaler, M., Yalcin, A., and Tuschl, T. (2004). The human DiGeorge syndrome critical region gene 8 and Its D. melanogaster homolog are required for miRNA biogenesis. *Curr Biol* 14, 2162-2167.
- Lane, H. C., Masur, H., Edgar, L. C., Whalen, G., Rook, A. H., and Fauci, A. S. (1983). Abnormalities of B-cell activation and immunoregulation in patients with the acquired immunodeficiency syndrome. *N Engl J Med* 309, 453-458.
- Lang, D. J., Garruto, R. M., and Gajdusek, D. C. (1977). Early acquisition of cytomegalovirus and Epstein-Barr virus antibody in several isolated Melanesian populations. *Am J Epidemiol* 105, 480-487.
- Lau, N. C., Lim, L. P., Weinstein, E. G., and Bartel, D. P. (2001). An abundant class of tiny RNAs with probable regulatory roles in *Caenorhabditis elegans*. *Science* 294, 858-862.
- Lee, R. C., Feinbaum, R. L., and Ambros, V. (1993). The *C. elegans* heterochronic gene *lin-4* encodes small RNAs with antisense complementarity to *lin-14*. *Cell* 75, 843-854.
- Lee, S. P., Brooks, J. M., Al-Jarrah, H., Thomas, W. A., Haigh, T. A., Taylor, G. S., Humme, S., Schepers, A., Hammerschmidt, W., Yates, J. L., et al. (2004). CD8 T cell recognition of endogenously expressed Epstein-Barr virus nuclear antigen 1. *J Exp Med* 199, 1409-1420.
- Lee, Y., Ahn, C., Han, J., Choi, H., Kim, J., Yim, J., Lee, J., Provost, P., Radmark, O., Kim, S., and Kim, V. N. (2003). The nuclear RNase III Drosha initiates microRNA processing. *Nature* 425, 415-419.
- Lee, Y., Jeon, K., Lee, J. T., Kim, S., and Kim, V. N. (2002). MicroRNA maturation: stepwise processing and subcellular localization. *Embo J* 21, 4663-4670.
- Leight, E. R., and Sugden, B. (2001). The cis-acting family of repeats can inhibit as well as stimulate establishment of an oriP replicon. *J Virol* 75, 10709-10720.
- Lewis, B. P., Burge, C. B., and Bartel, D. P. (2005). Conserved seed pairing, often flanked by adenosines, indicates that thousands of human genes are microRNA targets. *Cell* 120, 15-20.
- Lewis, B. P., Shih, I. H., Jones-Rhoades, M. W., Bartel, D. P., and Burge, C. B. (2003). Prediction of mammalian microRNA targets. *Cell* 115, 787-798.
- Li, Q., Turk, S. M., and Hutt-Fletcher, L. M. (1995). The Epstein-Barr virus (EBV) BZLF2 gene product associates with the gH and gL homologs of EBV and carries an epitope critical to infection of B cells but not of epithelial cells. *J Virol* 69, 3987-3994.
- Li, Z., Van Calcar, S., Qu, C., Cavenee, W. K., Zhang, M. Q., and Ren, B. (2003). A global transcriptional regulatory role for c-Myc in Burkitt's lymphoma cells. *Proc Natl Acad Sci U S A* 100, 8164-8169.
- Lim, L. P., Glasner, M. E., Yekta, S., Burge, C. B., and Bartel, D. P. (2003). Vertebrate microRNA genes. *Science* 299, 1540.
- Lim, L. P., Lau, N. C., Garrett-Engele, P., Grimson, A., Schelter, J. M., Castle, J., Bartel, D. P., Linsley, P. S., and Johnson, J. M. (2005). Microarray analysis shows that some microRNAs downregulate large numbers of target mRNAs. *Nature* 433, 769-773.
- Lin, J., and Cullen, B. R. (2007). Analysis of the interaction of primate retroviruses with the human RNA interference machinery. *J Virol* 81, 12218-12226.
- Lindner, S. E., and Sugden, B. (2007). The plasmid replicon of Epstein-Barr virus: mechanistic insights into efficient, licensed, extrachromosomal replication in human cells. *Plasmid* 58, 1-12.
- Lingel, A., and Sattler, M. (2005). Novel modes of protein-RNA recognition in the RNAi pathway. *Curr Opin Struct Biol* 15, 107-115.
- Liu, J., Carmell, M. A., Rivas, F. V., Marsden, C. G., Thomson, J. M., Song, J. J., Hammond, S. M., Joshua-Tor, L., and Hannon, G. J. (2004). Argonaute2 is the catalytic engine of mammalian RNAi. *Science* 305, 1437-1441.

- Liu, J., Rivas, F. V., Wohlschlegel, J., Yates, J. R., 3rd, Parker, R., and Hannon, G. J. (2005). A role for the P-body component GW182 in microRNA function. *Nat Cell Biol* 7, 1261-1266.
- Liu, Y. P., Vink, M. A., Westerink, J. T., Ramirez de Arellano, E., Konstantinova, P., Ter Brake, O., and Berkhout, B. (2010). Titers of lentiviral vectors encoding shRNAs and miRNAs are reduced by different mechanisms that require distinct repair strategies. *Rna* 16, 1328-1339.
- Lo, A. K., To, K. F., Lo, K. W., Lung, R. W., Hui, J. W., Liao, G., and Hayward, S. D. (2007). Modulation of LMP1 protein expression by EBV-encoded microRNAs. *Proc Natl Acad Sci U S A* 104, 16164-16169.
- Lu, J., Getz, G., Miska, E. A., Alvarez-Saavedra, E., Lamb, J., Peck, D., Sweet-Cordero, A., Ebert, B. L., Mak, R. H., Ferrando, A. A., *et al.* (2005). MicroRNA expression profiles classify human cancers. *Nature* 435, 834-838.
- Lung, R. W., Tong, J. H., Sung, Y. M., Leung, P. S., Ng, D. C., Chau, S. L., Chan, A. W., Ng, E. K., Lo, K. W., and To, K. F. (2009). Modulation of LMP2A expression by a newly identified Epstein-Barr virus-encoded microRNA miR-BART22. *Neoplasia* 11, 1174-1184.
- Luo, J., Deng, Z. L., Luo, X., Tang, N., Song, W. X., Chen, J., Sharff, K. A., Luu, H. H., Haydon, R. C., Kinzler, K. W., *et al.* (2007). A protocol for rapid generation of recombinant adenoviruses using the AdEasy system. *Nat Protoc* 2, 1236-1247.
- Ma, J. B., Yuan, Y. R., Meister, G., Pei, Y., Tuschl, T., and Patel, D. J. (2005). Structural basis for 5'-end-specific recognition of guide RNA by the *A. fulgidus* Piwi protein. *Nature* 434, 666-670.
- Mathews, M. B., and Shenk, T. (1991). Adenovirus virus-associated RNA and translation control. *J Virol* 65, 5657-5662.
- McClure, L. V., and Sullivan, C. S. (2008). Kaposi's sarcoma herpes virus taps into a host microRNA regulatory network. *Cell Host Microbe* 3, 1-3.
- McGeoch, D. J., and Cook, S. (1994). Molecular phylogeny of the alphaherpesvirinae subfamily and a proposed evolutionary timescale. *J Mol Biol* 238, 9-22.
- McGeoch, D. J., Cook, S., Dolan, A., Jamieson, F. E., and Telford, E. A. (1995). Molecular phylogeny and evolutionary timescale for the family of mammalian herpesviruses. *J Mol Biol* 247, 443-458.
- McGeoch, D. J., and Gatherer, D. (2005). Integrating reptilian herpesviruses into the family herpesviridae. *J Virol* 79, 725-731.
- McGeoch, D. J., Gatherer, D., and Dolan, A. (2005). On phylogenetic relationships among major lineages of the Gammaherpesvirinae. *J Gen Virol* 86, 307-316.
- McGeoch, D. J., Rixon, F. J., and Davison, A. J. (2006). Topics in herpesvirus genomics and evolution. *Virus Res* 117, 90-104.
- Meister, G., Landthaler, M., Patkaniowska, A., Dorsett, Y., Teng, G., and Tuschl, T. (2004). Human Argonaute2 mediates RNA cleavage targeted by miRNAs and siRNAs. *Mol Cell* 15, 185-197.
- Miller, C. L., Burkhardt, A. L., Lee, J. H., Stealey, B., Longnecker, R., Bolen, J. B., and Kieff, E. (1995). Integral membrane protein 2 of Epstein-Barr virus regulates reactivation from latency through dominant negative effects on protein-tyrosine kinases. *Immunity* 2, 155-166.
- Miller, N., and Hutt-Fletcher, L. M. (1988). A monoclonal antibody to glycoprotein gp85 inhibits fusion but not attachment of Epstein-Barr virus. *J Virol* 62, 2366-2372.
- Moghaddam, A., Rosenzweig, M., Lee-Parritz, D., Annis, B., Johnson, R. P., and Wang, F. (1997). An animal model for acute and persistent Epstein-Barr virus infection. *Science* 276, 2030-2033.
- Molesworth, S. J., Lake, C. M., Borza, C. M., Turk, S. M., and Hutt-Fletcher, L. M. (2000). Epstein-Barr virus gH is essential for penetration of B cells but also plays a role in attachment of virus to epithelial cells. *J Virol* 74, 6324-6332.
- Moormann, A. M., Chelimo, K., Sumba, P. O., Tisch, D. J., Rochford, R., and Kazura, J. W. (2007). Exposure to holoendemic malaria results in suppression of Epstein-Barr virus-specific T cell immunosurveillance in Kenyan children. *J Infect Dis* 195, 799-808.
- Morrow, R. H., Jr. (1985). Epidemiological evidence for the role of falciparum malaria in the pathogenesis of Burkitt's lymphoma. *IARC Sci Publ*, 177-186.
- Mourelatos, Z., Dostie, J., Paushkin, S., Sharma, A., Charroux, B., Abel, L., Rappsilber, J., Mann, M., and Dreyfuss, G. (2002). miRNPs: a novel class of ribonucleoproteins containing numerous microRNAs. *Genes Dev* 16, 720-728.
- Mullis, K., Faloona, F., Scharf, S., Saiki, R., Horn, G., and Erlich, H. (1986). Specific enzymatic amplification of DNA in vitro: the polymerase chain reaction. *Cold Spring Harb Symp Quant Biol* 51 Pt 1, 263-273.
- Murphy, E., Vanicek, J., Robins, H., Shenk, T., and Levine, A. J. (2008). Suppression of immediate-early viral gene expression by herpesvirus-coded microRNAs: implications for latency. *Proc Natl Acad Sci U S A* 105, 5453-5458.
- Nachmani, D., Stern-Ginossar, N., Sarid, R., and Mandelboim, O. (2009). Diverse herpesvirus microRNAs target the stress-induced immune ligand MICB to escape recognition by natural killer cells. *Cell Host Microbe* 5, 376-385.
- Nagahama, M., Hara, Y., Seki, A., Yamazoe, T., Kawate, Y., Shinohara, T., Hatsuzawa, K., Tani, K., and Tagaya, M. (2004). NVL2 is a nucleolar AAA-ATPase that interacts with ribosomal protein L5 through its nucleolar localization sequence. *Mol Biol Cell* 15, 5712-5723.

- Nanbo, A., Yoshiyama, H., and Takada, K. (2005). Epstein-Barr virus-encoded poly(A)- RNA confers resistance to apoptosis mediated through Fas by blocking the PKR pathway in human epithelial intestine 407 cells. *J Virol* 79, 12280-12285.
- Napoli, C., Lemieux, C., and Jorgensen, R. (1990). Introduction of a Chimeric Chalcone Synthase Gene into *Petunia* Results in Reversible Co-Suppression of Homologous Genes in trans. *Plant Cell* 2, 279-289.
- Nemerow, G. R., and Cooper, N. R. (1984). Early events in the infection of human B lymphocytes by Epstein-Barr virus: the internalization process. *Virology* 132, 186-198.
- Netherton, C. L., Simpson, J., Haller, O., Wileman, T. E., Takamatsu, H. H., Monaghan, P., and Taylor, G. (2009). Inhibition of a large double-stranded DNA virus by MxA protein. *J Virol* 83, 2310-2320.
- Niedobitek, G., Hansmann, M. L., Herbst, H., Young, L. S., Dienemann, D., Hartmann, C. A., Finn, T., Pitteroff, S., Welt, A., Anagnostopoulos, I., and et al. (1991). Epstein-Barr virus and carcinomas: undifferentiated carcinomas but not squamous cell carcinomas of the nasopharynx are regularly associated with the virus. *J Pathol* 165, 17-24.
- Nonkwelo, C., Skinner, J., Bell, A., Rickinson, A., and Sample, J. (1996). Transcription start sites downstream of the Epstein-Barr virus (EBV) Fp promoter in early-passage Burkitt lymphoma cells define a fourth promoter for expression of the EBV EBNA-1 protein. *J Virol* 70, 623-627.
- Nonkwelo, C. B., and Long, W. K. (1993). Regulation of Epstein-Barr virus BamHI-H divergent promoter by DNA methylation. *Virology* 197, 205-215.
- Norseen, J., Thomae, A., Sridharan, V., Aiyar, A., Schepers, A., and Lieberman, P. M. (2008). RNA-dependent recruitment of the origin recognition complex. *Embo J* 27, 3024-3035.
- Oda, T., Imai, S., Chiba, S., and Takada, K. (2000). Epstein-Barr virus lacking glycoprotein gp85 cannot infect B cells and epithelial cells. *Virology* 276, 52-58.
- Olsen, P. H., and Ambros, V. (1999). The lin-4 regulatory RNA controls developmental timing in *Caenorhabditis elegans* by blocking LIN-14 protein synthesis after the initiation of translation. *Dev Biol* 216, 671-680.
- Orzechowska, B. U., Powers, M. F., Sprague, J., Li, H., Yen, B., Searles, R. P., Axthelm, M. K., and Wong, S. W. (2008). Rhesus macaque rhadinovirus-associated non-Hodgkin lymphoma: animal model for KSHV-associated malignancies. *Blood* 112, 4227-4234.
- Ossareh-Nazari, B., Bachelier, F., and Dargemont, C. (1997). Evidence for a role of CRM1 in signal-mediated nuclear protein export. *Science* 278, 141-144.
- Ota, A., Tagawa, H., Karnan, S., Tsuzuki, S., Karpas, A., Kira, S., Yoshida, Y., and Seto, M. (2004). Identification and characterization of a novel gene, C13orf25, as a target for 13q31-q32 amplification in malignant lymphoma. *Cancer Res* 64, 3087-3095.
- Parker, G. A., Crook, T., Bain, M., Sara, E. A., Farrell, P. J., and Allday, M. J. (1996). Epstein-Barr virus nuclear antigen (EBNA)3C is an immortalizing oncoprotein with similar properties to adenovirus E1A and papillomavirus E7. *Oncogene* 13, 2541-2549.
- Parker, J. S., Roe, S. M., and Barford, D. (2005). Structural insights into mRNA recognition from a PIWI domain-siRNA guide complex. *Nature* 434, 663-666.
- Parker, R., and Song, H. (2004). The enzymes and control of eukaryotic mRNA turnover. *Nat Struct Mol Biol* 11, 121-127.
- Pascal, L. E., True, L. D., Campbell, D. S., Deutsch, E. W., Risk, M., Coleman, I. M., Eichner, L. J., Nelson, P. S., and Liu, A. Y. (2008). Correlation of mRNA and protein levels: cell type-specific gene expression of cluster designation antigens in the prostate. *BMC Genomics* 9, 246.
- Pauley, K. M., Satoh, M., Chan, A. L., Bubb, M. R., Reeves, W. H., and Chan, E. K. (2008). Upregulated miR-146a expression in peripheral blood mononuclear cells from rheumatoid arthritis patients. *Arthritis Res Ther* 10, R101.
- Paulson, E. J., Fingerroth, J. D., Yates, J. L., and Speck, S. H. (2002). Methylation of the EBV genome and establishment of restricted latency in low-passage EBV-infected 293 epithelial cells. *Virology* 299, 109-121.
- Pegtel, D. M., Middeldorp, J., and Thorley-Lawson, D. A. (2004). Epstein-Barr virus infection in ex vivo tonsil epithelial cell cultures of asymptomatic carriers. *J Virol* 78, 12613-12624.
- Pfeffer, S., Lagos-Quintana, M., and Tuschl, T. (2005a). Cloning of small RNA molecules. *Curr Protoc Mol Biol Chapter* 26, Unit 26 24.
- Pfeffer, S., Sewer, A., Lagos-Quintana, M., Sheridan, R., Sander, C., Grasser, F. A., van Dyk, L. F., Ho, C. K., Shuman, S., Chien, M., et al. (2005b). Identification of microRNAs of the herpesvirus family. *Nat Methods* 2, 269-276.
- Pfeffer, S., Zavolan, M., Grasser, F. A., Chien, M., Russo, J. J., Ju, J., John, B., Enright, A. J., Marks, D., Sander, C., and Tuschl, T. (2004). Identification of virus-encoded microRNAs. *Science* 304, 734-736.
- Pillai, R. S. (2005). MicroRNA function: multiple mechanisms for a tiny RNA? *Rna* 11, 1753-1761.
- Polack, A., Hortnagel, K., Pajic, A., Christoph, B., Baier, B., Falk, M., Mautner, J., Geltinger, C., Bornkamm, G. W., and Kempkes, B. (1996). c-myc activation renders proliferation of Epstein-Barr virus (EBV)-transformed cells independent of EBV nuclear antigen 2 and latent membrane protein 1. *Proc Natl Acad Sci U S A* 93, 10411-10416.

- Poluri, A., and Sutton, R. E. (2008). Titers of HIV-based vectors encoding shRNAs are reduced by a dicer-dependent mechanism. *Mol Ther* *16*, 378-386.
- Raab-Traub, N. (2002). Epstein-Barr virus in the pathogenesis of NPC. *Semin Cancer Biol* *12*, 431-441.
- Raab-Traub, N., and Flynn, K. (1986). The structure of the termini of the Epstein-Barr virus as a marker of clonal cellular proliferation. *Cell* *47*, 883-889.
- Rajewsky, N., and Socci, N. D. (2004). Computational identification of microRNA targets. *Dev Biol* *267*, 529-535.
- Randall, G., Panis, M., Cooper, J. D., Tellinghuisen, T. L., Sukhodolets, K. E., Pfeffer, S., Landthaler, M., Landgraf, P., Kan, S., Lindenbach, B. D., *et al.* (2007). Cellular cofactors affecting hepatitis C virus infection and replication. *Proc Natl Acad Sci U S A* *104*, 12884-12889.
- Rangan, S. R., Martin, L. N., Bozelka, B. E., Wang, N., and Gormus, B. J. (1986). Epstein-Barr virus-related herpesvirus from a rhesus monkey (*Macaca mulatta*) with malignant lymphoma. *Int J Cancer* *38*, 425-432.
- Raulet, D. H. (2003). Roles of the NKG2D immunoreceptor and its ligands. *Nat Rev Immunol* *3*, 781-790.
- Rawlins, D. R., Milman, G., Hayward, S. D., and Hayward, G. S. (1985). Sequence-specific DNA binding of the Epstein-Barr virus nuclear antigen (EBNA-1) to clustered sites in the plasmid maintenance region. *Cell* *42*, 859-868.
- Rehwinkel, J., Natalin, P., Stark, A., Brennecke, J., Cohen, S. M., and Izaurralde, E. (2006). Genome-wide analysis of mRNAs regulated by Droscha and Argonaute proteins in *Drosophila melanogaster*. *Mol Cell Biol* *26*, 2965-2975.
- Reinhart, B. J., Slack, F. J., Basson, M., Pasquinelli, A. E., Bettinger, J. C., Rougvie, A. E., Horvitz, H. R., and Ruvkun, G. (2000). The 21-nucleotide let-7 RNA regulates developmental timing in *Caenorhabditis elegans*. *Nature* *403*, 901-906.
- Rhoades, M. W., Reinhart, B. J., Lim, L. P., Burge, C. B., Bartel, B., and Bartel, D. P. (2002). Prediction of plant microRNA targets. *Cell* *110*, 513-520.
- Rickinson, A. B., Young, L. S., and Rowe, M. (1987). Influence of the Epstein-Barr virus nuclear antigen EBNA 2 on the growth phenotype of virus-transformed B cells. *J Virol* *61*, 1310-1317.
- Riley, K. J., Rabinowitz, G. S., and Steitz, J. A. (2010). Comprehensive analysis of Rhesus lymphocryptovirus microRNA expression. *J Virol* *84*, 5148-5157.
- Rivailler, P., Carville, A., Kaur, A., Rao, P., Quink, C., Kutok, J. L., Westmoreland, S., Klumpp, S., Simon, M., Aster, J. C., and Wang, F. (2004). Experimental rhesus lymphocryptovirus infection in immunosuppressed macaques: an animal model for Epstein-Barr virus pathogenesis in the immunosuppressed host. *Blood* *104*, 1482-1489.
- Rivailler, P., Cho, Y. G., and Wang, F. (2002). Complete genomic sequence of an Epstein-Barr virus-related herpesvirus naturally infecting a new world primate: a defining point in the evolution of oncogenic lymphocryptoviruses. *J Virol* *76*, 12055-12068.
- Rosa, M. D., Gottlieb, E., Lerner, M. R., and Steitz, J. A. (1981). Striking similarities are exhibited by two small Epstein-Barr virus-encoded ribonucleic acids and the adenovirus-associated ribonucleic acids VAI and VAII. *Mol Cell Biol* *1*, 785-796.
- Rose, T. M. (2005). CODEHOP-mediated PCR - a powerful technique for the identification and characterization of viral genomes. *Virol J* *2*, 20.
- Saeki, K., Suzuki, H., Tsuneoka, M., Maeda, M., Iwamoto, R., Hasuwa, H., Shida, S., Takahashi, T., Sakaguchi, M., Endo, T., *et al.* (2000). Identification of mammalian TOM22 as a subunit of the preprotein translocase of the mitochondrial outer membrane. *J Biol Chem* *275*, 31996-32002.
- Sakai, Y., Ohga, S., Tonegawa, Y., Takada, H., Nakao, F., Nakayama, H., Aoki, T., Yamamori, S., and Hara, T. (1998). Interferon-alpha therapy for chronic active Epstein-Barr virus infection: potential effect on the development of T-lymphoproliferative disease. *J Pediatr Hematol Oncol* *20*, 342-346.
- Sambrook, J., Russell, D. W., and Cold Spring Harbor Laboratory. (2001). *Molecular cloning : a laboratory manual*, 3rd. edn (Cold Spring Harbor, N.Y.: Cold Spring Harbor Laboratory).
- Samols, M. A., Hu, J., Skalsky, R. L., and Renne, R. (2005). Cloning and identification of a microRNA cluster within the latency-associated region of Kaposi's sarcoma-associated herpesvirus. *J Virol* *79*, 9301-9305.
- Samols, M. A., Skalsky, R. L., Maldonado, A. M., Riva, A., Lopez, M. C., Baker, H. V., and Renne, R. (2007). Identification of cellular genes targeted by KSHV-encoded microRNAs. *PLoS Pathog* *3*, e65.
- Sample, J., Young, L., Martin, B., Chatman, T., Kieff, E., Rickinson, A., and Kieff, E. (1990). Epstein-Barr virus types 1 and 2 differ in their EBNA-3A, EBNA-3B, and EBNA-3C genes. *J Virol* *64*, 4084-4092.
- Schafer, A., Cai, X., Bilello, J. P., Desrosiers, R. C., and Cullen, B. R. (2007). Cloning and analysis of microRNAs encoded by the primate gamma-herpesvirus rhesus monkey rhadinovirus. *Virology* *364*, 21-27.
- Schepers, A., Ritzi, M., Bousset, K., Kremmer, E., Yates, J. L., Harwood, J., Diffley, J. F., and Hammerschmidt, W. (2001). Human origin recognition complex binds to the region of the latent origin of DNA replication of Epstein-Barr virus. *Embo J* *20*, 4588-4602.
- Schmittgen, T. D., Jiang, J., Liu, Q., and Yang, L. (2004). A high-throughput method to monitor the expression of microRNA precursors. *Nucleic Acids Res* *32*, e43.
- Schuster, P., Fontana, W., Stadler, P. F., and Hofacker, I. L. (1994). From sequences to shapes and back: a case study in RNA secondary structures. *Proc Biol Sci* *255*, 279-284.

- Schwarz, D. S., Hutvagner, G., Du, T., Xu, Z., Aronin, N., and Zamore, P. D. (2003). Asymmetry in the assembly of the RNAi enzyme complex. *Cell* *115*, 199-208.
- Searles, R. P., Bergquam, E. P., Axthelm, M. K., and Wong, S. W. (1999). Sequence and genomic analysis of a Rhesus macaque rhadinovirus with similarity to Kaposi's sarcoma-associated herpesvirus/human herpesvirus 8. *J Virol* *73*, 3040-3053.
- Sears, J., Ujihara, M., Wong, S., Ott, C., Middeldorp, J., and Aiyar, A. (2004). The amino terminus of Epstein-Barr Virus (EBV) nuclear antigen 1 contains AT hooks that facilitate the replication and partitioning of latent EBV genomes by tethering them to cellular chromosomes. *J Virol* *78*, 11487-11505.
- Sen, G. L., and Blau, H. M. (2005). Argonaute 2/RISC resides in sites of mammalian mRNA decay known as cytoplasmic bodies. *Nat Cell Biol* *7*, 633-636.
- Seo, G. J., Chen, C. J., and Sullivan, C. S. (2009). Merkel cell polyomavirus encodes a microRNA with the ability to autoregulate viral gene expression. *Virology* *383*, 183-187.
- Seo, G. J., Fink, L. H., O'Hara, B., Atwood, W. J., and Sullivan, C. S. (2008). Evolutionarily conserved function of a viral microRNA. *J Virol* *82*, 9823-9828.
- Seto, E., Moosmann, A., Gromminger, S., Walz, N., Grundhoff, A., and Hammerschmidt, W. (2010). Micro RNAs of Epstein-Barr virus promote cell cycle progression and prevent apoptosis of primary human B cells. *PLoS Pathog* *6*.
- Shannon-Lowe, C. D., Neuhierl, B., Baldwin, G., Rickinson, A. B., and Delecluse, H. J. (2006). Resting B cells as a transfer vehicle for Epstein-Barr virus infection of epithelial cells. *Proc Natl Acad Sci U S A* *103*, 7065-7070.
- Sharp, T. V., Schwemmle, M., Jeffrey, I., Laing, K., Mellor, H., Proud, C. G., Hilse, K., and Clemens, M. J. (1993). Comparative analysis of the regulation of the interferon-inducible protein kinase PKR by Epstein-Barr virus RNAs EBER-1 and EBER-2 and adenovirus VAI RNA. *Nucleic Acids Res* *21*, 4483-4490.
- Shire, K., Ceccarelli, D. F., Avolio-Hunter, T. M., and Frappier, L. (1999). EBP2, a human protein that interacts with sequences of the Epstein-Barr virus nuclear antigen 1 important for plasmid maintenance. *J Virol* *73*, 2587-2595.
- Sinclair, A. J., Palmero, I., Peters, G., and Farrell, P. J. (1994). EBNA-2 and EBNA-LP cooperate to cause G0 to G1 transition during immortalization of resting human B lymphocytes by Epstein-Barr virus. *Embo J* *13*, 3321-3328.
- Skalsky, R. L., Samols, M. A., Plaisance, K. B., Boss, I. W., Riva, A., Lopez, M. C., Baker, H. V., and Renne, R. (2007). Kaposi's sarcoma-associated herpesvirus encodes an ortholog of miR-155. *J Virol* *81*, 12836-12845.
- Smith, P. (2001). Epstein-Barr virus complementary strand transcripts (CSTs/BARTs) and cancer. *Semin Cancer Biol* *11*, 469-476.
- Song, J. J., Smith, S. K., Hannon, G. J., and Joshua-Tor, L. (2004). Crystal structure of Argonaute and its implications for RISC slicer activity. *Science* *305*, 1434-1437.
- Sontheimer, E. J., and Carthew, R. W. (2005). Silence from within: endogenous siRNAs and miRNAs. *Cell* *122*, 9-12.
- Stanczyk, J., Pedrioli, D. M., Brentano, F., Sanchez-Pernaute, O., Kolling, C., Gay, R. E., Detmar, M., Gay, S., and Kyburz, D. (2008). Altered expression of MicroRNA in synovial fibroblasts and synovial tissue in rheumatoid arthritis. *Arthritis Rheum* *58*, 1001-1009.
- Stark, A., Brennecke, J., Russell, R. B., and Cohen, S. M. (2003). Identification of Drosophila MicroRNA targets. *PLoS Biol* *1*, E60.
- Stehlik, C., Lee, S. H., Dorfleutner, A., Stassinopoulos, A., Sagara, J., and Reed, J. C. (2003). Apoptosis-associated speck-like protein containing a caspase recruitment domain is a regulator of procaspase-1 activation. *J Immunol* *171*, 6154-6163.
- Steven, N. M., Annels, N. E., Kumar, A., Leese, A. M., Kurilla, M. G., and Rickinson, A. B. (1997). Immediate early and early lytic cycle proteins are frequent targets of the Epstein-Barr virus-induced cytotoxic T cell response. *J Exp Med* *185*, 1605-1617.
- Stevens, J. G. (1987). Defining herpes simplex genes involved in neurovirulence and neuroinvasiveness. *Curr Eye Res* *6*, 63-67.
- Strelow, L. I., and Leib, D. A. (1995). Role of the virion host shutoff (vhs) of herpes simplex virus type 1 in latency and pathogenesis. *J Virol* *69*, 6779-6786.
- Sullivan, C. S., and Ganem, D. (2005). MicroRNAs and viral infection. *Mol Cell* *20*, 3-7.
- Sullivan, C. S., Grundhoff, A. T., Tevethia, S., Pipas, J. M., and Ganem, D. (2005). SV40-encoded microRNAs regulate viral gene expression and reduce susceptibility to cytotoxic T cells. *Nature* *435*, 682-686.
- Sullivan, C. S., Sung, C. K., Pack, C. D., Grundhoff, A., Lukacher, A. E., Benjamin, T. L., and Ganem, D. (2009). Murine Polyomavirus encodes a microRNA that cleaves early RNA transcripts but is not essential for experimental infection. *Virology*.
- Sung, N. S., Kenney, S., Gutsch, D., and Pagano, J. S. (1991). EBNA-2 transactivates a lymphoid-specific enhancer in the BamHI C promoter of Epstein-Barr virus. *J Virol* *65*, 2164-2169.
- Szyf, M., Eliasson, L., Mann, V., Klein, G., and Razin, A. (1985). Cellular and viral DNA hypomethylation associated with induction of Epstein-Barr virus lytic cycle. *Proc Natl Acad Sci U S A* *82*, 8090-8094.

- Taganov, K. D., Boldin, M. P., Chang, K. J., and Baltimore, D. (2006). NF-kappaB-dependent induction of microRNA miR-146, an inhibitor targeted to signaling proteins of innate immune responses. *Proc Natl Acad Sci U S A* *103*, 12481-12486.
- Takada, K. (2001). Role of Epstein-Barr virus in Burkitt's lymphoma. *Curr Top Microbiol Immunol* *258*, 141-151.
- Takada, K., and Nanbo, A. (2001). The role of EBERs in oncogenesis. *Semin Cancer Biol* *11*, 461-467.
- Takada, K., and Ono, Y. (1989). Synchronous and sequential activation of latently infected Epstein-Barr virus genomes. *J Virol* *63*, 445-449.
- Takada, K., Shimizu, N., Sakuma, S., and Ono, Y. (1986). trans activation of the latent Epstein-Barr virus (EBV) genome after transfection of the EBV DNA fragment. *J Virol* *57*, 1016-1022.
- Tanner, J., Weis, J., Fearon, D., Whang, Y., and Kieff, E. (1987). Epstein-Barr virus gp350/220 binding to the B lymphocyte C3d receptor mediates adsorption, capping, and endocytosis. *Cell* *50*, 203-213.
- Tao, Q., Robertson, K. D., Manns, A., Hildesheim, A., and Ambinder, R. F. (1998). The Epstein-Barr virus major latent promoter Qp is constitutively active, hypomethylated, and methylation sensitive. *J Virol* *72*, 7075-7083.
- Teixeira, D., Sheth, U., Valencia-Sanchez, M. A., Brengues, M., and Parker, R. (2005). Processing bodies require RNA for assembly and contain nontranslating mRNAs. *Rna* *11*, 371-382.
- Tempera, I., Deng, Z., Atanasiu, C., Chen, C. J., D'Erme, M., and Lieberman, P. M. (2010). Regulation of Epstein-Barr virus OriP replication by poly(ADP-ribose) polymerase 1. *J Virol* *84*, 4988-4997.
- Thimmappaya, B., Weinberger, C., Schneider, R. J., and Shenk, T. (1982). Adenovirus VAI RNA is required for efficient translation of viral mRNAs at late times after infection. *Cell* *31*, 543-551.
- Thorley-Lawson, D. A. (2001). Epstein-Barr virus: exploiting the immune system. *Nat Rev Immunol* *1*, 75-82.
- Thornburg, N. J., Kusano, S., and Raab-Traub, N. (2004). Identification of Epstein-Barr virus RK-BARF0-interacting proteins and characterization of expression pattern. *J Virol* *78*, 12848-12856.
- Tomari, Y., and Zamore, P. D. (2005). Perspective: machines for RNAi. *Genes Dev* *19*, 517-529.
- Tsurumi, T., Fujita, M., and Kudoh, A. (2005). Latent and lytic Epstein-Barr virus replication strategies. *Rev Med Virol* *15*, 3-15.
- Tuzizov, S. M., Berline, J. W., and Palefsky, J. M. (2003). Epstein-Barr virus infection of polarized tongue and nasopharyngeal epithelial cells. *Nat Med* *9*, 307-314.
- Umbach, J. L., Strelow, L. I., Wong, S. W., and Cullen, B. R. (2010). Analysis of rhesus rhadinovirus microRNAs expressed in virus-induced tumors from infected rhesus macaques. *Virology* *405*, 592-599.
- van der Krol, A. R., Mur, L. A., de Lange, P., Mol, J. N., and Stuitje, A. R. (1990). Inhibition of flower pigmentation by antisense CHS genes: promoter and minimal sequence requirements for the antisense effect. *Plant Mol Biol* *14*, 457-466.
- Varkonyi-Gasic, E., Wu, R., Wood, M., Walton, E. F., and Hellens, R. P. (2007). Protocol: a highly sensitive RT-PCR method for detection and quantification of microRNAs. *Plant Methods* *3*, 12.
- Ventura, A., Meissner, A., Dillon, C. P., McManus, M., Sharp, P. A., Van Parijs, L., Jaenisch, R., and Jacks, T. (2004). Cre-lox-regulated conditional RNA interference from transgenes. *Proc Natl Acad Sci U S A* *101*, 10380-10385.
- Venturelli, D., Martinez, R., Melotti, P., Casella, I., Peschle, C., Cucco, C., Spampinato, G., Darzynkiewicz, Z., and Calabretta, B. (1995). Overexpression of DR-nm23, a protein encoded by a member of the nm23 gene family, inhibits granulocyte differentiation and induces apoptosis in 32Dc13 myeloid cells. *Proc Natl Acad Sci U S A* *92*, 7435-7439.
- Walz, N., Christalla, T., Tessmer, U., and Grundhoff, A. (2010). A global analysis of evolutionary conservation among known and predicted gammaherpesvirus microRNAs. *J Virol* *84*, 716-728.
- Wang, W. X., Rajeev, B. W., Stromberg, A. J., Ren, N., Tang, G., Huang, Q., Rigoutsos, I., and Nelson, P. T. (2008a). The expression of microRNA miR-107 decreases early in Alzheimer's disease and may accelerate disease progression through regulation of beta-site amyloid precursor protein-cleaving enzyme 1. *J Neurosci* *28*, 1213-1223.
- Wang, Y., Baskerville, S., Shenoy, A., Babiarz, J. E., Baehner, L., and Blelloch, R. (2008b). Embryonic stem cell-specific microRNAs regulate the G1-S transition and promote rapid proliferation. *Nat Genet* *40*, 1478-1483.
- Wen, K. W., and Damania, B. (2010). Kaposi sarcoma-associated herpesvirus (KSHV): molecular biology and oncogenesis. *Cancer Lett* *289*, 140-150.
- Wen, W., Iwakiri, D., Yamamoto, K., Maruo, S., Kanda, T., and Takada, K. (2007). Epstein-Barr virus BZLF1 gene, a switch from latency to lytic infection, is expressed as an immediate-early gene after primary infection of B lymphocytes. *J Virol* *81*, 1037-1042.
- Wightman, B., Ha, I., and Ruvkun, G. (1993). Posttranscriptional regulation of the heterochronic gene *lin-14* by *lin-4* mediates temporal pattern formation in *C. elegans*. *Cell* *75*, 855-862.
- Wilson, J. B., Bell, J. L., and Levine, A. J. (1996). Expression of Epstein-Barr virus nuclear antigen-1 induces B cell neoplasia in transgenic mice. *Embo J* *15*, 3117-3126.
- Witwer, K. W., Sisk, J. M., Gama, L., and Clements, J. E. (2010). MicroRNA regulation of IFN-beta protein expression: rapid and sensitive modulation of the innate immune response. *J Immunol* *184*, 2369-2376.

- Wong, S. W., Bergquam, E. P., Swanson, R. M., Lee, F. W., Shiigi, S. M., Avery, N. A., Fanton, J. W., and Axthelm, M. K. (1999). Induction of B cell hyperplasia in simian immunodeficiency virus-infected rhesus macaques with the simian homologue of Kaposi's sarcoma-associated herpesvirus. *J Exp Med* *190*, 827-840.
- Wu, H., Xu, H., Miraglia, L. J., and Crooke, S. T. (2000). Human RNase III is a 160-kDa protein involved in preribosomal RNA processing. *J Biol Chem* *275*, 36957-36965.
- Wu, L., Fan, J., and Belasco, J. G. (2006). MicroRNAs direct rapid deadenylation of mRNA. *Proc Natl Acad Sci U S A* *103*, 4034-4039.
- Xia, L., Zhang, D., Du, R., Pan, Y., Zhao, L., Sun, S., Hong, L., Liu, J., and Fan, D. (2008a). miR-15b and miR-16 modulate multidrug resistance by targeting BCL2 in human gastric cancer cells. *Int J Cancer* *123*, 372-379.
- Xia, T., O'Hara, A., Araujo, I., Barreto, J., Carvalho, E., Sapucaia, J. B., Ramos, J. C., Luz, E., Pedrosa, C., Manrique, M., *et al.* (2008b). EBV microRNAs in primary lymphomas and targeting of CXCL-11 by ebv-mir-BHRF1-3. *Cancer Res* *68*, 1436-1442.
- Yang, I. V., Wade, C. M., Kang, H. M., Alper, S., Rutledge, H., Lackford, B., Eskin, E., Daly, M. J., and Schwartz, D. A. (2009). Identification of novel genes that mediate innate immunity using inbred mice. *Genetics* *183*, 1535-1544.
- Yano, M., Hoogenraad, N., Terada, K., and Mori, M. (2000). Identification and functional analysis of human Tom22 for protein import into mitochondria. *Mol Cell Biol* *20*, 7205-7213.
- Yao, Q. Y., Croom-Carter, D. S., Tierney, R. J., Habeshaw, G., Wilde, J. T., Hill, F. G., Conlon, C., and Rickinson, A. B. (1998). Epidemiology of infection with Epstein-Barr virus types 1 and 2: lessons from the study of a T-cell-immunocompromised hemophilic cohort. *J Virol* *72*, 4352-4363.
- Yao, Y., Zhao, Y., Xu, H., Smith, L. P., Lawrie, C. H., Sewer, A., Zavolan, M., and Nair, V. (2007). Marek's disease virus type 2 (MDV-2)-encoded microRNAs show no sequence conservation with those encoded by MDV-1. *J Virol* *81*, 7164-7170.
- Yao, Y., Zhao, Y., Xu, H., Smith, L. P., Lawrie, C. H., Watson, M., and Nair, V. (2008). MicroRNA profile of Marek's disease virus-transformed T-cell line MSB-1: predominance of virus-encoded microRNAs. *J Virol* *82*, 4007-4015.
- Yekta, S., Shih, I. H., and Bartel, D. P. (2004). MicroRNA-directed cleavage of HOXB8 mRNA. *Science* *304*, 594-596.
- Yi, R., Poy, M. N., Stoffel, M., and Fuchs, E. (2008). A skin microRNA promotes differentiation by repressing 'stemness'. *Nature* *452*, 225-229.
- Yi, R., Qin, Y., Macara, I. G., and Cullen, B. R. (2003). Exportin-5 mediates the nuclear export of pre-microRNAs and short hairpin RNAs. *Genes Dev* *17*, 3011-3016.
- Young, L. S., Dawson, C. W., and Eliopoulos, A. G. (2000). The expression and function of Epstein-Barr virus encoded latent genes. *Mol Pathol* *53*, 238-247.
- Young, L. S., Yao, Q. Y., Rooney, C. M., Sculley, T. B., Moss, D. J., Rupani, H., Laux, G., Bornkamm, G. W., and Rickinson, A. B. (1987). New type B isolates of Epstein-Barr virus from Burkitt's lymphoma and from normal individuals in endemic areas. *J Gen Virol* *68 (Pt 11)*, 2853-2862.
- Yu, J., Ryan, D. G., Getsios, S., Oliveira-Fernandes, M., Fatima, A., and Lavker, R. M. (2008). MicroRNA-184 antagonizes microRNA-205 to maintain SHIP2 levels in epithelia. *Proc Natl Acad Sci U S A* *105*, 19300-19305.
- Yu, M. C., Ho, J. H., Henderson, B. E., and Armstrong, R. W. (1985). Epidemiology of nasopharyngeal carcinoma in Malaysia and Hong Kong. *Natl Cancer Inst Monogr* *69*, 203-207.
- Yu, M. C., and Yuan, J. M. (2002). Epidemiology of nasopharyngeal carcinoma. *Semin Cancer Biol* *12*, 421-429.
- Yu, X., Wang, Z., and Mertz, J. E. (2007). ZEB1 regulates the latent-lytic switch in infection by Epstein-Barr virus. *PLoS Pathog* *3*, e194.
- Zamore, P. D., Tuschl, T., Sharp, P. A., and Bartel, D. P. (2000). RNAi: double-stranded RNA directs the ATP-dependent cleavage of mRNA at 21 to 23 nucleotide intervals. *Cell* *101*, 25-33.
- Zeng, Y., and Cullen, B. R. (2003). Sequence requirements for micro RNA processing and function in human cells. *Rna* *9*, 112-123.
- Zeng, Y., and Cullen, B. R. (2004). Structural requirements for pre-microRNA binding and nuclear export by Exportin 5. *Nucleic Acids Res* *32*, 4776-4785.
- Zeng, Y., and Cullen, B. R. (2005). Efficient processing of primary microRNA hairpins by Drosha requires flanking nonstructured RNA sequences. *J Biol Chem* *280*, 27595-27603.
- Zeng, Y., Yi, R., and Cullen, B. R. (2003). MicroRNAs and small interfering RNAs can inhibit mRNA expression by similar mechanisms. *Proc Natl Acad Sci U S A* *100*, 9779-9784.
- Zeng, Y., Yi, R., and Cullen, B. R. (2005). Recognition and cleavage of primary microRNA precursors by the nuclear processing enzyme Drosha. *Embo J* *24*, 138-148.
- Zhang, C., Han, L., Zhang, A., Yang, W., Zhou, X., Pu, P., Du, Y., Zeng, H., and Kang, C. (2010). Global changes of mRNA expression reveals an increased activity of the interferon-induced signal transducer and activator of transcription (STAT) pathway by repression of miR-221/222 in glioblastoma U251 cells. *Int J Oncol* *36*, 1503-1512.

- Zhang, X., and Zeng, Y. (2010). The terminal loop region controls microRNA processing by Drosha and Dicer. *Nucleic Acids Res.*
- Zhang, Y. (2005). miRU: an automated plant miRNA target prediction server. *Nucleic Acids Res* 33, W701-704.
- Zhao, Q. Z., Zhao, S. Y., and Xia, G. M. (2005). [Research advances on the mechanism of RNA silencing in plants]. *Yi Chuan Xue Bao* 32, 104-110.
- Zhu, J. Y., Pfuhl, T., Motsch, N., Barth, S., Nicholls, J., Grasser, F., and Meister, G. (2009). Identification of novel Epstein-Barr virus microRNA genes from nasopharyngeal carcinomas. *J Virol* 83, 3333-3341.
- Ziegelbauer, J. M., Sullivan, C. S., and Ganem, D. (2009). Tandem array-based expression screens identify host mRNA targets of virus-encoded microRNAs. *Nat Genet* 41, 130-134.
- Zimber, U., Adldinger, H. K., Lenoir, G. M., Vuillaume, M., Knebel-Doeberitz, M. V., Laux, G., Desgranges, C., Wittmann, P., Freese, U. K., Schneider, U., and et al. (1986). Geographical prevalence of two types of Epstein-Barr virus. *Virology* 154, 56-66.
- Zimmermann, J., and Hammerschmidt, W. (1995). Structure and role of the terminal repeats of Epstein-Barr virus in processing and packaging of virion DNA. *J Virol* 69, 3147-3155.
- zur Hausen, H., Fresen, K. O., and Bornkamm, G. W. (1978). Epstein-Barr virus genomes and their biological functions: a review. *IARC Sci Publ*, 3-10.

8. Appendix

8.1. Safety-related Data

Table 8-1 R and S clauses for chemicals

Substance	Danger Symbol	R-Clause	S-Clause
2-Mercaptoethanol	T, N	R 20/22-24-34-51/53	S 26-36/37/39-45-61
2-Propanol	F,xi	R 10-36/38-67	S 7-16-24/25-26-36/37
p-Coumaric acid	Xi	R 36/37/38	S 26-36
Acetone	F,xi	R 11-36-66-67	S 9-16-26
Acetonitrile	F,xn	R 11-20/21/22-36	S 16-36/37
Acrylamid	T	R 45-46-20/21-25-36/38-43-48/23/24/25-62	S 53-26-36/37-45
Ampicillin	Xn	R 36/37/38-42/43	S 22-26-36/37
Ammonium persulfate (APS)	Q,xn	8-22-36/37/38-42/43	S 22-24-26-37
Bisacrylamid	Xn	R 22-20/21/22	S 24/25-36/37
Boric acid	T	R 60-61	S 53-45
Bromophenol Blue			S 22-24/25
Calcium chloride (CaCl ₂)	Xi	R 36	S 22-24
Chloroform	F,xn	R 11-22-36/38-40-48/20/22-66-67	S 9-16-26-36
Diethyl pyrocarbonate (DEPC)	Xn	R 22-36/37/38	S 26-36
N,N-Dimethylformamide	T	R 61-20/21-36	S 53-45
DL-Dithiothreitol (DTT)	Xn	R 22-36/37/38	S 26-36
Ethylendiaminetetraacetic acid (EDTA)	Xi	R 36-52/53	S 26-61
Glacial acetic acid	C	R 10-35	S 23-26-45
Ethanol	F	R 11	S 7-16
Ethidium bromide solution 10 mg/ml	T	R 23-68	S 36/37-45
Formaldehyde	T	R 23/24/25-34-39/23/24/25-40-43	S 26-36/37/39-45-51
Formamide	T	R 61	S 53-45
Glycin			S 22-24/25
Hydrochloric acid 37%	C	R 34-37	S 26-36/37/39-45
Hydrogen peroxide solution 30%	Xn	R 22-41	S 26-39
Isoamyl alcohol	Xn	R 10-20-37-66	S 46
Isopropyl-β-D-thio-galactopyranoside (IPTG)			S 22-24/25
Kanamycinsulfate	T	R 61	S 45-36/37/39
Luminol	Xi	R 36/37/38	S 26-36/37
Methanol	F, T	R 11-23/24/25-39/23-24/25	S 7-16-36/37-45
Magnesium chloride (MgCl ₂)			S 22-24/25
MgSO ₄			S 22-24/25
MOPS	Xi	R 36/37/38	S 26-36
N,N,N',N'-Tetramethylethylenediamine	F, C	R 11-20/22-34	S 16-26-36/37/39-45
Neomycin sulfate (G418)	T,xi	R 63-42/43-36 37/38	S 45-26-36/37/39
Neomycin sulfate	Xn	R 42/43	S 22-36/37-45
Nonidet™ P 40 Substitute	Xi	R 37-41	S 26-39
2-Nitrophenyl β-D-galactopyranoside (ONPG)			S22-24/25
Penicillin	Xn	R 42/43	S 22-36/37-45
Phenol	T, C	R 23/24/25-34-48/20/21/22-68	S 24/25-26-28-36/37/39-45
Polyethylenimine (PEI)	Xi	R 36/37/38	S 26-36
Potassium chloride			S 22-24/25
Proteinase K	Xn	R 36/37/38-42	S 22-24-26-36/37
Rubidium chloride (RbCl ₂)			S 22-24/25
Sodium azide	T+, N	R 28-32-50/53	S 28-45-60-61
Sodium acetate			S 22-24/25

Appendix

Sodium carbonate	Xi	R 36	S 22-26
Sodium dodecyl sulfate	F, xn	R 11-21/22-36/37/38	S 26-36/37
Sodium hydroxide	C	R 35	S 26-37/39-45
Streptomycin	Xn	R 22	
Trichloroacetic acid	C, N	R 35-50/53	S 26-36/37/39-45-60-61
Triton [®] X-100	Xi; N	R 22-41-51/53	S 26-36/39-61
TRIS base	Xi	R 36	S 26
Trypan blue	T	R 45	S 53-45
Trypsin	Xn	R 36/37/38-42	S 22-24-26-36/37
Xylene cyanol	Xi	R 36/37/38	S 26-36

8.4. Supplementary Table 1

Overlap of Regulated Genes Derived from DNA Microarrays

DNA microarrays were analyzed with Genepix software and filtered for genes, that are down-regulated in all setups and above a threshold of 1x stdv. Shown are genbank number and gene names. Genes that were further analyzed in luciferase reporter assays are highlighted in red (shown in this work) or in yellow (under investigation).

Overlap Epithelial Arrays		Overlap BJAB Arrays	
Genbank	Gene Name	Genbank	Gene Name
A_23_P255111	A_23_P255111	A_24_P255865	A_24_P255865
A_23_P255111	A_23_P255111	A_24_P552987	A_24_P552987
NM_004346	CASP3	NM_138764	BAX
NM_001753	CAV1	NM_003766	BECN1
ENST00000310773	ENST00000310773	BF869497	BF869497
NM_001315	MAPK14	BC011905	C15orf39
NM_005109	OXR1	NM_001039476	C16orf35
NM_000430	PAFAH1B1	NM_032587	CARD6
NM_001002811	PDE4DIP	NM_024296	CCDC28B
NM_002710	PPP1CC	NM_024098	CCDC86
NM_000944	PPP3CA	NM_058197	CDKN2A
NM_007173	PRSS23	NM_005507	CFL1
NM_006861	RAB35	NM_001326	CSTF3
NM_002950	RPN1	NM_001970	EIF5A
NM_005063	SCD	ENST00000318251	ENST00000318251
NM_001018067	SERBP1	NM_001005862	ERBB2
NM_005901	SMAD2	NM_013986	EWSR1
NM_001015892	TAF9	NM_001002901	FCRLM2
NM_003211	TDG	NM_080920	GGTLA4
NM_006287	TFPI	NM_133644	GTPBP3
NM_030755	TXNDC	NM_002109	HARS
		NM_003325	HIRA
		NM_000190	HMBS
		NM_153201	HSPA8
		NM_006546	IGF2BP1
		NM_176799	ILKAP
		NM_033453	ITPA
		NM_001033602	KIAA0774
		NM_017794	KIAA1797
		NM_015907	LAP3
		NM_005574	LMO2
		NM_181708	LOC144233
		NM_001010856	LOC147804
		NM_175063	LOC284361
		NM_032331	MGC2408
		NM_032355	MON1A
		NM_021107	MRPS12
		NM_003469	MX1
		NM_002467	MYC
		NM_005008	NHP2L1
		NM_006187	OAS3
		NM_002598	PDCD2
		NM_002695	POLR2E
		NM_001018051	POLR3H
		NM_000942	PP1B
		NM_000310	PPT1
		NM_005155	PPT2
		CR611847	PTRH1
		NM_006861	RAB35
		NM_015169	RRS1
		NM_003104	SORD
		NM_139266	STAT1
		NM_004710	SYNGR2
		NM_153649	TPM3
		NM_017735	TTC27
		NM_016505	ZCCHC17

8.5. Supplementary Table 2

Regulated Genes Derived from HNEpC DNA Microarrays

DNA microarrays were analyzed with Genespring GX10 software and filtered for genes, that are at least 1.2 fold down-regulated. Shown are genbank number and gene names. Genes that were further analyzed in luciferase reporter assays are highlighted in red (shown in this work) or in yellow (under investigation).

Genbank	Gene Name	Fold Regulation (down)	Genbank	Gene Name	Fold-Regulation (down)	Genbank	Gene Name	Fold Regulation (down)
NM_005159	ACTC1	18.007912	NM_001013398	IGFBP3	1.6878109	AI650707	AI650707	1.3851514
NM_201630	LRRN2	13.881205	NM_007220	CA5B	1.6767362	NM_000496	CRYBB2	1.3848639
NM_001008657	TCOF1	13.309102	ENST00000307366	MGC3196	1.6739197	NM_019037	EXOSC4	1.3842933
AK023827	RUNDC2B	11.847417	NM_003481	USP5	1.6735842	XR_015124	LOC730433	1.3812503
NM_178012	TUBB2B	9.338816	NM_032560	SMEK1	1.6723304	NM_145698	ACBD5	1.3810787
ENST00000380310	ENST00000380310	7.754641	NM_033518	SLC38A5	1.6710845	ENST00000379855	ENST00000379855	1.3803896
CB123670	CB123670	7.44589	NM_032373	PCGF5	1.6683607	NM_016573	GMIP	1.3797983
NM_002854	PVALB	6.851155	A_32_P196142	A_32_P196142	1.6681442	AB015331	BMP2K	1.379785
NM_003277	CLDN5	6.388837	NM_152903	KBTBD6	1.6666337	NM_015317	PUM2	1.3793787
AK094748	AK094748	6.221141	NM_138962	MSI2	1.6642671	ENST00000373457	ZBTB43	1.3791336
NM_018712	ELMOD1	5.8818564	NM_000366	TPM1	1.659177	NM_018049	PLEKHJ1	1.3750577
NM_017414	USP18	5.344877	NM_001664	RHOA	1.6584412	NM_177533	NUDT14	1.374268
NM_001613	ACTA2	4.9521856	NM_032207	C19orf44	1.6574916	NM_005321	HIST1H1E	1.3732089
NM_014061	MAGEH1	4.888273	NM_002372	MAN2A1	1.6562303	NM_015566	SIPA1L1	1.3730985
NM_020478	ANK1	4.865342	NM_012458	TIMM13	1.6554468	NM_052865	C20orf72	1.3723218
NM_006558	KHDRBS3	4.6062603	NM_001080510	LOC124512	1.6529584	NM_014765	TOMM20	1.3718469
M74509	M74509	4.5365987	NM_199329	SLC43A3	1.6521091	NM_003131	SRF	1.3709229
NM_002429	MMP19	4.31681	NM_032325	MGC11102	1.6510795	NM_032831	TMEM142B	1.3670186
NM_003004	SECTM1	4.163174	NM_001664	RHOA	1.6459731	A_24_P101503	A_24_P101503	1.3666827
NM_024312	GNPTAB	3.975226	NM_138493	C6orf129	1.6456369	NM_00102234	SCN1M1	1.366586
NM_001008495	TMEM64	3.908164	NM_022774	C1orf176	1.644139	NM_015528	RNF167	1.3659976
NM_006379	SEMA3C	3.5738974	NM_018167	BTBD7	1.6427159	NM_001780	CD63	1.3652728
NM_003528	HIST2H2BE	3.5338736	AK021933	AK021933	1.6389657	A_32_P46351	A_32_P46351	1.362479
AK023048	FLJ12986	3.5088527	BC036645	BC036645	1.6377323	NM_025182	KIAA1539	1.3624166
NM_001976	ENO3	3.4420066	BX117168	BX117168	1.6352074	NM_002128	HMG1	1.3618342
NM_172244	SGCD	3.4112227	NM_206949	FAM14B	1.6332104	NM_004640	BAT1	1.3616629
NM_002514	NOV	3.380341	NM_006607	PTTG2	1.6330065	NM_080430	SELM	1.3615686
AL833294	SYNPO2	3.3315756	AL035301	PIGC	1.6322519	NM_032823	C9orf3	1.3615217
NM_014391	ANKRD1	3.3225129	THC2675272	THC2675272	1.631937	AF075027	AF075027	1.3599782
NM_015393	DKFZP564O0823	3.2971947	NM_080425	GNAS	1.6317536	NM_002526	NF05	1.3593208
NM_021020	LZTS1	3.1965096	XR_016822	LOC645251	1.6281431	AK024934	KIAA1641	1.3586413
NR_003127	ZNF542	3.156974	NM_015120	ALMS1	1.6271094	NM_002480	PPP1R12A	1.3576643
CR601496	CR601496	3.038592	NM_014836	RHOBTB1	1.6235399	ENST00000371008	SLC35D1	1.3575562
AL832817	AL832817	3.0361729	NM_022765	MICAL1	1.6195868	NM_005610	RBBP4	1.3572139
ENST00000366930	TGFB2	3.0153136	NM_013974	DDAH2	1.6182835	A_24_P32735	A_24_P32735	1.3567922
BX097190	BX097190	2.9986663	NM_177439	FTSJ1	1.6182779	NM_144573	NEXN	1.3565482
AF086011	AF086011	2.9887938	NM_032627	SSBP4	1.6116773	NM_015544	TMEM98	1.3558217
A_24_P928993	A_24_P928993	2.9511812	NM_032591	SLC9A7	1.6115023	BC004943	MGC10814	1.3556331
THC2504565	THC2504565	2.9313252	NM_017813	IMPAD1	1.6112357	NM_033224	PURB	1.3554832
BC030118	BC030118	2.8792257	NM_005858	AKAP8	1.6069949	NM_006559	KHDRBS1	1.3551273
NM_015359	MKS3	2.867459	NM_021103	TMSB10	1.6039145	NM_021210	TRAPPC1	1.3548559
NM_138659	C6orf142	2.7808332	AK001998	AK001998	1.6035681	NM_032226	ZCCHC7	1.3537991
NM_147161	ACOT11	2.759855	NM_020987	ANK3	1.6034021	NM_032593	HINT2	1.353171
THC2642537	THC2642537	2.757246	NM_008661	RAB35	1.6010522	BC009264	LOC151534	1.3498931
NM_138689	PPP1R14B	2.719817	NM_004309	ARHGDI1A	1.6003542	NM_004120	GBP2	1.3485887
NM_003211	TDG	2.7103693	XR_019552	LOC652912	1.6000625	NM_014994	MAPKBP1	1.3468289
ENST00000310773	ENST00000310773	2.7044902	AK123679	AK123679	1.5996326	NM_017828	COMMD4	1.3450551
NM_00101522	TAGLN	2.690072	NM_004514	FOXK2	1.5991278	THC2571921	THC2571921	1.3449395
ENST00000256367	TTC9	2.672882	NM_030925	CAB39L	1.597295	NM_021168	RAB40C	1.3414475
THC2687538	THC2687538	2.6404028	AK024926	AK024926	1.5923767	NR_003192	SNHG8	1.3399222
NM_015455	CNO16	2.6325932	NM_017614	BHMT2	1.5908396	NM_001008735	HMG1L1	1.3392429
NM_003211	TDG	2.590372	NM_006749	SLC20A2	1.5903323	NM_017934	PHIP	1.3389907
NM_022648	TNS1	2.5549319	ENST00000285605	ENST00000285605	1.5893512	NM_183057	VPS28	1.3386146
A_24_P827738	A_24_P827738	2.5346673	THC2538067	THC2538067	1.5881617	NM_022085	TXNDC5	1.3367121
NM_001823	CKB	2.5177937	NM_001014979	LOC90835	1.5840029	NM_001014999	GlyD1	1.3343345
NM_000337	SGCD	2.5133545	NM_121551	LYSMD1	1.582391	NM_003011	SET	1.3324436
NM_003739	AKR1C3	2.4814255	NM_033215	PPP1R3F	1.5804027	ENST00000360524	LOC731479	1.3322256
NM_006482	DYRK2	2.4747307	AK094772	FLJ37453	1.5760376	ENST00000367846	BRP44	1.3300837
NM_033300	LRP8	2.4403982	NM_003004	SECTM1	1.5748236	NM_001024457	RGPD1	1.3256427
NM_014757	MAML1	2.4291239	NM_020062	SLC2A4RG	1.5686668	NM_001261	CDK9	1.3230965
NM_001080416	MYBL1	2.4273994	THC2651023	THC2651023	1.5626724	NM_080678	UBE2F	1.3216109
THC2519484	THC2519484	2.39308	NM_004313	ARRB2	1.5621392	NM_005706	TSSC4	1.3202213
NM_003246	THBS1	2.389389	NM_002546	TNFRSF11B	1.5592631	NM_006003	UQCRF51	1.3185529
AK002023	AK002023	2.3788908	AL117621	AL117621	1.5588782	NM_015665	AAAS	1.3141003
NM_016448	DTL	2.3617465	NM_003532	HIST1H3E	1.5568016	NM_173354	SNF1LK	1.3134011
NM_019044	ELP4	2.3544584	NM_002507	NGFR	1.5540332	NM_016488	TMEM69	1.3124323
NM_181847	AMIGO2	2.3512805	NM_183050	BCKDHB	1.5501117	NM_032937	C9orf37	1.3116957
NM_004933	CDH15	2.2982082	BC067871	LOC150383	1.5423994	NM_002310	LIFR	1.3099576
NM_005864	EPS	2.2776532	NM_016277	RAB23	1.5411509	NM_198576	AGRN	1.3094859
AK022059	AK022059	2.2553976	NM_006808	PHTF1	1.5379193	NM_153256	C10orf47	1.3079104
NM_001953	ECGF1	2.2483954	NM_006820	IF144L	1.5361255	NM_178037	ERC1	1.3075504
CD511705	CD511705	2.2447536	NM_001014764	TMEM93	1.5356985	NM_001567	INPPL1	1.3069161
NM_003211	TDG	2.235747	NM_002107	H3F3A	1.5340635	NM_025124	TMEM134	1.3051686
NM_006674	HCP5	2.2254922	NM_007175	ERLIN2	1.5297203	NM_004068	AP2M1	1.3038846
AK057740	AK057740	2.215729	NM_002950	RPN1	1.5276407	BC112973	BC112973	1.3026346
CF124646	CF124646	2.1879597	NM_017567	NAGK	1.5199846	NM_022103	ZNF667	1.3019791
THC2603732	THC2603732	2.1878145	THC2613107	THC2613107	1.5199556	NM_004629	FANCG	1.2998365
NM_005253	FOSL2	2.1850502	NM_004356	CD81	1.5198873	NM_004606	TAF1	1.2986594
NM_016091	EIF3S6IP	2.1702378	AL136736	KIAA1549	1.5198538	NM_024595	C1orf108	1.2980042
NM_198401	ANKRD46	2.1696043	THC2597357	THC2597357	1.5194887	NR_002933	LOC493754	1.2965322
AK054902	AK054902	2.1673284	NM_016587	CBX3	1.5175767	NM_001005291	SREBF1	1.2964299
NM_030929	KAZALD1	2.1592052	NM_001011515	PDLIM5	1.5171905	NM_145290	GPR125	1.2949516
NM_006674	HCP5	2.132715	THC2689749	THC2689749	1.5162704	BID03432	BID03432	1.2949058
NM_001001415	ZNF429	2.1192405	NM_002317	LOX	1.5142559	NM_201434	RAB5C	1.293422
NM_001007553	CSDE1	2.1032917	AL832783	LMLN	1.507477	NM_003944	DYSF	1.2911243
BG327427	BG327427	2.1030827	NM_006915	RP2	1.5072109	NM_016479	SCOTIN	1.2909013
NM_152742	GPC2	2.0944972	NM_174910	TCF3	1.5059662	A_24_P24230	A_24_P24230	1.2904181
NM_001001522	TAGLN	2.088888	NM_004155	SERPINB9	1.5050279	NM_016145	C19orf56	1.2901534
NM_206827	SYTL2	2.0853767	NM_022098	FN1	1.5019478	NM_054016	FUSP1	1.2900256
NM_178830	C19orf47	2.0823958	NM_004317	XPNPEP3	1.5015475	ENST00000381655	ENST00000381655	1.2877952
BC066852	ACYP2	2.0823753	NM_006827	ASNA1	1.501281	NM_018973	DPM3	1.2864629
AK021980	AK021980	2.081175	NM_002040	TMED10	1.4994353	BC042539	LOC442421	1.2862551
NM_020731	AHRR	2.0732262	XR_016752	GABPA	1.4991155	A_23_P72330	A_23_P72330	1.2855799
NM_013305	ST8SIA5	2.06796	NM_005184	LOC644651	1.498126	NM_001679	AT1B3	1.285093
NM_173872	CLCN3	2.0637033	NM_006475	CALM3	1.4963969	NM_004859	CLTC	1.2836305
THC2575678	THC2575678	2.063389	NM_001425	POSTN	1.493969	NM_177559	CSNK2A1	1.2824707
				EMP3	1.493115	NM_145261	DNAJC19	1.2817637

BC018086	MGC13017	2.0629175	NM 002107	H3F3A	1.4912753	NM 152736	ZNF187	1.2794946
NM 005689	ABC66	2.0607903	NM 019607	C8orf44	1.4890314	NM 024537	CARS2	1.2784231
XR 016196	LOC642652	2.0501173	NM 003196	TCEA3	1.4887308	NM 002812	PSMD8	1.2783915
NM 005382	NEFM	2.046952	BM129308	BM129308	1.4884369	NM 003429	ZNF85	1.2774656
NM 138689	PPP1R14B	2.044391	NM 080678	UBE2F	1.488073	NM 174891	C14orf79	1.2771204
NM 145201	NPART1	2.03516	NM 152726	EFHA1	1.4879869	NM 152407	GRPEL2	1.2766935
NM 015999	ADIPOR1	2.0171876	ENST00000332101	ENST00000332101	1.4856168	NM 138799	MBOAT2	1.2766589
NM 181643	C1orf88	2.0107348	AK094159	FLJ36840	1.4855459	NM 007214	SEC63	1.2746094
BQ071182	BQ071182	2.0100777	NM 007169	PEMT	1.4852701	NM 198794	MWAP45	1.2728791
NM 001221	CAMK2D	2.005298	NM 002128	HMG1B1	1.4843673	NM 020243	TOMM22	1.2725484
NM 000660	TGFB1	2.0052278	NM 152409	C5orf24	1.4819937	NM 033200	TMEM112B	1.2714876
NM 017980	LIMS2	1.9965395	NM 020198	CCDC47	1.479477	NM 012200	B3GAT3	1.2709302
NM 152399	TMEM155	1.9962537	THC2558699	THC2558699	1.4750572	NM 014284	NCDN	1.2707301
BC033127	C4orf12	1.9946331	NM 002513	NME3	1.4747623	NM 021159	RAP1GDS1	1.2701893
NM 020433	JPH2	1.992491	NR 002807	TMED10P	1.4740455	NM 003498	SNN	1.2700337
NM 032348	MXRA8	1.9766691	NM 020428	SLC44A2	1.4733227	NM 152267	RNF185	1.2688055
NM 002871	RAB1F	1.9693686	NM 006111	ACAA2	1.4722551	NM 001039650	ZMYM5	1.2654338
NM 016147	PPME1	1.9670216	NM 022346	NCAPG	1.4697887	NM 006373	VAT1	1.264197
NM 032440	LCOR	1.9551027	AL832059	Sep 13	1.46917	NM 152574	C8orf52	1.2617489
THC2501739	THC2501739	1.9517038	A 24 P16291	A 24 P16291	1.4686108	NM 005674	ZNF239	1.2615555
NM 005628	SLC1A5	1.9507275	BC009364	TOE1	1.4665316	ENST00000278505	ENDOD1	1.2612162
A 24 P76210	A 24 P76210	1.9391563	NM 005600	NIT1	1.4656568	NM 214710	PRSSL1	1.2601863
THC2753400	THC2753400	1.9383483	XR 018867	LOC650440	1.4644215	NM 006003	UCRFS1	1.2601599
NM 004717	DGKI	1.9340973	NM 148912	ABHD11	1.4636477	NM 000075	CDK4	1.2598392
A 24 P775812	A 24 P775812	1.928502	NM 006807	CBX1	1.4610976	NM 173852	KRTCAP2	1.2589363
NM 032483	PPAPDC1B	1.9199312	NM 002796	PSMB4	1.4601377	XR 015322	LOC730556	1.2577206
NM 005225	EZF1	1.9189113	NM 004656	BAP1	1.4598616	CN272797	CN272797	1.2570897
THC2542546	THC2542546	1.9155598	NM 013986	EWSR1	1.45917	NM 203330	CD59	1.2570636
NM 057159	EDG2	1.908272	NM 022873	IFI6	1.4588512	NM 006826	YWHAQ	1.255897
H15635	H15635	1.9042927	BQ072652	BQ072652	1.4582803	NM 052873	C14orf179	1.2554811
NM 012216	MID2	1.903979	AK021784	C15orf28	1.4576057	AK097411	FLJ40092	1.2517556
XM 946374	LOC654342	1.9030082	NM 006556	PMVK	1.4569839	NM 010780	CD63	1.2506992
NM 006888	CALM1	1.8992136	NM 017760	NCAPG2	1.4561815	NM 206833	CTXN1	1.2479441
NM 006080	SEMA3A	1.8930424	AI084055	AI084055	1.4558679	NM 003507	FZD7	1.2468201
AK026131	AK026131	1.8903996	AX721128	AX721128	1.4553112	NM 005005	NDFUFB9	1.2467935
NM 006459	ERLIN1	1.8862203	NM 021913	AXL	1.4552027	AK098134	AK098134	1.2461145
THC2724046	THC2724046	1.8861808	AL713796	LOC389831	1.4546782	NM 002791	PSMA6	1.2451414
NM 003969	UBE2M	1.8701481	NM 005620	S100A11	1.4546627	NM 001281	TBCB	1.2431103
NR 002837	UBE2MP1	1.8579308	NM 024038	C19orf43	1.4543234	THC2726401	THC2726401	1.2430105
NM 032476	MRP56	1.8475903	XR 015796	LOC732268	1.4528949	NM 018049	PLEKHJ1	1.2423595
NM 006107	CROP	1.8453441	AF307448	CECR4	1.4504137	NM 017626	DNAJB12	1.2421218
AK025721	DDX52	1.8445623	NM 004609	TCF15	1.450065	NM 005078	TE3	1.2403799
THC2685750	THC2685750	1.8376415	NM 000933	PLCB4	1.4467584	NM 002128	HMG1B1	1.239674
NM 005966	NAB1	1.8318725	BC071773	BC071773	1.4457935	NM 032374	C14orf153	1.2356464
NM 198440	DERL3	1.8282814	NM 005034	POLR2K	1.4450747	NM 032193	RNASEH2C	1.2351347
NM 024734	CLMN	1.8270723	NM 006335	TIMM17A	1.4396602	NM 014970	KIFAP3	1.2347152
AK092083	AK092083	1.8131789	NM 004729	ZBED1	1.439202	NM 005544	IRS1	1.2338821
NM 001975	ENO2	1.8126607	NM 001743	CALM2	1.4388534	NM 006284	TAF10	1.2335196
NM 003139	TCF4	1.8095328	NM 004111	FEN1	1.438829	NM 004788	UBE4A	1.2323196
NM 001418	EIF4G2	1.8065978	AK095607	ZNF776	1.4338362	NM 032786	ZC3H10	1.2306714
NM 001980	STX2	1.7959285	NM 002634	NVL	1.4335887	NM 002791	PSMA6	1.2301501
NM 018084	KIAA1212	1.7950632	NM 003134	SRP14	1.4321573	NM 032349	NUDT16L1	1.2286622
NM 012137	DDAH1	1.7912968	NM 015379	BRIS	1.4305478	NM 021163	RBAK	1.2255745
NM 022455	NSD1	1.7849886	NM 002201	ISG20	1.4303824	NM 018061	PRPF38B	1.2245369
NM 005506	SCARB2	1.780352	NM 005399	PRKAB2	1.4289649	ENST00000288911	ENST00000288911	1.2236309
THC2701372	THC2701372	1.7751065	NM 004219	PTTG1	1.424308	NM 003400	XPO1	1.2236274
NM 000582	SPP1	1.774633	NM 014584	ERO1L	1.4240211	NM 006640	Sep 09	1.2228316
NM 152353	SIPA1	1.7717806	NM 014743	KIAA0232	1.4236758	NM 015392	NPDC1	1.2227292
NM 199188	LARP4	1.764809	NM 032632	PAPOLA	1.4222667	NM 025235	TNKS2	1.2226024
NM 018956	C9orf9	1.7619617	NM 153461	IL17RC	1.4210732	NM 001013845	CXorf40B	1.2223457
NM 001012754	RP11-50D16.3	1.7550852	BC062473	BC062473	1.4194739	NM 004520	KIF2A	1.2220706
NM 001845	LOC4A1	1.7533946	NM 033133	CNP	1.418218	NM 018048	FLJ10292	1.22167
NM 001040078	LOC654346	1.7471955	AI344752	AI344752	1.4179772	AF292100	DCUN1D1	1.221318
AI936672	AI936672	1.746398	AK098256	LOC728723	1.4168087	XR 018803	LOC649915	1.2170353
NM 020428	SLC44A2	1.7412723	NM 004491	GRFL1	1.4118034	THC2540738	THC2540738	1.2167537
THC2727205	THC2727205	1.7392979	AL049447	AL049447	1.4115882	BG208131	BG208131	1.2141956
NM 001033	RRM1	1.737849	NM 199050	C21orf25	1.4113652	NM 014948	UBOX5	1.2139723
BC033590	BC033590	1.7366854	AB017007	PMS2L2	1.4111711	NM 032316	NICN1	1.2138565
NM 005407	SALL2	1.7344108	A 32 P128399	A 32 P128399	1.4098954	NM 018064	C6orf166	1.2126775
NM 031934	RAB34	1.7323625	NM 014302	SEC61G	1.4098481	NM 025010	KLHL18	1.2126601
NM 172037	RDH10	1.7301909	NM 152415	VPS37A	1.4088414	NM 201575	SEZ6L2	1.2110176
NM 018566	YOD1	1.7284127	NM 024120	C20orf7	1.4073912	NM 005005	NDFUFB9	1.2102737
AF092095	HTATIP2	1.7282436	NM 172171	CAMK2G	1.4072312	NM 017883	WDR13	1.2102126
NM 020374	C12orf4	1.7157396	NM 138286	ZNF681	1.4068414	BC067244	BC067244	1.2086201
NM 001481	GAS8	1.7135366	NM 003377	VEGFB	1.4067777	AW467174	AW467174	1.2083391
ENST00000369562	C6orf165	1.7129242	NM 203473	PORCN	1.4024283	BC062368	LOC152217	1.2082741
THC2499508	THC2499508	1.7107896	NM 000023	SGCA	1.4023188	NM 016073	HDFFRP3	1.2064381
NM 173546	KLHDC8B	1.7086718	NM 012338	TSPAN12	1.400876	NM 007273	PHB2	1.2045327
NM 080797	DIDO1	1.7080722	BC067830	LOC653391	1.3954026	NM 016456	TMEM9	1.2040309
NM 032476	MRP36	1.7059143	NR 003273	SRP14P1	1.3946575	BC051368	BC051368	1.203762
NM 024075	TSEN34	1.7042263	A 24 P480464	A 24 P480464	1.3935097	NM 030578	MGC4093	1.202964
NM 006466	POLR3F	1.6972085	NM 032423	ZNF528	1.3933187	NM 032121	RP11-217H1.1	1.202462
NM 032639	PLEKHA8	1.6964449	A 24 P279760	A 24 P279760	1.3885108	AK091483	LOC339778	1.2017461
NM 014363	SACS	1.6942294	DB451431	DB451431	1.3883749	NM 005159	ACTC1	1.8007912
NM 001394	DUSP4	1.693187	NM 175910	ZNF493	1.3870609	NM 201630	LRRN2	1.881205
NM 002800	PSMB9	1.6931696	NM 017588	WDR5	1.3867426	NM 001008657	TCOF1	1.309102
NM 001101	ACTB	1.6901766	NM 020353	PLSCR4	1.3861562	AI650707	AI650707	1.3851514
NM 032348	MXRA8	1.6895443	NM 002489	NDUFA4	1.3856694	NM 000496	CRYBB2	1.3846639
NM 005159	ACTC1	1.8007912	NM 001013398	IGFBP3	1.6878109	NM 019037	EXOSC4	1.3842933
NM 201630	LRRN2	1.881205	NM 007220	CA5B	1.6767362	XR 015124	LOC730433	1.3812503
NM 001008657	TCOF1	1.309102	ENST00000307366	MGC3196	1.6739197	NM 145698	ACBD5	1.3810787
AK023827	RUNDC2B	1.1847417	NM 003481	USP5	1.6735842	ENST00000379855	ENST00000379855	1.3803896
NM 178012	TUBB2B	9.338816	NM 032560	SMEK1	1.6723304	NM 016573	GMIP	1.3797983
ENST00000380310	ENST00000380310	7.754641	NM 033518	SLC38A5	1.6710845	AB015331	BMP2K	1.379785
CB123670	CB123670	7.44589	NM 032373	PCGF5	1.6683607	NM 015317	PUM2	1.3793787
NM 002854	PVALB	6.851155	A 32 P196142	A 32 P196142	1.6681442	ENST00000373457	ZBTB43	1.3791336
NM 003277	CLDN5	6.388837	NM 152903	KBTD6	1.6656337	NM 018049	PLEKHJ1	1.3750577
AK094748	AK094748	6.221141	NM 138962	MSI2	1.6642671			
NM 018712	ELMOD1	5.8818564	NM 000366	TPM1	1.659177			

9. Acknowledgment

First and foremost I would like to express my gratitude to Dr. Adam Grundhoff for the opportunity to perform this doctoral thesis in his lab. Furthermore, I would like to thank him for his ideas, support and fruitful discussions as well as the relaxed atmosphere. It is a pleasure to work in this group.

I would like to thank Prof. Deppert for the supervision of the work on behalf of the Heinrich-Pette-Institute and the University of Hamburg, as well as Prof. Hahn for his willingness to review this thesis.

I would like to say a big thank you to everyone from AG75 (Thomas Günther, Christine Henning, Thomas Christalla, Uwe Tessmer, Philipp Schult, Ina Kowalski and Sophie Borchert) for their support in the lab, helpful discussions and a lot of fun in the lab and after work and last but not least for listening to all kinds of problems - you are gorgeous. My special thanks go to Uwe Tessmer for his great support with many experiments.

Furthermore I would like to thank Peter Groitl (Laboratory of Prof. Dobner) and Ina Kowalski (Diploma Student in our lab) for their help in establishing adenoviruses. In addition, I would like to thank Dr. Nicole Fischer and her lab for good collaboration. Kristin Stieler I thank for many nice evenings on diverse congresses and after work.

I would like to express my gratitude to Uwe, Thomas, Christine, Kristin, Sophie and Benni for reading and correcting the manuscript. My special thanks go to Dr. Carol Stocking and in particular Sarah Kinkley for correcting my english grammar.

Isabel Unterstrasser I would like to thank for the great time during our studies and the lasting friendship, although she moved away as far as possible in germany.

I would like to thank my friends, especially Vanessa Lange, Jennifer Lübbke and Cora Karg for their support in everyday live.

I thank Dr. Benjamin Dälken for his steadfast optimism and his support.

Last but not least, I would like to thank my parents who have always believed in me and have supported me all the time. This work is dedicated to them.

Curriculum Vitae

Personal Details

Name: Nicole Walz
Date of Birth: 27.01.82
Place of Birth: Saarbrücken
Nationality: German

Education

Since 09/2006: PhD Thesis, Heinrich-Pette-Institute, Hamburg,
Junior Research Group of Dr. Adam Grundhoff: Identification and
Analysis of microRNAs encoded by γ -Herpesviruses

11/2005 - 05/2006: Diploma Thesis Georg-Speyer-Haus, Frankfurt am Main, Group of
Dr. Ursula Dietrich: Genetic and biologic characterization of HIV-1
viruses derived from non-progressing HIV-positive patients

2001 - 2006: Studies in Biochemistry,
Johann-Wolfgang-Goethe University, Frankfurt am Main

Practical courses:

06 - 07/2005 Sanofi-Aventis, Frankfurt,
Group of Dr. Günter Müller:
Lipid Metabolism
02 - 03/2005 Research Centre Borstel,
Group of Dr. Frey: Mucosa Immunology
06 - 07/2004 Johann-Wolfgang-Goethe University,
Group of Prof. Dr. Robert Tampé:
Characterization of human
ribonuclease L inhibitor (RLI)

2001: General Qualification for University Entrance,
Secondary School Dörpsweg, Hamburg

Publications, Presentations and Awards

Publications:

Walz N, Tessmer U, Wong S, Grundhoff A.; JMHV and RRV encoded miRNAs share extensive sequence conservation.; Manuscript in preparation

Hildebrand J, Rütze M, Walz N, Gallinat S, Wenck H, Deppert W, Grundhoff A, Knott A.; A comprehensive analysis of microRNA expression during human keratinocyte differentiation in vitro and in vivo.; *J Invest Dermatol.* 2010 Sep 9. [Epub ahead of print]

Seto E, Moosmann A, Grömminger S, Walz N, Grundhoff A, Hammerschmidt W.; Micro RNAs of Epstein-Barr virus promote cell cycle progression and prevent apoptosis of primary human B cells.; *PLoS Pathog.* 2010 Aug 19;6(8).

Walz N, Christalla T, Tessmer U, and Grundhoff A.; A Global analysis of evolutionary conservation among known and predicted gammaherpesvirus miRNAs.; *J Virol.* 2010 Jan;84(2):716-28. Epub 2009 Nov 4.

Müller G, Wied S, Walz N, Jung C.; Translocation of glycosylphosphatidylinositol-anchored proteins from plasma membrane microdomains to lipid droplets in rat adipocytes is induced by palmitate, H₂O₂, and the sulfonylurea drug glimepiride.; *Mol Pharmacol.* 2008 May;73(5):1513-29. Epub 2008 Feb 13.

Antoni S, Walz N, Landersz M, Humbert M, Seidl C, Dittmar MT, Dietrich U.; Genetic and biological characterization of recombinant HIV-1 with Env derived from long-term non-progressor (LTNP) viruses.; *AIDS Res Hum Retroviruses*, 2007, 23 (11); 1377-1386

Oral and Poster Presentations:

Walz N, Christalla T, Henning C, Tessmer U, Grundhoff A.; A global analysis of evolutionary conservation among known and predicted gammaherpesvirus miRNAs; Poster, First International Symposium on Structural Systems Biology, 2009, Hamburg, Germany

Walz N, Christalla T, Tessmer U, Grundhoff A.; A global analysis of evolutionary conservation among known and predicted gammaherpesvirus miRNAs; Poster, "Gesellschaft für Virologie" Annual Meeting, 2009, Leipzig, Germany

Walz N, Christalla T, Tessmer U, Grundhoff A.; Identification of conserved γ -herpesvirus microRNAs; Oral Presentation, 3rd European Congress of Virology 2007, Nuremberg, Germany

Antoni S, Humbert M, Landersz M, Walz N, Rodes B, Soriano V, Knechten H, Staszewski S, von Laer D, Dittmar M, Dietrich U; Enhanced humoral neutralization capacity of long-term non-progressor plasma; Poster, "Gesellschaft für Virologie" Annual Meeting, 2006, Munich, Germany

Awards:

HPI PhD Award 2009 for outstanding publications:

Walz N, Christalla T, Tessmer U, and Grundhoff A.; A Global analysis of evolutionary conservation among known and predicted gammaherpesvirus miRNAs.; *J Virol.* 2010 Jan;84(2):716-28. Epub 2009 Nov 4.

Eidesstattliche Erklärung

Ich erkläre hiermit an Eides statt, dass ich die vorliegende Arbeit selbständig sowie ohne unzulässige Hilfe Dritter und ohne Benutzung anderer als der angegebenen Hilfsmittel angefertigt habe. Die aus anderen Quellen direkt oder indirekt übernommenen Daten und Konzepte sind unter Angabe der Quelle gekennzeichnet.

Des weiteren versichere ich, dass ich diese Dissertation noch keiner anderen Fakultät oder Universität im In- oder Ausland zur Prüfung vorgelegt habe, sowie dass ich mich noch nicht anderweitig um einen Doktorgrad beworben habe bzw. einen solchen bereits besitze.

Nicole Walz

(Ort, Datum)

(Unterschrift)